Hicham Zejli

Janus Cosmological Model

Bimetric Universe: Perspectives & Challenges

Preface by Jean-Pierre Petit

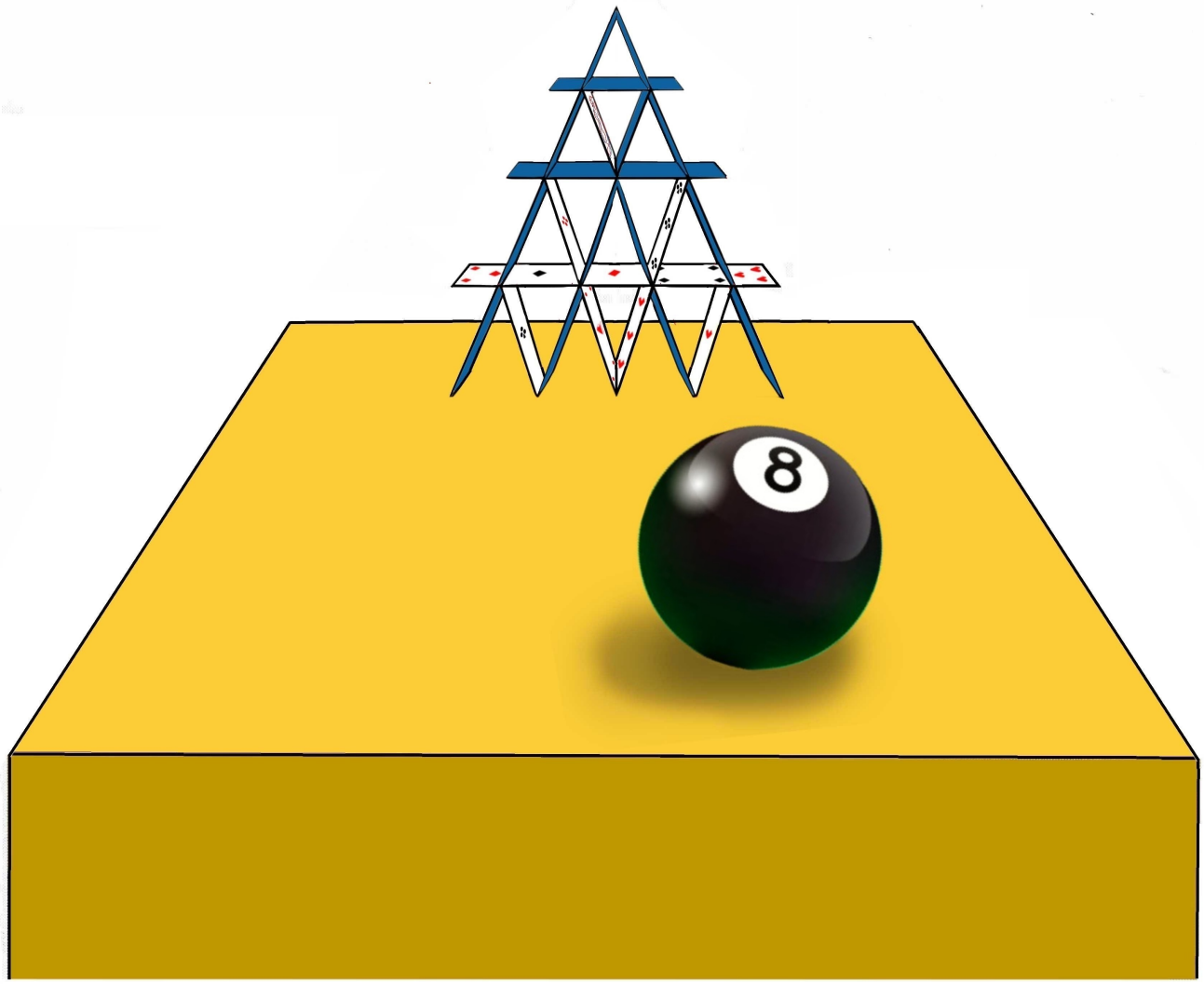

ISBN 978-29-59189-30-2

Updated digital version :

Contents

Preface by Jean-Pierre Petit (France)

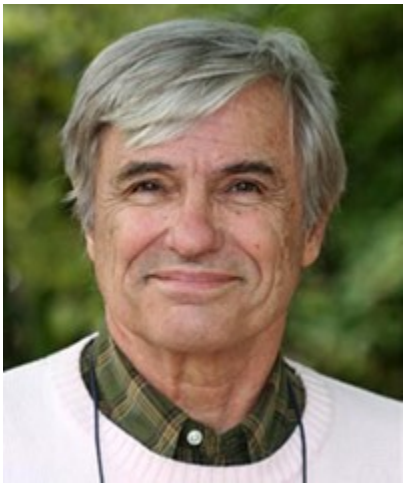

The year is 2024. Do the math. I was born in 1937. As I write these lines, I will be 87 years old. Time passes so quickly that by the time you read these lines I may no longer be of this world. I'm writing these pages, and I think Hicham feels the same way, like throwing a bottle into the sea, containing a message of appeal.

I feel like saying: what's going on in the scientific world?

As you know, more than a century ago, the scientific world underwent the upheaval resulting from the sudden emergence of two new disciplines: quantum mechanics and cosmology. So, for the next seventy years, scientific progress followed one another at a fantastic pace. Either theorists provided explanations for long-known phenomena, such as the advance of Mercury's perihelion, which Newtonian mechanics was unable to account for. Or they were new observations, such as the discovery of the expansion of the universe, which the Russian Alexander Friedman was quick to account for by producing the first unsteady solution to the equation introduced by Einstein in 1915, which now forms the basis of this new worldview, general relativity.

Occasionally, theorists come up with a new vision, proposing strange objects that

they use to make their calculations more balanced. An example is antimatter, the existence of which was conjectured by Englishman Paul Dirac in 1928.

Anecdotally, let's quote the reaction of Dane Niels Bohr, after reading this article:
"This theory seems ideal for capturing elephants in Africa. We hang Dirac's article on a tree. An elephant comes along and reads Dirac's article. It's so amazed that it's easy to capture."

But Nature proved to be Dirac's good friend, and in 1931 confirmed the existence of antielectrons in cosmic rays. At the time, we were unable to recreate this antimatter in particle colliders. Gamma-ray photons from the depths of the cosmos were transformed into an electron-anti-electron pair, an object known as a positron.

This revolution, described as a paradigm shift, began in 1895, with discoveries made by Conrad Röntgen, Henri Becquerel and J.J. Thomson, heralding the dramatic entry of particles and atomic phenomena onto the scientific scene. For decades, theorists on one side, experimenters and observers on the other, resembled two groups of thoroughbreds galloping side by side, some a short neck ahead of others.

All this continued for a very few decades after the Second World War. Among these major discoveries was the accidental discovery, in 1967, of the cosmic ray background, a population of low-energy photons, providing evidence that a fantastic annihilation of pairs of matter and as much antimatter had occurred, at the beginning of the universe.

At the end of the 1960s, cosmologists were preoccupied with determining the average density of the universe. If this was greater than 10^{-29} grams per cubic centimeter, then the universe was evolving in a cyclical fashion. After a phase of expansion, it collapses in on itself, producing a Big Crunch. If this density is lower, then in the distant future of the universe galaxies will move away from each other, indefinitely, at speeds that will become constant. And if this density were equal to this value, then let's say that evolution lies between these two extremes.

I remember this perfectly: it was at this time that I began my research career, at the end of the sixties.

What happens next? Very quickly, the mechanics went haywire and everything went from bad to worse.

The theorists of particle physics, which came into being as the century progressed, thanks to the increased energies brought into play in gas pedals, predicted the appearance of new objects, which they called superparticles.

But nothing happened.

At the dawn of the eighties, to account for the rotation speed of stars in galaxies, and to explain why centrifugal force doesn't cause them to explode, the existence of dark matter, accounting for four-fifths of the mass, was proposed.

In 1989, observations by the COBE satellite revealed the extreme homogeneity of the early universe. To justify this, a young Russian, Andreï Linde, proposed his theory of inflation, according to which the universe, when it was only 10^{-33} second old, underwent a sudden expansion by a factor of 10^{26}, caused by a new field, made up of new particles to which we give the name of inflatons.

Today, there are as many models of inflatons as there are researchers who specialize in this field.

In 2011, a Nobel Prize was awarded for another discovery: that of the acceleration of cosmic expansion, attributed to dark energy. Translating its importance using Einstein's expression $E = mc^2$, this time 75% of the cosmic content escapes observation.

In 2024, as I write these lines, there is no credible model of dark energy.

When all is said and done, ordinary, observable matter now accounts for just 4% of the cosmic soup.

Various candidates have been proposed for dark matter, the main one being that representative of the hypothetical superparticle family, the neutralino. But not only is it impossible to make it appear in powerful colliders, it also eludes all attempts at detection in costly experiments carried out in tunnels and mines, protected from cosmic radiation by a thick layer of rock.

And on the theoretical front?

At the turn of the seventies, when the lack of results from high-energy physics experiments, prompted a new paradigm shift, a group of researchers proposed representing both material particles and those associated with radiation by a new model, made up of vibrating strings, open or closed. The majority of theorists embarked on what they saw as a new and promising path. Research and teaching posts were created in every country. Teams were formed. The players at the heart of this movement went so far as to dream of building a theory of everything.

This current of thought gave rise to mountains of articles and doctoral theses.

What's the situation at the dawn of the third millennium?

Nothing: the mountain is giving birth to a mouse.

The current situation is reminiscent of Hans Christian Andersen's short story *"The Emperor's New Clothes"*. When, at the end of the story, a child writes: *"he's naked!"*

Hicham's book is the story of a paradigm shift project, which can be summed up in one sentence: *The universe is made up of positive and negative masses*

Why not, after all?

But this idea is like a thread, sticking out. We pull on this thread: a string follows. You pull on the string, and a rope is attached. You pull on the rope, and a heavy cable follows, whose pull shakes the edifice.

What building? Albert Einstein's sacrosanct general relativity, whose equation is carved in stone in physics institutes the world over.

Does this mean that the theory is false? No. It's only one side of the coin. It must be integrated into a system of two coupled field equations. In the pages of this book you'll find all that has emerged from this sacrilegious idea.

In January 2023, being the only one to carry this heavy project for forty years, I give a conference in Paris, attended by Hicham.

New ideas are like the traps used in Africa to capture small monkeys. A hollow shell is placed within reach, with a hole drilled in it. Inside the shell is a piece of fruit, which they love, but whose diameter is exactly that of the hole. This means that when the monkey slips his hand into the hole, it's impossible for him to pull out both the hand and the fruit. I myself fell victim to a similar trap forty years ago. A passing idea took hold of me and took possession of my neurons. When an idea is logical, functional and fruitful, it's very difficult to get rid of it. And, finally, if that idea is consistent with observations, rejecting it simply becomes impossible, which complicates your life a great deal by making you a kind of mutant, an outsider within your scientific community.

Unless you decide to stay in the labyrinth.

In 1959 an Englishman, Arthur Koestler, wrote a liter entitled: *"The sleepwalkers"*. He wrote of scientists as people who walk in their sleep, eyes closed, both hands outstretched to find their way. They are walking, unknowingly, in a labyrinth. Not understanding how it's constructed, they sometimes pass by a wide-open door without being able to see it, as they embark on a path that turns out to be a dead end.

This idea is not new. A similar, more static idea can be found in Plato's myth of

the cave.

Let me now turn to what happened to Hicham Zejli. In January 2023, while working as a computer engineer for a French company, he was intrigued by the content of a lecture I was giving in Paris on my cosmological model Janus. He watches the thirty videos I created in 2017 and reads all the books related to the topic to present the main features of this model. He redoes all the calculations he finds in the pdf files I've placed on the Internet, and which accompany my videos. And then the trap closes.

Hicham Zejli during his presentation at the CITV conference in Bastia in April 2024

If you read his book, beware! You may fall victim to it yourself. These pages may lead you to open your eyes and climb up one of the walls of the labyrinth. Then you'll see the world of science differently. As was the case with Hicham, you will suddenly perceive people, sometimes awarded the most prestigious prizes, wandering like sleepwalkers, going round and round in a loop of the labyrinth.

Models that have been accepted by the so-called scientific community will then appear to you as the obvious consequence of blatant miscalculations. You'll see how these somnambulists pass over and over again new, wide-open paths, magnificently in tune with a mass of observation, unable to see them, clinging to ideas that are no more than

planks, rotten, feverishly nailed to the breaches that the reefs of harsh reality have caused in a standard model that is leaking on all sides.

And you'll want to cry out, like the Andersen character, *"the king is naked!"*

The work Hicham has accomplished in less than a year is considerable, and this despite the fact that he has done it all outside his professional activities, in what could be described as his spare time. In twelve months, he has understood and assimilated in depth, rather than superficially, an astonishing mass of things relating to the various fields affected by my Janus model. I've never seen anyone swallow and digest so much, so complex, in so little time.

Becoming the first chronicler of this fantastic adventure that is the Janus model and all that flows from it, he bears witness to it in this book, which had to be written. He has already been actively involved in writing articles for months, and doesn't want to miss a thing of this adventure. More than a witness, he wants to be one of the players.

To ensure the widest possible distribution, the book he has written is in the form of freely downloadable PDFs, in all languages, and should continue to be developed in this spirit. What's special about knowledge is that once it's given, it can't be taken back, and to a certain extent, it's difficult to make it your own.

This book also serves as a logbook, whose content continues to gradually expand. I commit to indicating the date of the latest update in front of the download link. This is where the project becomes particularly interesting. By accessing the most recent version, readers will be able to stay informed of the continuous progress of our research. This research evolves constantly. For example, at the time of writing this new version of the preface, on May 19, 2024, a significant new result has been obtained, which Hicham will detail in the pages of this book-journal.

1967: To explain the absence of primordial antimatter, Sakharov had imagined placing it in a twin universe, CPT symmetric to ours, sharing only the Big Bang singularity (or, in place of that, a tube eliminating this singular aspect).

- T-symmetry: the time coordinate is antiparallel to that of our universe.
- P-symmetry: this second universe is enantiomorphic, that is, a mirror image of ours.
- C-symmetry: what is matter in our universe becomes antimatter in this second universe.

1970: Mathematician Jean-Marie Souriau sheds light on the issue of inverting the time coordinate, synonymous with energy inversion, and thus mass inversion.

1975: I meet the blind mathematician Bernard Morin (1931-2018), who introduces me to sphere eversion.

1979: In January, I publish the first description of his eversion in the journal *Pour la Science*. At the same time, I invent a torus eversion through the two-sheeted covering of the Klein bottle:

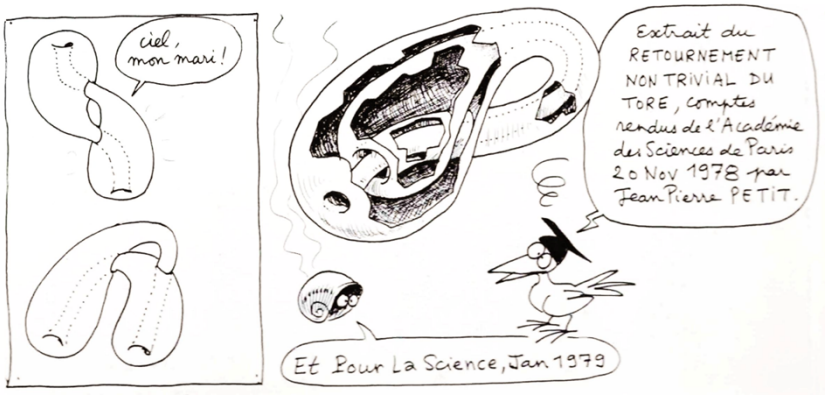

Things then become clearer. The first torus eversion, due to the American mathematician Anthony Phillips and published in 1966 in *Scientific American* (totally unreadable), passes through the two-sheeted covering of the Boy surface, as I explain in my comic book *Topologicon* in 1985:

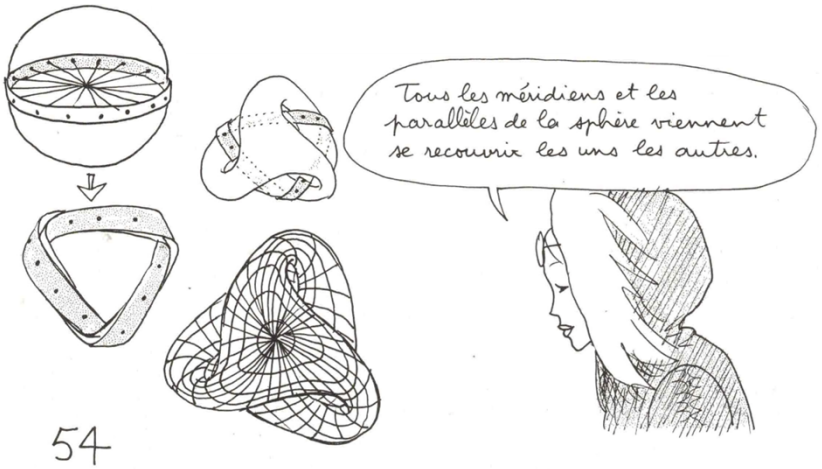

If we consider a sphere S^4 covering a projective P^4 (analogous to the Boy surface in four dimensions), then the operation generates PT symmetry. By adding an even

number of closed dimensions, quantum numbers are created, the first being electric charge. If this hypersphere S^{4+p} is configured as a two-sheeted covering of a projective P^{4+p}, this operation generates CPT symmetry. Along the way, it is shown that if we consider increasing the number of dimensions, it can only be done by adding an even number. Why? You will discover this in a new chapter.

The conclusion that emerges from this presentation is that the Janus Cosmological Model is entirely rooted in topological considerations. This perspective is a recent contribution to the discipline.

Who introduces and develops these new ideas, as if forged in a furnace? A retired 87-year-old and a 44-year-old engineer, in his spare time! Like castaways perched on a makeshift raft, sending messages in bottles, in different languages, trusting them to the currents.

These new ideas are extremely necessary today. One must be blind and deaf not to see a major, unprecedented crisis spreading. The standard model is like an old inner tube, covered in patches: dark matter, dark energy, inflation, strings.

In 2024, here is what has emerged:

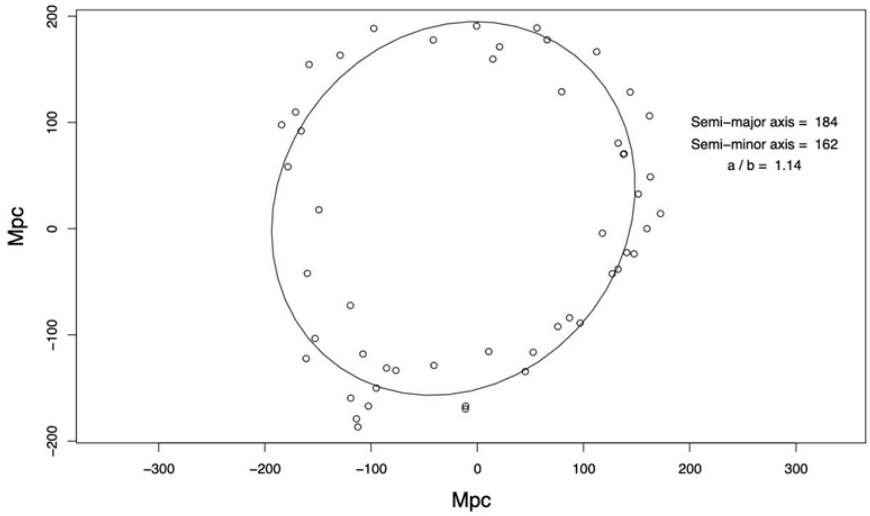

Figure 23: The visually-identified BR absorber members projected onto the plane perpendicular to w_0 with an added fitted ellipse.

The discovery was made by a student from the University of Lancashire, England, who funds her studies by giving violin lessons. To view this discovery, refer to the following video:

https://www.youtube.com/watch?v=S36MqEzUzIw

At the 1 minute and 32 seconds mark, you will hear the opening measures of a solo violin piece by Bach, one of my favorite compositions.

And she handles the bow remarkably well, this young woman!

She initially identified *The Big Arc* in 2021, followed by *The Big Ring*, which corresponds to a collection of galaxies or galaxy clusters located 9.2 billion light-years away and with a diameter of 1.3 billion light-years. These discoveries provide substantial support for the Janus model. In my view, these two structures result from density waves generated by the abrupt formation of the large-scale, lacunary structure of the universe. Alternatively, they could result from simultaneous metric fluctuations, or a combination of both phenomena. Hicham will elaborate on these points in detail.

In April, a symposium titled *"Challenging the Standard Model"* took place at the Royal Astronomical Society in London. Unfortunately, our absence from this significant event was regrettable.

We live in an exceptional period characterized by major upheavals in the scientific world. Particularly in cosmology, a paradigm shift is to be expected.

By the time you read these lines, I may no longer be with you. Time passes so quickly. What will become of all this? I don't know.

I have a vague feeling that humanity today has an appointment with its destiny, that beyond this cosmological model lies a different, even more vast vision of the universe. To illustrate this, I'd like to quote the end of Andréi Sakharov's 1975 Nobel Peace Prize acceptance speech. Words I make my own:
"Thousands of years ago, human tribes suffered great hardship in their struggle for existence. At that time, it was important not only to know how to wield a club, but to possess the ability to think intelligently, to take into account the knowledge and experience accumulated by the tribe, and to develop the bonds that would lay the foundations for cooperation with other tribes. Today, the human race faces a similar test. Many civilizations could exist in infinite space, including societies that might be wiser and more "successful" than our own. I support the cosmological hypothesis that the development of the universe repeats itself an infinite number of times, according to essential characteristics. Other civilizations, including some of the most "successful", are inscribed an infinite number of times on the "next" or "previous" pages of the Book of the Universe. Nevertheless, we should not minimize our sacred efforts in this world, where like faint gleams in the darkness, we have emerged for a moment from the nothingness of obscure unconsciousness to material existence. We must respect the demands of reason and create a life worthy of ourselves and of the goals we barely perceive."

Jean-Pierre Petit, citizen of the world - jean-pierre.petit@manaty.net

Hicham ZEJLI - Born on September 22, 1979 - French Nationality
Master of Engineering, Graduate from ENSISA - hicham.zejli@manaty.net

Chapter 1

Introduction

1.1 Presentation of the Context & Objectives of the Book

In the current landscape of cosmology and theoretical physics, exploring new models to explain observed phenomena in our universe continues to be a vibrant and contentious field of research. This book proposes to explore and present an innovative and revolutionary cosmological model, the Janus Cosmological Model (JCM).

As an engineer with an advanced background in mathematics and physics, I identified in the study of the Janus Cosmological Model, an innovative and intellectually enriching approach to explore and interpret some of the most enigmatic phenomena of the universe. This approach also paves the way for the development of multiple practical applications at local scales, drawing on the fundamental principles derived from this model.

This book aims to achieve two main objectives:

Firstly, to provide a detailed explanation of the Janus Cosmological Model, its foundations, and its implications through some studies, accessible to scientists with a background like mine, namely an advanced level in mathematics and theoretical physics.

Secondly, despite an intense, enriching, and diverse collaboration within our team, I would like to emphasize the marked contrast caused by the lack of communication with the referees consulted by major peer-reviewed journals. This situation highlights the challenges that innovative ideas can face in emerging and refining without significant dialogue among researchers.

1.2 Brief Introduction to the Janus Cosmological Model & Its Importance

The Janus Cosmological Model (JCM) stands out in the landscape of theoretical physics with its bold proposition: to describe the universe as a Riemannian manifold with two metrics. This construction is based on Einstein's theory of general relativity and integrates elements from particle physics and symplectic geometry. The model takes root in the works of Andrei Sakharov and Jean-Marie Souriau, establishing a link between time inversion, energy inversion, and consequently, mass inversion.

One of the major contributions of the model is its ability to address the problem of the baryonic asymmetry of the universe. This issue, at the heart of current debates in cosmology, concerns the observed predominance of matter over antimatter, defying the predictions of the Big Bang model. The Janus Cosmological Model offers a new perspective on this problem by postulating the existence of a bimetric universe from the same singularity which is dominated by matter and antimatter.

The originality of the model also lies in its bimetric approach to the universe, where two *"layers"* of space-time interact through gravitational effect, offering alternative explanations for phenomena such as dark energy, dark matter, and potentially opening new understandings of interstellar travel.

In summary, this book aims to present this model as an innovative approach, challenging current perspectives in cosmology and theoretical physics, and inviting deep reflection on the unexplored possibilities of our understanding of the universe.

Chapter 2

Theoretical Foundations

2.1 Newton's Law of Gravitation

Newton's law, formulated in Euclidean space, states that when a mass m is subjected to the influence of the gravitational force G generated by another mass M, this force F is inversely proportional to the square of the distance d that separates the two masses, and it can be expressed by the following equation:

$$F = \frac{G \cdot m \cdot M}{d^2} \tag{2.1.1}$$

The larger the masses, the greater the force, but this force decreases rapidly as the distance increases due to the d^2 term in the denominator. This law is essential for understanding gravity and the movements of celestial objects.

In physics, this law of gravitation has been fundamental in understanding gravitational interactions between celestial bodies, from Earth to planets and stars. It remains a foundational law of classical mechanics and has played a crucial role in the development of astronomy and astrophysics. It has also been confirmed by numerous observations and experiments over the centuries, further reinforcing its validity in understanding the universe.

However, while Newton's gravitational law has proven to be remarkably powerful and precise in numerous scenarios, it began to reveal its limitations when applied to situations involving speeds approaching the speed of light and phenomena at an astronomical scale. This marked the point at which Albert Einstein's Theory of Special Relativity emerged, heralding a paradigm shift in our understanding of the fundamental concepts of space, time, and gravitation. In the ensuing section, we will meticulously delve into the foundational principles of Special Relativity, which will lay the groundwork for our subsequent exploration of General Relativity. This will lead us towards a more profound comprehension of the intricacies of the cosmos.

2.2 Introduction to Special Relativity

In the early 20^{th} century, physics underwent a conceptual revolution that would challenge the foundations established by Sir Isaac Newton in the 17^{th} century. As observations and experiments became increasingly precise, anomalies emerged when dealing with speeds close to that of light and extreme cosmic environments. In this context, Albert Einstein's Special Relativity made its entrance, disrupting our traditional understanding of space, time, and gravity.

2.2.1 Minkowski Spacetime & Proper Time

Special Relativity invites us to abandon the idea that the universe unfolds in a three-dimensional Euclidean space where time is a separate entity. Instead, it presents a model in which we reside in a hypersurface of four dimensions, where the three dimensions of space are perpendicular to a temporal dimension. This fusion of space and time forms what is known as Minkowski spacetime, with a metric signature of $(-+++)$[1].

To better grasp this concept, envision a point M moving in this spacetime described by two coordinates: time (t) and spatial position (x). As this point evolves, a neighboring point M' corresponds to slightly modified values: $(t + \mathrm{d}t,\, x + \mathrm{d}x)$, where $\mathrm{d}t$ and $\mathrm{d}x$ represent small increments of time and space. If we consider that this increment occurs along a trajectory described by $x = ct$ (where c is the speed of light), then $\mathrm{d}x = c\mathrm{d}t$.

At this juncture, we introduce the concept of *"proper time"*. The quantity s, known as proper time, is a measure of time that governs the life of an object moving at a velocity v. To calculate s, we use the equation:

$$\mathrm{d}s^2 = c^2\mathrm{d}t^2 - \mathrm{d}x^2 \tag{2.2.1}$$

This equation demonstrates how proper time (s) is related to changes in time ($\mathrm{d}t$) and space ($\mathrm{d}x$) when an object moves at a velocity v (here equals c)[2]. It also reveals that proper time can vary based on the velocity and trajectory of the object, leading to phenomena such as time dilation.

In Einstein's theory of special relativity, time is not absolute but depends on the relative velocity of the observer. The next mathematical development describes the relationship between the proper time τ, which is the time measured by the clock in motion (onboard the spaceship), and the coordinate time t, which is the time measured

[1] The metric signature is an important characteristic of spacetime that indicates how time and space intervals are combined in the equations of special relativity. In this $(-+++)$ signature, the first term corresponds to the time interval, which is subtracted from the three subsequent terms corresponding to space intervals. This means that time has a negative sign in the metric, while the three spatial dimensions have positive signs. This specific signature is crucial for understanding how distances and time intervals are measured within the framework of special relativity.

[2] Hence, $v = \frac{\mathrm{d}x}{\mathrm{d}t}$.

by the clock that has remained on the ground (at rest with respect to the observer).

$$\begin{aligned} s = c\tau \Rightarrow \mathrm{d}s = c\mathrm{d}\tau \quad & \Rightarrow c^2\mathrm{d}\tau^2 = c^2\mathrm{d}t^2 - \mathrm{d}x^2 \\ \Rightarrow \mathrm{d}\tau^2 = \mathrm{d}t^2 - \frac{1}{c^2}\mathrm{d}x^2 \quad & \Rightarrow \frac{\mathrm{d}\tau^2}{\mathrm{d}t^2} = 1 - \frac{1}{c^2}\left(\frac{\mathrm{d}x}{\mathrm{d}t}\right)^2 \end{aligned} \tag{2.2.2}$$

We can thus deduce the proper time through the following calculation:

$$\begin{aligned} \left(\frac{\mathrm{d}\tau}{\mathrm{d}t}\right)^2 = 1 - \frac{v^2}{c^2} \quad \Rightarrow \quad \frac{\mathrm{d}\tau}{\mathrm{d}t} = \sqrt{1 - \frac{v^2}{c^2}} \quad \Rightarrow \quad \mathrm{d}\tau = \mathrm{d}t\sqrt{1 - \frac{v^2}{c^2}} \\ \Rightarrow \quad \tau = t\sqrt{1 - \frac{v^2}{c^2}} + \mathrm{Cst} \end{aligned} \tag{2.2.3}$$

Let us determine the value of the integration constant based on the principles of special relativity. Consider that if the velocity v is zero, there is no relative velocity difference between two clocks[3]. Consequently, they should measure the same proper time τ as the time coordinate t. Thus, based on equation 2.2.3, if $v = 0$, then we obtain $\tau = t + \mathrm{Cst}$. If the two clocks are synchronized at the start, then τ and t must be equal at the initial moment, which implies that the constant must be zero. Since the integration constant does not depend on the velocity v as it remains constant for all values of v, it must therefore be zero in all cases. Thus, the relationship between the proper time τ and the time coordinate t is simply given by:

$$\tau = t\sqrt{1 - \frac{v^2}{c^2}}. \tag{2.2.4}$$

This implies that in a scenario where t represents the time measured by a stationary observer equipped with a ground-based clock, and v is the velocity of an object equipped with an onboard clock moving at this speed relative to this assumed stillness, then the proper time τ that will elapse in this object will be affected by time dilation described by $\frac{1}{\sqrt{1-\frac{v^2}{c^2}}}$ known as the *"Lorentz factor"*.

2.2.2 The Speed of Light as a Limit

It is important to note that in this spacetime, the speed of light is constrained by the properties of spacetime (along with its contents) in which it propagates.

Indeed, if we assume that x represents the spatial coordinate, t is the time coordinate, and c is the speed of light, then we can define a velocity v using the expression $v = \frac{\mathrm{d}x}{\mathrm{d}t}$.

Starting with the hypothesis that the proper time variation is always greater than or equal to 0[4], it follows that the speed of light in a vacuum is the ultimate speed limit

[3] One moving and the other at rest.

[4] $\mathrm{d}s^2 = c^2\mathrm{d}t^2 - \mathrm{d}x^2 \geq 0$

for objects in motion with a positive rest mass, as $v \leq c$. Photons, in contrast, follow trajectories for which $v = c$, leading to unique properties associated with light.

Special Relativity is a theory confined to the study of inertial reference frames, specifically those in uniform rectilinear motion (in spaces without curvature, moving in straight lines at a constant velocity).

2.2.3 Fundamental Concepts

Special relativity is primarily based on three concepts:

- **Postulate of the Invariance of the Speed of Light:** This postulate asserts that the speed of light in a vacuum is a universal constant, and it remains the same for all observers, regardless of their relative motion. In other words, the speed of light cannot be added to or subtracted from an observer's velocity. This fundamental idea was confirmed by the famous Michelson-Morley experiment ([44]).

- **Cosmological Principle:** The cosmological principle posits that the universe is homogenous and isotropic. This means that its properties are uniform and identical in all directions and scales. This principle allows us to extend the application of the laws of special relativity to the cosmic scale, considering the universe as a whole.

- **Principle of Special Relativity:** The principle of special relativity asserts that the laws of physics are consistent in all inertial frames of reference. Inertial frames are those moving at a constant velocity relative to each other. This principle generalizes Galileo's concept of relativity and challenges the notion of an absolute reference frame. It demonstrates that the laws of physics remain consistent and invariant, regardless of the relative velocities of observers.

2.2.4 The Equivalence of Mass & Energy

One of the most iconic equations in the realm of physics is Albert Einstein's mass-energy equivalence equation. This equation signifies a profound connection between mass (m) and energy (E), revealing that they are interchangeable in the universe.

Albert Einstein's groundbreaking insight, which led to the formulation of this equivalence, emerged from his special theory of relativity. In this theory, Einstein postulated that energy and mass are intrinsically linked, and the equation serves as the keystone of this union.

The equation's core concept is straightforward: it states that the energy (E) of an object is directly proportional to its mass (m), with the speed of light in a vacuum (c) as the proportionality constant. Mathematically, it can be expressed as:

$$E = mc^2 \tag{2.2.5}$$

Let's explore this equation further through a simple example. Suppose we have a small object with a mass of 1 gram (0,001 kilograms). By applying Einstein's equation, we can calculate the energy equivalent of this mass:

$$E = (0,001\,\text{kg}) \times (3 \times 10^8\,\text{m/s})^2 = 9 \times 10^{13}\,\text{J} \tag{2.2.6}$$

This astonishingly large amount of energy underscores the profound impact of Equation 2.2.5. It demonstrates that even a small mass can produce an enormous amount of energy when converted using this equation. This equation plays a pivotal role in understanding nuclear reactions, such as those occurring in stars and nuclear power plants, where tiny mass changes result in substantial energy releases.

Einstein's equation, with its capacity to bridge mass and energy, remains a cornerstone of modern physics, profoundly influencing our comprehension of the universe's workings.

While Special Relativity has allowed us to explore fascinating aspects of the cosmos by guiding us through journeys at speeds close to that of light and revealing how spacetime bends in response to our motion, it is confined to a specific framework, that of inertial reference frames and uniform rectilinear motions. However, what happens when gravity comes into play? How does the structure of spacetime evolve in the presence of massive objects or significant curvature? This is where Albert Einstein's General Relativity takes over in the next section.

2.3 Introduction to General Relativity

2.3.1 A Revolution in Physics

The law of Newton is a theory that works well in many situations as explained on Section 2.1, but it cannot explain certain phenomena observed at speeds close to that of light or in the presence of strong gravitational fields. Albert Einstein's General Relativity (GR) is a more comprehensive theory that encompasses these gravitational effects. General Relativity, a cornerstone of modern physics, revolutionized our understanding of gravity and the universe. Proposed by Albert Einstein in 1915, this theory is based on the principle that gravity is a manifestation of the curvature of space-time, induced by the presence of mass and energy. The Einstein field equation, at the heart of this theory, describe how matter and energy influence the geometry of space-time and, in turn, how this curved geometry guides the motion of matter and energy.

Indeed, the Einstein field equation, published for the first time on November 25,

1915, is the main partial differential equation of general relativity[5]:

$$G_{\mu\nu} = R_{\mu\nu} - \frac{1}{2} g_{\mu\nu} R = \frac{8\pi G}{c^4} T_{\mu\nu} \tag{2.3.1}$$

It is a dynamic equation that describes how matter and energy modify the geometry of space-time. This curvature of geometry around a matter source is then interpreted as the gravitational field of that source. The movement of objects in this field is very precisely described by their geodesic equation. The metric $g_{\mu\nu}$ produces a family of geodesics. It is noteworthy that particles with positive or negative gravitational mass would behave in the same way by following the same geodesics when deflected by the gravitational potential created by a significant mass M, for example in Earth or solar gravity. Thus, a massive object, such as a star, influences spacetime not only through its mass but also through the energy it emits, like radiation. In general relativity, the energy of an object - including its rest mass energy represented by mc^2 and any additional forms of energy like radiation - contributes to the gravitational field it produces. This combined energy-mass contribution is what curves spacetime around the object. Its second term accounts for the content of the universe at every point in space-time :

- **If it is non-zero**, then the geometric solution that emerges from this equation will describe the interior of a mass.
- **If it is zero**, the solution induced by this equation will refer to a completely empty portion of the universe around this mass.

[5]The different terms of this relationship will be explained in detail later.

2.3.2 Observable Effects & Experimental Confirmations

Among the phenomena explained by GR is the deviation of the plane of rotation of the planet Mercury when it is closest to the Sun, known as the precession of the perihelion. This phenomenon was measured with a precision of 45 seconds of arc per century, a value that could not be accounted for by Newton's law.

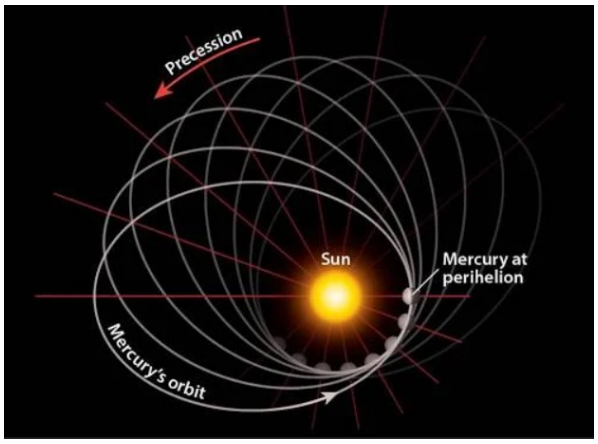

Figure 2.1: Precession of Mercury's perihelion

Another observed phenomenon is the apparent bending of light around the Sun. During the solar eclipse of 1919, Sir Arthur Eddington noticed that light rays appeared to bend around the Sun. In reality, these light rays follow the shortest paths in curved spacetime, known as geodesics. This apparent bending of light is due to the deformation of spacetime caused by the presence of mass, an effect that GR accurately explained ([24]).

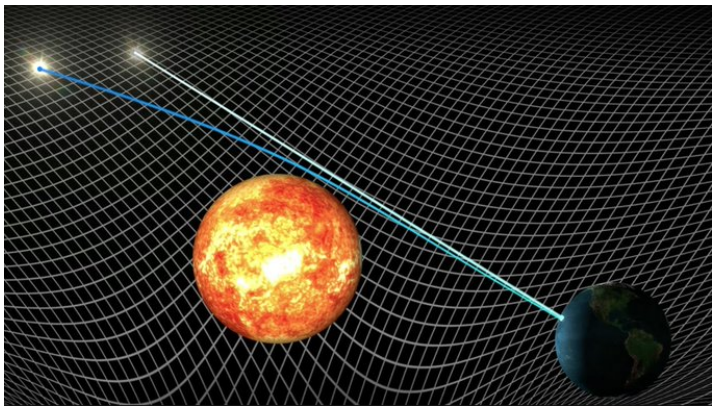

Figure 2.2: Starlight Bending During the Solar Eclipse

These phenomena are considered non-linear because they can only be explained by the theory of GR. However, under conditions where relativistic effects are negligible, Newton's law can provide valid approximations. GR has thus expanded our understanding of gravity beyond the limits of Newton's law, paving the way for a better understanding of gravitational interactions on a large scale and at high speeds.

2.3.3 Geometry of Spacetime & Geodesic Equation

Let's recall Einstein's equivalence principle regarding an inertial frame in free fall:

> *"In a gravitational field, it is always possible at any point in spacetime to choose a locally inertial coordinate system such that, in a sufficiently small region, the laws of physics are identical to those in the absence of gravity."*

In this free-falling frame of reference, the inertial force experienced by a freely falling body cancels out the gravitational force, meaning that the object is not subject to any force (a state of weightlessness). Therefore, the inertial frame is the fundamental frame for studying interacting objects (referred to as the frame of special relativity) before analyzing them in a second Galilean frame known as the *"laboratory frame"*, where these objects are subject to the effects of gravity. This latter frame is, in fact, accelerated upwards ($a = -g$) relative to the natural inertial frame (imagine that *"the ground on Earth is accelerating you upwards"*).

In the theory of special relativity, an inertial frame is described by the Minkowski metric, which is a mathematical representation of flat spacetime. This metric applies in regions where the effects of gravity are absent. In such a context, object paths are determined by the equations of motion derived from the principles of special relativity. While *"geodesic"* is used in general relativity for curved spacetime under gravity, in Minkowski metric of special relativity, these paths are better described as straight lines representing constant velocity motion. In this framework, objects in inertial frames move in straight lines at constant velocity, a special case of a geodesic in flat spacetime.

Inertial Frame and Coordinates

First of all, let's position ourselves in this inertial frame and define the coordinates of a point mass in this frame: We consider the coordinates ξ^α with $\xi^0 = ct$, $\xi^1 = x$, $\xi^2 = y$, $\xi^3 = z$ within the framework of our analysis. Since this body is not subjected to any force (constant velocity), we can deduce that:

$$\frac{\mathrm{d}^2\xi^\alpha}{\mathrm{d}\tau^2} = 0 \tag{2.3.2}$$

With

$$\mathrm{d}\tau^2 = c^2\mathrm{d}t^2 - \mathrm{d}x^2 - \mathrm{d}y^2 - \mathrm{d}z^2 \tag{2.3.3}$$

Where τ corresponds to the metric or interval in this space, which we could also denote as s, and it's important to note that this metric is invariant regardless of the reference frame.

Coordinate Transformation to an Accelerated Laboratory Reference Frame

Let's apply now a coordinate transformation into a new Galilean laboratory reference frame that is *"accelerated upward"* relative to the previous inertial reference frame :

$$x^\mu(x^0, x^1, x^2, x^3)$$

However, each coordinate of the new Galilean frame depends on the coordinates of the inertial frame and vice versa:

$$x^\mu(\xi^0, \xi^1, \xi^2, \xi^3), \quad \xi^\mu(x^0, x^1, x^2, x^3)$$

And it must be remembered that ξ depends on τ :

$$\xi^\mu(\tau)(x^0, x^1, x^2, x^3)$$

So, each parameter of ξ in the new reference frame also depends on τ. Therefore, we can deduce that:

$$\frac{\mathrm{d}\xi^0}{\mathrm{d}\tau} = \frac{\mathrm{d}x^0}{\mathrm{d}\tau}\frac{\partial\xi^0}{\partial x^0} + \frac{\mathrm{d}x^1}{\mathrm{d}\tau}\frac{\partial\xi^0}{\partial x^1} + \frac{\mathrm{d}x^2}{\mathrm{d}\tau}\frac{\partial\xi^0}{\partial x^2} + \frac{\mathrm{d}x^3}{\mathrm{d}\tau}\frac{\partial\xi^0}{\partial x^3} \tag{2.3.4}$$

This can be expressed using Einstein summation convention for repeated indices:

$$\frac{\mathrm{d}\xi^\alpha}{\mathrm{d}\tau} = \sum_{\mu=0}^{3}\frac{\partial\xi^\alpha}{\partial x^\mu}\frac{\mathrm{d}x^\mu}{\mathrm{d}\tau} = \underbrace{\frac{\partial\xi^\alpha}{\partial x^\mu}\frac{\mathrm{d}x^\mu}{\mathrm{d}\tau}}_{\substack{\text{Einstein}\\ \text{summation}\\ \text{convention}}} \tag{2.3.5}$$

NB: In mathematics, Einstein summation convention is a way to compactly represent the summation of a series of terms. When an indice appears both as a subscript and as a superscript in an expression, it typically implies a summation over that indice, meaning that all possible values of that indice are added together. This notation is commonly used in various fields of mathematics and physics to simplify the representation of equations involving repeated indices.

Now, we wish to derive with respect to τ the expression 2.3.5:

$$\frac{\mathrm{d}}{\mathrm{d}t}\left(\frac{\mathrm{d}\xi^\alpha}{\mathrm{d}\tau}\right) = \frac{\mathrm{d}}{\mathrm{d}\tau}\left(\frac{\partial\xi^\alpha}{\partial x^\mu}\right)\frac{\mathrm{d}x^\mu}{\mathrm{d}\tau} + \left(\frac{\partial\xi^\alpha}{\partial x^\mu}\right)\frac{\mathrm{d}^2x^\mu}{\mathrm{d}\tau^2} \tag{2.3.6}$$

However, $\frac{\mathrm{d}}{\mathrm{d}t}\left(\frac{\mathrm{d}\xi^\alpha}{\mathrm{d}\tau}\right) = \frac{\mathrm{d}^2\xi^\alpha}{\mathrm{d}\tau^2}$, therefore, according to 2.3.2, we can deduce that:

$$\frac{\mathrm{d}}{\mathrm{d}\tau}\left(\frac{\partial\xi^\alpha}{\partial x^\mu}\right)\frac{\mathrm{d}x^\mu}{\mathrm{d}\tau} + \left(\frac{\partial\xi^\alpha}{\partial x^\mu}\right)\frac{\mathrm{d}^2x^\mu}{\mathrm{d}\tau^2} = 0 \tag{2.3.7}$$

We then apply 2.3.5 to $\frac{\partial \xi^\alpha}{\partial x^\mu}$ using this time the dummy variable ν:

$$\frac{\mathrm{d}}{\mathrm{d}\tau}\left(\frac{\partial \xi^\alpha}{\partial x^\mu}\right) = \frac{\partial}{\partial x^\nu}\left(\frac{\partial \xi^\alpha}{\partial x^\mu}\right)\frac{\mathrm{d}x^\nu}{\mathrm{d}\tau} \tag{2.3.8}$$

2.3.7 becomes then:

$$\frac{\partial}{\partial x^\nu}\left(\frac{\partial \xi^\alpha}{\partial x^\mu}\right)\frac{\mathrm{d}x^\nu}{\mathrm{d}\tau}\frac{\mathrm{d}x^\mu}{\mathrm{d}\tau} + \left(\frac{\partial \xi^\alpha}{\partial x^\mu}\right)\frac{\mathrm{d}^2x^\mu}{\mathrm{d}\tau^2} = 0 \tag{2.3.9}$$

Hence:

$$\frac{\mathrm{d}x^\nu}{\mathrm{d}\tau}\frac{\partial^2 \xi^\alpha}{\partial x^\mu \partial x^\nu}\frac{\mathrm{d}x^\mu}{\mathrm{d}\tau} + \frac{\partial \xi^\alpha}{\partial x^\mu}\frac{\mathrm{d}^2x^\mu}{\mathrm{d}\tau^2} = 0 \tag{2.3.10}$$

To achieve summation over repeated indices as following:

$$\frac{\partial \xi^\alpha}{\partial x^\mu} \times \frac{\partial x^\beta}{\partial \xi^\alpha} = \sum_{\alpha=0}^{3} \frac{\partial \xi^\alpha}{\partial x^\mu} \times \frac{\partial x^\beta}{\partial \xi^\alpha} \tag{2.3.11}$$

We must do this operation:

$$\left(\frac{\partial x^\beta}{\partial \xi^\alpha}\right)\frac{\mathrm{d}x^\nu}{\mathrm{d}\tau}\frac{\partial^2 \xi^\alpha}{\partial x^\mu \partial x^\nu}\frac{\mathrm{d}x^\mu}{\mathrm{d}\tau} + \frac{\partial \xi^\alpha}{\partial x^\mu}\frac{\mathrm{d}^2x^\mu}{\mathrm{d}\tau^2}\left(\frac{\partial x^\beta}{\partial \xi^\alpha}\right) = 0 \tag{2.3.12}$$

However, for $\beta \neq \mu$, the partial derivatives of one coordinate with respect to another coordinate in the same coordinate system are zero (e.g., $\frac{\partial t}{\partial x} = 0$), and for $\beta = \mu$, the partial derivative is equal to 1. This corresponds to the Kronecker symbol (δ^β_μ):

$$\frac{\partial \xi^\alpha}{\partial x^\mu} \times \frac{\partial x^\beta}{\partial \xi^\alpha} = \frac{\partial x^\beta}{\partial x^\mu} = \delta^\beta_\mu \tag{2.3.13}$$

NB: When β and μ represent different coordinates in the same coordinate system, the partial derivative of β with respect to μ is zero because it means these coordinates are mutually independent in the system. However, when β and μ represent the same coordinate, the partial derivative is equal to 1, indicating that the coordinate changes with itself, as represented by the Kronecker symbol (δ^β_μ).

Thus, we obtain:

$$0 = \left(\frac{\partial x^\beta}{\partial \xi^\alpha}\right)\frac{\mathrm{d}x^\nu}{\mathrm{d}\tau}\frac{\partial^2 \xi^\alpha}{\partial x^\mu \partial x^\nu}\frac{\mathrm{d}x^\mu}{\mathrm{d}\tau} + \delta^\beta_\mu \frac{\mathrm{d}^2x^\mu}{\mathrm{d}\tau^2} \tag{2.3.14}$$

However, if we replace μ with β ($\beta = \mu$), then $\delta^\beta_\mu = \delta^\beta_\beta = 1$, and $\frac{\mathrm{d}^2x^\mu}{\mathrm{d}\tau^2} = \frac{\mathrm{d}^2x^\beta}{\mathrm{d}\tau^2}$. Consequently, we get:

$$0 = \left(\frac{\partial x^\beta}{\partial \xi^\alpha}\right)\frac{\mathrm{d}x^\nu}{\mathrm{d}\tau}\frac{\partial^2 \xi^\alpha}{\partial x^\mu \partial x^\nu}\frac{\mathrm{d}x^\mu}{\mathrm{d}\tau} + \frac{\mathrm{d}^2x^\beta}{\mathrm{d}\tau^2} \tag{2.3.15}$$

Therefore, by introducing the *Christoffel symbols* as follows:

$$\Gamma^{\beta}_{\mu\nu} = \frac{\partial x^{\beta}}{\partial \xi^{\alpha}} \frac{\partial^2 \xi^{\alpha}}{\partial x^{\mu} \partial x^{\nu}} \tag{2.3.16}$$

We can deduce the following *equation of geodesics*:

$$\frac{\mathrm{d}^2 x^{\beta}}{\mathrm{d}\tau^2} + \Gamma^{\beta}_{\mu\nu} \frac{\mathrm{d}x^{\mu}}{\mathrm{d}\tau} \frac{\mathrm{d}x^{\nu}}{\mathrm{d}\tau} = 0 \tag{2.3.17}$$

This represents a general expression for the *Christoffel symbols* $\Gamma^{\beta}_{\mu\nu}$ in terms of the derivatives of the coordinate transformation functions. The Christoffel symbols, as we will see it later, are used in the mathematics of general relativity and differential geometry to describe how coordinate systems change locally.

What does this equation of geodesics teach us?

- The second derivative of coordinates in the *"accelerated"* Galilean reference frame is no longer zero but is equal to the equivalent of inertial forces applied in general relativity (in this case, gravity). From 2.3.17, we can deduce:

$$\frac{\mathrm{d}^2 x^{\beta}}{\mathrm{d}\tau^2} = -\Gamma^{\beta}_{\mu\nu} \frac{\mathrm{d}x^{\mu}}{\mathrm{d}\tau} \frac{\mathrm{d}x^{\nu}}{\mathrm{d}\tau} \tag{2.3.18}$$

  Indeed, if x^{μ} and x^{ν} are space coordinates, then their derivative with respect to τ corresponds to a *"velocity"*.

- Any object in motion in the *"accelerated"* laboratory Galilean reference frame will obey this equation when subjected to the force of Earth's gravity.

- The form of this equation informs us about the shortest or longest (extremums) paths on a curved surface (manifold). More precisely, geodesics correspond to stationary paths whose physical properties remain constant over time (absence of applied external forces).

- We can describe gravity as a purely geometric effect related to the geodesics traversed by objects in curved spacetime (how spacetime is curved is described by the Christoffel symbols). An analogy would be to consider two objects traveling parallel, identical paths at the same speed from a point on Earth towards the North; they will eventually cross at the North Pole due to Earth's curvature. This crossing can be analyzed either by the fact that a force attracted them (analogy with Newtonian mechanics) or by a purely geometric effect related to Earth's curvature (analogy with relativistic mechanics). According to general relativity, gravity is thus a curvature of spacetime that causes objects in locally straight-line motion to follow these geodesics. General relativity allows us to determine the curvature of spacetime based on its components (matter, energy) and then describe the trajectories of moving particles within this spacetime.

- The Christoffel symbols are calculated from the metric and its partial derivatives, capturing information about the curvature of spacetime. They allow us to calculate how geodesics are affected by the curvature of spacetime.

2.3.4 Definition of Tensors

Tensors are mathematical objects from multilinear algebra that were introduced in physics to represent the state of stress and deformation of a volume subjected to forces, hence their name (tensions).

To illustrate the nature of a *tensor*, let us consider a tensor function T that associates two vectors[6] $\vec{u}$ and $\vec{v}$ to a scalar[7] $T(\vec{u}, \vec{v})$ in the set of real numbers $\mathbb{R}$. This function must respect the following linearity conditions:

- The function produces a scalar, that is $T(\vec{u}, \vec{v}) \in \mathbb{R}$.

- The multiplication of one of the vectors by a scalar α must conform to the property of linearity, namely:
$$T(\alpha\vec{u}, \vec{v}) = \alpha T(\vec{u}, \vec{v}) \tag{2.3.19}$$

- The addition of two vectors in one of the function's arguments is distributed linearly as follows:
$$T(\vec{u} + \vec{w}, \vec{v}) = T(\vec{u}, \vec{v}) + T(\vec{w}, \vec{v}) \tag{2.3.20}$$

A *tensor* can therefore be defined as an application or a function in a vector space[8] that associates a set of vectors with a scalar and must obey the following linear properties:

- When one of the vectors is multiplied by a scalar, the tensor multiplies the result by that same scalar.

- When an addition operation is applied to one of the vectors, the tensor distributes the addition through the result of the operation on both vectors.

[6] These are rank 1 tensors which can be represented as a list of numbers (components) that change in a specific way with each change of coordinate system.

[7] These are rank 0 tensors which are simply real or complex numbers and do not change depending on the coordinate system used.

[8] A *vector space* is a collection of vectors, which are objects that can be added together and multiplied ("stretched" or "contracted") by numbers, called scalars in this context. Scalars are often taken to be real numbers, but there can be cases with complex scalars or other types. In a vector space, every linear combination of vectors must also be a vector in that space.

In this context, our tensor is said to be of order 2, which means it takes two vectors as parameters, and is thus qualified as *bilinear*. A tensor of order 1 corresponds to a vector. There are also tensors that can accept three or n vectors as parameters[9].

Thus, tensors allow us to generalize *scalars* and *vectors*:

- **Scalars**:

  Consider 2 coordinate systems, one x'^{μ} being the transformation of the first x^{μ} according to the following relation:

  $$x^{\mu} \to x'^{\mu} \tag{2.3.21}$$

  The scalar allows for the transition of a point from one coordinate system S to a new coordinate system S'. Indeed, if we wish to transition a point M from a Cartesian coordinate system S: $x^{\mu}(x, y)$ to a new polar coordinate system S': $x'^{\mu}(r, \theta)$ (Figure 2.3):

[9] These are called higher-order tensors, going up to order n

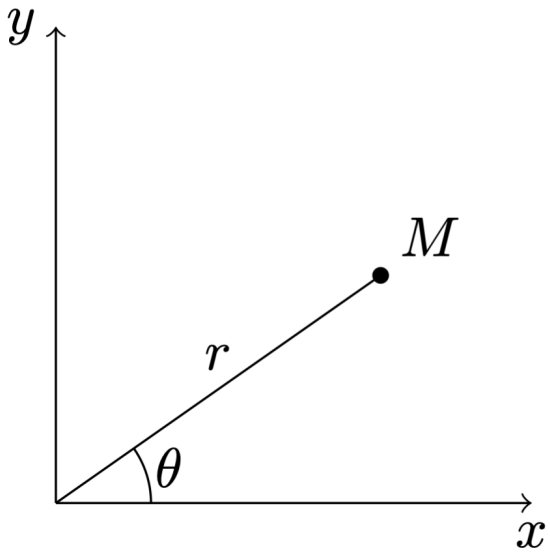

Figure 2.3: Polar Coordinates

This transformation must be operated:

$$S'(x'^{\mu}) = S(x^{\mu}) \tag{2.3.22}$$

- **Vectors**:
  Consider the following figure 2.4:

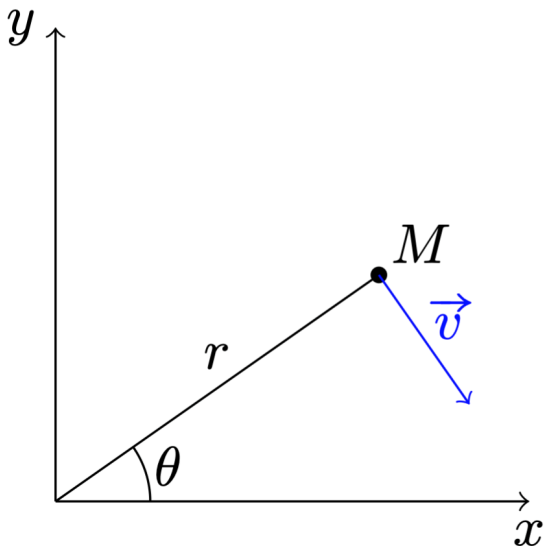

Figure 2.4: Vector in Polar Coordinates

Let's express the coordinates of the vector in terms of r, θ in the new coordinate system as well as in terms of new base vectors $(\vec{u}_r, \vec{u}_\theta)$:

$$\vec{v}(x,y) = v_x(x,y)\vec{u}_x + v_y(x,y)\vec{u}_y \tag{2.3.23}$$

$$\vec{v'}(r,\theta) = v_r(r,\theta)\vec{u}_r + v_\theta(r,\theta)\vec{u}_\theta \tag{2.3.24}$$

Thus, a scalar is a simple number that is associated with each point in space, while a vector is characterized by its length, direction, and sense in space.

The transformation of vectors from one coordinate system to another is a more elaborate operation than the transformation of scalars. There are mainly two types of vectors, each with its own rule of transformation:

- **Contravariant vectors**: these transform by deriving the coordinates of the new reference frame x'^μ with respect to those of the old x^ν. The law of transformation is given by:

$$v'^\mu = \frac{\partial x'^\mu}{\partial x^\nu} v^\nu \tag{2.3.25}$$

- **Covariant vectors**: in this case, the transformation is performed by deriving the coordinates of the old reference frame x^ν with respect to those of the new x'^μ. The rule of transformation is expressed by:

$$v'_\mu = \frac{\partial x^\nu}{\partial x'^\mu} v_\nu \tag{2.3.26}$$

These relations illustrate how contravariant and covariant vectors transform under a change of coordinates.

Proof. Consider an elementary displacement vector that connects 2 distinct events in spacetime separated by $(\mathrm{d}t', \mathrm{d}x', \mathrm{d}y', \mathrm{d}z')$, which can collectively be denoted as $\mathrm{d}x'^\mu$. Then:

$$\mathrm{d}x'^\mu = \frac{\partial x'^\mu}{\partial x^\nu} \mathrm{d}x^\nu \tag{2.3.27}$$

However, the total differential of a function $f(x,y,z)$, which measures the variations of f with respect to its variables x, y, z, also incorporates the changes in its implicit variables according to the following relationship[10]:

[10] Indeed, when the variables x, y, z are themselves functions of another implicit variable, t, a variation in t induces a variation in each of the variables x, y, z through their derivatives with respect to t. In other words, the variation in t results in variations in x, y, z that are quantified by their derivatives with respect to t. Consequently, the total differential of f with respect to t involves the use of partial derivatives of f with respect to its variables x, y, z, as well as the derivatives of these variables with respect to t, to capture the full effect of variations in t on f

$$\mathrm{d}f(x(t),y(t),z(t)) = \frac{\partial f}{\partial x}\frac{\mathrm{d}x}{\mathrm{d}t}\mathrm{d}t + \frac{\partial f}{\partial y}\frac{\mathrm{d}y}{\mathrm{d}t}\mathrm{d}t + \frac{\partial f}{\partial z}\frac{\mathrm{d}z}{\mathrm{d}t}\mathrm{d}t = \frac{\partial f}{\partial x}\mathrm{d}x + \frac{\partial f}{\partial y}\mathrm{d}y + \frac{\partial f}{\partial z}\mathrm{d}z \quad (2.3.28)$$

Hence the contravariant elementary displacement vector[11]:

$$\mathrm{d}x'^{\mu} = \frac{\partial x'^{\mu}}{\partial x^{\nu}}\mathrm{d}x^{\nu} \Leftrightarrow v'^{\mu} = \frac{\partial x'^{\mu}}{\partial x^{\nu}}v^{\nu}$$

□

We will now demonstrate that the norm of the vector $\vec{v}$ is given by the following relation:

$$v_{\mu}v^{\mu} = ||\vec{v}||^2 \quad (2.3.29)$$

Proof. Consider a non-orthogonal frame (Oxy) in figure 2.5 in which the vector $\vec{v}$ has both covariant and contravariant components.

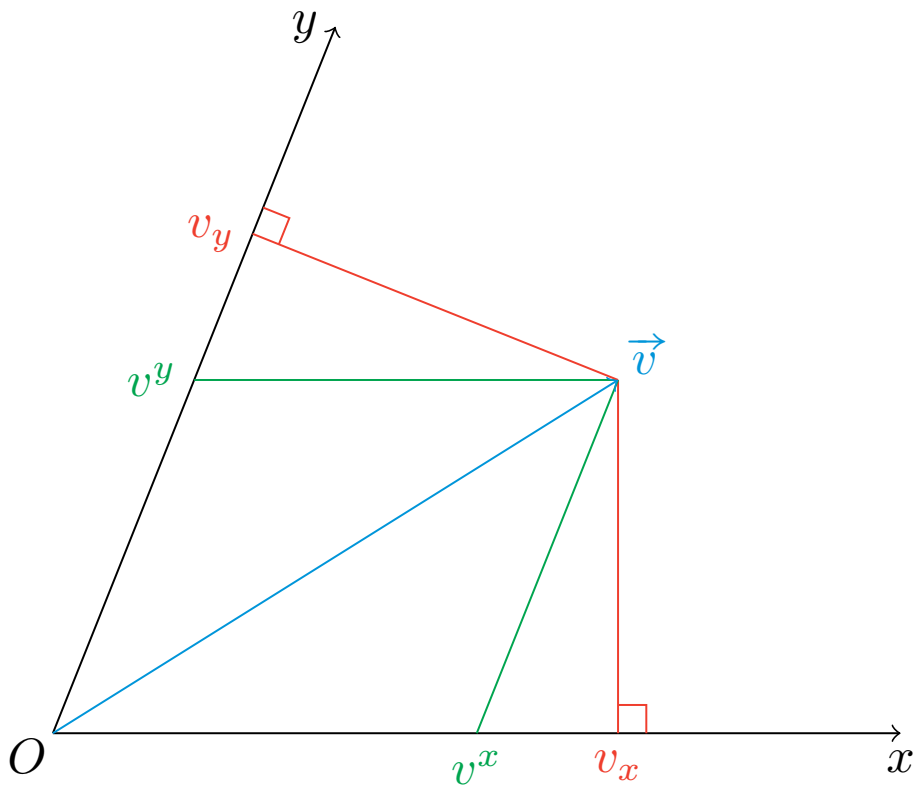

Figure 2.5: $||\vec{v}||^2 = v_x v^x + v_y v^y$

[11] Where μ can take the values 0,1,2,3.

Hence, we obtain:

$$v^2 = h^2 + v_y^2 \tag{2.3.30}$$
$$(v^x)^2 = h^2 + (v_y - v^y)^2 \tag{2.3.31}$$
$$(v^x)^2 = h^2 + v_y^2 + (v^y)^2 - 2v_y v^y \tag{2.3.32}$$
$$(v^x)^2 = v^2 + (v^y)^2 - 2v_y v^y \tag{2.3.33}$$
$$v^2 = (v^x)^2 - (v^y)^2 + 2v_y v^y \tag{2.3.34}$$

However, the second right-angled triangle allows us to obtain the following relation:

$$v^2 = (v^y)^2 - (v^x)^2 + 2v_x v^x \tag{2.3.35}$$

By summing the two, we can therefore deduce that:

$$v^2 = v_x v^x + v_y v^y \tag{2.3.36}$$

□

Thus, a rank 2 tensor simply allows us to manipulate two indices instead of one:

- **Covariant**:
$$T'_{\mu\nu} = \frac{\partial x^\alpha}{\partial x'^\mu}\frac{\partial x^\beta}{\partial x'^\nu}T_{\alpha\beta} \tag{2.3.37}$$
- **Contravariant**:
$$T'^{\mu\nu} = \frac{\partial x'^\mu}{\partial x^\alpha}\frac{\partial x'^\nu}{\partial x^\beta}T^{\alpha\beta} \tag{2.3.38}$$
- **Mixed**:
$$T'^\mu_\nu = \frac{\partial x^\alpha}{\partial x'^\mu}\frac{\partial x'^\nu}{\partial x^\beta}T^\beta_\alpha \tag{2.3.39}$$

We deduce that a rank 2 tensor is, essentially, a matrix or a two-index array that represents a physical quantity in a given space.

Let's observe the transformation of a rank 2 tensor from one coordinate system to another, using the partial derivatives $\frac{\partial x^\alpha}{\partial x'^\mu}$ and $\frac{\partial x^\beta}{\partial x'^\nu}$ to establish how the coordinates in the new system x'^μ are related to the coordinates in the old system x^α. By applying this transformation to the initial rank 2 tensor $T_{\alpha\beta}$, we obtain a new tensor $T'_{\mu\nu}$ of the same rank in the new coordinate system.

Now, to perform a tensor transformation from its contravariant to its covariant form, or vice versa (using implicit summation over ν), it is necessary to introduce the metric tensor[12], with the following relations illustrating this transformation:

$$V_\mu = g_{\mu\nu}V^\nu \tag{2.3.40}$$
$$V^\mu = g^{\mu\nu}V_\nu \tag{2.3.41}$$

[12] which will be studied in the following section.

Indeed, as we will study in the following section, the definition of the metric tensor[13] is expressed by the relation 2.3.54.

Let's try to express this metric tensor in another reference frame:

$$g'_{\mu\nu} = \eta_{\alpha\beta}\frac{\partial\xi^{\alpha}}{\partial x'^{\mu}}\frac{\partial\xi^{\beta}}{\partial x'^{\nu}} \tag{2.3.42}$$

$$g'_{\mu\nu} = \eta_{\alpha\beta}\frac{\partial\xi^{\alpha}}{\partial x^{\sigma}}\frac{\partial x^{\sigma}}{\partial x'^{\mu}}\frac{\partial\xi^{\beta}}{\partial x^{\rho}}\frac{\partial x^{\rho}}{\partial x'^{\nu}} \tag{2.3.43}$$

$$g'_{\mu\nu} = \eta_{\alpha\beta}\frac{\partial\xi^{\alpha}}{\partial x^{\sigma}}\frac{\partial\xi^{\beta}}{\partial x^{\rho}}\frac{\partial x^{\sigma}}{\partial x'^{\mu}}\frac{\partial x^{\rho}}{\partial x'^{\nu}} \tag{2.3.44}$$

Then:

$$g'_{\mu\nu} = \eta_{\sigma\rho}\frac{\partial x^{\sigma}}{\partial x'^{\mu}}\frac{\partial x^{\rho}}{\partial x'^{\nu}} \tag{2.3.45}$$

$$\tag{2.3.46}$$

This clearly demonstrates that $g'_{\mu\nu}$ is indeed a tensor since tensorial equalities (among tensors of the same type) hold true in all reference frames.

Tensor Properties:

- Any linear combination of tensors is a tensor[14].
- The product of two tensors results in a higher-rank tensor. For example, for a rank-2 tensor, $T_{\mu\nu}$, where μ and ν can each take 4 values, the product with another rank-2 tensor results in a rank-4 tensor with $4 \times 4 = 16$ components, giving a total of $16 \times 16 = 256$ components. Thus, if two rank-2 tensors are multiplied, the resulting tensor is of rank 4. The total number of components of the new tensor is the product of the number of components of the two initial tensors.
- The contraction of two tensors yields a tensor[15] according to the following relation:

$$T_{\mu\alpha}V^{\alpha\nu} = W^{\nu}_{\mu} \tag{2.3.47}$$

2.3.5 Metric Tensors

We will now delve into metric tensors and their connection with the previously determined Christoffel symbols.

[13] which transforms coordinates from an inertial frame to any frame such as a Galilean frame.

[14] Considering two tensors $A_{\mu\nu}$ and $B_{\mu\nu}$, and two scalars a and b, then $C_{\mu\nu} = aA_{\mu\nu} + bB_{\mu\nu}$ is also a tensor. This property arises from the definition of tensors in terms of their behavior under coordinate transformation, which preserves linear operations.

[15] by implicit summation over the corresponding indices α of the two tensors.

Consider the Minkowski metric described using the spacetime coordinates of an object in motion within an inertial reference frame, as shown in equation (2.3.3), and expressed as:

$$\mathrm{d}\tau^2 = (\mathrm{d}\xi^0)^2 - (\mathrm{d}\xi^1)^2 - (\mathrm{d}\xi^2)^2 - (\mathrm{d}\xi^3)^2 \tag{2.3.48}$$

It can also be written in this way, where one can denote a summation over indices α and β:

$$\mathrm{d}\tau^2 = \eta_{\alpha\beta}\mathrm{d}\xi^\alpha \mathrm{d}\xi^\beta \tag{2.3.49}$$

This equation uses the metric tensor $\eta_{\alpha\beta}$ of Minkowski space (which describes flat spacetime in special relativity) to calculate the spacetime interval $\mathrm{d}\tau^2$ in terms of the differentials of the coordinates $\mathrm{d}\xi^\alpha$ and $\mathrm{d}\xi^\beta$. The Minkowski metric tensor $\eta_{\alpha\beta}$ has components that are -1 for time-like intervals and +1 for space-like intervals on the diagonal, and 0 off the diagonal like this:

$$\eta_{\alpha\beta} = \begin{pmatrix} 1 & 0 & 0 & 0 \\ 0 & -1 & 0 & 0 \\ 0 & 0 & -1 & 0 \\ 0 & 0 & 0 & -1 \end{pmatrix} \tag{2.3.50}$$

Let's recall that next expressions represent the differential transformation rules between two coordinate systems. They demonstrate how a small change in the set of coordinates x^μ and x^ν results in a small change in an another set of coordinates ξ^α and ξ^β.

$$\mathrm{d}\xi^\alpha = \frac{\partial \xi^\alpha}{\partial x^\mu}\mathrm{d}x^\mu \tag{2.3.51}$$

$$\mathrm{d}\xi^\beta = \frac{\partial \xi^\beta}{\partial x^\nu}\mathrm{d}x^\nu \tag{2.3.52}$$

Now, if we substitute these two differential forms into the expression 2.3.49, we can deduce the following expression:

$$\mathrm{d}\tau^2 = \eta_{\alpha\beta}\frac{\partial \xi^\alpha}{\partial x^\mu}\frac{\partial \xi^\beta}{\partial x^\nu}\mathrm{d}x^\mu \mathrm{d}x^\nu \tag{2.3.53}$$

From where one can extract the following metric tensor:

$$g_{\mu\nu} = \eta_{\alpha\beta}\frac{\partial \xi^\alpha}{\partial x^\mu}\frac{\partial \xi^\beta}{\partial x^\nu} \tag{2.3.54}$$

The metric tensor plays a fundamental role in general relativity as it determines the geometry of spacetime and how gravity acts between two objects located at coordinates x^μ and x^ν in the same reference frame. It enables the transformation from the coordinates of these objects to the distance that separates them, while taking into account the local curvature of spacetime, which can vary depending on the distribution of matter and energy. Unlike classical intuition, the distance between two points in curved spacetime depends on this curvature and can vary significantly. Therefore, the

metric tensor is a crucial mathematical tool for calculating the interval between two events, which also includes the measurement of the time elapsed between them in the presence of a gravitational field.

Since the indices μ and ν are dummy and repeated, they are subject to Einstein's summation convention and can thus be interchanged in the metric tensor expression. This implies that the metric tensor $g_{\mu\nu}$ is symmetric[16].

NB : Now, let us denote $g^{\mu\nu}$ as the inverse of $g_{\mu\nu}$, which is expressed by the following relation with a summation over the repeated indice α, yielding the Kronecker symbol:

$$g^{\mu\alpha}g_{\alpha\nu} = \delta^{\mu}_{\nu} \tag{2.3.55}$$

where δ^{μ}_{ν} is the Kronecker symbol, which as we have seen previously, equals 1 when $\mu = \nu$ and 0 otherwise. This relation defines the nature of the inverse of the metric tensor in differential geometry and general relativity.

2.3.6 Christoffel Symbols

The Christoffel symbols, denoted by $\Gamma^{\beta}_{\mu\nu}$, are derived from the metric tensor and provide essential information about the geometry of spacetime. They are not tensors themselves but are derived from the metric tensor, which is a true tensor.

To calculate the Christoffel symbols, we take the partial derivatives of the metric tensor components and then apply a specific combination of these derivatives. The formula for the Christoffel symbols of the second kind is given by:

$$\Gamma^{\beta}_{\mu\nu} = \frac{1}{2}g^{\beta\alpha}\left(\frac{\partial g_{\alpha\nu}}{\partial x^{\mu}} + \frac{\partial g_{\alpha\mu}}{\partial x^{\nu}} - \frac{\partial g_{\mu\nu}}{\partial x^{\alpha}}\right) \tag{2.3.56}$$

Each term involves a partial derivative of the metric tensor with respect to the coordinates, and $g^{\beta\alpha}$ is the inverse of the metric tensor, ensuring that we are summing over the appropriate indices. As we will see later, Christoffel symbols play a central role in determining geodesics, which describe the trajectory of particles and light in curved spacetime and are used in the equations of motion in General Relativity.

Proof. We will now express the Christoffel symbols in terms of the metric tensor $g_{\mu\nu}$. To do this, we consider the partial derivative of $g_{\mu\nu}$ with respect to the coordinates x^{λ}. This operation introduces the second derivatives of the coordinate transformation functions ξ^{α}, which can then be incorporated into the expression for the Christoffel symbols 2.3.16.

Before we begin our calculations, here are a few preliminary tips to simplify them:

- The metric tensor is symmetric, hence $g_{\mu\nu} = g_{\nu\mu}$.

[16] $g_{\mu\nu} = g_{\nu\mu}$

- To replace ν with α, we must first substitute the existing dummy indice α with σ.

We obtain the metric tensor as following:

$$g_{\alpha\mu} = \eta_{\sigma\beta}\frac{\partial\xi^{\sigma}}{\partial x^{\mu}}\frac{\partial\xi^{\beta}}{\partial x^{\alpha}} \tag{2.3.57}$$

By applying the product rule for differentiation, and remembering that $\eta_{\sigma\beta}$ is a constant, we get:

$$\frac{\partial g_{\alpha\mu}}{\partial x^{\nu}} = \frac{\partial}{\partial x^{\nu}}\left(\eta_{\sigma\beta}\frac{\partial\xi^{\sigma}}{\partial x^{\mu}}\frac{\partial\xi^{\beta}}{\partial x^{\alpha}}\right) \tag{2.3.58}$$

We see the expected second partial derivatives appearing in the right-hand side of the equation (twice):

$$\frac{\partial g_{\alpha\mu}}{\partial x^{\nu}} = \eta_{\sigma\beta}\frac{\partial^2\xi^{\sigma}}{\partial x^{\nu}\partial x^{\mu}}\frac{\partial\xi^{\beta}}{\partial x^{\alpha}} + \eta_{\sigma\beta}\frac{\partial\xi^{\sigma}}{\partial x^{\mu}}\frac{\partial^2\xi^{\beta}}{\partial x^{\alpha}\partial x^{\nu}} \tag{2.3.59}$$

To integrate the expression for the Christoffel symbols 2.3.16 into this relationship, we must apply the following transformation to both sides to isolate the partial derivative and introduce a sum over the repeated indice β:

$$\frac{\partial\xi^{\sigma}}{\partial x^{\beta}}\Gamma^{\beta}_{\mu\nu} = \frac{\partial x^{\boldsymbol{\beta}}}{\partial\xi^{\lambda}}\frac{\partial^2\xi^{\lambda}}{\partial x^{\mu}\partial x^{\nu}}\left(\frac{\partial\xi^{\sigma}}{\partial x^{\boldsymbol{\beta}}}\right) \tag{2.3.60}$$

However, we know that:

$$\frac{\partial x^{\beta}}{\partial\xi^{\lambda}}\frac{\partial\xi^{\sigma}}{\partial x^{\beta}} = \frac{\partial\xi^{\sigma}}{\partial\xi^{\lambda}} = \delta^{\sigma}_{\lambda} \tag{2.3.61}$$

and according to 2.3.55, this Kronecker symbol equals 1 when $\sigma = \lambda$, thus:

$$\frac{\partial\xi^{\lambda}}{\partial x^{\beta}}\Gamma^{\beta}_{\mu\nu} = \frac{\partial^2\xi^{\lambda}}{\partial x^{\mu}\partial x^{\nu}} \tag{2.3.62}$$

We can then replace it in expression 2.3.59, ensuring that we reformulate the corresponding indices in the new expression analogously:

$$\frac{\partial^2\xi^{\sigma}}{\partial x^{\nu}\partial x^{\mu}} = \frac{\partial\xi^{\sigma}}{\partial x^{\boldsymbol{\rho}}}\Gamma^{\boldsymbol{\rho}}_{\mu\nu} \tag{2.3.63}$$

$$\frac{\partial^2 x^{\beta}}{\partial x^{\nu}\partial x^{\mu}} = \frac{\partial\xi^{\beta}}{\partial x^{\boldsymbol{\rho}}}\Gamma^{\boldsymbol{\rho}}_{\nu\alpha} \tag{2.3.64}$$

NB : We do not place β on the Christoffel symbol because it is a dummy summation indice in the term where we want to assign it, so we will choose another letter, ρ:

$$\frac{\partial g_{\alpha\mu}}{\partial x^{\nu}} = \eta_{\sigma\beta}\frac{\partial^2\xi^{\sigma}}{\partial x^{\nu}\partial x^{\mu}}\frac{\partial\xi^{\boldsymbol{\beta}}}{\partial x^{\alpha}} + \eta_{\sigma\beta}\frac{\partial\xi^{\sigma}}{\partial x^{\mu}}\frac{\partial^2\xi^{\beta}}{\partial x^{\alpha}\partial x^{\nu}} \tag{2.3.65}$$

Finaly, we can deduce from 2.3.59:

$$\frac{\partial g_{\alpha\mu}}{\partial x^\nu} = \eta_{\sigma\beta}\frac{\partial \xi^\sigma}{\partial x^\rho}\Gamma^\rho_{\mu\nu}\frac{\partial \xi^\beta}{\partial x^\alpha} + \eta_{\sigma\beta}\frac{\partial \xi^\sigma}{\partial x^\mu}\frac{\partial \xi^\beta}{\partial x^\rho}\Gamma^\rho_{\nu\alpha} \tag{2.3.66}$$

Therefore, the differentiation of the metric tensor can be expressed in 3 different ways (the last 2 involving new indices by swapping ν and μ and replacing μ with α):

$$\frac{\partial g_{\alpha\mu}}{\partial x^\nu} = g_{\rho\alpha}\Gamma^\rho_{\mu\nu} + g_{\mu\rho}\Gamma^\rho_{\nu\alpha} \tag{2.3.67}$$

$$\frac{\partial g_{\alpha\nu}}{\partial x^\mu} = g_{\rho\alpha}\Gamma^\rho_{\mu\nu} + g_{\nu\rho}\Gamma^\rho_{\mu\alpha} \tag{2.3.68}$$

$$\frac{\partial g_{\mu\nu}}{\partial x^\alpha} = g_{\rho\mu}\Gamma^\rho_{\alpha\nu} + g_{\nu\rho}\Gamma^\rho_{\mu\alpha} \tag{2.3.69}$$

These three ways of expressing this differentiation allow us to obtain a simplified result by adding the first two and subtracting the last one: 2.3.67 + 2.3.68 - 2.3.69:

$$g_{\alpha\rho}\Gamma^\rho_{\mu\nu} = \frac{1}{2}\left(\frac{\partial g_{\mu\alpha}}{\partial x^\nu} + \frac{\partial g_{\nu\alpha}}{\partial x^\mu} - \frac{\partial g_{\mu\nu}}{\partial x^\alpha}\right) \tag{2.3.70}$$

$$g^{\beta\alpha}g_{\alpha\rho}\Gamma^\rho_{\mu\nu} = \frac{1}{2}\left(\frac{\partial g_{\mu\alpha}}{\partial x^\nu} + \frac{\partial g_{\nu\alpha}}{\partial x^\mu} - \frac{\partial g_{\mu\nu}}{\partial x^\alpha}\right) g^{\beta\alpha} \tag{2.3.71}$$

$$\delta^\beta_\rho\Gamma^\rho_{\mu\nu} = \frac{1}{2}\left(\frac{\partial g_{\mu\alpha}}{\partial x^\nu} + \frac{\partial g_{\nu\alpha}}{\partial x^\mu} - \frac{\partial g_{\mu\nu}}{\partial x^\alpha}\right) g^{\beta\alpha} \tag{2.3.72}$$

So, finally:

$$\Gamma^\beta_{\mu\nu} = \frac{1}{2}g^{\beta\alpha}\left(\frac{\partial g_{\mu\alpha}}{\partial x^\nu} + \frac{\partial g_{\nu\alpha}}{\partial x^\mu} - \frac{\partial g_{\mu\nu}}{\partial x^\alpha}\right) \tag{2.3.73}$$

This expression of the Christoffel symbol[17] enables us to establish a connection between the curvature of spacetime induced by gravitational force and the spatial derivatives of the metric tensor. It is essential for formulating the equations governing geodesics in the theory of General Relativity. □

Example of Calculating Christoffel Symbols for a Spherical Metric:

In spherical coordinates, the line element ds^2 for a three-dimensional space is expressed as:

$$\begin{aligned}
\mathrm{d}s^2 &= g_{\mu\nu}\mathrm{d}x^\mu\mathrm{d}x^\nu \\
\mathrm{d}s^2 &= g_{11}(\mathrm{d}x^1)^2 + 2g_{12}\mathrm{d}x^1\mathrm{d}x^2 + 2g_{13}\mathrm{d}x^1\mathrm{d}x^3 + g_{22}(\mathrm{d}x^2)^2 + 2g_{23}\mathrm{d}x^2\mathrm{d}x^3 + g_{33}(\mathrm{d}x^3)^2 \\
\mathrm{d}s^2 &= \mathrm{d}r^2 + r^2\mathrm{d}\theta^2 + r^2\sin^2(\theta)\mathrm{d}\phi^2
\end{aligned} \tag{2.3.74}$$

[17] Also known as the affine connection.

where dr, $d\theta$, and $d\phi$ are the differentials of the radial coordinate r, the polar angle θ, and the azimuthal angle ϕ, respectively. The corresponding metric tensor $g_{\mu\nu}$ in spherical coordinates is diagonal and is given by:

$$g_{\mu\nu} = \begin{bmatrix} g_{11} & g_{12} & g_{13} \\ g_{21} & g_{22} & g_{23} \\ g_{31} & g_{32} & g_{33} \end{bmatrix} = \begin{bmatrix} 1 & 0 & 0 \\ 0 & r^2 & 0 \\ 0 & 0 & r^2 \sin^2(\theta) \end{bmatrix} \tag{2.3.75}$$

Proof. The relationship between cartesian and spherical coordinates can be deduced from the Figure 2.6:

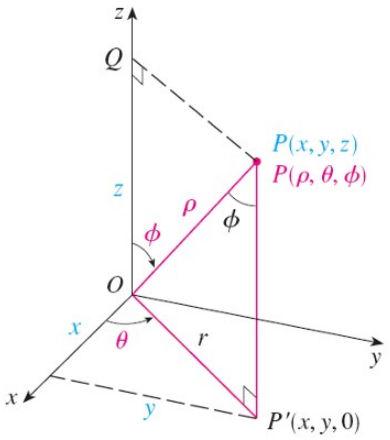

Figure 2.6: The position of point P is defined by the distance ρ and the angles θ (colatitude) and ϕ (longitude)

If we consider triangles OPQ and OPP', we have: $z = \rho\cos\phi$, $r = \rho\sin\phi$, where $x = r\cos\theta$ and $y = r\sin\theta$. Therefore:

$$\begin{aligned} x &= \rho\sin\phi\cos\theta \\ y &= \rho\sin\phi\sin\theta \\ z &= \rho\cos\phi \end{aligned} \tag{2.3.76}$$

Using the physical notations according to the Figure 2.9, the transition to cartesian coordinates is given by:

$$\begin{aligned} x &= r\sin\phi\cos\theta \\ y &= r\sin\phi\sin\theta \\ z &= r\cos\phi \end{aligned} \tag{2.3.77}$$

However, the metric in cartesian coordinates is given by:

$$\mathrm{d}s^2 = \mathrm{d}x^2 + \mathrm{d}y^2 + \mathrm{d}z^2 \tag{2.3.78}$$

To express this in spherical coordinates, we replace x, y, and z with their equivalents in spherical coordinates, yielding 2.3.74. □

To compute the Christoffel symbols $\Gamma^{\beta}_{\mu\nu}$, we first find the inverse of the metric tensor, which for a diagonal metric is simply:

$$g^{\mu\nu} = \begin{bmatrix} 1 & 0 & 0 \\ 0 & \frac{1}{r^2} & 0 \\ 0 & 0 & \frac{1}{r^2 \sin^2(\theta)} \end{bmatrix} \tag{2.3.79}$$

For the given metric tensor, we calculate the partial derivatives required for the Christoffel symbols:

$$\begin{aligned} \frac{\partial g_{\theta\theta}}{\partial r} &= 2r, \\ \frac{\partial g_{\phi\phi}}{\partial r} &= 2r \sin^2(\theta), \\ \frac{\partial g_{\phi\phi}}{\partial \theta} &= 2r^2 \sin(\theta)\cos(\theta). \end{aligned}$$

Inserting these partial derivatives into the formula for the Christoffel symbols 2.3.73, we calculate them by summing over the repeated indice α. For the given metric tensor, most of the Christoffel symbols will be zero because it is diagonal and only depends on r and θ. The non-zero Christoffel symbols are:

$$\Gamma^{r}_{\theta\theta} = -r \tag{2.3.80}$$
$$\Gamma^{r}_{\phi\phi} = -r \sin^2(\theta) \tag{2.3.81}$$
$$\Gamma^{\theta}_{r\theta} = \Gamma^{\theta}_{\theta r} = \frac{1}{r} \tag{2.3.82}$$
$$\Gamma^{\theta}_{\phi\phi} = -\sin(\theta)\cos(\theta) \tag{2.3.83}$$
$$\Gamma^{\phi}_{r\phi} = \Gamma^{\phi}_{\phi r} = \frac{1}{r} \tag{2.3.84}$$
$$\Gamma^{\phi}_{\theta\phi} = \Gamma^{\phi}_{\phi\theta} = \cot(\theta) \tag{2.3.85}$$

NB:

- The Christoffel symbol $\Gamma^{r}_{\theta\theta}$ is calculated as follows:

$$\Gamma^{r}_{\theta\theta} = \frac{1}{2} g^{rr} \left(-\frac{\partial g_{\theta\theta}}{\partial x^r} \right)$$

since the only non-zero derivative of $g_{\theta\theta}$ is with respect to r. Substituting the values, we get:

$$\Gamma^{r}_{\theta\theta} = \frac{1}{2} \left(-\frac{\partial (r^2)}{\partial r} \right) = -r.$$

- Another example is the Christoffel symbol $\Gamma^{\theta}_{r\theta}$, which is calculated as:

$$\Gamma^{\theta}_{r\theta} = \frac{1}{2} g^{\theta\theta} \left(\frac{\partial g_{r\theta}}{\partial x^{\theta}} + \frac{\partial g_{\theta\theta}}{\partial x^{r}} - \frac{\partial g_{r\theta}}{\partial x^{\theta}} \right)$$

  where the only non-zero term is $\frac{\partial g_{\theta\theta}}{\partial x^{r}}$. This gives us:

$$\Gamma^{\theta}_{r\theta} = \frac{1}{2} g^{\theta\theta} \left(\frac{\partial g_{\theta\theta}}{\partial r} \right) = \frac{1}{2} \left(\frac{1}{r^2} \right) (2r) = \frac{1}{r}.$$

Calculating the Riemann Tensor, Ricci Tensor & Ricci Scalar

In this spherical space, all components of the Riemann tensor and the Ricci tensor, as well as the Ricci scalar, are zero, illustrating flat space geometry.

Proof. The Riemann curvature tensor is defined by the expression:

$$R^{\rho}_{\sigma\mu\nu} = \partial_{\mu}\Gamma^{\rho}_{\nu\sigma} - \partial_{\nu}\Gamma^{\rho}_{\mu\sigma} + \Gamma^{\rho}_{\mu\lambda}\Gamma^{\lambda}_{\nu\sigma} - \Gamma^{\rho}_{\nu\lambda}\Gamma^{\lambda}_{\mu\sigma} \tag{2.3.86}$$

Taking for example the Christoffel symbols provided by 2.3.80:

$$\begin{aligned} \Gamma^{\theta}_{\phi\phi} &= -\sin(\theta)\cos(\theta), \\ \Gamma^{\theta}_{r\theta} &= \Gamma^{\theta}_{\theta r} = \frac{1}{r} \end{aligned} \tag{2.3.87}$$

We can proceed to compute the components of the Riemann tensor. As an example, we'll calculate $R^{\theta}_{r\theta r}$:

$$R^{\theta}_{r\theta r} = \partial_{\theta}\Gamma^{\theta}_{rr} - \partial_{r}\Gamma^{\theta}_{\theta r} + \Gamma^{\theta}_{\theta\lambda}\Gamma^{\lambda}_{rr} - \Gamma^{\theta}_{r\lambda}\Gamma^{\lambda}_{\theta r} \tag{2.3.88}$$

Thus, for the calculation of the Riemann tensor component $R^{\theta}_{r\theta r}$, we have:

- The first term $\partial_{\theta}\Gamma^{\theta}_{rr}$ is zero since Γ^{θ}_{rr} is zero.
- The second term $\partial_{r}\Gamma^{\theta}_{\theta r}$ involves the partial derivative of $\Gamma^{\theta}_{\theta r}$ with respect to r, which is $-\frac{1}{r^2}$.
- The third term is the sum over λ of $\Gamma^{\theta}_{\theta\lambda}\Gamma^{\lambda}_{rr}$, but since Γ^{λ}_{rr} is zero for $\lambda \neq r$, this term is zero.
- The fourth term is the sum over λ of $\Gamma^{\theta}_{r\lambda}\Gamma^{\lambda}_{\theta r}$, which for $\lambda = \theta$ gives $\left(\frac{1}{r}\right)\left(\frac{1}{r}\right) = \frac{1}{r^2}$.

The sum of the two non-zero terms (terms 2 and 4) is:

$$-\frac{1}{r^2} + \frac{1}{r^2} = 0$$

Thus, the component $R^{\theta}_{r\theta r}$ of the Riemann tensor is zero.

The Ricci tensor, obtained by contracting the Riemann tensor over its first and third indices, is given by:

$$R_{\mu\nu} = R^{\lambda}_{\mu\lambda\nu} \tag{2.3.89}$$

Finally, the Ricci scalar, which is the trace of the Ricci tensor, is calculated as follows:

$$R = g^{\mu\nu} R_{\mu\nu} \tag{2.3.90}$$

As the Riemann tensor is zero, it follows that the Ricci tensor and its scalar are also zero.

□

Mathematica calculation code:

```
(*Import package*)
(*--------------------*)
Needs["OGRe`"]
(*Definition of the coordinates*)
TNewCoordinates["Spherical", {r, \[Theta], \[Phi]}]
(*Definition of the Metric Tensor*) TShow@
 TNewMetric["SphericalMetricTensor", "Spherical",
  DiagonalMatrix[{1, r^2, r^2 Sin[\[Theta]]^2}]]
(*Line element using integrated function TLineElement*)
TLineElement["SphericalMetricTensor"]
(*Calculation of the Christoffel symbols using TCalcChristoffel*)
TList@TCalcChristoffel["SphericalMetricTensor"]
(*Calculation of the Riemann Tensor using TCalcRiemannTensor*)
TList@TCalcRiemannTensor["SphericalMetricTensor"]
(*Calculation of the Ricci Tensor using TCalcRicciTensor*)
TList@TCalcRicciTensor["SphericalMetricTensor"]
(*Calculation of the Ricci Scalar using TCalcRicciScalar*)
TList@TCalcRicciScalar["SphericalMetricTensor"]
```

2.3.7 Application of the Geodesic Equation in the Weak Field Limit

We denote the expression of the Christoffel symbol and the geodesic equation as follows (if $\nu = 0$: time coordinate, otherwise it is a spatial coordinate x, y, z):

$$\Gamma^{\lambda}_{\mu\nu} = \frac{1}{2} g^{\lambda\sigma} \left(g_{\mu\sigma,\nu} + g_{\nu\sigma,\mu} - g_{\mu\nu,\sigma} \right) \tag{2.3.91}$$

$$\frac{\mathrm{d}^2 x^{\lambda}}{\mathrm{d}s^2} + \Gamma^{\lambda}_{\mu\nu} \frac{\mathrm{d}x^{\mu}}{\mathrm{d}s} \frac{\mathrm{d}x^{\nu}}{\mathrm{d}s} = 0 \tag{2.3.92}$$

where

$$\frac{\partial g_{\mu\sigma}}{\partial x^{\nu}} = g_{\mu\sigma,\nu} \tag{2.3.93}$$

NB :

- This equation represents the partial derivative of the metric tensor component $g_{\mu\sigma}$ with respect to the coordinate x^{ν}, and it's often written with a comma followed by the indice of differentiation, which in this case is ν. The comma notation $g_{\mu\sigma,\nu}$ is a common shorthand in general relativity for denoting partial derivatives of tensor components.

- In the context of special relativity, it is common to use a system of units where the speed of light c is defined as equal to 1 ($c = 1$). This simplifies equations and allows for the easier expression of certain quantities. In this unit system, distances are expressed in units of time (for example, light-years instead of meters) due to the equivalence $c = 1$. To do this, time must be expressed in seconds, and the units of length become a distance traveled by light in one second, which is expressed in light-seconds (equivalent to *"light-years"*). We can thus express the metric as follows:

  $$\mathrm{d}s^2 = \mathrm{d}\tau^2 = g_{\mu\nu}\mathrm{d}x^{\mu}\mathrm{d}x^{\nu} \tag{2.3.94}$$

  Nevertheless, we will now consider that the time t, expressed up to this point, will be the proper time τ in the metric expression, in order to express it as follows:

  $$\mathrm{d}s^2 = \mathrm{d}\tau^2 - \mathrm{d}x^2 - \mathrm{d}y^2 - \mathrm{d}z^2 \tag{2.3.95}$$

We will now demonstrate that the equation 2.3.92 reduces to the Newtonian equation of motion when gravitational fields are weak and static[18], and when velocities are much smaller than the speed of light[19], which can be expressed as follows:

$$g_{\mu\nu} = \eta_{\mu\nu} + h_{\mu\nu} \quad with \quad h_{\mu\nu} \ll \eta_{\mu\nu} \tag{2.3.96}$$

NB : In the theory of linearized gravity, we start by assuming that spacetime is nearly flat. To do this, we represent the total metric tensor $g_{\mu\nu}$ as the sum of the Minkowski metric $\eta_{\mu\nu}$, which describes flat spacetime as seen before, and a small *"perturbation"* $h_{\mu\nu}$, which represents deviations from this flatness due to the presence of mass or energy. We will see it later on the dipole repeller study for a stationary system.

By integrating this metric tensor into the expression 2.3.91, we realize that the partial derivatives of the metric tensor depend only on $h_{\mu\nu}$, since $\eta_{\mu\nu}$ is constant and its derivatives are zero. Hence, in the linearized theory of gravity, the Christoffel symbols can be approximated by considering only the contributions from the perturbation $h_{\mu\nu}$. This is because the Christoffel symbols are defined by the first derivatives of the metric

[18] In special relativity where $g_{\mu\nu}$ is very close to $\eta_{\mu\nu}$ and time-independent.

[19] $v/c \ll 1$

tensor, and in a weak gravitational field, $h_{\mu\nu}$ is small compared to $\eta_{\mu\nu}$. Thus, when we calculate the Christoffel symbols for a weak gravitational field, we neglect the derivatives of $\eta_{\mu\nu}$ and take into account only the derivatives of $h_{\mu\nu}$. Thus, we obtain:

$$g_{\mu\sigma,\nu} = h_{\mu\sigma,\nu} \quad and \quad g_{\mu\nu,\sigma} = h_{\mu\nu,\sigma} \quad and \quad g_{\nu\sigma,\mu} = h_{\nu\sigma,\mu} \tag{2.3.97}$$

$$\Gamma^{\lambda}_{\mu\nu} = \frac{1}{2}(\eta^{\lambda\sigma} + h^{\lambda\sigma})(h_{\mu\sigma,\nu} + h_{\nu\sigma,\mu} - h_{\mu\nu,\sigma}) \tag{2.3.98}$$

Given that $h_{\mu\nu}$ is small, we realize that the product of $h^{\lambda\sigma}$ with its partial derivatives will contribute terms that are second-order or higher (e.g., h^2, h^3, etc.). These higher-order terms will be significantly smaller compared to the first-order terms we are interested in. Therefore, when computing the Christoffel symbols, we neglect the products of $h_{\mu\nu}$ and its derivatives, which implies that the contributions from $h^{\lambda\sigma}$ are negligible in comparison to those from $\eta^{\lambda\sigma}$. Consequently, we obtain:

$$\Gamma^{\lambda}_{\mu\nu} \approx \frac{1}{2}\eta^{\lambda\sigma}(h_{\mu\sigma,\nu} + h_{\nu\sigma,\mu} - h_{\mu\nu,\sigma}) \tag{2.3.99}$$

This approximation streamlines the process of computing spacetime curvature in weak gravitational fields and is foundational in the analysis of gravitational waves, where the perturbations $h_{\mu\nu}$ represent ripples in the curvature of spacetime.

Now, let's consider 2 cases :

- For $\lambda = 0$, which corresponds to the time coordinate in general relativity, the equation for the Christoffel symbols of the first kind becomes specific to the time coordinate. Utilizing the Minkowski metric tensor η and the perturbation h, the Christoffel symbol for $\lambda = 0$ is given by the equation:

$$\Gamma^{0}_{\mu\nu} = \frac{1}{2}\eta^{0\sigma}\left(h_{\mu\sigma,\nu} + h_{\nu\sigma,\mu} - h_{\mu\nu,\sigma}\right) \tag{2.3.100}$$

  Now, considering that $\eta^{0\sigma}$ is not zero only when $\sigma = 0$, which leads to $\eta^{00} = 1$, we arrive at the following relation:

$$\Gamma^{0}_{\mu\nu} = \frac{1}{2}\left(h_{\mu 0,\nu} + h_{\nu 0,\mu} - h_{\mu\nu,0}\right) \tag{2.3.101}$$

  However, given that the gravitational field is static[20]. Consequently, the partial derivative of the metric tensor with respect to time ($\frac{\partial h_{\mu\nu}}{\partial t}$) is zero. This allows us to consider the system as being in a stationary regime with respect to the spacetime metric:

$$\Gamma^{0}_{\mu\nu} = \frac{1}{2}\left(h_{\mu 0,\nu} + h_{\nu 0,\mu}\right) \tag{2.3.102}$$

[20]The spacetime metric does not vary with time.

- For spatial coordinates denoted by $\lambda = i$ (where i, j, k represent spatial indices), the Christoffel symbols can be computed using the perturbation metric $h_{\mu\nu}$. The Minkowski metric $\eta^{i\sigma}$ is used to raise the indice, and it is equal to -1 when the indices match. Thus, the Christoffel symbols for spatial coordinates are given by:

$$\Gamma^i_{\mu\nu} = \frac{1}{2}\eta^{i\sigma}\left(h_{\mu\sigma,\nu} + h_{\nu\sigma,\mu} - h_{\mu\nu,\sigma}\right) \tag{2.3.103}$$

  However, considering the negative sign of the spatial components of $\eta^{i\sigma}$, the equation for $\sigma = i$ simplifies to:

$$\Gamma^i_{\mu\nu} = -\frac{1}{2}\left(h_{\mu i,\nu} + h_{\nu i,\mu} - h_{\mu\nu,i}\right) \tag{2.3.104}$$

  This negative sign reflects the opposite sign convention for the spatial components of the Minkowski metric in comparison to the time component.

Now, let's integrate these results into the geodesic equation 2.3.92 for each case:

- For $\lambda = 0$, we know that $x^\lambda = x^0 = ct$, then:

$$c^2\frac{\mathrm{d}^2 t}{\mathrm{d}s^2} + \frac{1}{2}\left(h_{\mu 0,\nu} + h_{\nu 0,\mu}\right)\frac{\mathrm{d}x^\mu}{\mathrm{d}s}\frac{\mathrm{d}x^\nu}{\mathrm{d}s} = 0 \tag{2.3.105}$$

  However,the following product will generate a sum over repeated indices μ and ν of quantities of orders 0, 1, and 2:

$$(h_{\mu 0,\nu} + h_{\nu 0,\mu})\frac{\mathrm{d}x^\mu}{\mathrm{d}s}\frac{\mathrm{d}x^\nu}{\mathrm{d}s} \tag{2.3.106}$$

  Considering that higher-order quantities, specifically of order 1 and 2, are highly negligible, particularly since they are based on the already small quantity $h_{\mu\nu}$ which is much less than $\eta_{\mu\nu}$, we will only retain the zeroth-order terms. In this context, zeroth-order refers to the terms where μ and ν are both equal to 0, which correspond to the temporal components. This simplification leads us to the following equation:

$$c^2\frac{\mathrm{d}^2 t}{\mathrm{d}s^2} + \frac{1}{2}\left(h_{00,0} + h_{00,0}\right)c^2\frac{\mathrm{d}t}{\mathrm{d}s}\frac{\mathrm{d}t}{\mathrm{d}s} = 0 \tag{2.3.107}$$

  In this approximation, only the terms involving the time coordinate contribute significantly to the equation of motion, simplifying the analysis of spacetime geodesics in a weak gravitational field.

  However, given that the gravitational field is static, these quantities are zero, then:

$$c^2\frac{\mathrm{d}^2 t}{\mathrm{d}s^2} = 0 \tag{2.3.108}$$

  This implies that t is proportional to s, which means:

$$s = ct \tag{2.3.109}$$

- For spatial coordinates denoted by $\lambda = i$, from 2.3.109, we obtain:

$$\frac{1}{c^2}\frac{\mathrm{d}^2x^i}{\mathrm{d}t^2} - \frac{1}{2}\left(h_{\mu i,\nu} + h_{\nu i,\mu} - h_{\mu\nu,i}\right)\frac{1}{c^2}\frac{\mathrm{d}x^\mu}{\mathrm{d}t}\frac{\mathrm{d}x^\nu}{\mathrm{d}t} = 0 \tag{2.3.110}$$

  However, as mentioned earlier, we will only keep quantities of order 0 for μ and ν which are equal to 0. Due to the static nature of the gravitational fields, we obtain the following equation:

$$\frac{1}{c^2}\frac{\mathrm{d}^2x^i}{\mathrm{d}t^2} + \frac{1}{2}h_{00,i} = 0 \tag{2.3.111}$$

$$\frac{\mathrm{d}^2x^i}{\mathrm{d}t^2} = -\frac{c^2}{2}h_{00,i} \tag{2.3.112}$$

  Since i is a spatial indice taking values 1, 2, or 3, we thus find a form of *"Acceleration - Force"* equivalence that can be represented in vector form:

$$\frac{\mathrm{d}^2\vec{r}}{\mathrm{d}t^2} = -\overrightarrow{\mathrm{grad}}\phi \tag{2.3.113}$$

  with

$$\phi = \frac{c^2h_{00}}{2} \tag{2.3.114}$$

The connection between the gravitational potential and the temporal component of the metric tensor can be established by introducing 2.3.114 into 2.3.96, thus we obtain:

$$g_{00} = 1 + \frac{2\phi}{c^2} \tag{2.3.115}$$

The gravitational potential ϕ is equivalent to a speed squared (c^2). Knowing that $h_{\mu\nu} \ll \eta_{\mu\nu}$, we can locally verify that for Earth, $h_{00} = \frac{2\phi}{c^2} = \frac{2G\cdot M_t}{R_t\cdot c^2} = 10^{-9} \ll \eta_{00} = 1$ using the well-known expression for gravitational potential calculation:

$$\phi = \frac{GM}{R} \tag{2.3.116}$$

2.3.8 The Solutions of Karl Schwarzschild & Ludwig Flamm

Karl Schwarzschild then developed a complete geometric solution to this equation, consisting of two metrics published in two separate papers[21], whose expanded forms[22] are as follows:

- **The first solution**, described by metric 2.3.117, depicts the exterior geometry of empty spacetime around a spherically symmetric mass, such as a star with a radius r_n, as illustrated in Figure 2.7:

$$\mathrm{d}s^2 = \left(1 - \frac{8\pi G\rho r_n^3}{3c^2r}\right)c^2\mathrm{d}t^2 - \frac{\mathrm{d}r^2}{1 - \frac{8\pi G\rho r_n^3}{3c^2r}} - r^2\left(\mathrm{d}\theta^2 + \sin^2\theta\mathrm{d}\phi^2\right) \tag{2.3.117}$$

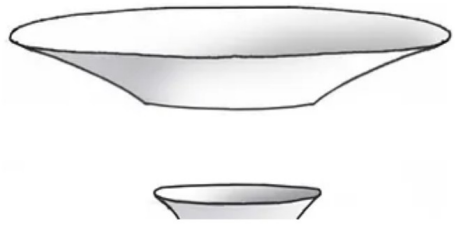

Figure 2.7: Portion of a Flamm hypersurface

- **The second solution**, often referred to as the interior Schwarzschild solution structured by metric 2.3.118, describes the spacetime geometry within a static, spherically symmetric body composed of an incompressible fluid, such as a star with a radius r_n, as depicted in Figure 2.8:

$$\begin{aligned} \mathrm{d}s^2 = &- \frac{\mathrm{d}r^2}{1 - \frac{8\pi G\rho r^2}{3c^2}} - r^2\left(\mathrm{d}\theta^2 + \sin^2\theta \mathrm{d}\phi^2\right) \\ &+ \left[\frac{3}{2}\sqrt{1 - \frac{8\pi G\rho r_n^2}{3c^2}} - \frac{1}{2}\sqrt{1 - \frac{8\pi G\rho r^2}{3c^2}}\right]^2 c^2\mathrm{d}t^2 \end{aligned} \tag{2.3.118}$$

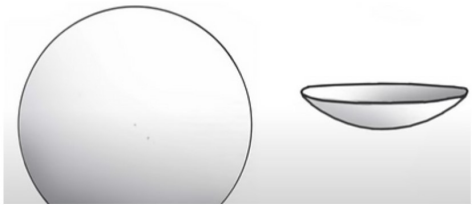

Figure 2.8: Portion of a sphere

This approach entails matching two segments of spacetime solutions, specifically two regions of hypersurfaces, each characterized by their distinct metrics. The matching is performed at a common boundary, ensuring the continuity of the spacetime geometry and the physical consistency of the combined solution across the interface.

That same year, a young mathematician offered his own interpretation of Schwarzschild's work. His name was Ludwig Flamm. His work and his name remained unknown to most

[21] [75] and [74]
[22] [1]

cosmology specialists for a simple reason: his paper was not translated into English until 2012. He had a perfect mastery of the geometry of objects such as three-dimensional Riemannian hypersurfaces ([29],[30]).

Kruskal, building upon the exterior Schwarzschild metric, developed his renowned model, considered as the foundation of black hole theory. Indeed, by analytically extending the exterior Schwarzschild solution, he eliminates *"algebraically"* the coordinate singularity found at the *"event horizon"* for $r = R_s$ (Schwarzschild Radius), through the introduction of a new coordinate system. This system is designed to make the metric regular everywhere, except at the *"central physical singularity"* for $r = 0$ ([42],[77]). But does this model truly have a physical meaning ?

2.3.9 Construction of Geodesics for the Schwarzschild Exterior Metric

Let's consider the Schwarzschild exterior metric (6.53) extracted from [1] (Page 194):

$$\mathrm{d}s^2 = \left(1 - \frac{2m}{r}\right)(\mathrm{d}x^0)^2 - \left(\frac{\mathrm{d}r^2}{1 - \frac{2m}{r}}\right) - r^2(\mathrm{d}\theta^2 + \sin^2\theta\,\mathrm{d}\phi^2) \tag{2.3.119}$$

where m is a simple integration constant (a length), x^0 is a chronological marker (also a length), and s is the length measured on the 4D hypersurface.

The authors write:

$$x^0 = ct \tag{2.3.120}$$

A geodesic is a path inscribed on the hypersurface, which corresponds to a minimal length:

$$\delta \int \mathrm{d}s = 0 \tag{2.3.121}$$

This means that this length:

$$\int_a^b \left\{ \left(1 - \frac{2m}{r}\right) c^2 \mathrm{d}t^2 - \frac{\mathrm{d}r^2}{1 - \frac{2m}{r}} - r^2 \left(\mathrm{d}\theta^2 + \sin^2\theta\,\mathrm{d}\phi^2\right) \right\} \tag{2.3.122}$$

has a minimal value along a path thus configured: $t(s)$, $r(s)$, $\theta(s)$, $\phi(s)$.

Let's write:

$$\dot{t} = \frac{\mathrm{d}t}{\mathrm{d}s}, \quad \dot{r} = \frac{\mathrm{d}r}{\mathrm{d}s}, \quad \dot{\theta} = \frac{\mathrm{d}\theta}{\mathrm{d}s}, \quad \dot{\phi} = \frac{\mathrm{d}\phi}{\mathrm{d}s} \tag{2.3.123}$$

This amounts to searching for paths that minimize:

$$\int_a^b \left\{ \left(1 - \frac{2m}{r}\right) c^2 \dot{t}^2 - \frac{\dot{r}^2}{1 - \frac{2m}{r}} - r^2(\dot{\theta}^2 + \sin^2\theta\,\dot{\phi}^2) \right\} \mathrm{d}s \tag{2.3.124}$$

The quantity in brackets is:

$$L = L(t, r, \theta, \phi, \dot{t}, \dot{r}, \dot{\theta}, \dot{\phi}) \quad \text{or} \quad L = L(x^i, \dot{x}^i) \tag{2.3.125}$$

This problem was solved by the French mathematician Lagrange, which led to what are now known as the Lagrange equations.

The calculation of the geodesics is a problem of *"bounded extremum"*. This is because we consider all paths connecting two points a and b, hence linked to these points. The geodesics are then given by the equations:

$$\frac{\mathrm{d}}{\mathrm{d}s}\left(\frac{\partial L}{\partial \dot{x}^i}\right) = \frac{\partial L}{\partial x} \tag{2.3.126}$$

With:

$$L = \left(1 - \frac{2m}{r}\right) c^2\dot{t}^2 - \frac{\dot{r}^2}{1 - \frac{2m}{r}} - r^2\left(\dot{\theta}^2 + \sin^2\theta\dot{\phi}^2\right) \tag{2.3.127}$$

$$\frac{\partial L}{\partial t} = \frac{\partial L}{\partial \phi} = 0, \quad \frac{\partial L}{\partial \theta} = -2r^2\sin\theta\cos\theta\dot{\phi}^2 \tag{2.3.128}$$

The first three Lagrange equations (6.75), (6.76), (6.77) extracted from [1], corresponding to the variables θ, ϕ and t, are the following:

$$\frac{\mathrm{d}}{\mathrm{d}s}(r^2\dot{\theta}) = r^2\sin\theta\cos\theta\dot{\phi}^2 \tag{2.3.129}$$

$$\frac{\mathrm{d}}{\mathrm{d}s}(r^2\sin^2\theta\dot{\phi}) = 0 \tag{2.3.130}$$

$$\frac{\mathrm{d}}{\mathrm{d}s}\left[\left(1 - \frac{2m}{r}\right)\dot{t}\right] = 0 \tag{2.3.131}$$

If we divide each term of the metric 2.3.119 by ds^2:

$$1 = \left(1 - \frac{2m}{r}\right) c^2\dot{t}^2 - \frac{\dot{r}^2}{1 - \frac{2m}{r}} - r^2\left(\dot{\theta}^2 + \sin^2\theta\dot{\phi}^2\right) \tag{2.3.132}$$

In general relativity, exploiting the spherical symmetry of a solution can simplify the analysis of geodesics. In the case of the Schwarzschild metric, which is indeed spherically symmetric, this symmetry can be exploited to reduce the problem to two dimensions.

The Schwarzschild metric, in spherical coordinates, depends on the variables r, θ, ϕ, and t. Spherical symmetry indicates that the metric does not change when rotations are made around the center. This property allows us to simplify the problem by choosing geodesics that remain in a constant plane. It is common to choose the equatorial plane to simplify calculations, corresponding to setting $\theta = \pi/2$. In this plane, the θ

coordinate does not change, which means that $\mathrm{d}\theta = 0$ and therefore the component of the metric involving $\mathrm{d}\theta$ disappears (see the Figure 2.9).

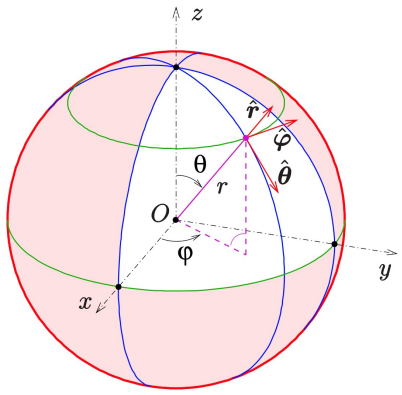

Figure 2.9: Unit vectors in spherical coordinates

Then, by examining the Lagrangian (which is a function that summarizes the dynamics of a system) associated with this metric, we can find the equations of motion for the geodesics. For an object moving in the equatorial plane, the azimuthal component of its angular momentum, related to ϕ, is conserved, which is a consequence of the axial symmetry of the metric with respect to the axis perpendicular to the equatorial plane. Mathematically, this is expressed by the equation:

$$r^2\dot{\phi} = h = \text{constant} \tag{2.3.133}$$

where h is a constant of motion (angular momentum per unit mass), r is the radial coordinate, and $\dot{\phi}$ is the derivative of the azimuthal coordinate ϕ with respect to proper time s (the time measured by a clock moving with the object).

This tells us that the quantity $r^2\dot{\phi}$ remains constant along the geodesic.

The equation 2.3.131 above integrates and gives:

$$\left(1 - \frac{2m}{r}\right)\dot{t} = l = \text{constant} \tag{2.3.134}$$

By substitution, we then obtain the differential equation:

$$1 = \left(1 - \frac{2m}{r}\right)^{-1} c^2 l^2 - \left(1 - \frac{2m}{r}\right)^{-1} \dot{r}^2 - \frac{h^2}{r^2} \tag{2.3.135}$$

which gives r as a function of the parameter s. But by using an equation presented earlier, we can switch to a differential equation featuring the derivative:

$$r' = \frac{\mathrm{d}r}{\mathrm{d}\phi} = \frac{\dot{r}}{\dot{\phi}} \tag{2.3.136}$$

From 2.3.133 and 2.3.134, we then obtain:

$$\dot{r} = \dot{\phi} r' = \frac{h}{r^2} r' \tag{2.3.137}$$

We can then obtain the differential equation relating r and l:

$$\left(1 - \frac{2m}{r}\right) = c^2 l^2 - \frac{h^2}{r^4} r'^2 - \frac{h^2}{r^2}\left(1 - \frac{2m}{r}\right) \tag{2.3.138}$$

We can then do the transition from the variable r to a variable u such that:

$$u = \frac{1}{r} \quad \Longrightarrow \quad r' = -\frac{u'}{u^2} \tag{2.3.139}$$

Then, from 2.3.136, we can deduce:

$$\mathrm{d}\phi = \frac{\mathrm{d}r}{r'} = \frac{\mathrm{d}u}{u'} \tag{2.3.140}$$

Which leads us to:

$$(1 - 2mu) = c^2 l^2 - h^2 u'^2 - h^2 u^2 (1 - 2mu) \tag{2.3.141}$$

which reduces to:

$$u'^2 = \left(\frac{c^2 l^2 - 1}{h^2}\right) + \frac{2m}{h^2} u - u^2 + 2mu^3 \tag{2.3.142}$$

Thus, from 2.3.140, the integration gives:

$$\phi = \phi_0 + \int_{u_0}^{u} \frac{\mathrm{d}v}{\sqrt{\frac{c^2 l^2 - 1}{h^2} + \frac{2m}{h^2} v - v^2 + 2mv^3}} \tag{2.3.143}$$

This constitutes an exact solution to Einstein's equation which expresses the angle ϕ as an integral of $u = \frac{1}{r}$, and conversely it gives us u as the inverse (implicit) function of ϕ and results in *"quasi-elliptical"* geodesics, depending on the two integration constants l and h.

Indeed, if h is large, it means that the geodesic traversed by a test particle will deviate from a radial free-fall trajectory because it will have a significant amount of specific angular momentum. Consequently, its trajectory will be less affected by the gravitational pull directly towards the central body, causing it to veer away from a direct radial fall and follow a more curved or *"quasi-elliptical"* path.

Ignoring the region inside the Schwarzschild sphere (r<2m), it is possible to represent in 3D the plane geodesics associated with this stationary metric. The representation of the Schwarzschild sphere, can be envisioned as a circle that projects into spacetime along the Schwarzschild time dimension t_s. If we consider a neutron star with a radius

of 10 km, it will remain stable at the Tolman-Oppenheimer-Volkoff (TOV) limit of approximately 2 solar masses. The TOV limit represents the critical maximum mass a neutron star can have while remaining stable. This places the '*horizon*' of a point mass equivalent at a distance from its center of about 6 km ($r_s = \alpha$). Given that the star's radius is approximately 3/2 times r_s, we position the '*horizon*' of this object at $r_s = 2$ for a radius of 3. This setup allowed me to represent, using Mathematica, the geodesic of a test particle following a falling trajectory toward this object, as depicted in the Figure 2.10.

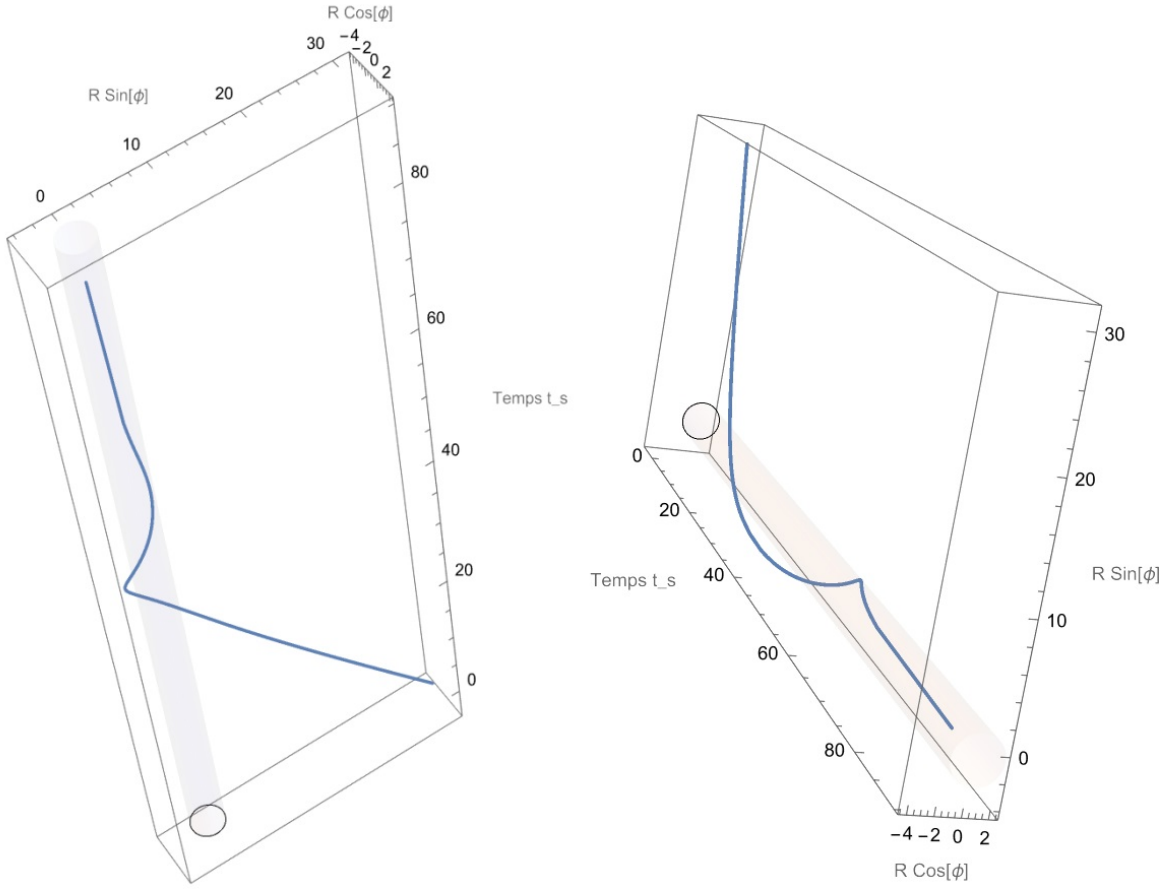

Figure 2.10: Representation of a Falling Geodesic in the Coordinate System (r, ϕ, t_s)

Regardless of the geodesic's direction of travel, centripetal in this case, with this choice of temporal coordinate, approaching the Schwarzschild sphere would require an infinite duration. Indeed, as we can see Figures 2.11 and 2.12, for a distant observer, any object approaching the horizon of either a neutron star near its physical criticality or a supermassive object, such as those whose alternative approach will be studied in the chapter 8, would experience time dilation near what is known as the Schwarzschild radius. However, for the object itself (or an observer moving with the object), time

would continue to progress normally (Respectively, the blue curve compared to the dashed curve).

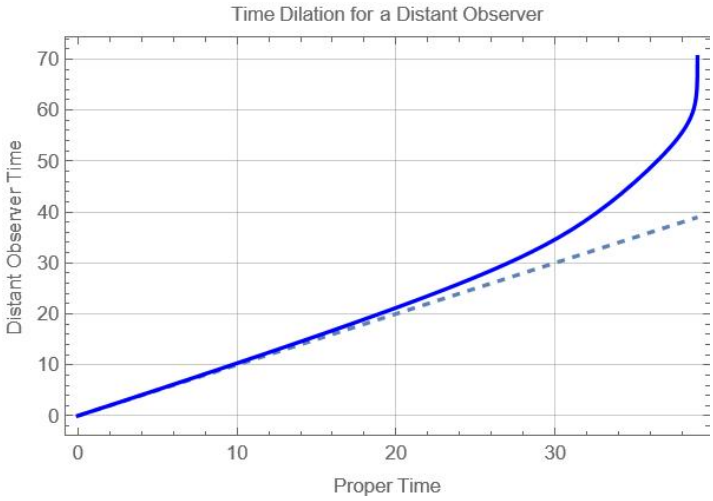

Figure 2.11: Time Dilation for a Distant Observer

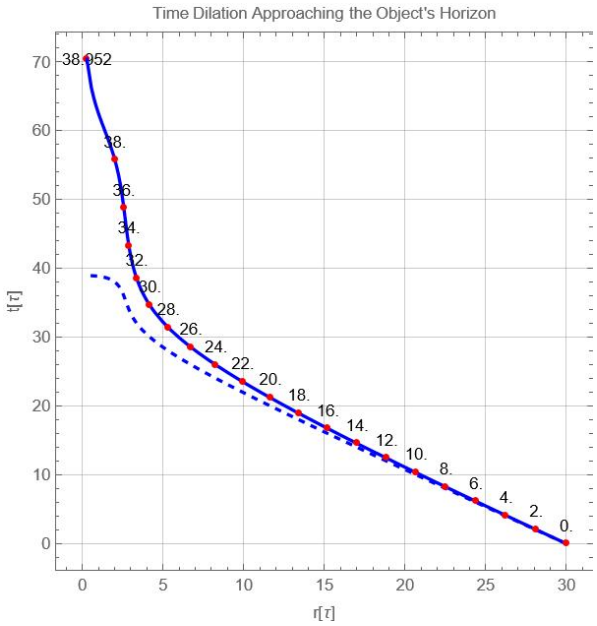

Figure 2.12: Time Dilation Approaching the Object's Horizon

From the perspective of this distant observer, the object would take an apparently infinite amount of time to reach this horizon. As a result, it would be perceived as slowing down progressively, appearing almost frozen or making a freeze-frame near the

horizon.

This phenomenon is a consequence of general relativity, which predicts that the presence of a significant mass curves space-time. This curvature affects the passage of time, leading to time dilation in intense gravitational fields.

This aspect forms one of the cornerstones of black hole theory. But is there another alternative? This is what we will explore later in the chapter 6.

2.3.10 The Solution of Roy Kerr

In 1963, Roy Kerr, an eminent New Zealand mathematician, revolutionized the understanding of general relativity in the context of the black hole model by proposing a new solution to the Einstein's field equation. Unlike the Schwarzschild exterior metric ([75]), which is used as the foundation of the static and spherically symmetric black hole model, the Kerr solution is axisymmetric, representing a rotating black hole ([39]). This discovery was particularly significant at the time because it provided a more realistic model for numerous celestial objects.

The Kerr metric is expressed in Boyer-Lindquist coordinates (t, r, θ, ϕ) ([17]), and its line element is given for $c = 1$ by:

$$\begin{aligned} \mathrm{d}s^2 = &- \left(1 - \frac{2GMr}{\rho^2}\right) \mathrm{d}t^2 - \frac{4GMar\sin^2\theta}{\rho^2}\mathrm{d}t\mathrm{d}\phi + \frac{\rho^2}{\Delta}\mathrm{d}r^2 \\ &+ \rho^2\mathrm{d}\theta^2 + \left(r^2 + a^2 + \frac{2GMra^2\sin^2\theta}{\rho^2}\right)\sin^2\theta\mathrm{d}\phi^2 \end{aligned} \tag{2.3.144}$$

where

$$\begin{aligned} \Delta &= r^2 - 2GMr + a^2, \\ \rho^2 &= r^2 + a^2\cos^2\theta. \end{aligned}$$

M is the mass of the central rotating object, often a black hole, influencing the surrounding spacetime and a is the specific angular momentum of the rotating object. The important term to note here is $-\frac{4GaMr\sin^2\theta}{\rho^2}\mathrm{d}t\mathrm{d}\phi$, which represents the spacetime dragging effect due to the rotation of the object, typically a black hole. This characteristic can be interpreted as a manifestation of Ernst Mach's idea of the relativity of motion, where spacetime itself seems to be influenced by the presence of moving matter.

The relevance of the Kerr solution was further underscored by the discovery of pulsars in 1967, initially understood as neutron stars rotating at incredibly high speeds, sometimes reaching a thousand rotations per second. Although the Kerr metric is primarily applied to the black hole model, its implications for understanding other compact

astrophysical objects, such as neutron stars, are also significant.

Renowned astrophysicist Subrahmanyan Chandrasekhar praised the Kerr solution, considering it a major advance in applied mathematical research in theoretical physics ([15]).

What is important to emphasize through this Kerr approach is the possibility of exploring other representation properties, such as introducing, for example, a $drdt$ term into the Schwarzschild exterior metric, whose implications will be studied in the chapter 6.

2.4 The Works of Andrei Sakharov & Jean-Marie Souriau

The Janus cosmological model compiles Albert Einstein's theory of general relativity, the work of Andrei Sakharov in particle physics and cosmology, as well as the work of Jean-Marie Souriau in symplectic geometry. According to the theory of dynamical groups, it explains how time inversion implies an inversion of energy and therefore mass.

Indeed, the baryonic asymmetry of the universe is considered one of the most significant problems in current physics. More specifically, it refers to the observation that there is a net quantity of baryons (particles made up of three quarks, such as protons and neutrons) in the universe, but almost no antibaryons (particles composed of three antiquarks). The universe should have been created with an equal amount of baryonic matter and antibaryonic antimatter since the Big Bang, which would have led to their mutual annihilation, their mass transforming into photons. But where did this primordial antimatter go?

In the 1960s, scientists discovered that the rate of matter production (from the combination of primordial quarks) occurs slightly faster than the rate of antimatter production (from the combination of antiquarks), a phenomenon known as *"CP violation"* ([20]). This was paradoxical because such combination processes were previously thought to be symmetrical. However, because of this *CP violation*, more matter was synthesized in the primordial universe and prevailed over antimatter.

The Russian physicist Andrei Sakharov was the first, starting in 1967, to restore a global symmetry, considering that the universe was not composed of a single entity but of two twin universes emanating from the same Big Bang singularity, having two opposing time arrows from the moment $t = 0$. The initial singularity Φ not only reverses time (*T-symmetry*) but also parity (*P-symmetry*, also called *"enantiomorphy"*) as well as charge conjugation (*C-symmetry*, which transforms a particle into its antiparticle, and vice versa), inducing complete *CPT-symmetry* ([69],[70],[71]). The *CP-symmetry* violation is also reversed in the twin universe, meaning that antimatter prevailed over

matter. It should be noted that Sakharov focused on describing *CPT-symmetry* only within the context of particle physics, thus without involving gravitation in his model, so that the twin universes never interact except at the moment of their birth as on the Figure 2.13:

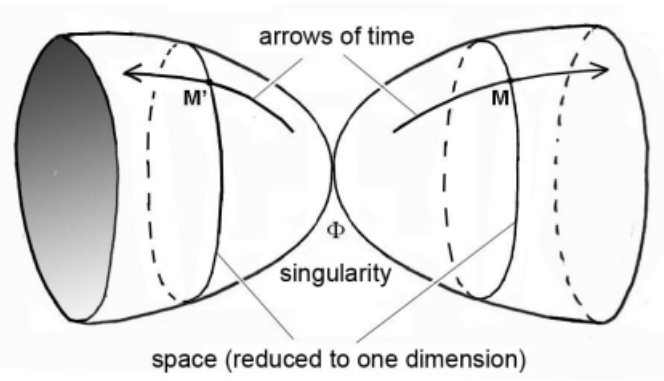

Figure 2.13: Sakharov Cosmological Model

2.5 Bimetric Approach Introduced by Hyperbolic Riemannian Geometry

Hyperbolic Riemannian geometry plays a crucial role in the Janus cosmological model. This branch of geometry studies curved spaces with a constant negative curvature. This geometry allows for the conceptualization of spaces with both positive and negative curvatures. However, it is important to note that currently, there is no bimetric or multimetric mathematical theory introduced in hyperbolic Riemannian geometry on which a bimetric cosmological model can be based. Indeed, current theoretical models remain heuristic. For example, two approaches were attempted in 2002 and 2008 by Thibauld Damour ([22]) and Sabine Hossenfelder ([37]), respectively. One was based on the introduction of heavy and light gravitons in a bimetric field equation system, and the other was more or less similar to our model. Indeed, Damour and Kogan attempt to construct a *"two-branes"* theory, involving a spectrum of massive gravitons, but this 40-page paper ends in a fishtail. In passing, they show that such bigravity must obey a system of two coupled field equations:

$$2M_L^2\left(R_{\mu\nu}(g^L)-\frac{1}{2}g^L_{\mu\nu}R(g^L)\right)+\Lambda_L g^L_{\mu\nu}=t^L_{\mu\nu}+T^L_{\mu\nu} \tag{2.5.1}$$

$$2M_R^2\left(R_{\mu\nu}(g^R)-\frac{1}{2}g^R_{\mu\nu}R(g^R)\right)+\Lambda_R g^R_{\mu\nu}=t^R_{\mu\nu}+T^R_{\mu\nu} \tag{2.5.2}$$

Then, Sabine Hossenfelder proposes a refined model addressing the concept of negative mass in the universe. However, in 1957, Hermann Bondi attempted to introduce

these masses into Albert Einstein's model. Nevertheless, the so-called runaway phenomenon reveals physical contradictions that the model violates, such as fundamental principles of physics like the principle of action-reaction and equivalence ([10]). Hossenfelder goes further to formulate a pair of new coupled field equations:

$$ {}^{(g)}R_{vk} - \frac{1}{2} g_{vk} {}^{(g)}R = T_{kv} - \underline{V} \sqrt{\frac{\underline{h}}{g}} a_{\underline{v}}^{v} a_{\underline{k}}^{k} \tag{2.5.3} $$

$$ {}^{(\underline{h})}R_{\underline{vk}} - \frac{1}{2} h_{\underline{vk}} {}^{(\underline{h})}R = \underline{T}_{\underline{vk}} - W \sqrt{\frac{g}{\underline{h}}} a_{\underline{k}}^{k} a_{\underline{v}}^{v} T_{kv} \tag{2.5.4} $$

Next, as she could not resolve the inconsistency with physical principles and believed it to be inextricably linked to *"bimetric gravity"*, she gave up.

The common point between these two approaches is that they are purely theoretical and have not provided any results validated by observations. The only credit that can be attributed to our cosmological model, compared to the previous two, is that it has many anchoring points with observation and several physical predictions that we'll see on the Section 3.2

Hyperbolic Riemannian geometry is a branch of Riemannian geometry that studies curved spaces with a constant negative curvature, mathematically corresponding to a hyperbolic shape often described as being *"saddle-shaped"*. More precisely, the constant negative curvature of hyperbolic space can be described as the asymptotic behavior of the hyperbola in both directions: the branches of the hyperbola diverge infinitely without ever converging. This characteristic is an important property of hyperbolic space and can be used to distinguish it from Euclidean geometry and spherical Riemannian geometry.

For example, on the Figure 2.14, the red lines drawing the triangles are the *geodesics* of the surface. Put simply, a *geodesic* is the shortest path between two points in space. Imagine you're in a flat Euclidean space, like on a large sheet of paper; here, this path is just a straight line. But on curved surfaces, whether they are positively curved (Spherical geometry) or negatively curved (Hyperbolic geometry like a horse's saddle), a *geodesic* can be drawn using a rope or an elastic stretched tight between two points on that surface, representing the shortest path. Thus, contrary to Euclidean geometry where the sum of the angles of a triangle equals 180 degrees, this sum exceeds 180 degrees in spherical (Riemannian) geometry and is less than 180 degrees in hyperbolic geometry (also a type of Riemannian geometry).

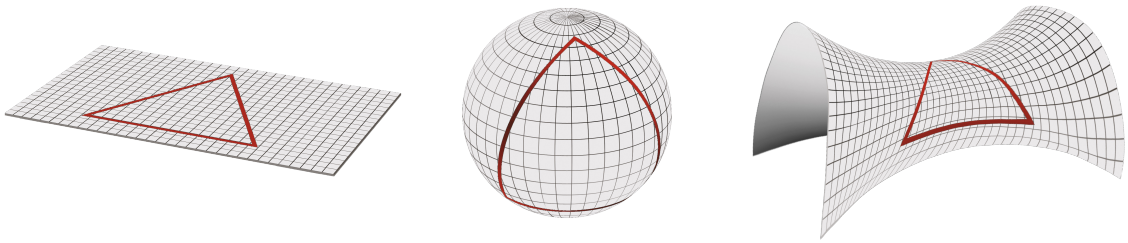

Figure 2.14: Types of Spatial Curvature

It's important to note that a *"flat"* Euclidean space[23], is not necessarily a flat plane. Take the earlier example of the sheet: even if it's bent several times, like corrugated iron, its curvature remains zero everywhere. This means that the *geodesic* traced on its surface don't change, because the sheet isn't stretching. The same goes for closed Euclidean surfaces like a cylinder or a cone: contrary to what one might think, they don't have any curvature. According to Euclidean geometry, although they appear curved, they can be considered *"flat"* because their surface can be unfolded into a plane without stretching.

The concept of the Janus Cosmological Model, which will be developed on the next chapter, is to associate it with a *"twin geometry"* defined by a relationship between spaces with positive curvature and spaces with negative curvature, according to a system of two coupled bimetric field equations.

[23]A space with zero curvature.

Chapter 3

Janus Cosmological Model

3.1 Description

The Janus Cosmological Model (JCM) proposes a revolutionary vision of the universe, characterized by a Riemannian manifold with two distinct metrics. These metrics manage positive and negative masses in a unique way, offering a coherent interpretation within the framework of general relativity, confirmed by observations, while avoiding traditional paradoxes.

Based on Andrei Sakharov's cosmological model of non-interacting twin bimetric universes, a new model has been developed as a unique universe consisting of a single Riemannian manifold with two metrics, namely a four-dimensional hypersurface with two layers folded onto each other in *CPT-Symmetry* but this time interacting through gravitational effect.

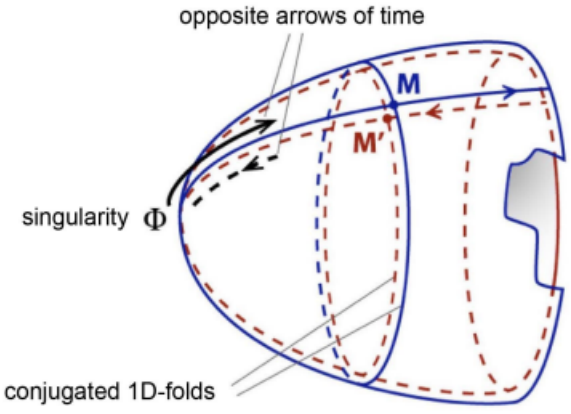

Figure 3.1: Janus Cosmological Model

The first layer is gridded with a certain unit of length providing a metric traversed by matter of positive energy and mass between two points of this spacetime at a speed c, limited by the theory of special relativity (Section 2.2.2). And its counterpart, folded on top but gridded according to a unit of length 100 times shorter and a speed 10 times higher for matter of negative energy and mass (the photons evolving in the same proportions), resulting in a traversal time 1000 times faster. This model thus provides two families of geodesics traversing spacetime in two different ways and at different speeds making interstellar travel possible, and explaining several physical phenomena such as the missing primordial antimatter as well as the confinement of galaxies ([54],[58],[57]).

It also demonstrates that negative energy states are compatible with quantum mechanics.

This model is built on two coupled field equations that is an extension of Einstein's field equation, offering a credible alternative to the presence of dark energy (repulsive power) and dark matter (flattening of galactic rotation curves) in the cosmos while successfully integrating negative masses into General Relativity.

It's based on the derivation of equations from a concept called the "*Lagrangian*". In physics, we often use principles to explain how objects or particles move and interact with each other. In our case, we employ principles of variation, which are mathematical formulas that describe how a physical system evolves over time by minimizing a specific quantity called "*action*". This concept of variation must be "*covariant*", meaning it remains the same regardless of the chosen inertial reference frame. This implies that it applies to all observers, regardless of their velocity.

The logical derivation from these principles should lead us to equations that describe the motions and interactions of a system of particles in a way that makes them valid for all observers, regardless of their relative motion. The "*Action*" is defined as the integral of the "*Lagrangian*" over a certain period of time, enabling us to describe the kinetics and dynamics of a physical system. The "*Lagrangian*" is a function computed from the kinetic and potential energy of the system, as well as other factors that may influence its behavior. By using the principle of least action, we seek to find the system's trajectory that minimizes "*action*", meaning the path for which the "*action's*" value is as low as possible. The equations of motion are obtained by differentiating this minimal action trajectory with respect to time.

3.2 Implications

Cosmology is in crisis. Indeed, the first example is the rate of expansion of the Universe, which, like a gigantic balloon, has been inflating for 13.8 billion years. When astrophysicists measured the current rate of this expansion with their telescopes, known as the Hubble constant (or H_0), they found a value incompatible with that predicted by

the standard model of cosmology (the ΛCDM model), the theory that best describes the history of the Universe for the time being, from its origin (the Big Bang) and the first atoms to today, including the first stars and galaxies.

The Hubble constant (H_0) is a key parameter in cosmology that measures the rate of expansion of the Universe. It indicates how fast galaxies are moving away from each other as a function of their distance. However, recently, two main methods of measurement have yielded significantly different results:

- On the one hand, local measurements using direct observation of galaxies and the cosmic distance scale based on standard candles such as Cepheids and Type Ia supernovae give a value of H_0 of 73 km/s/Mpc[1]. This measurement comes from the Shoes collaboration led by American Adam Riess.

- On the other hand, data from the Cosmic Microwave Background[2], analyzed within the framework of the standard model of cosmology, suggest a lower value, of 67.4 kilometers per second per megaparsec (km/s/Mpc). This method relies on data from the Planck satellite.

This divergence, if not attributable to measurement errors, necessitates a reevaluation of some fundamental aspects of the standard model, such as the role of dark energy in the acceleration of cosmic expansion. The Janus Cosmological Model attributes this anti-gravitational effect to negative masses and specifies its nature, a subject that we will study into later in the dedicated section 3.3.

Another example is the James Webb Space Telescope (JWST), with its advanced infrared observation capabilities, which is designed to observe the Universe at very early stages of its evolution, including the formation of the first galaxies. Recent observations from the JWST reveal objects or behaviors that do not match the predictions of the standard model, leading to a complete revision of its foundations.

Indeed, according to the standard model of cosmology, the universe experienced a dark period after the Big Bang, followed by the formation of the first stars and proto-galaxies a few hundred million years later. These initial structures evolved into large galaxies over the first billion years, a process driven by the gravity of dark matter. Galaxies continued to develop and cluster over billions of years, forming the various types observed today.

[1] One megaparsec is approximately equivalent to 3.26 million light-years. For every megaparsec of distance, the expansion of the Universe increases the speed of separation of galaxies by 73 kilometers per second.

[2] The Cosmic Microwave Background (CMB) is the electromagnetic radiation emitted about 380,000 years after the Big Bang, when the universe had cooled enough for electrons and protons to combine into atoms.

Dark matter and dark energy are thought to play crucial roles in this process, influencing the formation of structures and the expansion of the universe, respectively.

Moreover, a recent study published in *Nature Astronomy* [12] discusses the discovery by Mike Boylan-Kolchin, associate professor of astronomy at the University of Texas at Austin, of several galaxies forming earlier than expected at high redshifts (between 500 and 700 million years after the Big Bang), which are much more massive than ours (10 billion solar masses).

For example, *Abell 2744 Y1* is a galaxy cluster located in the Sculptor constellation at a distance of approximately 13.2 billion light-years away, and thus, it appears to us as it was when the universe was only 650 million years old (Figure 3.2).

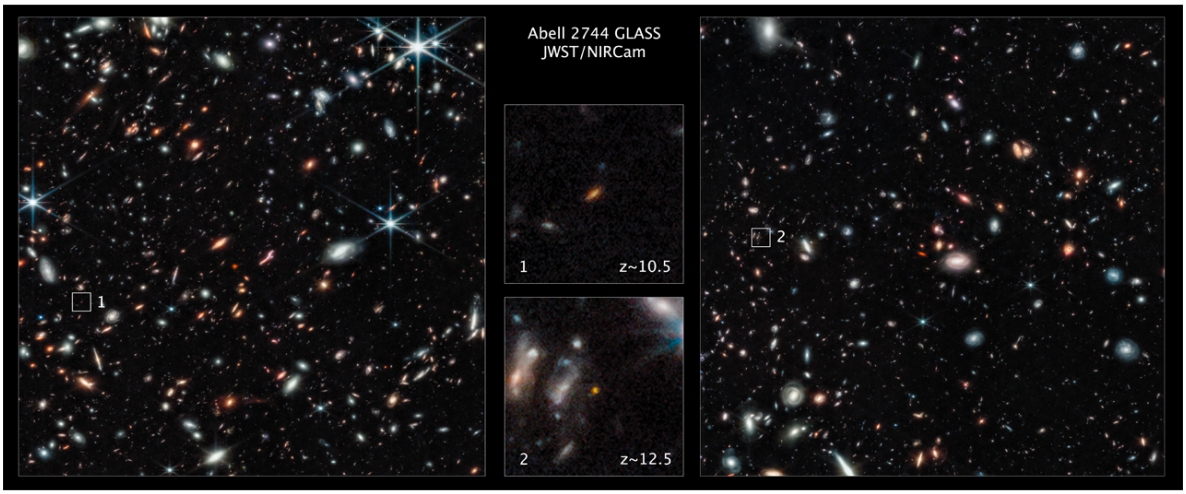

Figure 3.2: James Webb Space Telescope Image - Abell 2744 Y1

This observation from the James Webb Space Telescope once again confirms one of the predictions of the Janus Cosmological Model.

The Janus Cosmological Model therefore sheds new light on key cosmological questions, the answers to which are confirmed by numerous observations and predictions, of which here is a non-exhaustive list:

- Explanation of the confinement of galaxies by lacunar spaces occupied by negative masses contributing to their stability.

- Explanation of the shape of galaxy rotation curves (flattening)

- This model explains the greater-than-expected gravitational acceleration of stars orbiting at the outskirts of galaxies due to the presence of negative masses.

- Explanation for the high velocity of galaxies within clusters due to the anti-gravitational contribution of negative masses.

- It provides a mathematically detailed description of the behavior of galaxies, relying on a common approach to Vlasov and Poisson equations. It predicts that the velocities of stars within a galaxy organize themselves into an ellipsoid oriented toward the galactic center, an assumption confirmed by the measurement of residual velocities of stars near the solar system (Chapter 4).

- It explains the gravitational lensing effects around galaxies as on 3.3.

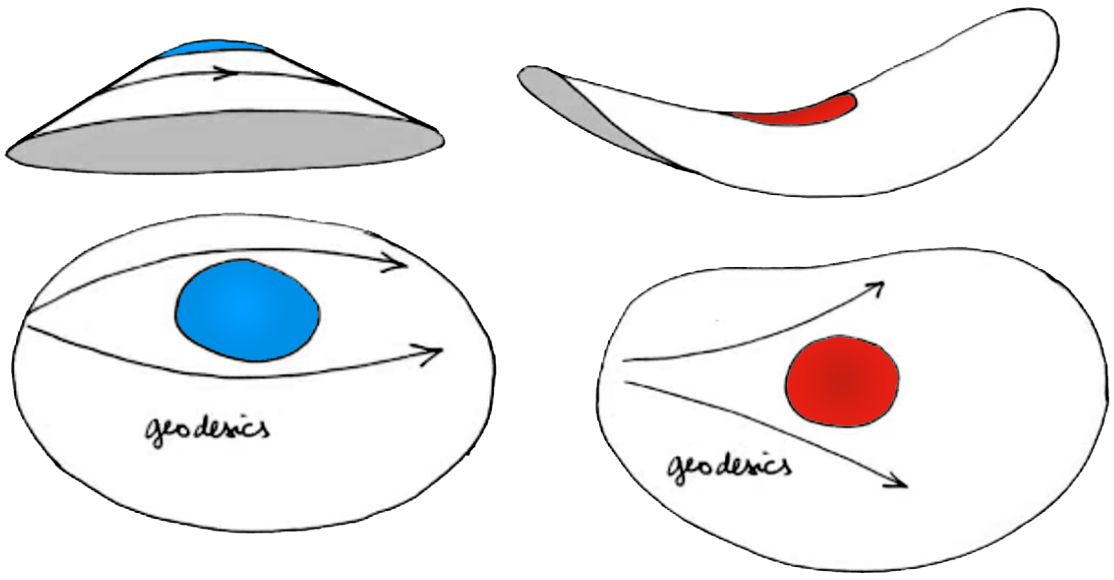

Figure 3.3: Gravitational lensing effects

- Explanation of the void-like structure of the universe occupied by clusters of negative masses in the form of interconnected soap bubbles as on 3.4.

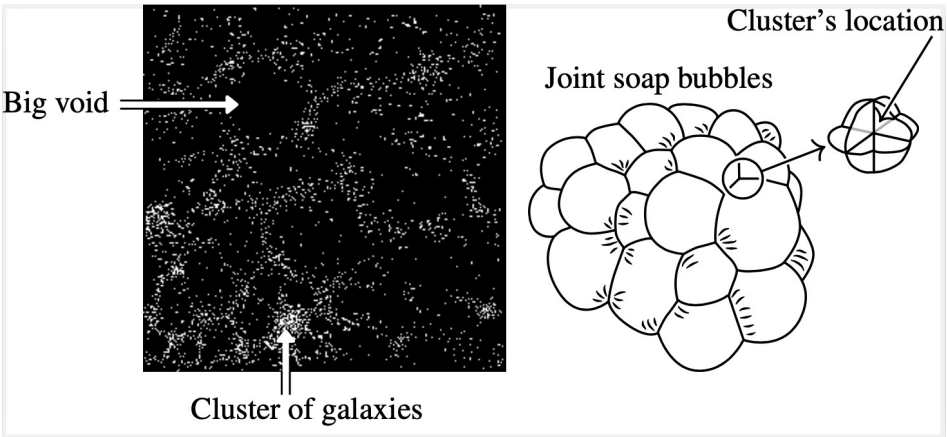

Figure 3.4: Lacunar structure

This structure was also established in 2018 by Tsvi Piran in his article [66], where he highlights the distribution of galaxies in what he refers to as *"walls"* due to the anti-gravitational compression of underdense regions of negative masses concentrated within the dark matter of empty spaces. Observations show that these empty spaces occupy a significant portion of the Universe's volume. The correlation between voids in the distribution of galaxies and regions of low dark matter density clearly demonstrates the gravitational origin of these voids. The primordial underdense regions, known as *"negative cosmological voids"*, act as gravitational negative masses and serve as the seeds for the observed voids. The centers of these underdense regions are effective gravitational masses that repel matter, aligning it along the walls between the centers. Voids are centered around these masses and are surrounded by walls of galaxies. Eventually, the walls crack, causing the void spaces to merge with other voids, creating a larger network of voids that confines galaxies within.

- Prediction and confirmation of the early formation of all galaxies recently observed by the James Webb Space Telescope ([28]). Indeed, the model suggests that all galaxies formed together during the first 100 million years of the universe's history (primordial). This formation occurred when positive mass was violently compressed between multiple clusters of negative masses, creating high pressure. The strong contraction of matter and gases due to the anti-gravitational effect of negative masses induced significant heating, leading to rapid cooling facilitated by a sheet-like structure. This cooling time allowed the attainment of a sufficient temperature to initiate thermonuclear fusion reactions, thus enabling the first stars to be born and gather to form the galaxies we know today.

- Explanation of distant galaxies with a high redshift (> 7) appearing as dwarfs (reduced luminosity). Indeed, clusters of negative masses (as in the region of the

Dipole Repeller that we will study in the Section 3.3) create a negative gravitational lensing effect on their photons, which has the effect of attenuating their brightness.

- Local relativistic verifications confirmed, such as the advance of Mercury's perihelion or the deflection of light rays by the Sun. Indeed, since both types of masses repel each other and considering that the density of negative mass is nearly negligible in the vicinity of the Sun, the first equation of the system corresponds to Einstein's field equation (see the Section 3.3.4).

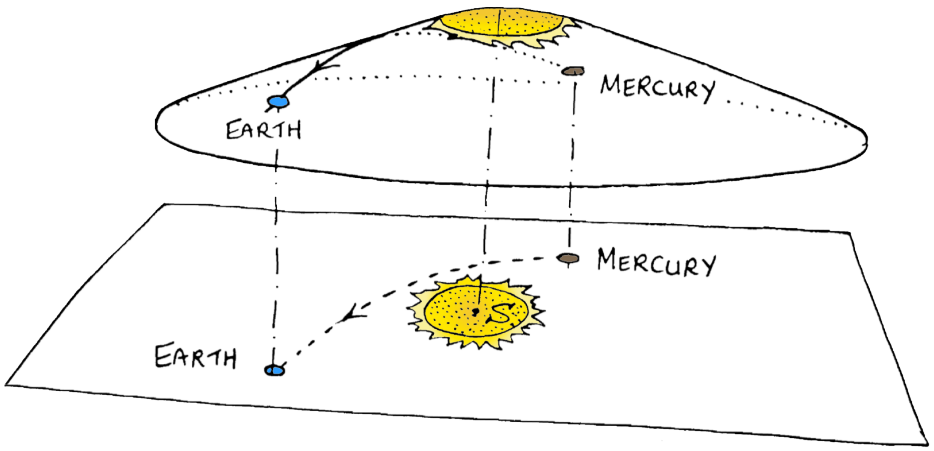

Figure 3.5: Space-Time Warping Induced by the Sun's Mass

- Exploiting the asymmetry between the two populations of positive and negative masses has led to consistency with the data from observations of type Ia supernovae. The observation of type Ia supernovae has been a crucial tool for determining the distances of celestial objects and studying the universe's expansion. Type Ia supernovae are supernova explosions that occur in binary stellar systems where a star known as a white dwarf absorbs matter from a companion star until it reaches a critical mass, causing an explosion. This asymmetry could be caused by processes such as the rotation or magnetic field of the companion star, which transfers matter to the white dwarf. If the asymmetry exists, it could result in a difference in brightness between type Ia supernovae, which could explain the observations.

- Explanation of the nature of the Great Repeller discovered in January 2017 (see the Section 3.3), where it was shown to exist in an apparently empty region of the universe, opposite to that of the Shapley Attractor, which appeared to repel all matter.

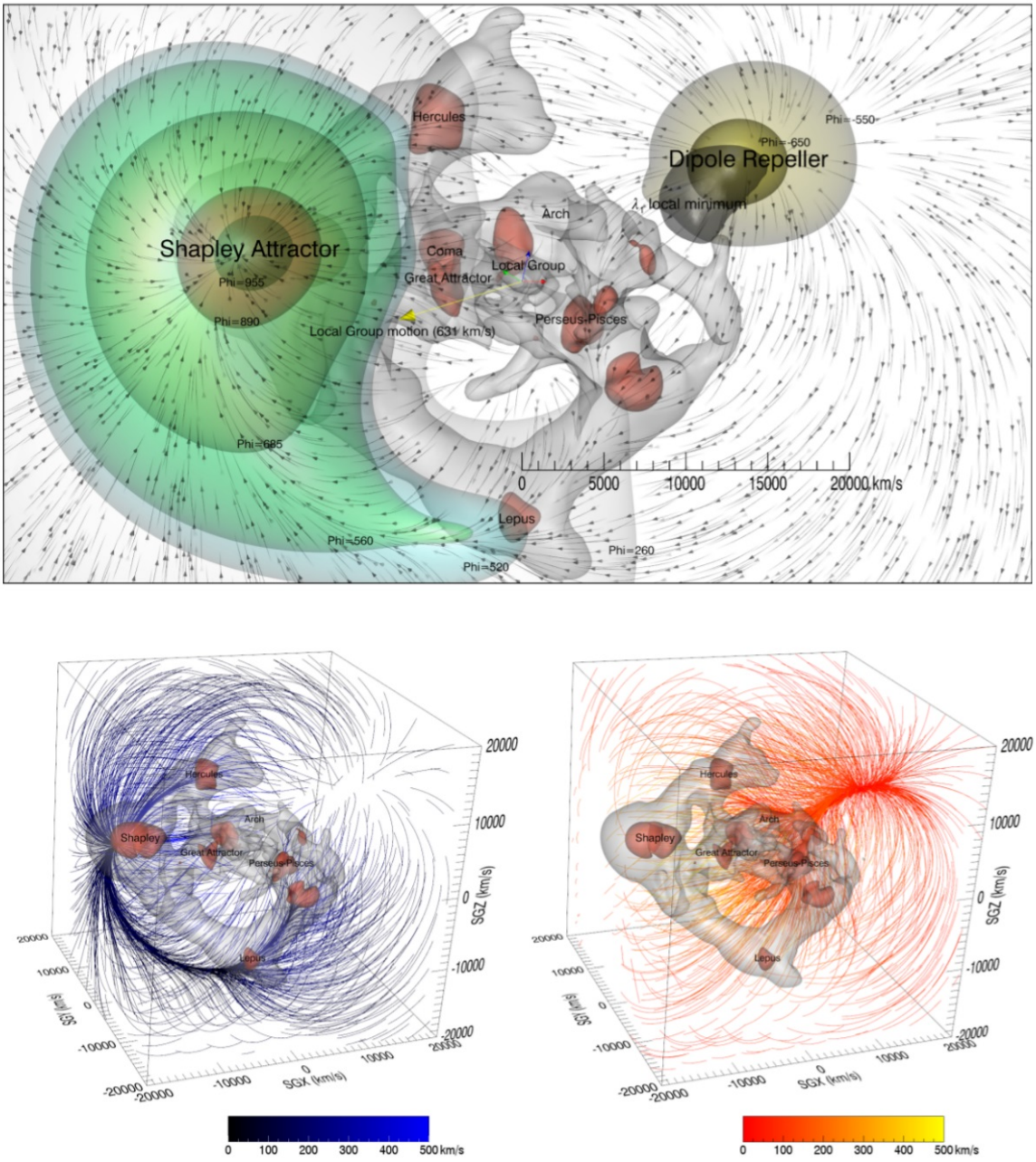

Figure 3.6: The great repeller from [36]. The figure shows the location of the Dipole Repeller (highlighted by the red circle) within the large-scale structure of the universe. The Dipole Repeller is a hypothesized region of space where galaxies are pushed away from, counteracting the attractive force of the Shapley Supercluster.

- The model highlights a sustainable galactic spiral structure model ensured by dynamic friction that continuously transfers momentum to the less dense environment of negative mass, allowing the spiral arms to persistently and stably revolve around the galaxy.

As depicted on next figures 3.7 and 3.8, when the arms traverse regions of high density (positive masses), they slow down and lose energy, whereas when they pass through low-density regions, they accelerate and gain energy. This creates density waves that propagate through the galaxy, transferring momentum to the negative mass environment.

In the context of the Standard Model, the rotation and spiral arms of galaxies are primarily explained by gravity and differential rotation, where density waves form and act as compression zones. These allow stars and interstellar gas orbiting around the galaxy's center to pass through them. These compression zones can trigger the formation of stars by compressing interstellar gas, contributing to the appearance of bright spiral arms.

In the Janus model, spiral galaxies also form through exchange with their external environment, consisting of negative masses that confine them. It is important to note that for these waves to imprint a lasting spiral rotation on a galaxy, they must interact with the waves of another medium.

Currently, scientists study the spiral structures of galaxies in the same way they would analyze sea wave motion, without considering their interactions with the wind. Indeed, if we set aside various other factors like water depth, seabed topography, the strength and direction of the wind, etc., when wind blows over the surface of the water, it generates ripples on the surface, thus creating wave propagation through the water. These ripples are essentially surface waves, also known as gravity waves. They propagate on the water's surface due to the gravity and surface tension of the liquid. When the wind blows over the water, it transfers kinetic energy to the water's surface, thereby creating surface waves. This transfer of energy implies an exchange of waves. Surface waves result from this interaction between the wind and the water's surface.

Another example to illustrate would be the spiral of cream in a coffee, created by stirring with a spoon. This spiral is induced by its interaction with the cup. Without the cup, there would be no spiral.

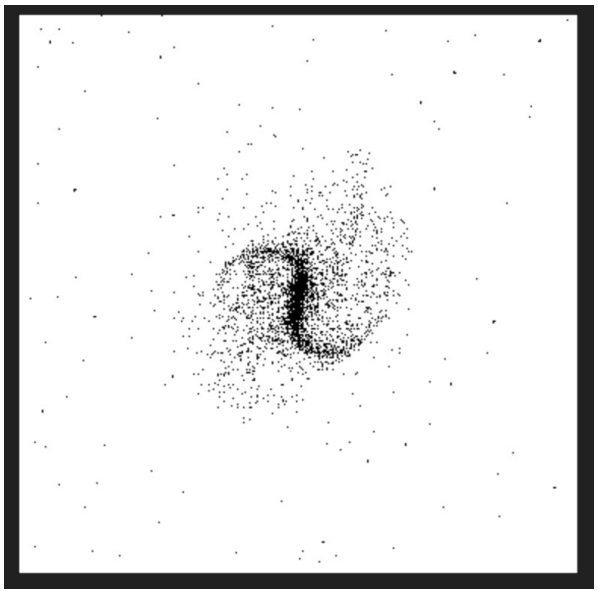

Figure 3.7: Barred spiral from a numerical simulation (1992: 20,000 points)

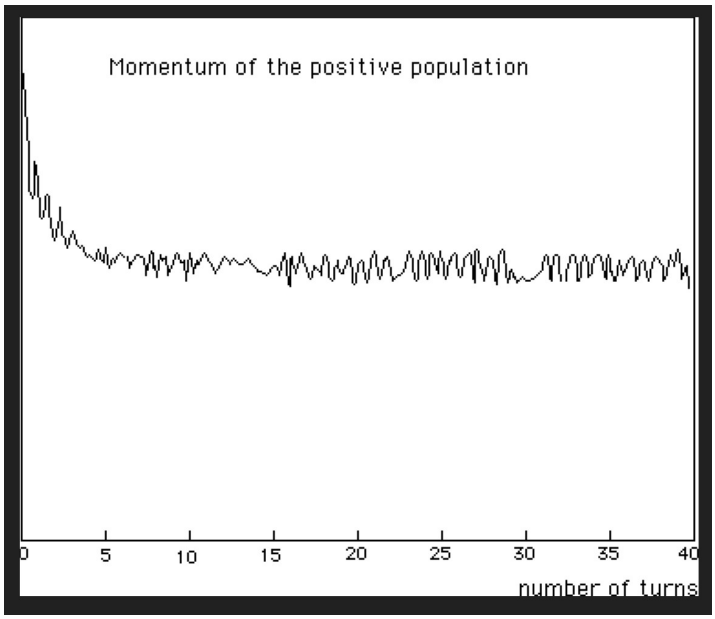

Figure 3.8: Evolution of the kinetic moment (1992: 20,000 points)

- Explanation for the lack of observation of cosmic antimatter, as it emits photons with negative energy.

- Explanation of the nature of the invisible components of the universe: antiprotons, antineutrons, antielectrons, antihydrogen, and antihelium with negative mass. These elements make up the primordial antimatter, eluding observation as they emit photons with negative energy.
- **Conjecture confirmed recently on September 2023 [5]**: C-symmetric antimatter (charge symmetry), developed in the laboratory and emitting photons of positive energy, is gravitationally pushed downwards just like ordinary matter.
- The model offers its own interpretation of the Cosmic Microwave Background fluctuations by attributing them to the response of ordinary matter with positive mass to density fluctuations in adjacent universe cells populated by a distribution of negative mass matter. This situation is linked to the gravitational instability that manifests within these cells. The analysis of these fluctuations serves as a means to evaluate the ratio between the scale factors of the two types of matter. It is observed that the ratio $\frac{a(+)}{a(-)}$ is of the order of 100. Consequently, it can be deduced that the ratio $\frac{c(-)}{c(+)}$ is of the order of 10 ([57]). This implies that the overall effect would be to reduce the required time for interstellar travel by a factor of a thousand for objects that succeed in reversing their mass, thereby enabling them to move along the geodesics described by the metric $h_{\mu\nu}$ of the second field equation 3.3.36, as we will study in the following section.

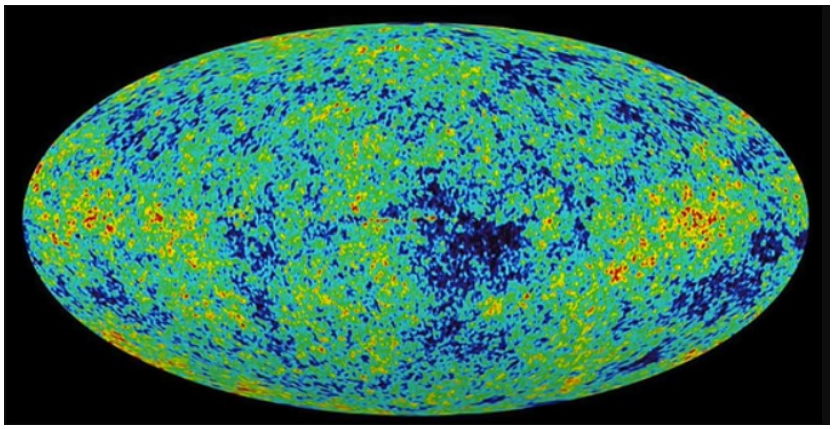

Figure 3.9: Cosmic Microwave Background (Source : Wikipedia)

- Gravitational redshift of 3 deduced from the first two images of supermassive objects located at the centers of galaxies M87 and the Milky Way (See the study conducted in the section 8).
- There is currently no answer to the question: *"What was it before the Big Bang?"* According to the Janus Cosmological Model, a topological structure of the universe, *"interacting with its anti-chronal counterpart"*, eliminates this questioning

by invalidating the meaning of the adverb *"before"*. Indeed, as we'll see in chapter 7, at the moment of the Big Bang, the arrow of time reverses.

3.3 The Dipole Repeller

3.3.1 Introduction

In 2017, Yehudi Hoffman, B. Tully, H. Courtois, and D. Pomarède published the first highly detailed map of the universe [36]. This map was not only based on the positions of galaxies but also incorporated their velocity field by subtracting the influence of the Hubble expansion from the raw measurements of their redshift. The results were incredibly impressive and are considered among the most significant observational discoveries in cosmology today, comparable in importance to Edwin Hubble's discovery a century ago. Prior to this study, it was known that certain galaxies exhibited convergent motions towards a region known as the Great Attractor. The 2017 analysis revealed the influence of another, larger structure located beyond the Great Attractor, named the Shapley Attractor. However, the most remarkable finding was the identification of a region nearly opposite to these two formations, where no galaxies were detected. Instead, there was a significant void surrounded by neighboring galaxies exhibiting a motion away from this region, forming a *"flight"* pattern centered on this void. Initially called the Dipole Repeller, it was later named the Dipole Attractor when it was understood to be connected to the attractive formations. Understanding this phenomenon, which cannot be attributed to measurement artifacts, undoubtedly requires significant progress in our understanding of cosmic dynamics.

3.3.2 Some Attempts at Interpretation

Four years after the initial discovery, there have been few attempts to model the phenomenon of the dipole repeller. In his recent article [47], Neiser does not focus on this question but instead proposes hypotheses about the nature of the Big Bang, the quantum vacuum, and the origin of the universe. Neiser speculates that antimatter could have a repulsive gravitational effect, leading to the formation of neutrino stars and antineutrino stars that repel each other. Similar repulsive aspects of primordial antimatter are mentioned by Benoit-Lévy et al. in 2012 ([7]), but without further justification. Heald in his article [34] mentions the situation of Laniakea, which is pushed by the dipole repeller and pulled by the Shapley Attractor. Again, the idea of a repulsion between matter and antimatter is suggested as a possible explanation for the large-scale structure of the universe and the organization of voids. However, no concrete model is given for the center object in the great void, and the lack of emitted light remains unexplained. In 2018, Hoffman et al. used numerical simulations to reconstruct a dark matter distribution consistent with observational data [35]. They suggest the existence of a bias (or discrepancy) in the dark matter distribution compared to the distribution of galaxy luminosity. Observations have revealed that the expansion of the universe

is accelerating, indicating the presence of a component with negative pressure ([52], [68], [73]). One model proposed to explain this phenomenon suggests the existence of negative masses that could contribute to these antigravitational effects, combining the repulsive influences of dark matter and dark energy on positive mass components. This hypothesis is at the center of the works corresponding to the references [56] [58] [59] [62] [63] [60] [61].

3.3.3 Interpretation through Dark Matter Voids

Let's study the possibility that a void in dark matter could produce the observed repulsive effect. We can begin by considering a spherical void within a uniform distribution of dark matter and use the Poisson equation to analyze this system:

$$\frac{\mathrm{d}^2\Psi}{\mathrm{d}r^2} + \frac{2}{r}\frac{\mathrm{d}\Psi}{\mathrm{d}r} = 4\pi G\rho_{\mathrm{dm}} \tag{3.3.1}$$

This equation is linear and describes the gravitational potential as a function of density. By superimposing two density distributions ρ_1 and ρ_2, the resulting gravitational potential is the sum of the potentials associated with these two distributions: $\Psi = \Psi_1 + \Psi_2$.

Considering a uniform density distribution $\rho_{\mathrm{dm}}^{\mathrm{unif}}$, we obtain a potential Ψ_1, which is the solution of the Poisson equation 3.3.1:

$$\Psi_1 = \frac{4\pi G\rho_{\mathrm{dm}}^{\mathrm{unif}} r^2}{3} \quad \text{et} \quad \vec{g}_1 = -\frac{8\pi G\rho_{\mathrm{dm}}^{\mathrm{unif}}}{3}\vec{r} \tag{3.3.2}$$

Now, by introducing a volume with an opposite density equal to $-\rho_{\mathrm{dm}}^{\mathrm{unif}}$, we create a potential Ψ_2, which is the solution of the following Poisson equation:

$$\frac{\mathrm{d}^2\Psi_2}{\mathrm{d}r^2} + \frac{2}{r}\frac{\mathrm{d}\Psi_2}{\mathrm{d}r} = -4\pi G\rho_{\mathrm{dm}}^{\mathrm{unif}} \tag{3.3.3}$$

This solution is:

$$\Psi_2 = -\frac{4\pi G\rho_{\mathrm{dm}}^{\mathrm{unif}} r^2}{3}, \quad \vec{g}_2 = \frac{8\pi G\rho_{\mathrm{dm}}^{\mathrm{unif}}}{3}\vec{r} \tag{3.3.4}$$

Thus, we obtain the same gravitational field but with opposite sign. It's therefore repulsive and proportional to the distance from the center of the sphere.

Next, by calculating the gravitational potentials associated with these two distributions, we can observe that the resulting gravitational potential is zero inside the void. In other words, the gravitational force exerted by the uniform distribution of dark matter is exactly counterbalanced by the gravitational force exerted by the opposite density creating the void:

$$\vec{g} = \vec{g}_1 + \vec{g}_2 \tag{3.3.5}$$

However, regardless of the chosen position as the origin of coordinates, the gravitational field remains nonzero inside the void. This means that the gravitational force

is not perfectly balanced, which seems contradictory to the idea of a void creating a repulsive gravitational field.

To solve this paradox, the Poisson equation must be considered as the linearized version of the Einstein equation in a stationary situation, which defines the gravitational potential in terms of a perturbation of the Lorentz metric:

$$g_{\mu\nu} = \eta_{\mu\nu} + \varepsilon\gamma_{\mu\nu} \tag{3.3.6}$$

The classical calculation gives for proper-density ρ_0 ([1]):

$$\varepsilon \sum_{i=0}^{3} \gamma_{00|i|i} = -\chi\rho_0 \tag{3.3.7}$$

NB: In the context of the weak field limit as studied in the Section 2.3.7, the equation 3.3.7 relates the second spatial derivatives of the time component γ_{00} of the metric tensor to gravitational sources, represented by the local mass-energy density ρ_0. It helps us understand how the curvature of space-time responds to the distribution of mass-energy, while maintaining a precise relationship between these two aspects.

Thus, the gravitational potential is defined as 2.3.112 by:

$$\Psi = -\frac{c^2}{2}\varepsilon\gamma_{00} \tag{3.3.8}$$

Then, 3.3.7 can be identified with the Poisson equation. However, this approach cannot be applied to an infinite uniform distribution of dark matter. The conclusion is that it is simply impossible to define a gravitational potential within a uniform matter distribution. Consequently, the problem of the existence of large voids in the large-scale structure of the universe remains unresolved, as gravitational instability tends to lead to the formation of clusters, not voids, and there is no clear framework for the formation of such voids.

3.3.4 Interpretation through the Janus Cosmological Model

Let's now consider the interaction between two entities: ordinary matter with positive mass interacting with negative mass through gravitational effects. This model involving negative mass takes into account the influence of both dark matter and dark energy.

We can describe this system of two entities with respective metrics $g_{\mu\nu}$ and $h_{\mu\nu}$. Let G and H be the corresponding Ricci scalars. We then consider the following two-layers action[3]:

$$A = \int_{\mathscr{E}} \left(\frac{1}{2\Gamma^{(g)}} G + S_{(g)} + S_{(h,g)} \right) \sqrt{|g|}\, \mathrm{d}^4x + \int_{\mathscr{E}} \left(\frac{\kappa}{2\Gamma^{(h)}} H + S_{(h)} + S_{(g,h)} \right) \sqrt{|h|}\, \mathrm{d}^4x \tag{3.3.9}$$

[3]Integration over $\mathscr{E}$ using the element d^4x is a method for calculating the total action in bimetric spacetime, reflecting the four-dimensional nature of this bimetric universe. This implies considering the

The terms $S_{(g)}$ and $S_{(h)}$ will yield the source terms related to the populations of the two entities, while the terms $S_{(h,g)}$ and $S_{(g,h)}$ will generate the interaction tensors. $\Gamma^{(g)}$ and $\Gamma^{(h)}$ are the gravitational constants of Einstein for each entity. g and h are the determinants of the metrics $g_{\mu\nu}$ and $h_{\mu\nu}$. For $\kappa = \pm 1$, we apply the principle of least action. The Lagrangian derivation of this action gives us:

$$\begin{aligned}
0 &= \delta A \\
&= \int_{\mathscr{E}} \delta \left(\frac{1}{2\Gamma^{(g)}} G + S_{(g)} + S_{(h,g)} \right) \sqrt{|g|}\, \mathrm{d}^4x + \int_{\mathscr{E}} \delta \left(\frac{\kappa}{2\Gamma^{(h)}} H + S_{(h)} + S_{(g,h)} \right) \sqrt{|h|}\, \mathrm{d}^4x \\
&= \int_{\mathscr{E}} \delta \left[\frac{1}{2\Gamma^{(g)}} \left(\frac{\delta G}{\delta g^{\mu\nu}} + \frac{G}{\sqrt{|g|}} \frac{\delta \sqrt{|g|}}{\delta g^{\mu\nu}} \right) + \frac{1}{\sqrt{|g|}} \frac{\delta(\sqrt{|g|} S_{(g)})}{\delta g^{\mu\nu}} + \frac{1}{\sqrt{|g|}} \frac{\delta(\sqrt{|g|} S_{(h,g)})}{\delta g^{\mu\nu}} \right] \delta g^{\mu\nu} \sqrt{|g|}\, \mathrm{d}^4x \\
&\quad + \int_{\mathscr{E}} \delta \left[\frac{\kappa}{2\Gamma^{(h)}} \left(\frac{\delta H}{\delta h^{\mu\nu}} + \frac{H}{\sqrt{|h|}} \frac{\delta \sqrt{|h|}}{\delta h^{\mu\nu}} \right) + \frac{1}{\sqrt{|h|}} \frac{\delta(\sqrt{|h|} S_{(h)})}{\delta h^{\mu\nu}} + \frac{1}{\sqrt{|h|}} \frac{\delta(\sqrt{|h|} S_{(g,h)})}{\delta h^{\mu\nu}} \right] \delta h^{\mu\nu} \sqrt{|h|}\, \mathrm{d}^4x
\end{aligned} \tag{3.3.10}$$

For any variation $\delta g^{\mu\nu}$ and any variation $\delta h^{\mu\nu}$, we obtain locally:

$$\frac{1}{2\Gamma^{(g)}} \left(\frac{\delta G}{\delta g^{\mu\nu}} + \frac{G}{\sqrt{|g|}} \frac{\delta \sqrt{|g|}}{\delta g^{\mu\nu}} \right) + \frac{1}{\sqrt{|g|}} \frac{\delta(\sqrt{|g|} S_{(g)})}{\delta g^{\mu\nu}} + \frac{1}{\sqrt{|g|}} \frac{\delta(\sqrt{|g|} S_{(h,g)})}{\delta g^{\mu\nu}} = 0 \tag{3.3.11}$$

$$\frac{\kappa}{2\Gamma^{(h)}} \left(\frac{\delta H}{\delta h^{\mu\nu}} + \frac{H}{\sqrt{|h|}} \frac{\delta \sqrt{|h|}}{\delta h^{\mu\nu}} \right) + \frac{1}{\sqrt{|h|}} \frac{\delta(\sqrt{|h|} S_{(h)})}{\delta h^{\mu\nu}} + \frac{1}{\sqrt{|h|}} \frac{\delta(\sqrt{|h|} S_{(g,h)})}{\delta h^{\mu\nu}} = 0 \tag{3.3.12}$$

Let us introduce the following tensors:

$$T^{(g,g)}_{\mu\nu} = -\frac{2}{\sqrt{|g|}} \frac{\delta(\sqrt{|g|} S_{(g)})}{\delta g^{\mu\nu}} = -2 \frac{\delta S_{(g)}}{\delta g^{\mu\nu}} + g_{\mu\nu} S_{(g)} \tag{3.3.13}$$

$$T^{(h,h)}_{\mu\nu} = -\frac{2}{\sqrt{|h|}} \frac{\delta(\sqrt{|h|} S_{(h)})}{\delta h^{\mu\nu}} = -2 \frac{\delta S_{(h)}}{\delta h^{\mu\nu}} + h_{\mu\nu} S_{(h)} \tag{3.3.14}$$

$$T^{(h,g)}_{\mu\nu} = -\frac{2}{\sqrt{|h|}} \frac{\delta(\sqrt{|g|} S_{(h,g)})}{\delta g^{\mu\nu}} \tag{3.3.15}$$

$$T^{(g,h)}_{\mu\nu} = -\frac{2}{\sqrt{|g|}} \frac{\delta(\sqrt{|h|} S_{(g,h)})}{\delta h^{\mu\nu}} \tag{3.3.16}$$

Indeed, in general relativity, the covariant derivative is a way to generalize the notion of the partial derivative to curved spaces. Unlike an ordinary partial derivative, the covariant derivative accounts for the curvature of space-time.

entirety of spacetime as the domain of integration, integrating the contributions from every point to the action. The term d^4x represents an infinitesimal element of hypervolume in this bimetric spacetime, serving to *"measure"* each segment during integration. Hence, it is a multiple volume integral carried out over the four dimensions of spacetime, accumulating the contributions to the total action from each four-dimensional volume segment, corresponding to each metric.

Then, for a tensor $A^{\rho}_{\nu\sigma}$, its covariant derivative along an indice μ is given by the expression:

$$\nabla_{\mu} A^{\rho}_{\nu\sigma} = \partial_{\mu} A^{\rho}_{\nu\sigma} + \Gamma^{\rho}_{\mu\lambda} A^{\lambda}_{\nu\sigma} - \Gamma^{\lambda}_{\mu\nu} A^{\rho}_{\lambda\sigma} - \Gamma^{\lambda}_{\mu\sigma} A^{\rho}_{\nu\lambda} \tag{3.3.17}$$

So, we can deduce both expressions :

$$\nabla_{\mu} \delta\Gamma^{\rho}_{\nu\sigma} = \partial_{\mu} \delta\Gamma^{\rho}_{\nu\sigma} + \Gamma^{\rho}_{\mu\lambda} \delta\Gamma^{\lambda}_{\nu\sigma} - \Gamma^{\lambda}_{\mu\nu} \delta\Gamma^{\rho}_{\lambda\sigma} - \Gamma^{\lambda}_{\mu\sigma} \delta\Gamma^{\rho}_{\nu\lambda} \tag{3.3.18}$$

$$\nabla_{\nu} \delta\Gamma^{\rho}_{\mu\sigma} = \partial_{\nu} \delta\Gamma^{\rho}_{\mu\sigma} + \Gamma^{\rho}_{\nu\lambda} \delta\Gamma^{\lambda}_{\mu\sigma} - \Gamma^{\lambda}_{\nu\mu} \delta\Gamma^{\rho}_{\lambda\sigma} - \Gamma^{\lambda}_{\nu\sigma} \delta\Gamma^{\rho}_{\mu\lambda} \tag{3.3.19}$$

NB :

- 3.3.19 is obtained from 3.3.18 by simply swapping μ and ν
- The term $\partial_{\mu} A^{\rho}_{\nu\sigma}$ is the ordinary partial derivative of the tensor. If spacetime were flat (as in Newtonian physics), this would be enough to describe the variation of the tensor.
- The terms with the Christoffel symbols $\Gamma^{\rho}_{\mu\lambda}$, $\Gamma^{\lambda}_{\mu\nu}$, and $\Gamma^{\lambda}_{\mu\sigma}$ represent the correction due to the connection of space-time, which takes into account how space-time is curved. Indeed, in curved space, the connection (represented by the Christoffel symbols Γ) introduces a correction. This correction is necessary because the bases of the tangent space (the space in which the tensor lives) change from one point in spacetime to another. So, $\Gamma^{\rho}_{\mu\lambda} A^{\lambda}_{\nu\sigma}$ is the term that corrects for the change in the component $A^{\lambda}_{\nu\sigma}$ as we move in the μ direction for the upper indice ρ. $\Gamma^{\lambda}_{\mu\nu} A^{\rho}_{\lambda\sigma}$ and $\Gamma^{\lambda}_{\mu\sigma} A^{\rho}_{\nu\lambda}$ are terms that subtract the contribution due to the change in the lower indices ν and σ. These terms ensure that the covariant derivative respects the tensor transformation rules.

  In summary, the covariant derivative ∇_{μ} of a tensor is a combination of its ordinary partial derivative and terms that compensate for changes in spacetime geometry. It is constructed such that the derivative of the tensor is itself a tensor, which is not the case for the ordinary partial derivative.

Then, the Riemann tensor is related to the Christoffel symbols by the equation:

$$R^{\rho}{}_{\sigma\mu\nu} = \partial_{\mu} \Gamma^{\rho}_{\nu\sigma} - \partial_{\nu} \Gamma^{\rho}_{\mu\sigma} + \Gamma^{\rho}_{\mu\lambda} \Gamma^{\lambda}_{\nu\sigma} - \Gamma^{\rho}_{\nu\lambda} \Gamma^{\lambda}_{\mu\sigma} \tag{3.3.20}$$

NB: The Riemann tensor $R^{\rho}{}_{\sigma\mu\nu}$ is a mathematical quantity in general relativity that describes the intrinsic curvature of spacetime. It is defined by the difference between the partial derivatives of the Christoffel symbols and the sum of the products of the Christoffel symbols themselves. The term $\partial_{\mu} \Gamma^{\rho}_{\nu\sigma}$ is the partial derivative of the Christoffel symbol $\Gamma^{\rho}_{\nu\sigma}$ with respect to the coordinate x^{μ}. This term measures how the Christoffel symbol varies when moving in the μ direction. The term $\partial_{\nu} \Gamma^{\rho}_{\mu\sigma}$ is similar to the first term but with the partial derivative taken in a different direction, x^{ν}. The

terms $\Gamma^{\rho}_{\mu\lambda}\Gamma^{\lambda}_{\nu\sigma}$ and $\Gamma^{\rho}_{\nu\lambda}\Gamma^{\lambda}_{\mu\sigma}$ describe the product of two Christoffel symbols that represents the interaction between two spacetime connections. It measures how curvature in one direction influences curvature in another direction.

Then, we get:

$$\delta R^{\rho}{}_{\sigma\mu\nu} = \partial_{\mu}\delta\Gamma^{\rho}_{\nu\sigma} - \partial_{\nu}\delta\Gamma^{\rho}_{\mu\sigma} + \delta\Gamma^{\rho}_{\mu\lambda}\Gamma^{\lambda}_{\nu\sigma} + \Gamma^{\rho}_{\mu\lambda}\delta\Gamma^{\lambda}_{\nu\sigma} - \delta\Gamma^{\rho}_{\nu\lambda}\Gamma^{\lambda}_{\mu\sigma} - \Gamma^{\rho}_{\nu\lambda}\delta\Gamma^{\lambda}_{\mu\sigma} \tag{3.3.21}$$

Thus, we obtain :

$$\delta R^{\rho}{}_{\sigma\mu\nu} = \nabla_{\mu}\delta\Gamma^{\rho}_{\nu\sigma} - \nabla_{\nu}\delta\Gamma^{\rho}_{\mu\sigma} \tag{3.3.22}$$

By contracting the indices ρ and σ in the previous relation using the Einstein summation convention, which states that when an indice is repeated, there is an implicit summation over that indice, we can express the variation of the Ricci curvature tensor which meets the Palatini identity ([83],[50]):

$$\delta R_{\sigma\nu} = \delta R^{\rho}{}_{\sigma\rho\nu} = \nabla_{\rho}(\delta\Gamma^{\rho}_{\nu\sigma}) - \nabla_{\nu}(\delta\Gamma^{\rho}_{\rho\sigma}) \tag{3.3.23}$$

NB : In general relativity, the geometry of spacetime is described by a quantity called the metric tensor, denoted by $g_{\mu\nu}$. This tensor contains all the information about distances and angles in spacetime.

The Ricci scalar, denoted by R, is a measure of the curvature of spacetime at a point. It is computed by summing (or contracting) the components of the Ricci tensor $R_{\sigma\nu}$ with the metric tensor $g^{\sigma\nu}$. Mathematically, it is as if you were multiplying the matrices of the Ricci tensor and the metric tensor and then adding up the terms along the diagonal.

Plus, we must have the covariant derivative of the metric tensor equal to zero[4]. In other words, as you move through spacetime, the way you measure distances and angles does not change. This is a fundamental property of spacetime in general relativity that says the local geometry does not change as you move, regardless of the overall curvature.

In summary, the Ricci scalar R gives us an idea of how much spacetime is curved at a point, and the fact that $\nabla_{\sigma}g^{\mu\nu} = 0$ ensures that the shape of spacetime remains consistent as we move, regardless of the global curvature[5].

Next, we can deduce :

$$\begin{aligned}
\delta R &= R_{\sigma\nu}\delta g^{\sigma\nu} + g^{\sigma\nu}\delta R_{\sigma\nu} \\
&= R_{\sigma\nu}\delta g^{\sigma\nu} + g^{\sigma\nu}\left(\nabla_{\rho}(\delta\Gamma^{\rho}_{\nu\sigma}) - \nabla_{\nu}(\delta\Gamma^{\rho}_{\rho\sigma})\right) \\
&= R_{\sigma\nu}\delta g^{\sigma\nu} + \nabla_{\rho}\left(g^{\sigma\nu}\delta\Gamma^{\rho}_{\nu\sigma}\right) - g^{\sigma\nu}\nabla_{\nu}\delta\Gamma^{\rho}_{\rho\sigma} \\
&= R_{\sigma\nu}\delta g^{\sigma\nu} + \nabla_{\rho}(g^{\sigma\nu}\delta\Gamma^{\rho}_{\nu\sigma} - g^{\sigma\rho}\delta\Gamma^{\mu}_{\mu\sigma}) \\
&= R_{\sigma\nu}\delta g^{\sigma\nu} + \nabla_{\rho}B^{\rho}
\end{aligned} \tag{3.3.24}$$

[4] $\nabla_{\sigma}g^{\mu\nu} = 0$

[5] This consistency is ensured by the metric's compatibility with the Levi-Civita connection, which guarantees that geometric concepts such as lengths and angles remain constant when they are transported through spacetime.

NB : For the calculation above, we must consider two rules :

- The properties of the covariant derivative and the Leibniz rule (the product rule of differentiation). The Leibniz rule for the covariant derivative is similar to that of the ordinary derivative and is written as:

$$\nabla_\rho(AB) = (\nabla_\rho A)B + A(\nabla_\rho B)$$

  where A and B can be scalar, vector, or tensor fields.

- As noted before, repeated indices are referred to as *silent* or *dummy* indices according to the Einstein summation convention. Indeed, it is useful to recall that when an indice of a variable appears twice in a term, once in an upper position and once in a lower position, it implies summation over all possible values that the indice can take. For example, $A^\mu B_\mu$ implies $\sum_\mu A^\mu B_\mu$. Let's consider the Christoffel symbols $\Gamma^\mu_{\mu\sigma}$ and $\Gamma^\rho_{\rho\sigma}$. In these expressions, the indices μ and ρ are examples of dummy indices according to the Einstein summation convention. This means that the expression $\Gamma^\mu_{\mu\sigma}$, where the sum is taken over all possible values of μ, is identical to $\Gamma^\rho_{\rho\sigma}$, where the sum is taken over all possible values of ρ. Thus, we can apply the summation indices $(\rho, \nu) \to (\mu, \rho)$ in the last term.

By calculating in two different ways, we have:

$$\nabla_\mu(\sqrt{|g|}\delta B^\mu) = \nabla_\mu(\sqrt{|g|})B^\mu + \sqrt{|g|}\nabla_\mu(\delta B^\mu) = \sqrt{|g|}\nabla_\mu\delta B^\mu + 0 = \sqrt{|g|}\nabla_\mu\delta B^\mu \tag{3.3.25}$$

$$\nabla_\mu(\sqrt{|g|}\delta B^\mu) = \partial_\mu(\sqrt{|g|}\delta B^\mu) + \Gamma^\mu_{\mu\nu}\sqrt{|g|}\delta B^\nu = \partial_\mu(\sqrt{|g|}\delta B^\mu) + 0 = \partial_\mu(\sqrt{|g|}\delta B^\mu) \tag{3.3.26}$$

NB : Similarly, the derivative of the determinant of the metric tensor, represented as $\sqrt{|g|}$, is also zero when taken covariantly[6]. This latter property simplifies the expression of volume integrals and is fundamental to the application of the divergence theorem in curved spacetime.

Then ,we can deduce:

$$\sqrt{|g|}\nabla_\mu\delta B^\mu = \partial_\mu(\sqrt{|g|}\delta B^\mu) \tag{3.3.27}$$

Let's now consider the contribution of $\sqrt{|g|}\nabla_\mu\delta B^\mu$ in the action. Let n^μ be a unit vector normal to $\partial\mathscr{E}$, $\varepsilon = n^\mu n_\mu, y^a$ representing coordinates adapted to the boundary $\partial\mathscr{E}$, and h_{ab} representing the metric induced by g_{ab} on the boundary. We have $|\varepsilon| = 1$, and $\sqrt{|h|}\mathrm{d}^3y$ is an $(n-1)$-volume form on the boundary with $h = \det(h_{ab})$. By the Stokes' theorem, we have:

$$\int_{\mathscr{E}} \sqrt{|g|}\nabla_\mu\delta B^\mu\sqrt{-g}\mathrm{d}^4x = \int_{\mathscr{E}} \partial_\mu(\sqrt{|g|}\delta B^\mu)\mathrm{d}^4x \tag{3.3.28}$$

$$= \int_{\delta\mathscr{E}} \varepsilon\delta B^\mu n_\mu\sqrt{|h|}\mathrm{d}^3y \tag{3.3.29}$$

[6] $\nabla_\mu\sqrt{|g|} = 0$

We will assume that the metric does not vary at the boundary (or that there is no boundary). In this case, the term $\nabla_\mu \delta B^\mu \sqrt{-g}$ does not contribute to the action, so we have:

$$\frac{\delta R}{\delta g^{\mu\nu}} = R_{\mu\nu} + \frac{\nabla_\rho B^\rho}{\delta g^{\mu\nu}} \approx R_{\mu\nu} \tag{3.3.30}$$

However, from the corollary with $a = \frac{1}{2}$, we have:

$$\delta\sqrt{-g} = \frac{1}{2}\sqrt{-g} g^{\mu\nu} \delta g_{\mu\nu} = -\frac{1}{2}\sqrt{-g} g_{\mu\nu} \delta g^{\mu\nu} \tag{3.3.31}$$

So, we can deduce:

$$\frac{R\,\delta\sqrt{-g}}{\sqrt{-g}\,\delta g^{\mu\nu}} = -\frac{1}{2} g_{\mu\nu} R \tag{3.3.32}$$

NB : For the calculation above, we need to explain two things:

- The variation of the determinant of the metric tensor, denoted as δg, is related to the variation of the metric tensor itself, $\delta g_{\mu\nu}$, through the relationship $\delta g = g g^{\mu\nu} \delta g_{\mu\nu}$, where g is the determinant of the metric tensor and $g^{\mu\nu}$ is its inverse. This relationship arises from the mathematical property of determinants, where the derivative of a determinant can be expressed as the determinant multiplied by the trace of the product of the inverse of the matrix and the derivative of the matrix. In the case of a small variation, the variation of the square root of the negative determinant of the metric tensor, $\delta\sqrt{-g}$, is given by $\delta\sqrt{-g} = \frac{1}{2}\sqrt{-g} g^{\mu\nu} \delta g_{\mu\nu}$. This formula is pivotal in deriving the Einstein field equations from the Einstein-Hilbert action, as it allows for the integration of the action over the four-dimensional spacetime manifold.

- In our study, we utilize Stokes' theorem to simplify a crucial calculation. This theorem establishes an interesting relationship between the integral of a derivative of a vector field over a three-dimensional region and the integral of the same vector field along the boundary of that region.

  Let's consider a simple example: imagine a closed surface in space (like the surface of a sphere). If we want to calculate something within this surface (e.g., the sum of values of a field), Stokes' theorem allows us to do so by simply looking at what happens on the surface itself.

  The equation (3.3.28) we presented in our calculation follows this idea. It tells us that the integral of the derivative of a field ($\nabla_\mu \delta B^\mu$) over a four-dimensional region ($\mathscr{E}$) can be equivalent to the integral of the divergence of another field ($\sqrt{|g|}\delta B^\mu$) over the same region ($\mathscr{E}$). This equivalence is achieved through the metric and a four-dimensional volume element (d^4x).

  Next, equation (3.3.29) further simplifies the expression by bringing it to the boundary of the region ($\delta\mathscr{E}$). It shows us that this equivalence can be expressed as an integral along the boundary ($\delta\mathscr{E}$), using normal vectors (n_μ) to that boundary

and the induced metric on it ($\sqrt{|h|}\mathrm{d}^3y$). In other words, this equation allows us to understand what happens on the surface of our region without having to calculate what happens inside.

In summary, Stokes' theorem enables us to streamline our calculations by showing us how phenomena within a region can be understood by simply examining what happens on the boundary of that region. This mathematical trick is essential for solving those complex problems.

We obtain then from equations 3.3.15 and 3.3.16:

$$\sqrt{\frac{|h|}{|g|}}T^{(h,g)}_{\mu\nu} = \sqrt{\frac{|h|}{|g|}}\frac{-2}{\sqrt{|h|}}\frac{\delta(\sqrt{|g|}S_{(h,g)})}{\delta g^{\mu\nu}} = \frac{-2}{\sqrt{|g|}}\frac{\delta(\sqrt{|g|}S_{(h,g)})}{\sqrt{\delta g^{\mu\nu}}} = -2\frac{\delta S_{(h,g)}}{\delta g^{\mu\nu}} + g_{\mu\nu}S_{(h,g)} \tag{3.3.33}$$

$$\sqrt{\frac{|g|}{|h|}}T^{(g,h)}_{\mu\nu} = \sqrt{\frac{|g|}{|h|}}\frac{-2}{\sqrt{|g|}}\frac{\delta(\sqrt{|h|}S_{(g,h)})}{\delta h^{\mu\nu}} = \frac{-2}{\sqrt{|h|}}\frac{\delta(\sqrt{|h|}S_{(g,h)})}{\sqrt{\delta h^{\mu\nu}}} = -2\frac{\delta S_{(g,h)}}{\delta h^{\mu\nu}} + h_{\mu\nu}S_{(g,h)} \tag{3.3.34}$$

Introduced into 3.3.11 and 3.3.12, taking 3.3.30 into account, we can thus deduce the coupled field equations describing the system of the two entities:

$$R^{(g)}_{\mu\nu} - \frac{1}{2}g_{\mu\nu}G = \Gamma^{(g)}\left(T^{(g,g)}_{\mu\nu} + \sqrt{\frac{|h|}{|g|}}T^{(h,g)}_{\mu\nu}\right) \tag{3.3.35}$$

$$R^{(h)}_{\mu\nu} - \frac{1}{2}h_{\mu\nu}H = \kappa\Gamma^{(h)}\left(T^{(h,h)}_{\mu\nu} + \sqrt{\frac{|g|}{|h|}}T^{(g,h)}_{\mu\nu}\right) \tag{3.3.36}$$

Which $T^{(h,g)}_{\mu\nu}$ and $T^{(g,h)}_{\mu\nu}$ are the interaction tensors of the two entities system corresponding to the *"induced geometry"*, i.e., the way each matter distribution on one layer on the universe contributes to the geometry of the other[7]. This system must obey the Bianchi conditions, which are expressed by the following relationship:

$$\nabla^{(g)}_{\mu}T^{(h,g)}_{\mu\nu} = \nabla^{(h)}_{\mu}T^{(g,h)}_{\mu\nu} = 0 \tag{3.3.37}$$

Suppose the fluids within entities g and h are perfect, with energy densities corresponding to the following source tensors:

$$T^{(g,g)}_{\mu\nu} = \begin{pmatrix} \alpha^{(g)} & 0 & 0 & 0 \\ 0 & \beta^{(g)} & 0 & 0 \\ 0 & 0 & \beta^{(g)} & 0 \\ 0 & 0 & 0 & \beta^{(g)} \end{pmatrix}, T^{(h,h)}_{\mu\nu} = \begin{pmatrix} \alpha^{(h)} & 0 & 0 & 0 \\ 0 & \beta^{(h)} & 0 & 0 \\ 0 & 0 & \beta^{(h)} & 0 \\ 0 & 0 & 0 & \beta^{(h)} \end{pmatrix} \tag{3.3.38}$$

We will take $\{\alpha^{(g)} > 0, \beta^{(g)} > 0\}$ and $\{\alpha^{(h)} < 0, \beta^{(h)} < 0\}$. We will ensure that interaction laws are such that two particles belonging to the same entity attract each

[7]Interaction between populations of positive and negative masses.

other, while they repel each other when they belong to different entities. Let's introduce their interaction tensors:

$$T_{\mu\nu}^{(h,g)} = \begin{pmatrix} \alpha^{(h,g)} & 0 & 0 & 0 \\ 0 & \beta^{(h,g)} & 0 & 0 \\ 0 & 0 & \beta^{(h,g)} & 0 \\ 0 & 0 & 0 & \beta^{(h,g)} \end{pmatrix}, T_{\mu\nu}^{(g,h)} = \begin{pmatrix} \alpha^{(g,h)} & 0 & 0 & 0 \\ 0 & \beta^{(g,h)} & 0 & 0 \\ 0 & 0 & \beta^{(g,h)} & 0 \\ 0 & 0 & 0 & \beta^{(g,h)} \end{pmatrix} \tag{3.3.39}$$

To obtain the desired interaction laws under the Newtonian approximation, we must choose $\kappa = -1$. The system of equations then becomes:

$$R_{\mu\nu}^{(g)} - \frac{1}{2} g_{\mu\nu} G = \Gamma^{(g)} \left(T_{\mu\nu}^{(g,g)} + \sqrt{\frac{|h|}{|g|}} T_{\mu\nu}^{(h,g)} \right) = \Gamma^{(g)} \left(T_{\mu\nu}^{(g,g)} + \Phi T_{\mu\nu}^{(h,g)} \right) \tag{3.3.40}$$

$$R_{\mu\nu}^{(h)} - \frac{1}{2} h_{\mu\nu} H = -\Gamma^{(h)} \left(T_{\mu\nu}^{(h,h)} + \sqrt{\frac{|g|}{|h|}} T_{\mu\nu}^{(g,h)} \right) = -\Gamma^{(h)} \left(T_{\mu\nu}^{(h,h)} + \phi T_{\mu\nu}^{(g,h)} \right) \tag{3.3.41}$$

Verification for a non-steady, homogeneous and isotropic system

If we suppose that the bimetric universe, structured by the coupled field equations 3.3.40 and 3.3.41, is homogeneous and isotropic, the Robertson-Walker metric becomes, according to [1]:

$$(\mathrm{d}s^{(f)})^2 = (c^{(f)})^2 \mathrm{d}t^2 - (a^{(f)})^2 \left[\frac{\mathrm{d}r^2 + r^2(\mathrm{d}\theta^2 + \sin^2\theta \mathrm{d}\phi^2)}{(1 + k^{(f)} \frac{r^2}{4})^2} \right] \quad \text{where} \quad f \in \{g, h\} \tag{3.3.42}$$

Note that $a^{(f)}$ is the spatial scale factor, $k^{(f)}$, $c^{(f)}$, and $\Gamma^{(f)}$ are respectively the curvature indice, the speed of light, and the Einstein constant for each entity.

If we introduce these metrics into the system of equations 3.3.40 and 3.3.41 with pressures $p^{(g)} \approx 0$ and $p^{(h)} \approx 0$, we get the following classical system of equations:

$$\frac{3}{\left(c^{(g)}\right)^2 \left(a^{(g)}\right)^2} \left(\frac{\mathrm{d}a^{(g)}}{\mathrm{d}t} \right)^2 + \frac{3k^{(g)}}{(c^{(g)})^2 \left(a^{(g)}\right)^2} = -\Gamma^{(g)} \left[\rho^{(g)} \left(c^{(g)}\right)^2 + \Phi \rho^{(h)} \left(c^{(h)}\right)^2 \right] \tag{3.3.43}$$

$$\frac{2}{\left(c^{(g)}\right)^2 \left(a^{(g)}\right)^2} \frac{\mathrm{d}^2 a^{(g)}}{\mathrm{d}t^2} + \frac{1}{\left(c^{(g)}\right)^2 \left(a^{(g)}\right)^2} \left(\frac{\mathrm{d}a^{(g)}}{\mathrm{d}t} \right)^2 + \frac{k^{(g)}}{\left(c^{(g)}\right)^2 \left(a^{(g)}\right)^2} = 0 \tag{3.3.44}$$

$$\frac{3}{\left(c^{(h)}\right)^2 \left(a^{(h)}\right)^2} \left(\frac{\mathrm{d}a^{(h)}}{\mathrm{d}t} \right)^2 + \frac{3k^{(h)}}{\left(c^{(h)}\right)^2 \left(a^{(h)}\right)^2} = \Gamma^{(h)} \left[\phi \rho^{(g)} \left(c^{(g)}\right)^2 + \rho^{(h)} \left(c^{(h)}\right)^2 \right] \tag{3.3.45}$$

$$\frac{2}{\left(c^{(h)}\right)^2 \left(a^{(h)}\right)^2} \frac{\mathrm{d}^2 a^{(h)}}{\mathrm{d}t^2} + \frac{1}{\left(c^{(h)}\right)^2 \left(a^{(h)}\right)^2} \left(\frac{\mathrm{d}a^{(h)}}{\mathrm{d}t} \right)^2 + \frac{k^{(h)}}{\left(c^{(h)}\right)^2 \left(a^{(h)}\right)^2} = 0 \tag{3.3.46}$$

Applying classical mathematical methods by [1], the compatibility conditions of equations 3.3.43, 3.3.44, 3.3.45 and 3.3.46 gives:

$$3\frac{\mathrm{d}a^{(g)}}{a^{(g)}}+\frac{\mathrm{d}\left[\rho^{(g)}\left(c^{(g)}\right)^2+\Phi\rho^{(h)}\left(c^{(h)}\right)^2\right]}{\left[\rho^{(g)}\left(c^{(g)}\right)^2+\Phi\rho^{(h)}\left(c^{(h)}\right)^2\right]}=0 \tag{3.3.47}$$

$$3\frac{\mathrm{d}a^{(h)}}{a^{(h)}}+\frac{\mathrm{d}\left[\phi\rho^{(g)}\left(c^{(g)}\right)^2+\rho^{(h)}\left(c^{(h)}\right)^2\right]}{\left[\phi\rho^{(g)}\left(c^{(g)}\right)^2+\rho^{(h)}\left(c^{(h)}\right)^2\right]}=0 \tag{3.3.48}$$

So, the energy (and mass) is conserved for dust universe:

$$E=\rho^{(g)}\left(c^{(g)}\right)^2\left(a^{(g)}\right)^3+\rho^{(h)}\left(c^{(h)}\right)^2\left(a^{(h)}\right)^3 \tag{3.3.49}$$

If we have:

$$\Phi=\left(\frac{a^{(h)}}{a^{(g)}}\right)^3,\quad \phi=\left(\frac{a^{(g)}}{a^{(h)}}\right)^3,\quad \phi=\Phi^{-1} \tag{3.3.50}$$

The coupled field equations become:

$$R^{(g)}_{\mu\nu}-\frac{1}{2}g_{\mu\nu}G=\Gamma^{(g)}\left[T^{(g,g)}_{\mu\nu}+\left(\frac{a^{(h)}}{a^{(g)}}\right)^3T^{(h,g)}_{\mu\nu}\right] \tag{3.3.51}$$

$$R^{(h)}_{\mu\nu}-\frac{1}{2}h_{\mu\nu}H=-\Gamma^{(h)}\left[T^{(h,h)}_{\mu\nu}+\left(\frac{a^{(g)}}{a^{(h)}}\right)^3T^{(g,h)}_{\mu\nu}\right] \tag{3.3.52}$$

If both entities are dominated by radiation. The interaction tensor in mixed mode will be:

$$T^{\nu(f)}_{\mu}=\begin{pmatrix}\rho_r^{(f)}c^{(f)2} & 0 & 0 & 0\\ 0 & \frac{\rho_r^{(f)}c^{(f)2}}{3} & 0 & 0\\ 0 & 0 & \frac{\rho_r^{(f)}c^{(f)2}}{3} & 0\\ 0 & 0 & 0 & \frac{\rho_r^{(f)}c^{(f)2}}{3}\end{pmatrix}=\begin{pmatrix}\rho_r^{(f)}c^{(f)2} & 0 & 0 & 0\\ 0 & -p_r^{(f)} & 0 & 0\\ 0 & 0 & -p_r^{(f)} & 0\\ 0 & 0 & 0 & -p_r^{(f)}\end{pmatrix} \tag{3.3.53}$$

with

$$\begin{cases}\text{if } \rho_r^{(f)}>0 \text{ then } p_r^{(f)}>0 \text{ for } f=g\\ \text{if } \rho_r^{(f)}<0 \text{ then } p_r^{(f)}<0 \text{ for } f=h\end{cases}$$

NB:

- In a cosmological context, the energy-momentum tensor $T^{\nu(f)}_{\mu}$ is used to describe the distribution and interaction of matter and energy within the universe. For a specific field f, the temporal component $T^{0(f)}_{0}$ denotes the energy density, which is a primary determinant of space-time curvature. The spatial components $T^{i(f)}_{i}$,

on the other hand, represent the pressure exerted in spatial directions, also influencing the structure of space-time. In a bimetric model, where two distinct fields i.e., one for each layer of the universe, are considered, the associated conditions describe the relationships between the energy densities and pressures for each field, reflecting how these entities interact and collectively influence cosmic dynamics.

- The energy-momentum tensor is expressed in a diagonal form when considering the universe as isotropic and homogeneous, meaning that its physical properties are independent of direction and location. This assumption, fundamental to the standard cosmological model, is known as the cosmological principle (Section 2.2.3). Isotropy implies that the universe appears the same in all directions; there is no preferred direction where the distribution of matter or energy would differ. Homogeneity means that on large scales, every region of the universe resembles any other region. Consequently, transverse energy and momentum fluxes, which would be represented by non-diagonal terms in the tensor, are absent since there is no preferred motion or energy flow in any specific direction. Only the energy densities and pressures in spatial directions, which are uniform and do not vary with direction, are manifested in the energy-momentum tensor matrix, accounting for its diagonal shape.

- It is important to note that the *twin geometry* of the Janus model is described by two field equations, each including a mixed-mode coupling tensor $T_\mu^{\nu(g,h)}$ and $T_\mu^{\nu(h,g)}$ on the right-hand side, weighted by the square root of the ratio of the determinants of the two metrics[8]. We can then express expressions 3.3.51 and 3.3.52 in mixed form as follows:

$$R_\mu^{\nu(g)} - \frac{1}{2}\delta_\mu^\nu G = \Gamma^{(g)}\left[T_\mu^{\nu(g,g)} + \sqrt{\frac{h}{g}}T_\mu^{\nu(h,g)}\right] \tag{3.3.54}$$

$$R_\mu^{\nu(h)} - \frac{1}{2}\delta_\mu^\nu H = -\Gamma^{(h)}\left[T_\mu^{\nu(h,h)} + \sqrt{\frac{g}{h}}T_\mu^{\nu(g,h)}\right] \tag{3.3.55}$$

This tensor describes the negative gravitational lensing effect induced by the masses of one layer of spacetime on those of the other. However, as we do not know exactly how these populations affect each other, it is important to emphasize that we are free to define the interaction tensors $T_\mu^{\nu(g,h)}$ and $T_\mu^{\nu(h,g)}$ for each mass population in such a way that the Bianchi identities are satisfied.

[8]By performing the elementary calculation of the determinants of the metrics 3.3.42 for each species, using the same curvature indices $k^{(g)} = k^{(h)}$ and the same speeds of light $c^{(g)} = c^{(h)}$, we can deduce that the coefficients ϕ and Φ in 3.3.50 can respectively be identified with the square root of the ratio of the determinants $\sqrt{\frac{g}{h}}$ and its inverse.

For example, as we will see later in the study of the steady-state regime (Section 3.3.4), in the case where positive masses are predominant, the previous field equations reduce in mixed mode to 3.3.98 and 3.3.99 (Section 3.3.6). Thus, we can define the energy-momentum tensor $T_{\mu}^{\nu(g,g)}$[9] and the interaction tensor $T_{\mu}^{\nu(g,h)}$ as follows:

$$T_{\mu}^{\nu(g,g)} = \begin{pmatrix} \rho^{(g)} & 0 & 0 & 0 \\ 0 & -\frac{p^{(g)}}{c^{(g)^2}} & 0 & 0 \\ 0 & 0 & -\frac{p^{(g)}}{c^{(g)^2}} & 0 \\ 0 & 0 & 0 & -\frac{p^{(g)}}{c^{(g)^2}} \end{pmatrix} \tag{3.3.56}$$

$$T_{\mu}^{\nu(g,h)} = \begin{pmatrix} \rho^{(g)} & 0 & 0 & 0 \\ 0 & \frac{p^{(g)}}{c^{(g)^2}} & 0 & 0 \\ 0 & 0 & \frac{p^{(g)}}{c^{(g)^2}} & 0 \\ 0 & 0 & 0 & \frac{p^{(g)}}{c^{(g)^2}} \end{pmatrix} \tag{3.3.57}$$

By applying the Newtonian approximation[10] to the Tolman-Oppenheimer-Volkoff differential equations 3.3.182 and 3.3.225 that result, we find the Euler equation $\frac{\mathrm{d}p}{\mathrm{d}r}$ expressing the hydrostatic equilibrium[11] approximately equal to $-\frac{GM(r)\rho(r)}{r^2}$ for each equation. Thus, we obtain the pressure $\frac{p'}{c^2}$ as being approximately equal to $-\frac{\rho m}{r^2}$ for each equation (See the section 3.3.6 & the study of the Compatibility of Field Equations Near the Dipole Repeller). Therefore, both equations asymptotically satisfy the Bianchi identities in the Newtonian limit.

- From a physicist's perspective, the focus is primarily on observable or measurable phenomena. However, in our *"visible"* universe, made up of galaxies with a significant retinue of matter and gas, the density of negative mass is negligible according to the interaction principle of the Janus model where masses of opposite signs mutually exclude each other (Figure 3.12). Therefore, the modeling of the behavior of ordinary matter (including neutron stars) under the effect of gravitation aligns with the solutions of Einstein's field equation, without the need to consider interaction tensors, deemed negligible. Indeed, they only become significant in a spacetime dominated by negative masses such as the Dipole Repeller. With positive mass density in turn being negligible, equations 3.3.54 and 3.3.55 reduce to:

$$R_{\mu}^{\nu(g)} - \frac{1}{2}\delta_{\mu}^{\nu}G = \Gamma^{(g)}\sqrt{\frac{h}{g}}T_{\mu}^{\nu(h,g)} \tag{3.3.58}$$

$$R_{\mu}^{\nu(h)} - \frac{1}{2}\delta_{\mu}^{\nu}H = -\Gamma^{(h)}T_{\mu}^{\nu(h,h)} \tag{3.3.59}$$

[9] (13.1) page 425 de [1]

[10] $4\pi r^3 p \ll mc^2$ and $\frac{2Gm}{c^2 r} \ll 1$

[11] Where the pressure at the center of the star is balanced by the gravitational force as a function of density and mass

Thus, a physicist will only study what can be observed, namely the first equation 3.3.58, allowing, for example, to determine the geodesics traveled by photons (of positive energy) under the antigravitational effect generated by a spheroidal conglomerate of negative mass[12]. See the study of the Compatibility of Field Equations Near the Dipole Repeller.

Next, by introducing radiative pressure induced by each entity:

$$p_r^{(g)} = \frac{\rho_r^{(g)} \left(c^{(g)}\right)^2}{3}, \quad p_r^{(h)} = \frac{\rho_r^{(h)} \left(c^{(h)}\right)^2}{3} \tag{3.3.61}$$

We can then consider that the entity carried by the metric h, referred to as dark energy and dark matter, could be attributed to negative masses which, in the radiative phase, would obey the same equation of state:

$$\beta^{(h)} = \frac{\alpha^{(h)}}{3} \tag{3.3.62}$$

Under these conditions, the conservation relation is still expressed, in its radiative form, by the conservation of the sum of the two energies, that of the photon gas and that of the negative masses:

$$\rho_r^{(g)} (c^{(g)})^2 (a^{(g)})^4 + \alpha^{(h)} (a^{(h)})^4 = Constant \tag{3.3.63}$$

The exact solution of the system, for curvature indices $k^{(g)} = k^{(h)} = -1$ and $\Gamma^{(f)} = -\frac{8\pi G}{c^4}$ where $f \in \{g, h\}$, becomes a solution of the following equations:

$$a^{(g)^2} \frac{\mathrm{d}^2 a^{(g)}}{\mathrm{d}t^2} = \frac{\Gamma^{(g)}}{2} E \tag{3.3.64}$$

$$a^{(h)^2} \frac{\mathrm{d}^2 a^{(h)}}{\mathrm{d}t^2} = -\frac{\Gamma^{(h)}}{2} E \tag{3.3.65}$$

If we suppose that $E < 0$, then $a^{(g)} > 0$ and $a^{(h)} < 0$. Thus, we can conclude that the visible part of our universe accelerates, while the negative species decelerates. Here,

[12] This phenomenon of *negative gravitational lensing* cannot be produced by a neutron star of negative mass, since this conglomerate is composed only of antimatter with negative mass, which can form immense proto-stars where the agitation speed of these components is negligible compared to the speed of light in this medium (see section Nature of the primordial antimatter). The approximate form of the interaction tensor can then be reduced to the following expression:

$$T_\mu^{\nu(h,g)} \approx \begin{pmatrix} \rho^{(h)} c^{(h)^2} & 0 & 0 & 0 \\ 0 & 0 & 0 & 0 \\ 0 & 0 & 0 & 0 \\ 0 & 0 & 0 & 0 \end{pmatrix} \tag{3.3.60}$$

we observe the effect of the dominant negative species, which leads to the phenomenon of cosmic expansion acceleration, as the right-hand side of the first equation becomes positive ([61]):

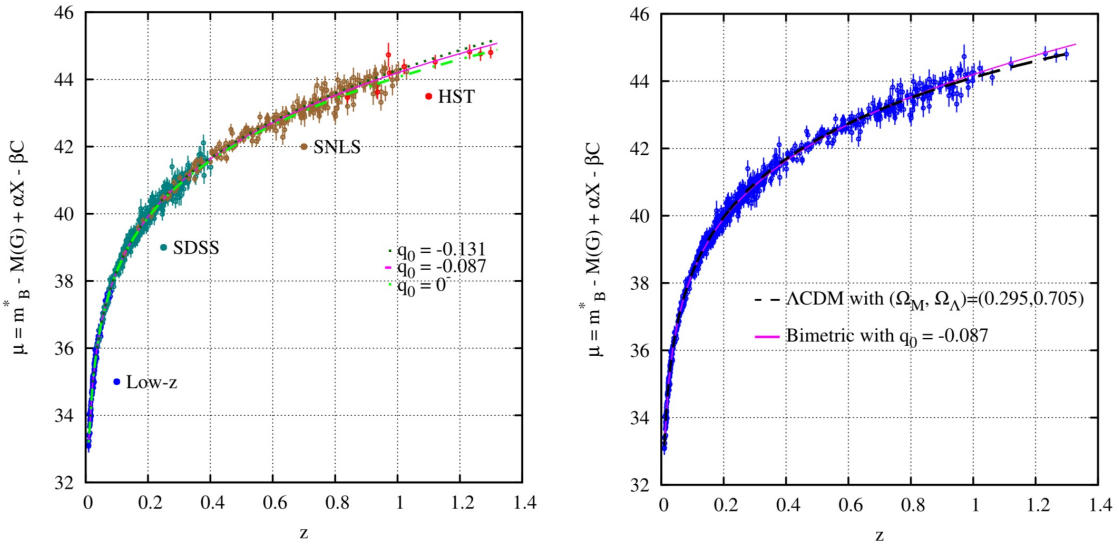

Figure 3.10: Hubble Diagram of the Two Models (Linear Redshift)

This two-species system allows for the consolidation of the effects attributed to dark matter and dark energy into a single entity composed of negative masses that combines both actions, as illustrated by the following diagram:

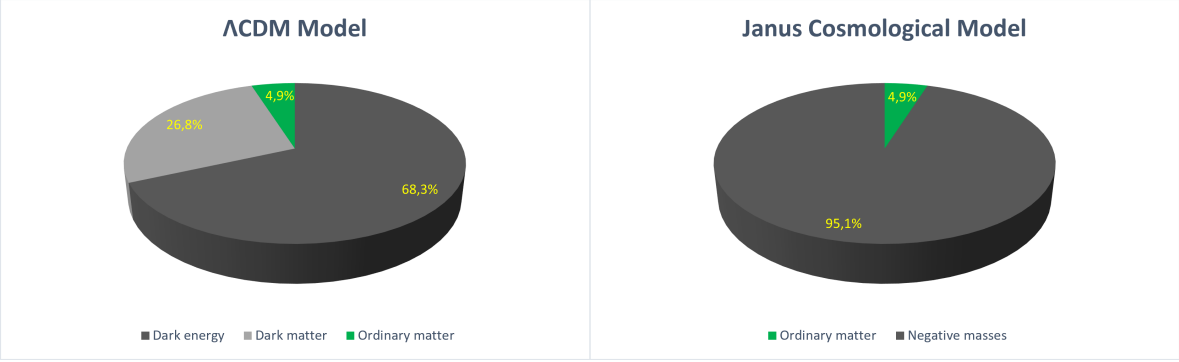

Figure 3.11: Models of the Universe

Local verification of a stationary system

In the study of the universe, we often simplify models to make them more manageable. One common simplification is to consider a small region of space as being effectively

empty and isolated from the vast complexities of the cosmos. This approach is particularly useful when we're interested in phenomena that occur over short periods, much shorter than the timescales on which the universe itself changes. In such cases, we can use *"time-independent"* metrics, which means we assume the structure of space doesn't change with time during our observation.

To add a bit of complexity, we sometimes introduce what are called *"perturbations"* to the model. These perturbations are small modifications of an otherwise simple space that we consider. They allow us to study how slight changes or disturbances might affect the system. In our case, these perturbations are represented by terms like $\gamma_{\mu\nu}^{(g)}$ and $\gamma_{\mu\nu}^{(h)}$, which signify small deviations in the geometrical structure of space, potentially representing different aspects or components of the universe.

$$g_{\mu\nu}^{(g)} = \eta_{\mu\nu}^{(g)} + \varepsilon\gamma_{\mu\nu}^{(g)}, \quad g_{\mu\nu}^{(h)} = \eta_{\mu\nu}^{(h)} + \varepsilon\gamma_{\mu\nu}^{(h)} \tag{3.3.66}$$

For the metrics, we have:

$$(\mathrm{d}s^{(g)})^2 = (c^{(g)})^2\mathrm{d}t^2 - (a^{(g)})^2[(\mathrm{d}\xi^1)^2 + (\mathrm{d}\xi^2)^2 + (\mathrm{d}\xi^3)^2] \tag{3.3.67}$$

$$(\mathrm{d}s^{(h)})^2 = (c^{(h)})^2\mathrm{d}t^2 - (a^{(h)})^2[(\mathrm{d}\xi^1)^2 + (\mathrm{d}\xi^2)^2 + (\mathrm{d}\xi^3)^2] \tag{3.3.68}$$

In cosmology, when we talk about *"quasi steady-state conditions"*, we mean a situation where certain aspects of the universe are assumed to be relatively constant over the period we're studying. Specifically, in this context, the *"spatial scale factors"* of the universe, which describe how the universe's size changes over time, are considered constant. This is a useful approximation for studying certain short-term phenomena.

To go deeper into the physics of such a scenario, we use what's known as a *"series expansion"* of the field equations. This is a mathematical technique where we break down complex equations into simpler, more manageable parts. However, we only focus on the most significant parts – in this case, we ignore the terms of second order and higher, as they have a minimal impact on the results for small-scale or short-term scenarios.

The resulting simplified equations, labeled as 3.3.69 and 3.3.70, describe the behavior of perturbations in this quasi steady-state universe. These equations involve terms like $\epsilon\gamma_{00}$ and $\delta\rho$, which represent small changes in the geometry of space and density of matter, respectively.

$$\varepsilon\gamma_{00|\beta|\beta}^{(g)} = -\Gamma^{(g)}\left[\delta\rho^{(g)}\left(c^{(g)}\right)^2 + \left(\frac{a^{(h)}}{a^{(g)}}\right)^3\delta\rho^{(h)}\left(c^{(h)}\right)^2\right] \tag{3.3.69}$$

$$\varepsilon\gamma_{00|\beta|\beta}^{(h)} = \Gamma^{(h)}\left[\delta\rho^{(h)}\left(c^{(h)}\right)^2 + \left(\frac{a^{(g)}}{a^{(h)}}\right)^3\delta\rho^{(g)}\left(c^{(g)}\right)^2\right] \tag{3.3.70}$$

Furthermore, we define *"gravitational potentials"* for each component of the universe, denoted as $\Psi^{(g)}$ and $\Psi^{(h)}$. These potentials are related to the changes in space geometry

and are key to understanding the gravitational effects in different regions or components of the universe (as 2.3.114).

$$\Psi^{(g)} = \frac{\left(c^{(g)}\right)^2}{2}\varepsilon\gamma_{00}^{(g)}, \quad \Psi^{(h)} = \frac{\left(c^{(h)}\right)^2}{2}\varepsilon\gamma_{00}^{(h)} \tag{3.3.71}$$

We obtain :

$$\sum_{\alpha=1}^{3}\frac{\partial^2\Psi^{(g)}}{\partial\xi^\alpha\partial\xi_\alpha} = -\Gamma^{(g)}\frac{\left(a^{(g)}\right)^2}{2}\left[\delta\rho^{(g)}\left(c^{(g)}\right)^2 + \left(\frac{a^{(h)}}{a^{(g)}}\right)^3\delta\rho^{(h)}\left(c^{(h)}\right)^2\right] \tag{3.3.72}$$

$$\sum_{\alpha=1}^{3}\frac{\partial^2\Psi^{(h)}}{\partial\xi^\alpha\partial\xi_\alpha} = \Gamma^{(h)}\frac{\left(a^{(h)}\right)^2}{2}\left[\delta\rho^{(h)}\left(c^{(h)}\right)^2 + \left(\frac{a^{(g)}}{a^{(h)}}\right)^3\delta\rho^{(g)}\left(c^{(g)}\right)^2\right] \tag{3.3.73}$$

In physics, particularly in the study of space and the universe, as we saw it on this section 2.3.9, *"geodesic equations"* describe how objects move under the influence of gravity. In simple terms, these equations tell us the path an object will take when it's moving only under the force of gravity. For example, how planets orbit stars or how objects fall on Earth.

In our scenario, we're dealing with two different layers (or sheets) of the universe, each with its own properties. The first layer, which we can think of as the ordinary matter universe, follows one set of rules. The second layer of negative masses, associated with dark matter and dark energy follows another set.

Next equations 3.3.74 and 3.3.75 are the way of mathematically expressing how objects would move in these two different layers (The layer of ordinary matter and that of negative masses respectively). These equations resemble the classical Poisson equation in physics, which is used to describe gravitational fields. However, the equations have a twist — they account for different *"speeds of light"* in each layer. This modification is crucial for exploring theories that go beyond our standard understanding of physics.

$$\frac{\mathrm{d}^2\xi^\alpha}{\mathrm{d}t^2} = -\frac{1}{\left(a^{(g)}\right)^2}\frac{\partial\Psi^{(g)}}{\partial\xi_\alpha} \tag{3.3.74}$$

$$\frac{\mathrm{d}^2\xi^\alpha}{\mathrm{d}t^2} = -\frac{1}{\left(a^{(h)}\right)^2}\frac{\partial\Psi^{(h)}}{\partial\xi_\alpha} \tag{3.3.75}$$

The interaction laws we have chosen ensure that the entities arising from the layers structured by the metrics g and h mutually exclude each other (3.12).

Figure 3.12: Laws of interaction between masses

Therefore, we can consider a region where only one of the two entities is present. Focusing on the reference frame structured by the metric g, which is populated by ordinary matter such as in the solar system, the system of coupled field equations simplifies to:

$$R^{(g)}_{\mu\nu} - \frac{1}{2} g_{\mu\nu} G = \Gamma^{(g)} T^{(g,g)}_{\mu\nu} \tag{3.3.76}$$

$$R^{(h)}_{\mu\nu} - \frac{1}{2} h_{\mu\nu} H = -\Gamma^{(h)} \sqrt{\frac{|g|}{|h|}} T^{(g,h)}_{\mu\nu} \tag{3.3.77}$$

The first equation can be identified with Einstein's equation without the cosmological constant Λ. This equation represents the standard model of gravity for ordinary matter. The second equation captures what might be termed *"the induced geometry effect"*. It describes how the geometry of space, influenced by the presence of ordinary matter within a sphere of radius r and density $\rho^{(g)} = \rho$, affects the geodesics of the negative masses layer. Consequently, we can deduce that this bimetric model, in which ordinary matter in one layer interacts with negative masses located in a second aligns with the standard tests of general relativity at the local level. Nevertheless, it remains crucial to verify the coherence of this system under stationary and non-homogeneous conditions.

Nature of the primordial antimatter

Following A. Sakharov's propositions in [69], [70] and [72], suppose that the matter/antimatter pair in the first layer of our universe consists of quarks and antiquarks with positive energy. Meanwhile, a matter/antimatter pair in a second layer is formed by quarks and antiquarks with negative energy. If the synthesis of matter in the first layer (the first pair) were faster, while the synthesis of antimatter in the second layer (the second pair) were slower, this could lead to the hypothesis that objects at the centers of large voids in the large-scale structure of the universe, as indicated by the dipole repeller phenomenon, are composed of antimatter. This antimatter includes antiprotons, antineutrons, and antielectrons of negative energy[13]. These could form spheroidal objects made of antihydrogen (light elements) with repulsive properties similar to immense proto-stars that formed during the primordial radiative phase (at the beginning of the universe).

The lacunar network of positive mass confines this space of negative density, preventing them from merging. Conversely, these conglomerates of negative mass act as anchor points for this porous network in the universe of positive masses, ensuring overall stability.

[13]Negative masses ([78]).

Indeed, the stars with positive mass initially resemble spheroidal clusters of gas, heated to high temperatures. These proto-stars gradually cool down, emitting radiation primarily in the red and infrared spectra. To transform into actual stars, matter and gases must undergo gravitational contraction, reaching sufficiently high temperatures and densities to initiate thermonuclear fusion reactions. This contraction process releases thermal energy, which is radiated from the star's surface in the form of electromagnetic radiation, including visible light. This energy release scales with the square of the star's radius. Larger stars have greater surface areas and can dissipate more heat. However, the amount of heat produced scales with the cube of the star's radius, which is tied to its volume. Thus, for very massive stars, the cooling rate can be relatively slow, and it can take a considerable amount of time before the temperature reaches the threshold necessary to trigger the thermonuclear fusion reactions that allow the star to shine.

In our positive world, it is considered that nuclear fusion reactions can begin at the core of a proto-star when the temperature reaches an optimal temperature of approximately 10 million degrees Celsius. It is at this temperature that the hydrogen nuclei, which make up the majority of the matter in the proto-star, acquire enough kinetic energy to overcome the electrostatic barrier due to their positive charge. When this barrier is crossed, the hydrogen nuclei can fuse to form helium, thus releasing a considerable amount of radiant and thermal energy. This optimal temperature enables a more efficient nuclear fusion reaction, producing the characteristic brilliance of stars.

Thus, a very massive and very hot negative mass proto-star can take a long time to cool down sufficiently for fusion reactions to begin because the proto-star's contraction process must generate enough heat to compensate for the heat loss at the surface.

As a result, these massive negative mass proto-stars have such long cooling times that they will never ignite (exceeding the age of the universe). Consequently, no galaxy, heavy element, molecule, or any other form of matter necessary for the development of life in the negative world can form.

2D numerical simulations

Two-dimensional numerical simulations have been performed using two sets of 5000 mass points, representing clusters of ordinary matter (population density $\rho^{(g)}$) and negative masses (population density $\rho^{(h)}$). A significant asymmetry was maintained between the two populations, with $|\rho^{(h)}|$ being much greater than $\rho^{(g)}$. Additionally, Maxwellian distributions of 2D thermal velocities were applied to both sets, with the average velocity of the negative mass distribution being four times higher than that of the ordinary matter.

These simulations revealed a lacunar structure of negative masses at the centers

of large voids in the large-scale structure of the universe. As the Jeans times vary inversely with the square root of the density, the development time for the negative mass distribution is shorter. This results in the formation of a regular network of spheroidal conglomerates. The distribution of ordinary matter, consequently, is forced to occupy the remaining space, leading to a lacunar structure similar to a set of joined soap bubbles in three-dimensional simulations. This pattern was also observed by Brennen in 1995 [13] (Figures 3.13 and 3.14), as cited by El-Ad in 1997 ([27]).

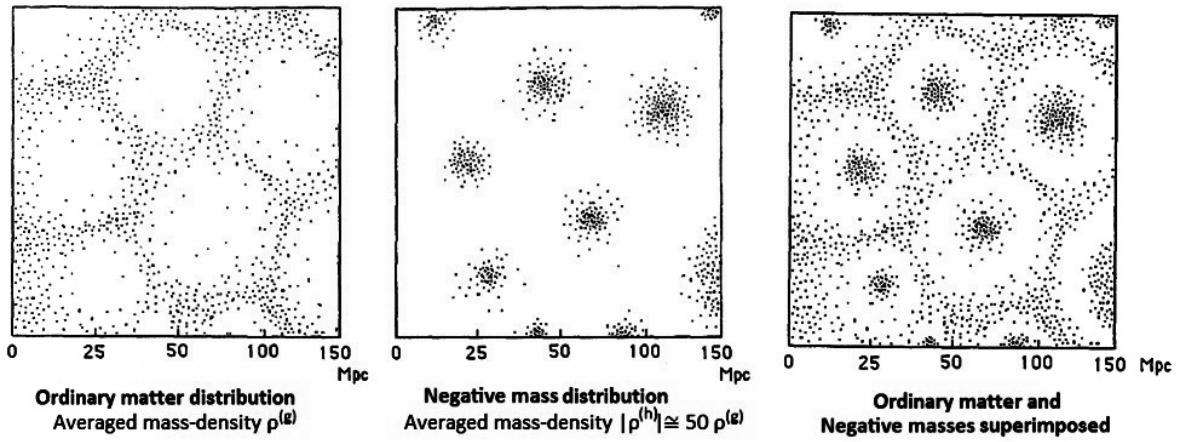

Figure 3.13: Distribution of Ordinary Matter and Negative Masses when $|\rho^{(h)}| \gg \rho^{(g)}$

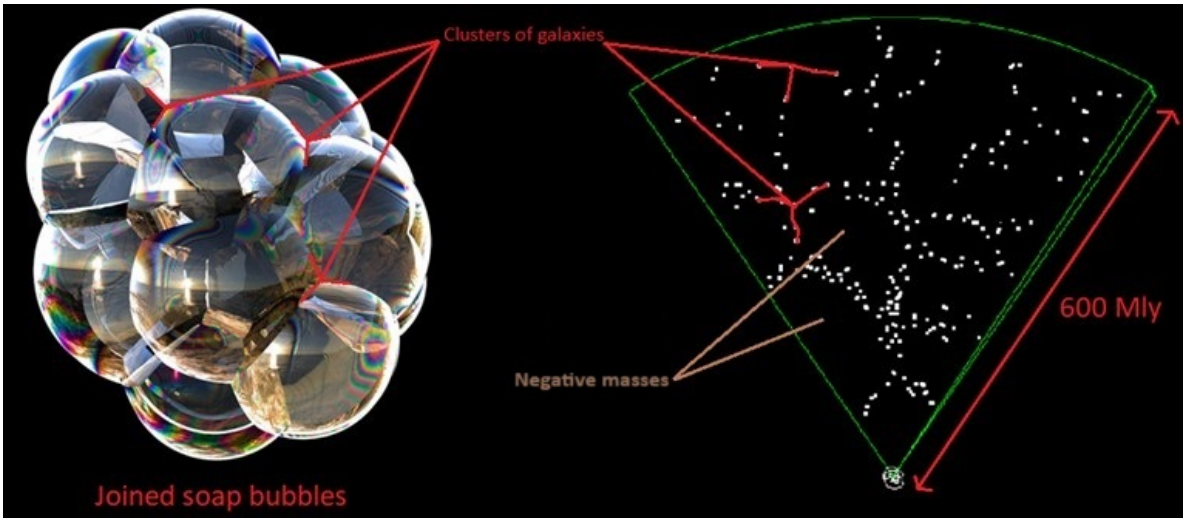

Figure 3.14: Spheroidal Lacunar Structure

It is important to consider that in the study of negative masses, we lack observational

data to compare with potential numerical predictions, except for the geometry effects induced by this reference frame (that of negative mass) through gravitational lensing phenomena that structure the metric $g_{\mu\nu}$. Therefore, the pressure derived from the Tolman-Oppenheimer-Volkoff (TOV) differential equation 3.3.225 in spacetime structured by the metric $h_{\mu\nu}$ will always remain hypothetical. As a result, it is impractical to attempt to structure the interaction tensor $T_{\mu}^{\nu(g,h)}$ from the second field equation 3.3.99 (Section 3.3.6). Indeed, we will never be able to compare the results obtained by calculating the geodesics of $h_{\mu\nu}$ with observational data related to the movement of particles with negative mass. Instead, we must work with a function $\beta(r)$ (unrelated to negative pressure) solely to ensure the existence of a solution in this frame of reference (3.3.104). The most important aspect is to define the tensors in mixed mode 3.3.56 and 3.3.57 of each field equation in such a way that the pressure $\frac{p'}{c^2}$ expressing the hydrostatic equilibrium for each equation is the same and thus asymptotically satisfies the Bianchi identities in the Newtonian limit.

To fully understand this induced geometry effect, one must place themselves within the context of the system with two coupled field equations of the model. Indeed, it is important to recall that it structures a 4D hypersurface according to 2 metrics associated with 2 distinct spacetime layers. Each type of mass is associated with its own metric, implying that a mass always creates a positive curvature in spacetime according to its own metric (where the mass emits photons of visible energy) and always a negative curvature in the conjugate metric (where the mass emits photons of invisible energy) as we can see on next figure 3.15.

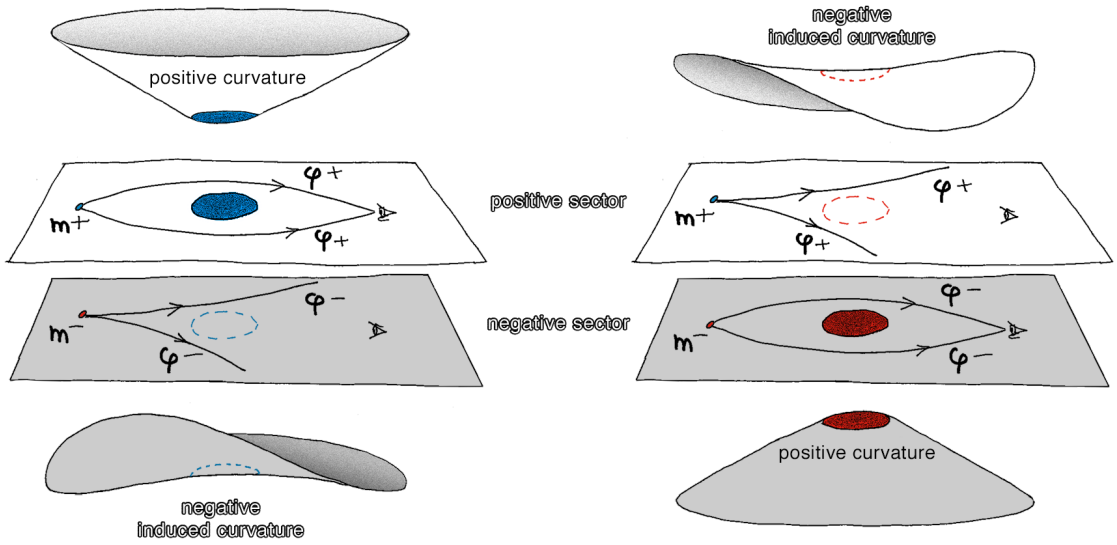

Figure 3.15: Induced geometry effect where photons can be represented by φ or γ symbol

At the left of the figure 3.15, the massive blue object belonging to the positive universe creates a positive curvature. Consequently, it produces a positive gravitational lensing effect on the image of a small positive mass m^+, causing the convergence of photons with positive energy φ^+ around the massive blue object. However, this massive object induces a negative curvature in the negative universe. Therefore, even though it is invisible, its apparent mass in the negative universe is *"felt"* as if it were negative.

Conversely, At the right of the figure 3.15, the massive red object belongs to the negative universe. It creates a positive curvature relative to its frame of reference (and not a negative one). This massive object induces a negative curvature that is perceived in our universe, even though its energy photons are invisible. Hence, we conclude that its apparent mass is negative. Indeed, it produces a negative gravitational lensing effect on the image of a small mass m^+, causing the divergence of photons with positive energy φ^+ around the invisible massive negative object, whose gravitational effect is still present.

We can deduce several corollaries from the concept of negative mass:

- Fundamentally, there is no negative mass (and therefore no negative energy). At least, the *"negativity of mass"* (and the *"negativity of energy"* as both are obviously linked) is not an intrinsic physical property of a *"negative mass particle"*. Indeed, the *"negativity"* or *"positivity"* of mass is merely a quantity of curvature measured locally in spacetime by an observer. The sign of this curvature is **relative** to the reference frame of the hypersurface or metric in which this mass is measured. It is, in fact, an apparent mass whose presence is only revealed by the curvature it induces in spacetime.

  In other words, all particles with mass in the universe possess exclusively positive inertial mass, but their gravitational mass is relative. The sign of their gravitational mass is opposite (positive or negative) depending on the perspective adopted: a mass distorts spacetime in its own metric, inducing a certain amount of curvature that is always positive. However, it will be perceived as an apparent mass in the opposite universe, from which an observer will perceive this curvature as negative. This is due to the coupled nature of the field equations, and it results in an effect known as *conjugate curvatures*. One could speak of *"the same mass inducing two opposite curvatures"*.

  For example, Earth, seen from our reference frame, possesses positive mass. Through an unknown process, imagine that you could reverse its energy (and its mass). Earth (and all the stars in the sky) would disappear because you can no longer perceive photons with positive energy. However, you can still perceive and measure the curvature it continues to induce in our spacetime. By performing this measurement, you would detect that the now-invisible Earth possesses a negative mass.

However, there is no distinct universe of positive energies and a universe of negative energies. It is merely an arbitrary choice in nomenclature. Both are equivalent. By convention, we refer to the sector of the universe where we live as the one composed of positive mass matter. The reversal of the arrow of time does not mean that we start living *"backward"* and become younger. It is manifested physically by the inversion of particle energies. Once again, this inversion is a relative observation. In practice, it translates to a transition to the opposite sector of the universe.

- It is important to note that particles of negative energy (and their photons) cannot be detected by optical instruments because they follow geodesics of their own metric $h_{\mu\nu}$, distinct from the geodesics of our metric $g_{\mu\nu}$. There are, therefore, two sets of geodesics that never *"cross"* each other. Since positive-energy species and negative-energy species cannot see each other and evolve along two distinct families of geodesics, the two spacetime reference frames in which they reside are respectively referred to as the positive mass frame and the negative mass frame. Thus, these are two frames within the same 4D hypersurface, structured by two coupled field equations, not just one. However, even though negative masses are invisible to us because they do not interact electromagnetically with our sector without exchanging photons, they only reveal their presence through an anti-gravitational effect, as they induce opposite curvatures in our observable sector.

- Negative masses are distributed throughout the universe, but their proportions vary depending on the region of space we are in. They exist solely to contribute to its stability through an anti-gravitational effect. The universe can be defined by a hypersurface structured by two metrics that allow distances between points to be measured in two different ways, using two distinct sets of coordinates (three spatial coordinates and one temporal coordinate). In a didactic manner, one can envision this universe as a sheet of paper with two different measuring grids on each of its two sides.

3.3.5 Future Perspective

Experimental Approach to Mass Inversion

The scientific approach to understanding a phenomenon can be summarized in the ability to reproduce and measure it. It is important to note that it is entirely possible to demonstrate the phenomenon of mass inversion in a laboratory by inverting an infinitesimal amount of matter, provided that a significant disruption of this matter can be induced by producing electromagnetic parameters on the order of tens of millions of tesla for a very short time, using explosives, for example. The Soviet Union had already achieved a production of 100 million amperes by compressing a magnetic flux with the help of explosives in the 1950s, using a magneto-cumulative generator ([51]). It would

then be possible to demonstrate this mass inversion by measuring the gravitational waves emitted and detected by the Virgo and Ligo laser interferometers.

Experimental Protocol for the Study of Mass Inversion via Nuclear Metastable States

This approach proposes to explore the phenomenon of mass inversion in the laboratory by exploiting the metastable states of specific atomic nuclei, such as those of platinum, iridium, cobalt, and xenon. The goal is to store energy in these metastable states before releasing it to induce a disruption of matter. The detection and characterization of this phenomenon would be carried out by observing the emitted gravitational waves, measured using finely calibrated interferometers.

Nuclear Excitation: The first step of the protocol requires the excitation of atomic nuclei to their metastable states. The energy levels required for such excitations are significantly higher than those provided by standard laboratory lasers, lying in the range of MeV (Mega Electron Volts) to GeV (Giga Electron Volts). Consequently, this procedure requires the use of a particle accelerator capable of generating and concentrating these high energies on the targeted atomic nuclei.

Isotope Selection: A meticulous selection of the appropriate isotope is essential. The chosen isotope must have a metastable state whose half-life corresponds to the desired time frame for energy storage. This half-life must be short enough to allow controlled release of the energy, yet long enough to ensure temporary storage of the injected energy. The ideal half-life would be on the order of a fraction of a second.

Measurement of Gravitational Waves: The detection of mass inversion would be carried out by measuring the gravitational waves emitted during the disruption of matter. This step involves the use of high-precision interferometers, calibrated to detect extremely subtle variations in the gravitational field resulting from the experiment.

Conclusion: This experimental protocol proposes an innovative method to study mass inversion, a still theoretical phenomenon at local scale. The experimentation requires cutting-edge equipment, notably a particle accelerator, and expertise in nuclear physics, optics, and the measurement of gravitational waves.

Quantification of Gravity

An unification of the Theory of Relativity with Quantum Mechanics would only be possible through the quantization of gravity. However, there is no concept of energy quantization in the Theory of Relativity, except for the mass-energy equivalence since Einstein's field equation does not fundamentally describe particles. This is why string theory is the only contemporary approach accepted and acceptable to bridge the gap

between Relativity and Quantum Mechanics. Nevertheless, this unification is impossible within this approach because Quantum Mechanics considers forces in terms of fields, and a particle is required in these fields to convey interaction. For instance, the photon is the elementary particle that conveys the electromagnetic field, and its quantization is possible because of the consideration of positive and negative electric charges. Conversely, the only particle emerging from string theory to convey gravity is the graviton, but this pseudo-particle has never been experimentally observed. Indeed, the concept of quantum gravity remains speculative within this model. An alternative conjecture for quantizing gravity at the quantum scale would involve considering the existence of masses with opposite signs that exhibit repulsive properties within the model, similar to the model of photons with oppositely charged electric charges to convey interaction.

3.3.6 Response to Criticisms Published by Dr. Thibault Damour on the IHES Website

The physical and mathematical coherence of the Janus model was questioned by the academician Thibault Damour in a correspondence dated January 7, 2019, sent by registered mail with acknowledgment of receipt to my home[14].

Here is its content:

Thibault Damour
IHES, Bures-sur-Yvette,
7 Janvier 2019

à Jean-Pierre Petit, BP 55, 84122 Pertuis

Copies: Je me réserve le droit d'envoyer des copies de cette lettre à toutes les personnes que vous citez sur votre site, dans vos vidéos, et dans vos lettres, ainsi qu'à toute personne s'intéressant au "modèle Janus".

Objet: "modèle Janus".

Monsieur,

j'ai bien reçu votre lettre du 7 décembre 2018. En revanche je n'ai pas souvenir d'avoir reçu (précédemment) de vous une réponse aux objections et critiques que je vous avais communiquées dans ma lettre du 12 mars 2014, écrite après réception des prépublications de vos articles récents, et notamment: J. P. Petit. et G. d'Agostini, "Negative mass hypothesis in cosmology and the nature of dark energy", Astrophys. Space Sci DOI 10.1007/s10509-014-2106-5); et J. P. Petit, et G. dAgostini, "Cosmological bimetric model with interacting positive and negative masses and two different speeds of light, in agreement with the observed acceleration of the Universe". Mod. Phys. Lett. A Vol. 29 (no 34) (2014) 145082.

La réception de votre lettre m'a poussé à regarder de plus près la structure et les conséquences des équations de champ de ce que vous appelez "modèle Janus". J'ai en particulier poursuivi plus en détail les raisonnements et arguments que je vous avais indiqués dans ma lettre de 2014. J'ai ainsi démontré que *le "modèle Janus" était physiquement (et mathématiquement) incohérent.* Cette incohérence est particulièrement manifeste dans la limite quasi-newtonienne, où le "modèle Janus" implique que la matière ordinaire doit, à la fois, s'auto-attirer et s'auto-repousser gravitationnellement. J'ai posté mes raisonnements, et leurs conclusions, sur ma page web (lien "Sur le "modèle Janus de J. P. Petit" sur http://www.ihes.fr/~damour).

Vous comprendrez, après lecture, qu'il ne saurait être question de vous inviter à donner un séminaire à l'IHES, car vous n'avez pas de théorie cohérente, mathématiquement et physiquement bien définie, à présenter. [Notez d'ailleurs au passage que je ne suis pas, comme vous l'écrivez, "responsable du séminaire de cosmologie à l'IHES". Il n'y a en fait pas de séminaire régulier de cosmologie à l'IHES.]

Bien à vous,

Thibault Damour
Institut des Hautes Études Scientifiques
35, route de Chartres
91440 Bures-sur-Yvette (France)

P.S.: Quand j' ai évoqué le nom de Souriau à Genève (le 5 novembre 2018) en répondant à une question concernant vos travaux, je faisais allusion au manque d'une dérivation Lagrangienne pouvant (éventuellement) assurer la cohérence du "modèle Janus". Il est facile de voir que la dérivation variationnelle donnée dans l'article de Sabine Hossenfelder (PRD 78, 044015, 2008) est mathématiquement invalide.

[14] http://www.jp-petit.org/papers/cosmo/2019-Damour-lettre.pdf

Let's reexamine the context. Since 2014, we had vainly attempted to be received by T. Damour, wishing to present our work to him, but without receiving any response. Therefore, we undertook, starting in 2017, to publish online on the YouTube platform a lengthy series of 40 videos presenting the Janus model[15].

Annoyed by the growing public interest in this model, T. Damour decided to put an end to what he considered a scientific imposture. Thus, he sent us his arguments in a first article published online on the same day, January 4, 2019, on his page at the Institute of Advanced Studies in Bures-sur-Yvette. This document, still available, can be accessed[16].

Equations like those of the Janus model must indeed satisfy mathematical conditions called *"Bianchi conditions"*. For instance, the equations proposed in 2014, published in the journal *Astrophysics and Space Science* [59][17] in the article titled *Negative Mass hypothesis in cosmology and the nature of dark energy*, describing a non-stationary, homogeneous, and isotropic solution, are mathematically correct. T. Damour, unaware of the existence of this first paper, which accounts for the acceleration of cosmic expansion by attributing it to the universe's content in negative mass, focuses on a second article, published the same year in another journal *Modern Physics Letters A* [58], titled *Cosmological Bimetric model with interacting positive and negative masses and two different speeds of light, in agreement with the observed acceleration of the Universe*. In this article, the system of equations is described as follows:

In our model, the Universe is an M_4 manifold associated not to one single metric, but to two: $g^{(+)}_{\mu\nu}$ and $g^{(-)}_{\mu\nu}$, the former linked to species of positive mass and energy, the latter to species of negative mass and energy. From these metrics, one can build the associated Ricci tensors, $R^{(+)}_{\mu\nu}$ and $R^{(-)}_{\mu\nu}$. A system of two coupled field equations was then proposed:[20]

$$R^{(+)}_{\mu\nu} - \frac{1}{2}R^{(+)}g^{(+)}_{\mu\nu} = \chi(T^{(+)}_{\mu\nu} + T^{(-)}_{\mu\nu})\,, \tag{2a}$$

$$R^{(-)}_{\mu\nu} - \frac{1}{2}R^{(-)}g^{(-)}_{\mu\nu} = -\chi(T^{(+)}_{\mu\nu} + T^{(-)}_{\mu\nu})\,, \tag{2b}$$

where the tensors $T^{(+)}_{\mu\nu}$ and $T^{(+)}_{\mu\nu}$ represent positive and negative energy contents (and positive and negative mass contents as well). Previously, in 1957, Bondi[23]

[15] http://www.jp-petit.org/nouv_f/VIDEOS_JANUS.htm
[16] https://www.ihes.fr/~damour/publications/JanusJanvier2019-1.pdf
[17] https://jp-petit.org/papers/cosmo/2014-AstrophysSpaceSci2.pdf

In this article, we revisit the specific case of the time-dependent homogeneous and isotropic solution, for which the system of equations becomes, as published in the previous article:

So that our coupled field equation system becomes:

$$R_{\mu\nu}^{(+)} - \frac{1}{2}R^{(+)}g_{\mu\nu}^{(+)} = \chi^{(+)}\left[T_{\mu\nu}^{(+)} + \left(\frac{a^{(-)}}{a^{(+)}}\right)^3 T_{\mu\nu}^{(-)}\right], \tag{12a}$$

$$R_{\mu\nu}^{(-)} - \frac{1}{2}R^{(-)}g_{\mu\nu}^{(-)} = -\chi^{(-)}\left[\left(\frac{a^{(+)}}{a^{(-)}}\right)^3 T_{\mu\nu}^{(+)} + T_{\mu\nu}^{(-)}\right] \tag{12b}$$

The previous equations are recognized. This second article aimed to extend the previous one by showing that the speeds of light could be different in the two *"sheets"*. However, T. Damour's attention was drawn to the system of coupled field equations (2a) and (2b).

It should be noted that a model in cosmology or physics does not instantly emerge in a definitive form, perfectly coherent mathematically. We were fully aware of the issue that remained to be resolved in 2014. By the time T. Damour's entirely justified critique, focusing on this system (2a-2b), appeared, we had just resolved it, in the form of an article that had been published a few days earlier (the first in January 2019) in the journal *Progress in Physics* [63][18].

Therefore, we immediately wrote to T. Damour to send him our article, while recognizing the relevance of his critique, for which we are thankful.

What then is the subject of such criticism?

In the system of coupled field equations (2a-2b), the terms on the left-hand sides involve the Ricci tensors $R_{\mu\nu}^{(+)}$ and $R_{\mu\nu}^{(-)}$ and the corresponding Ricci scalars $R^{(+)}$ and $R^{(-)}$. These terms are calculated from the two metrics $g_{\mu\nu}^{(+)}$ and $g_{\mu\nu}^{(-)}$.

Using these two metrics, the form of two so-called *covariant derivative operators* $\nabla_\mu^{(+)}$ and $\nabla_\mu^{(-)}$ are then calculated. It turns out that, due to their form, the left-hand

[18] https://www.jp-petit.org/papers/cosmo/2019-Progress-in-Physics-1.pdf

sides of the two equations identically satisfy the following relation:

$$\nabla_{\mu}^{(+)}\left(R_{\mu\nu}^{(+)}-\frac{1}{2}R^{(+)}g_{\mu\nu}^{(+)}\right)=0 \tag{3.3.78}$$

$$\nabla_{\mu}^{(-)}\left(R_{\mu\nu}^{(-)}-\frac{1}{2}R^{(-)}g_{\mu\nu}^{(-)}\right)=0 \tag{3.3.79}$$

The two tensors, $T_{\mu\nu}^{(+)}$ and $T_{\mu\nu}^{(-)}$, also satisfy the following condition:

$$\nabla_{\mu}^{(+)}T_{\mu\nu}^{(+)}=0 \tag{3.3.80}$$

$$\nabla_{\mu}^{(-)}T_{\mu\nu}^{(-)}=0 \tag{3.3.81}$$

It follows that if the field equations correspond to those presented in 2014 in the journal *Modern Physics Letters A*, we should also have:

$$\nabla_{\mu}^{(+)}T_{\mu\nu}^{(-)}=0 \tag{3.3.82}$$

$$\nabla_{\mu}^{(-)}T_{\mu\nu}^{(+)}=0 \tag{3.3.83}$$

These are the equations that then lead to a contradiction.

Let us now speak the language of the physicist. What meaning is to be given to the tensors on the right-hand sides of the equations? They are the sources of the gravitational field.

There are two *"observers"*. One observer of positive mass, who perceives this gravitational field through the metric $g_{\mu\nu}^{(+)}$ by following the geodesics that emanate from it.

And an observer of negative masses, who perceives this gravitational field through the metric $g_{\mu\nu}^{(-)}$ by following the geodesics that emanate from it. Thus :

- The source of the field $T_{\mu\nu}^{(+)}$ represents the action of positive masses on positive masses.
- The source of the field $T_{\mu\nu}^{(-)}$ represents the action of negative masses on negative masses.

In the two right-hand sides are two source terms, which we can call *interaction tensors*, and which represent:

- The action of negative masses on positive masses. This could be denoted by $T_{\mu\nu}^{(-/+)}$.
- The action of positive masses on negative masses. This could be denoted by $T_{\mu\nu}^{(+/-)}$.

Under these conditions, this would have led us to write this system of equations in the following way:

$$R_{\mu\nu}^{(+)} - \frac{1}{2}R^{(+)}g_{\mu\nu}^{(+)} = \chi\left[T_{\mu\nu}^{(+)} + T_{\mu\nu}^{(-/+)}\right] \tag{3.3.84}$$

$$R_{\mu\nu}^{(-)} - \frac{1}{2}R^{(-)}g_{\mu\nu}^{(-)} = -\chi\left[T_{\mu\nu}^{(-)} + T_{\mu\nu}^{(+/-)}\right] \tag{3.3.85}$$

By a priori assuming the satisfaction of the following conditions:

$$\nabla_{\mu}^{(+)}T_{\mu\nu}^{(-/+)} = 0 \tag{3.3.86}$$

$$\nabla_{\mu}^{(-)}T_{\mu\nu}^{(+/-)} = 0 \tag{3.3.87}$$

Placing ourselves in a non-stationary, homogeneous, and isotropic regime, the system then became:

$$R_{\mu\nu}^{(+)} - \frac{1}{2}R^{(+)}g_{\mu\nu}^{(+)} = \chi\left[T_{\mu\nu}^{(+)} + \frac{{a^{(-)}}^3}{{a^{(+)}}^3}T_{\mu\nu}^{(-)}\right] \tag{3.3.88}$$

$$R_{\mu\nu}^{(-)} - \frac{1}{2}R^{(-)}g_{\mu\nu}^{(-)} = -\chi\left[T_{\mu\nu}^{(-)} + \frac{{a^{(+)}}^3}{{a^{(-)}}^3}T_{\mu\nu}^{(+)}\right] \tag{3.3.89}$$

Which was then mathematically and physically coherent. That is, in this case, our interaction tensors would become:

$$T_{\mu\nu}^{(-/+)} = \frac{{a^{(-)}}^3}{{a^{(+)}}^3}T_{\mu\nu}^{(-)} \tag{3.3.90}$$

$$T_{\mu\nu}^{(+/-)} = \frac{{a^{(+)}}^3}{{a^{(-)}}^3}T_{\mu\nu}^{(+)} \tag{3.3.91}$$

Why did we write the system of equations (2a-2b)? Which amounted to considering:

$$T_{\mu\nu}^{(-/+)} = T_{\mu\nu}^{(-)} \tag{3.3.92}$$

$$T_{\mu\nu}^{(+/-)} = T_{\mu\nu}^{(+)} \tag{3.3.93}$$

Why did we write the system of equations (2a-2b)? Which amounted to considering:

$$T_{\mu\nu}^{(-/+)} = T_{\mu\nu}^{(-)} \tag{3.3.94}$$

$$T_{\mu\nu}^{(+/-)} = T_{\mu\nu}^{(+)} \tag{3.3.95}$$

There was no real reason. It was a typographical error. All the more so since we immediately opted for the particular case of the non-stationary, homogeneous, isotropic solution represented by equations 3.3.88 and 3.3.89, which is physically and mathematically coherent.

We should have written the system of equations 3.3.84 and 3.3.85. But the fact is that it was presented this way. T. Damour, therefore, focused on this error, basing on this incorrect presentation, the idea that the entire body of work was marked by inconsistency.

Starting from this incorrect system of equations, let's see how the physical and mathematical inconsistency manifests itself.

The Bianchi conditions are of a mathematical essence. They have a physical meaning. In an isotropic, homogeneous, and non-stationary context, they translate into a generalized conservation of energy. Indeed, in the course of calculation, in the articles published in 2014 in both journals, we arrive at the energy conservation relation (Expression (10) of [58]).

It should be noted that, when considering Einstein's field equation, it implies the conservation of energy. In bimetric theory, relation (10) of [58], which translates into a generalized conservation of energy, is very satisfying for the physicist.

The conditions for mathematical coherence, in the non-stationary case, find their physical equivalent. When the situation is stationary, they express a state of balance between the force of gravity and the pressure force inside the mass, in the body of a massive star that creates the gravitational field.

Consider a massive body whose mass density is considered to be approximately constant, for example, the Earth. We know how to calculate the gravitational field inside the Earth: it is null at the center and maximal at the surface. We know that the (Newtonian) field produced by a spherical mass, at a distance r from the center of the system, is equal to the Newtonian field that would be produced by a mass $M(r)$ concentrated at the geometric center, which is:

$$M(r) = \frac{4}{3}\pi r^3 \rho \tag{3.3.96}$$

The gravitational field is then proportional to the distance from the center, equal to $\frac{4}{3}\pi G r \rho$.

By stating that this field balances the pressure force, we arrive at Euler's relation expressing hydrostatic equilibrium, namely the balance between the gravitational force and the pressure force in a fluid of uniform density:

$$\frac{\mathrm{d}p}{\mathrm{d}r} = -\frac{GM\rho}{r^2} \tag{3.3.97}$$

Calculating the Bianchi condition should yield this relationship for a massive body with constant mass density.

Let's see how this type of calculation is managed in relativity.

We will now move away from the notations of the publications with their metrics $g^{(+)}_{\mu\nu}$ and $g^{(-)}_{\mu\nu}$. In this work, we opt for $g_{\mu\nu}$ and $h_{\mu\nu}$.

The Ricci tensors are $R^{(g)}_{\mu\nu}$ and $R^{(h)}_{\mu\nu}$, and the Ricci scalars G and H.

This refers us to page 65 of this work. The derivation of the field equation system has revealed the square root of the ratio of the determinants of the two metrics, which is also found in the article [37] by S. Hossenfelder. The system is then written in mixed tensor notations 3.3.54 and 3.3.55.

Relation 3.3.37 allows retrieving the condition for the nullity of the covariant derivative of the interaction tensors.

In general relativity, analysis focuses on specific cases that are mathematically manageable, often associated with extreme physical situations. These situations include:

- A homogeneous and isotropic universe that is dynamic rather than static.
- Stationary solutions exhibiting spherical symmetry, invariant under the action of the SO(3) group. For these cases, it is possible to determine metric solutions that describe both the interior and exterior of spheroidal bodies.
- Stationary and axisymmetric solutions, invariant under the action of the SO(2) group. Here, only the exterior metric is known, as in the case of the Kerr metric. The ongoing challenge in cosmology is to find a corresponding interior metric.

These scenarios define the framework of the study.

In the context of the Janus model, the approach is similar. As masses of opposite signs repel each other, they do not coexist. Therefore, the study will be limited to situations where either one or the other of the two types of masses is predominant, the other having a density considered negligible in the region of space in question.

When positive mass is dominant, the field equations become:

$$R^{\nu(g)}_{\mu} - \frac{1}{2}\delta^{\nu}_{\mu}G = \chi T^{\nu(g,g)}_{\mu} \tag{3.3.98}$$

$$R^{\nu(h)}_{\mu} - \frac{1}{2}\delta^{\nu}_{\mu}H = -\chi\sqrt{\frac{|g|}{|h|}}T^{\nu(g,h)}_{\mu} \tag{3.3.99}$$

It is the same system of equations, tensorial, but written in mixed notation. Under these conditions, the metric tensors are identified with the Kronecker delta symbol

(2.3.55). The advantage is that the source tensors are expressed in a simple way:

$$T_{\mu}^{\nu(g,g)} = \begin{pmatrix} \rho^{(g)}c^{(g)2} & 0 & 0 & 0 \\ 0 & -p^{(g)} & 0 & 0 \\ 0 & 0 & -p^{(g)} & 0 \\ 0 & 0 & 0 & -p^{(g)} \end{pmatrix} \tag{3.3.100}$$

$$T_{\mu}^{\nu(h,h)} = \begin{pmatrix} \rho^{(h)}c^{(h)2} & 0 & 0 & 0 \\ 0 & -p^{(h)} & 0 & 0 \\ 0 & 0 & -p^{(h)} & 0 \\ 0 & 0 & 0 & -p^{(h)} \end{pmatrix} \tag{3.3.101}$$

When, on the contrary, it is the negative mass that dominates (as in the case of the *"Dipole Repeller"*), the system of equations becomes:

$$R_{\mu}^{\nu(g)} - \frac{1}{2}\delta_{\mu}^{\nu}G = \chi\sqrt{\frac{|h|}{|g|}}T_{\mu}^{\nu(h,g)} \tag{3.3.102}$$

$$R_{\mu}^{\nu(h)} - \frac{1}{2}\delta_{\mu}^{\nu}H = -\chi T_{\mu}^{\nu(h,h)} \tag{3.3.103}$$

In the continuation of our analysis, it will be sufficient to consider one of the two cases. We will rely on the equation system 3.3.98 and 3.3.99, as treated by T. Damour in his January 2019 article[19].

In the context of this symmetry, the interaction tensor to be defined must have a specific form:

$$T_{\mu}^{\nu(g,h)} = \begin{pmatrix} \alpha & 0 & 0 & 0 \\ 0 & \beta & 0 & 0 \\ 0 & 0 & \beta & 0 \\ 0 & 0 & 0 & \beta \end{pmatrix} \tag{3.3.104}$$

This is necessary to satisfy condition 3.3.37, which describes the influence of species g on species h, that is, the effect of *induced geometry* by one population on the other.

Applying the zero divergence condition to equation 3.3.98 leads us to Euler's equation expressing hydrostatic equilibrium:

$$\frac{\mathrm{d}p^{(g)}}{\mathrm{d}r} = -\frac{GM(r)\rho(r)^{(g)}}{r^2} \tag{3.3.105}$$

Based on the system composed of the two equations (2a-2b) resulting from the typographical error in our 2014 publication in *Modern Physics Letters A*, we must

[19]The full detail of the calculations giving the metric solutions is presented in the study of the Compatibility of Field Equations in the Limit of Weak Fields. The second case is treated in the study of the Compatibility of Field Equations Near the Dipole Repeller.

express the interaction tensor as follows:

$$T_{\mu}^{\nu(g,h)} = \begin{pmatrix} \rho^{(g)}{c^{(g)}}^2 & 0 & 0 & 0 \\ 0 & -p^{(g)} & 0 & 0 \\ 0 & 0 & -p^{(g)} & 0 \\ 0 & 0 & 0 & -p^{(g)} \end{pmatrix} \tag{3.3.106}$$

Under these conditions, as demonstrated by T. Damour in his January 2019 article, the zero divergence condition leads to the following relation contradicting 3.3.105:

$$\frac{\mathrm{d}p^{(g)}}{\mathrm{d}r} = +\frac{GM(r)\rho(r)^{(g)}}{r^2} \tag{3.3.107}$$

There is obviously a physical and mathematical inconsistency, which results from an inappropriate choice of the interaction tensor. Indeed, nothing a priori requires us to adopt the expression 3.3.106. The zero divergence condition can be satisfied by using two functions, $\alpha(r)$ and $\beta(r)$, whose nature remains to be defined and constructed.

On the other hand, what we were able to establish in 2019 is that the choice of the following interaction tensor:

$$T_{\mu}^{\nu(g,h)} = \begin{pmatrix} \rho^{(g)}{c^{(g)}}^2 & 0 & 0 & 0 \\ 0 & p^{(g)} & 0 & 0 \\ 0 & 0 & p^{(g)} & 0 \\ 0 & 0 & 0 & p^{(g)} \end{pmatrix} \tag{3.3.108}$$

eliminated this inconsistency, in the case of the Newtonian approximation, the foundations of which are recalled as follows:

- The velocities considered are small compared to the speed of light
- The effects of space curvature remain moderate.

How do we interpret the first condition?

The cosmic fluid is assimilated to a perfect gas. Under this assumption, if $\langle v^2 \rangle$ represents the mean square velocity (associated with thermal agitation), the pressure can be expressed by the following relation:

$$p^{(g)} = \frac{\rho^{(g)}\langle v^{(g)} \rangle^2}{3} \tag{3.3.109}$$

Thus, we can deduce that:

$$v^{(g)} \ll c^{(g)} \implies |p^{(g)}| \ll \rho^{(g)}{c^{(g)}}^2 \tag{3.3.110}$$

Recalling that pressure is nothing but a volumetric density of kinetic energy related to thermal agitation, how can we manage the condition of weak curvature?

The inequality $r \gg 2m$ (where m is often replaced by $\frac{GM}{c^2}$ to obtain a dimension of length, M being the mass of the object) indicates that we are sufficiently far from the gravitational source for the effects of general relativity to be negligible. Indeed, at large distances, the length $\frac{2GM}{c^2}$[20] is completely negligible.

It is important to note that for a star like the Sun, the Schwarzschild radius, which depends solely on mass, is about 3 km, which is negligible compared to the diameter of the star. This observation is valid for all observable celestial objects, except for neutron stars where space-time curvature effects become significant. Similarly, hypermassive objects located at the heart of galaxies are excluded, their nature remaining to be specified in more detail.

Therefore, this approach restricts the field of study to objects that fall within the framework of the Newtonian approximation, which represents 99% of observable objects.

As will be demonstrated in the detailed analysis that follows, by choosing the interaction tensor in the form 3.3.108 and taking into account these Newtonian conditions, we retrieve the relation 3.3.105 and the apparent contradiction is resolved.

Before detailing this analysis, let's go back to our exchanges with T. Damour. In vain, we attempted to communicate this point to him in 2019. We received no response to our letters, nor to our invitation to an informal meeting "in front of a blackboard, without recording or witnesses." For five years, we made similar approaches, including to Étienne Ghys, an eminent mathematician and geometer, as well as the perpetual secretary of the Academy of Sciences, regarding these theoretical questions.

At the end of 2019, in the absence of responses, we posted the details of this calculation on our website so that our scientific colleagues, teachers, engineers, and students could access it[21].

It provides a complete explanation of the calculations.

The detail of the calculations is presented in the study of the Compatibility of Field Equations in the Limit of Weak Fields and attention can be focused on equations 3.3.182 and 3.3.225, which, as explained, both lead to Euler's relation under the Newtonian approximation, namely equation 3.3.105, resolving the apparent mathematical and physical contradiction.

We had informed T. Damour of our observation after the publication of his article

[20] corresponding to the gravitational characteristic length called the *"Schwarzschild radius"*

[21] `http://www.jp-petit.org/papers/cosmo/2019-to-Damour-3.pdf`

on January 7, 2019. However, it seems that he did not become aware of this text until November 2022.

Several scientific and academic colleagues, having incorporated the detail of this calculation and being dismayed by T. Damour's silence for three years, sent him a registered letter with acknowledgment of receipt on November 2, 2022, asking him to respond to our questions[22].

In response, T. Damour quickly published a new article online on December 12, 2022[23].

Allow me to quote an excerpt from this article:

> Dans le document "Sur le "modèle Janus" de J. P. Petit" (mis en ligne sur http://www.ihes.fr/~damour le 4 Janvier 2019), j'avais expliqué en grand détail l'incohérence physique et mathématique de la version du modèle Janus publiée en 2014 par J. P. Petit and G. d'Agostini; c.a.d.
>
> J. P. Petit. et G. d'Agostini, "Negative mass hypothesis in cosmology and the nature of dark energy", Astrophys. Space Sci DOI 10.1007/s10509-014-2106-5);
>
> J. P. Petit, et G. d'Agostini, "Cosmological bimetric model with interacting positive and negative masses and two different speeds of light, in agreement with the observed acceleration of the Universe". Mod. Phys. Lett. A Vol. 29 (no 34) (2014) 145082.
>
> Quelques mois plus tard (le 12 Mars 2019), j'ai reçu une lettre de J. P. Petit affirmant qu'il avait maintenant résolu l'incohérence (que j'avais signalée) de la version 2014 du modèle Janus dans un nouvel article:
>
> Jean-Pierre Petit, Gilles D'Agostini and Nathalie Debergh [disons PDD19], " Physical and Mathematical Consistency of the Janus Cosmological Model (JCM)", Progress in Physics, **15**, issue 1, (2019) (http://www.ptep-online.com)[1]
>
> Dans sa lettre du 12 mars 2019 (et dans un courriel ultérieur du 3 avril 2019) J. P. Petit affirmait qu'il avait corrigé l'incohérence que j'avais pointée du doigt par "une légère modification des seconds membres des équations Janus", et me demandait de modifier mon document du 4 janvier 2019 pour prendre en compte son travail de 2019. J'ai répondu à J. P. Petit dans un courriel d'avril 2019 en y disant que: "Dans votre dernier article, "Physical and Mathematical Consistency of the JCM" (January 2019), vous dites avoir corrigé l'incohérence (soulignée dans mon texte) du modèle Janus par "une légère modification des seconds membres des équations Janus". Mais, les sections 3 et 4 de votre article, loin de fournir une déduction bien définie d'une théorie modifiée cohérente, sont mathématiquement incohérentes, et conduisent, selon votre article lui-même, à une incohérence mathématico-physique."
>
> Malgré cette réponse, il semble que ni J.P. Petit, ni ses collaborateurs (ni plusieurs de ses amis qui m'ont inondé de lettres recommandées ces derniers mois) n'ont apprécié l'incohérence mathématico-physique des équations de champ publiées dans leur article de 2019. Pour clarifier cette situation, je discute ci-

[22] https://www.jp-petit.org/papers/cosmo/2022-11-02-Duval-to-Damour.pdf
[23] https://www.jp-petit.org/papers/cosmo/2022-12-12-Damour-IHES.pdf

And he writes, further on:

Une première nouvelle incohérence concerne l'idée de base du modèle Janus (tel qu'il a été défini dans un cadre newtonien), cad le fait que, dans ce modèle, *les masses positives attirent les masses positives; les masses négatives attirent les masses négatives, mais les masses positives et négatives se repoussent.*

In his analysis, T. Damour questions this interaction scheme by writing:

Cette loi de conservation (par rapport à la connexion ∇_- de la métrique $g^-_{\mu\nu}$) implique, comme il est bien connu, qu'une particule d'épreuve à masse négative doit suivre une *géodésique* de la métrique $g^-_{\mu\nu}$. En particulier, une particule d'épreuve à masse négative autour d'une solution de Schwarzschild de masse négative, sera *repoussée*, et non attirée par la masse centrale négative. Nous avons donc ici une violation frappante d'une des idées de base du modèle Janus. Cela montre que les deux équations de champ (1) ne réussissent pas à donner une description relativiste de la situation physique qu'elles sont censées décrire.

And ends by concluding:

doit suivre une *géodésique* de la métrique $g^-_{\mu\nu}$. En particulier, une particule d'épreuve à masse négative autour d'une solution de Schwarzschild de masse négative, sera *repoussée*, et non attirée par la masse centrale négative. Nous avons donc ici une violation frappante d'une des idées de base du modèle Janus.

This shows that T. Damour did not take into account the effect of the *"minus"* sign present in the right-hand side of the second field equation, whose solution is the metric $h_{\mu\nu}$, from which derive the geodesics followed by negative masses:

$$R^{(g)}_{\mu\nu} - \frac{1}{2} g_{\mu\nu} G = \chi \left(T^{(g,g)}_{\mu\nu} + \sqrt{\frac{|h|}{|g|}} T^{(h,g)}_{\mu\nu} \right) \quad (3.3.35) \qquad (3.3.111)$$

$$R^{(h)}_{\mu\nu} - \frac{1}{2} h_{\mu\nu} H = -\chi \left(T^{(h,h)}_{\mu\nu} + \sqrt{\frac{|g|}{|h|}} T^{(g,h)}_{\mu\nu} \right) \quad (3.3.36) \qquad (3.3.112)$$

We have used the notations of this work. Thus, without the *"minus"* sign, negative masses would repel negative masses, which corresponds to the contribution of the term $T^{(h,h)}_{\mu\nu}$ to the field. Conversely, positive masses attract each other, as indicated by the contribution of the term $\sqrt{\frac{|g|}{|h|}} T^{(g,h)}_{\mu\nu}$. However, it is the *"minus"* sign that

reverses the direction of these forces, a detail that T. Damour seems to have overlooked.

In the continuation of his article, T. Damour addresses the issue of satisfying the Bianchi conditions in the Newtonian approximation regime, a point he seems to have recently discovered, three years late. He states:

équation (5). Il est vrai que cette modification élimine la violente contradiction entre les deux équations newtoniennes (5), en les replaçant par l'unique (et correcte) équation de structure newtonienne

$$p'_+ = -G\rho_+ \frac{M_+(r)}{r^2} \,. \tag{6}$$

Then, he writes the two equations of state:

où la source $T^+_{\mu\nu}$ est stationnaire et à symétrie sphérique. Ces solutions ont été écrites[2] dans les éqs. (45), (46) de PDD19, c-a-d (avec $' = d/dr$)

$$\begin{aligned} p'_+ &= -G\left(\rho_+ + \frac{p_+}{c^2}\right)\frac{M_+(r) + 4\pi p_+ r^3/c^2}{r(r - 2GM_+(r)/c^2)} \,, \\ p'_+ &= -G\left(\rho_+ - \frac{p_+}{c^2}\right)\frac{M_+(r) - 4\pi p_+ r^3/c^2}{r(r + 2GM_+(r)/c^2)} \,, \end{aligned} \tag{7}$$

où $p_+(r)$ est la pression (de la matière ordinaire), $\rho_+(r)$ sa densité, et $M_+(r) = 4\pi \int_0^r dr r^2 \rho_+(r)$ est la masse (positive) contenue dans le rayon r. Notons que l'on passe de la première équation (7) à la seconde par les changements: $p_+ \to -p_+$ et $G \to -G$.

Il est vrai que si l'on prend formellement la limite newtonienne $\frac{1}{c^2} \to 0$ dans les équations (7), ces deux équations deviennent compatibles, car elles deviennent toutes deux identiques à l'unique équation de structure newtonienne (6).

Agreeing three years later, that the previously observed contradiction disappears within the framework of the Newtonian approximation.

We immediately wrote to T. Damour to point out that his interpretation regarding the direction of the forces was incorrect, and that the contradiction related to the laws of interaction stemmed solely from his calculation errors[24].

We then write to him:

[24] https://www.jp-petit.org/papers/cosmo/2022-12-14-to-Damour.pdf

Vous écrivez, je vous cite :

- *Une nouvelle incohérence concerne l'idée de base du modèle Janus (tel qu'il a été défini dans un cadre newtonien), c'est-à-dire le fait que, dans ce modèle, les masses positives attirent les masses positives ; les masses négatives attirent les masses négatives, mais les masses positives et négatives se repoussent. Une conséquence particulière de ce principe fondamental du modèle Janus doit être qu'une étoile de masse négative doit attirer les masses d'épreuve négatives dans son voisinage. Mais de fait les équation Janus impliquent le contraire, les masses d'épreuve négatives sont repoussées.*

Si c'était vrai, cela serait effectivement très grave et constituerait une incohérence ingérable, rhédibitoire.

Malheureusement, c'est complètement faux !

Votre conclusion montre que vous n'avez rien compris au modèle, dont la propriété centrale est, grâce au signe moins (que vous oubliez) qui précède la constante d'Einstein dans le second membre de la seconde équation, de reconstituer les principes d'équivalence et d'action-réaction, donc de produire des lois d'interaction permettant d'échapper à l'ingérable paradoxe runaway. Et tel était son but, pour permettre à des masses négatives de constituer une nouvelle donne en cosmologie.

T. Damour withdraws his version dated December 12, 2022, and replaces it with a new article on December 28, 2022[25].

Let's quote him:

$$\begin{aligned} \frac{dv_+^i}{dt} &= -c^2\Gamma_{i0}^{+0} = +\frac{1}{2}c^2\partial_i g_{00}^{+} = +\partial_i U\,, \\ \frac{dv_+^i}{dt} &= -c^2\Gamma_{i0}^{-0} = +\frac{1}{2}c^2\partial_i g_{00}^{-} = -\partial_i U\,. \end{aligned} \tag{9}$$

La première de ces équations implique qu'une masse d'épreuve positive est attirée par une masse-source positive et repoussée par une masse-source négative, alors que la deuxième de ces équations implique l'inverse: une masse d'épreuve positive doit aussi [comme conséquence nécessaire des éqs (1)] être repoussée par une masse-source positive et attirée par une masse-source négative. En refaisant ce raisonnement à partir d'une source d'épreuve constituée d'une répartition continue de *"poussière" à masse négative*, c.a.d. $T^{1-}_{\mu\nu} = \rho_1^- u_\mu^- u_\nu^-$, on obtiendrait, mutatis mutandis, deux autres équations similairement contradictoires pour la variation de vitesse $\frac{dv_-^i}{dt}$ d'une masse d'épreuve négative. Ceci montre de façon frappante l'incohérence du modèle Janus (ici au niveau newtonien).

Despite the clarification provided in our correspondence of December 12, 2022, T.

[25] https://www.jp-petit.org/papers/cosmo/2022-12-28-Damour-IHES.pdf

Damour maintained his conclusion on the inconsistency of the laws of force. This demonstrates that he either did not grasp or did not wish to grasp the explanations provided.

It is then noteworthy, upon reexamining his text from December 12, 2022, that although the Newtonian approximation eliminates the contradiction, he revisits the case of a relativistic solution for the interior of neutron stars, where such approximations are inadequate. Indeed, the terms $\alpha(r)$ and $\beta(r)$ present in the interaction tensor must be chosen so as to satisfy the zero divergence condition 3.3.37. This would theoretically allow for the construction of the metric $h_{\mu\nu}$. However, what tangible observation would this yield? **None**.

Indeed, this would allow modeling the geodesics taken by photons of negative energy, which remain unobservable. Therefore, we are not obliged to construct this second metric. However, it is perfectly possible to construct the interior metric $g_{\mu\nu}$ in its nonlinear form, namely that of a *"Schwarzschild interior solution"*, which leads to the famous TOV equation of state. This solution had already been proposed by Karl Schwarzschild in his second article of February 1916 [74].

What then, when the field is generated by a negative mass? We observe this in regions where the repulsive effect is evident, on both masses and negative energy photons, due to the presence of a conglomerate of negative mass acting as the *"Dipole Repeller"*.

In such cases, where the object is extended, the Newtonian approximation is entirely adequate. The thermal agitation speeds of atoms of negative mass antimatter are insignificant compared to the speed of negative energy light. Similarly, the Schwarzschild radius associated with the object is negligible compared to its diameter.

The only situation where relativistic corrections might be necessary would be in the case of a neutron star with negative mass. However, such objects do not exist according to our approach (see the section Nature of the primordial antimatter).

Thus, we have established a theoretical framework capable of covering all possible cases and addressing the objections raised by T. Damour.

T. Damour finally acknowledged, after three years of delay in his articles of December 12 and 28, 2022, that there is no manifest inconsistency within the framework of the Newtonian approximation. Therefore, he is not obliged to provide a detailed explanation of the calculation leading to the equations of state. Nonetheless, we consider this necessary to convince the reader.

However, it is not essential to provide a detailed analysis of the calculation of the covariant derivative operators. The contradiction outside the Newtonian framework

simply manifests in the effort to construct a metric solution based on simple symmetry assumptions, namely:

- Stationarity
- Invariance under the action of the SO(3) group

It could be objected that this limits the examination to systems presenting spherical symmetry and free of rotation. But to be rigorous, one should consider:

- The exterior metric, namely that of Kerr.
- An interior metric describing the geometry inside a rotating mass.

The construction of this second metric, which would complement that of Kerr, remains to this day an unfinished task.

Therefore, the focus is on constructing the interior solution with spherical symmetry. This refers to the calculation described starting from page 22 of the article sent to T. Damour in 2019[26]. The relevant detail of these calculations being presented in the Compatibility of Field Equations in the Limit of Weak Fields section.

[26] http://www.jp-petit.org/papers/cosmo/2019-to-Damour-3.pdf

3.3.7 Compatibility of Field Equations in the Limit of Weak Fields

To achieve a complete geometric solution, the model must be capable of reproducing the solution initially developed by K. Schwarzschild in 1916 [75], and extending it to the internal geometry of a sphere filled with incompressible fluid [74].

Mastery of this solution is crucial for calculating the attenuation of the brightness of a distant source, after the light rays it emits have passed through a cluster of negative mass. Indeed, while photons of positive energy interact with positive mass matter[27], they only undergo an anti-gravitational interaction when passing through a negative mass. The schematic representation of this phenomenon is illustrated in 3.16.

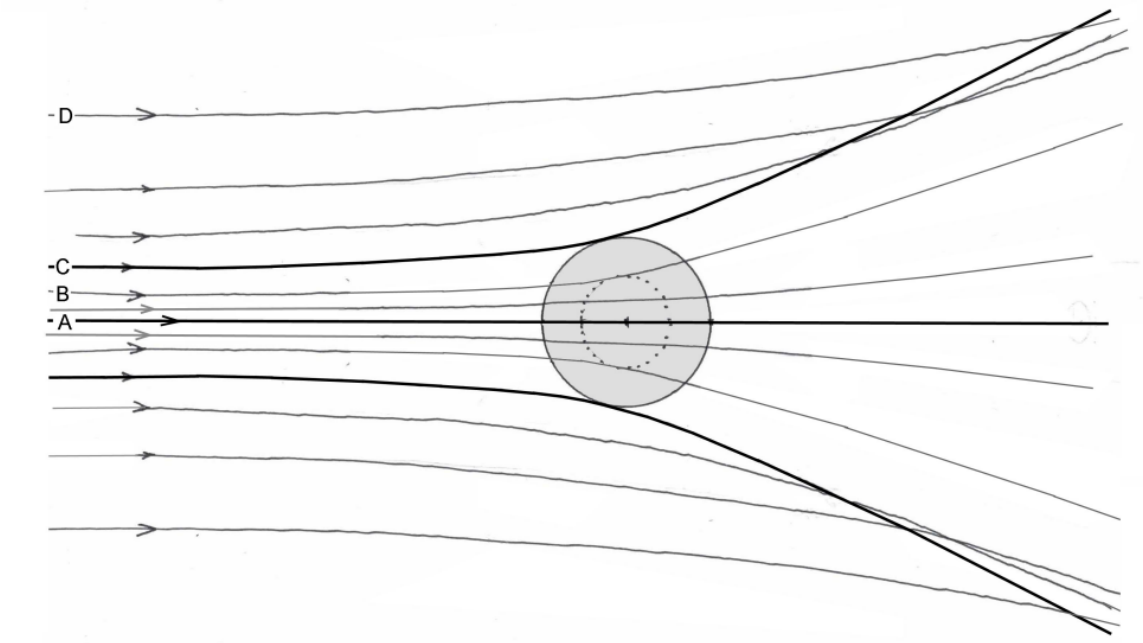

Figure 3.16: Deflection of photons of positive energy by a negative mass.

An analogous situation would arise if we considered a beam of parallel neutrinos of positive energy (or of low mass) passing through a homogeneous mass, also positive (figure 3.17). The trajectories, in both cases, when the curvature remains moderate, are very close to hyperbolas. In both cases, the angle of deviation, whether positive or negative, reaches a maximum (C) when the geodesic is tangent to the limit of the mass, positive or negative. It then decreases steadily to zero at very large distances (D). The angle of deviation is null, due to symmetry, when the geodesic passes through

[27] being emitted or absorbed by it

the center of the mass (A).

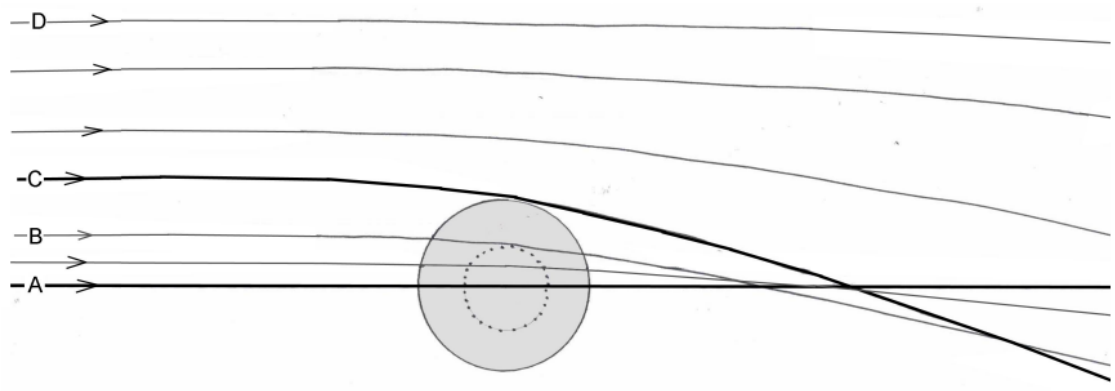

Figure 3.17: Deflection of positive energy neutrinos by a positive mass.

In this calculation of the geodesic trajectories corresponding to this *"Schwarzschild interior solution"* [74] and under quasi-Newtonian conditions, particles, with null or non-null mass, undergo the deviation (B) which would correspond to the action of the mass contained within the dotted sphere, concentrated at the center. A sphere tangent to the line (C) corresponds to the maximum deviation. For line (A), passing through the center of the sphere, it is null. At distance (D), the deviation tends towards zero.

By developing a calculation similar to the construction of the interior metric (14.47) of [1], we can write:

$$\mathrm{d}s^{(g)2} = -e^{\nu^{(g)}}\mathrm{d}x^{0\,2} + e^{\lambda^{(g)}}\mathrm{d}r^2 + r^2\mathrm{d}\phi^2 + r^2\sin^2\theta\mathrm{d}\phi^2 \tag{3.3.113}$$

$$\mathrm{d}s^{(h)2} = -e^{\nu^{(h)}}\mathrm{d}x^{0\,2} + e^{\lambda^{(h)}}\mathrm{d}r^2 + r^2\mathrm{d}\phi^2 + r^2\sin^2\theta\mathrm{d}\phi^2 \tag{3.3.114}$$

Let us now consider these two metrics under the signature $(+---)$:

$$\mathrm{d}s^{(g)\,2} = e^{\nu(r)^{(g)}}\mathrm{d}x^{0\,2} - e^{\lambda(r)^{(g)}}\mathrm{d}r^2 - r^2\mathrm{d}\phi^2 - r^2\sin^2\theta\mathrm{d}\phi^2 \tag{3.3.115}$$

$$\mathrm{d}s^{(h)\,2} = e^{\nu(r)^{(h)}}\mathrm{d}x^{0\,2} - e^{\lambda(r)^{(h)}}\mathrm{d}r^2 - r^2\mathrm{d}\phi^2 - r^2\sin^2\theta\mathrm{d}\phi^2 \tag{3.3.116}$$

In the framework of general relativity, the form of the metric describing a spherically symmetric and static spacetime is often expressed in terms of specific functions to facilitate the analysis of Einstein's equations. One of the most suited solutions to these equations is the exterior Schwarzschild metric 2.3.117, which describes the spacetime around a point mass in empty space. This solution does not explicitly make use of exponential functions in its most well-known form, but more general forms of spherically

symmetric metrics can introduce them to model various matter configurations.

In situations where the matter distribution is not point-like or in regimes of strong spatio-temporal curvature, exponential functions such as $e^{\nu(r)}$ and $e^{\lambda(r)}$ can be introduced to describe the gravitational potential and the curvature of space. These exponential functions facilitate the mathematical handling of differential equations by ensuring certain physical properties, such as the flatness of spacetime at infinity[28].

The function $\nu(r)$ is related to the gravitational potential perceived by an observer at infinity, while $\lambda(r)$ concerns the space curvature due to the presence of matter. For a general spherically symmetric metric, the line element can be written in the form 3.3.115. This formulation allows adapting the metric to different matter distributions and capturing the behavior of gravity in varied contexts, ranging from weak gravitational fields to extreme regimes near supermassive objects such as neutron stars. Thus, the gravitational potential can increase in an *"exponential"* manner near such objects, and exponential functions can capture this behavior accurately.

In the continuation of our analysis, we will rely on the system of equations 3.3.98 and 3.3.99 in the steady-state regime where negative masses are negligible compared to positive masses. We will then determine the solution for each of these field equations in the Newtonian limit.

Solution to the First Field Equation 3.3.98

We can express the metric tensor 3.3.115 as follows[29]:

$$g_{\mu\nu} = \begin{pmatrix} e^{\nu(r)} & 0 & 0 & 0 \\ 0 & -e^{\lambda(r)} & 0 & 0 \\ 0 & 0 & -r^2 & 0 \\ 0 & 0 & 0 & -r^2\sin^2\theta \end{pmatrix} \quad g^{\mu\nu} = \begin{pmatrix} e^{-\nu(r)} & 0 & 0 & 0 \\ 0 & -e^{-\lambda(r)} & 0 & 0 \\ 0 & 0 & -\frac{1}{r^2} & 0 \\ 0 & 0 & 0 & -\frac{1}{r^2\sin^2\theta} \end{pmatrix} \tag{3.3.117}$$

And we know that :

$$g^{\nu}_{\mu} = \delta^{\nu}_{\mu} \tag{3.3.118}$$

We will now calculate the Christoffel symbols[30] of the metric tensor 3.3.115 according to the relation 2.3.73.

[28] This is a characteristic of Minkowski spacetime.

[29] To simplify the notation, the exponent (g) will not be considered throughout the demonstration.

[30] The Christoffel symbols are also known as the Levi-Civita connection coefficients, as we have seen before.

It is noteworthy that this is a static and spherically symmetric metric often used in general relativity. The non-zero components of the metric tensor are:

$$g_{tt} = e^{\nu(r)} \tag{3.3.119}$$
$$g_{rr} = -e^{\lambda(r)} \tag{3.3.120}$$
$$g_{\theta\theta} = -r^2 \tag{3.3.121}$$
$$g_{\phi\phi} = -r^2 \sin^2\theta \tag{3.3.122}$$

And the components of the inverse metric $g^{\beta\alpha}$ are simply the inverse of the diagonal elements[31]:

$$g^{tt} = e^{-\nu(r)} \tag{3.3.123}$$
$$g^{rr} = -e^{-\lambda(r)} \tag{3.3.124}$$
$$g^{\theta\theta} = -\frac{1}{r^2} \tag{3.3.125}$$
$$g^{\phi\phi} = -\frac{1}{r^2 \sin^2\theta} \tag{3.3.126}$$

Given that this metric is diagonal, the calculation simplifies considerably. Many of the Christoffel symbols will be zero because the partial derivatives of the non-diagonal components are zero. We only need to calculate the non-zero components for:

- Γ^r_{tt} :

$$\Gamma^r_{tt} = \frac{1}{2}g^{rr}\left(-\frac{\partial g_{tt}}{\partial r}\right) = \frac{1}{2}(-e^{-\lambda})\left[-\frac{\mathrm{d}}{\mathrm{d}r}(e^{\nu})\right] = \frac{1}{2}e^{\nu-\lambda}\frac{\mathrm{d}\nu}{\mathrm{d}r} = \frac{1}{2}e^{\nu-\lambda}\nu' \tag{3.3.127}$$

- Γ^r_{rr} :

$$\Gamma^r_{rr} = \frac{1}{2}g^{rr}\left(\frac{\partial g_{rr}}{\partial r}\right) = \frac{1}{2}(-e^{-\lambda})\left[\frac{\mathrm{d}}{\mathrm{d}r}(-e^{\lambda})\right] = \frac{1}{2}\frac{\mathrm{d}\lambda}{\mathrm{d}r} = \frac{1}{2}\lambda' \tag{3.3.128}$$

- $\Gamma^r_{\theta\theta}$:

$$\Gamma^r_{\theta\theta} = \frac{1}{2}g^{rr}\left(-\frac{\partial g_{\theta\theta}}{\partial r}\right) = \frac{1}{2}(-e^{-\lambda})(-2r) = re^{-\lambda} \tag{3.3.129}$$

- $\Gamma^r_{\phi\phi}$:

$$\Gamma^r_{\phi\phi} = \frac{1}{2}g^{rr}\left(-\frac{\partial g_{\phi\phi}}{\partial r}\right) = \frac{1}{2}(-e^{-\lambda})(-2r\sin^2\theta) = re^{-\lambda}\sin^2\theta \tag{3.3.130}$$

[31] The non-diagonal elements are zero.

- $\Gamma^{\theta}_{r\theta}$ et $\Gamma^{\phi}_{r\phi}$:

$$\Gamma^{\theta}_{r\theta} = \Gamma^{\phi}_{r\phi} = \frac{1}{2} g^{\theta\theta} \left(\frac{\partial g_{\theta\theta}}{\partial r} \right) = \frac{1}{2} \left(-\frac{1}{r^2} \right) (-2r) = \frac{1}{r} \tag{3.3.131}$$

- $\Gamma^{\theta}_{\phi\phi}$:

$$\Gamma^{\theta}_{\phi\phi} = \frac{1}{2} g^{\theta\theta} \left(-\frac{\partial g_{\phi\phi}}{\partial \theta} \right) = \frac{1}{2} \left(-\frac{1}{r^2} \right) (-2r^2 \sin\theta \cos\theta) = \sin\theta \cos\theta \tag{3.3.132}$$

- $\Gamma^{\phi}_{\theta\phi}$:

$$\Gamma^{\phi}_{\theta\phi} = \frac{1}{2} g^{\phi\phi} \left(\frac{\partial g_{\phi\phi}}{\partial \theta} \right) = \frac{1}{2} \left(-\frac{1}{r^2 \sin^2\theta} \right) (2r^2 \sin\theta \cos\theta) = \cot\theta \tag{3.3.133}$$

- Γ^{t}_{rt} :

$$\Gamma^{t}_{rt} = \frac{1}{2} g^{tt} \left(\frac{\partial g_{tt}}{\partial r} \right) = \frac{1}{2} e^{-\nu} \left(\frac{d}{dr} e^{\nu} \right) = \frac{1}{2} \frac{d\nu}{dr} = \frac{1}{2} \nu' \tag{3.3.134}$$

We can then calculate the necessary components of the Riemann tensor to obtain one of the R_{tt} components of the Ricci tensor in a spherically symmetric spacetime according to the following relation (derived from 3.3.20):

$$R_{tt} = R^{r}_{trt} + R^{\theta}_{t\theta t} + R^{\phi}_{t\phi t} \tag{3.3.135}$$

However, the first component is given by:

$$R^{r}_{trt} = \partial_t \Gamma^{r}_{rt} - \partial_r \Gamma^{r}_{tt} + \Gamma^{r}_{t\lambda} \Gamma^{\lambda}_{rt} - \Gamma^{r}_{r\lambda} \Gamma^{\lambda}_{tt} \tag{3.3.136}$$

Thus, by substitifying each Christoffel symbol with its previously calculated value, and considering that the metric is static, we obtain:

$$R^{r}_{trt} = -\frac{1}{2} e^{\nu-\lambda} \left(\nu'' + \frac{\nu'^2}{2} - \frac{\lambda'\nu'}{2} \right) \tag{3.3.137}$$

The second necessary component $R^{\theta}_{t\theta t}$ is also trivially calculated:

$$R^{\theta}_{t\theta t} = -\Gamma^{\theta}_{\theta r} \Gamma^{r}_{tt} \tag{3.3.138}$$

$$R^{\theta}_{t\theta t} = -\frac{1}{r} \frac{1}{2} e^{\nu-\lambda} \nu' \tag{3.3.139}$$

$$R^{\theta}_{t\theta t} = -\frac{1}{2r} e^{\nu-\lambda} \nu' \tag{3.3.140}$$

$$\tag{3.3.141}$$

The last component $R^{\phi}_{t\phi t}$ is identical to $R^{\theta}_{t\theta t}$[32]:

$$R^{\phi}_{t\phi t} = -\frac{1}{2r}e^{\nu-\lambda}\nu' \tag{3.3.142}$$

Finally, by combining the different terms of the temporal component R_{tt} of the Ricci tensor, we obtain:

$$R_{tt} = e^{\nu-\lambda}\left(-\frac{\nu''}{2} - \frac{\nu'^2}{4} + \frac{\lambda'\nu'}{4} - \frac{\nu'}{r}\right) \tag{3.3.143}$$

Using the same method, we can deduce the other diagonal components of the Ricci tensor:

$$R_{rr} = \frac{\nu''}{2} - \frac{\nu'\lambda'}{4} + \frac{\nu'^2}{4} - \frac{\lambda'}{r} \tag{3.3.144}$$

$$R_{\theta\theta} = e^{-\lambda}\left(1 + \frac{\nu' r}{2} - \frac{\lambda' r}{2}\right) - 1 \tag{3.3.145}$$

$$R_{\phi\phi} = R_{\theta\theta}\sin^2\theta \tag{3.3.146}$$

To determine the Ricci scalar[33], we must first express the components of the Ricci tensor using mixed indices. For this, we raise an index using the inverse metric according to the following relation:

$$R^{\mu}_{\nu} = \sum_{\rho=0}^{3} g^{\mu\rho}R_{\rho\nu} \tag{3.3.147}$$

Thus, we obtain :

$$R^{t}_{t} = g^{tt}R_{tt} = -e^{-\lambda}\left(\frac{\nu''}{2} + \frac{\nu'^2}{4} - \frac{\lambda'\nu'}{4} + \frac{\nu'}{r}\right) \tag{3.3.148}$$

$$R^{r}_{r} = g^{rr}R_{rr} = -e^{-\lambda}\left(\frac{\nu''}{2} - \frac{\nu'\lambda'}{4} + \frac{\nu'^2}{4} - \frac{\lambda'}{r}\right) \tag{3.3.149}$$

$$R^{\theta}_{\theta} = g^{\theta\theta}R_{\theta\theta} = -e^{-\lambda}\left(\frac{1}{r^2} + \frac{\nu'}{2r} - \frac{\lambda'}{2r}\right) + \frac{1}{r^2} \tag{3.3.150}$$

$$R^{\phi}_{\phi} = R^{\theta}_{\theta} \tag{3.3.151}$$

We can deduce the Ricci scalar:

$$R = R^{\mu}_{\mu} = R^{t}_{t} + R^{r}_{r} + R^{\theta}_{\theta} + R^{\phi}_{\phi} \tag{3.3.152}$$

$$R = 2e^{-\lambda}\left(-\frac{\nu''}{2} + \frac{\lambda'\nu'}{4} - \frac{\nu'^2}{4} - \frac{\nu'}{r} + \frac{\lambda'}{r} - \frac{1}{r^2}\right) + \frac{2}{r^2} \tag{3.3.153}$$

[32]Due to the isotropy of the angular coordinates

[33]The Ricci scalar quantifies the total curvature of spacetime

However, the Einstein tensor in mixed mode is given by the following relation:

$$G_{\mu}^{\nu} = R_{\mu}^{\nu} - \frac{1}{2} R \delta_{\mu}^{\nu} \tag{3.3.154}$$

Thus, we can establish each of the components of the Einstein tensor:

$$G_t^t = R_t^t - \frac{1}{2} R \delta_t^t = R_t^t - \frac{1}{2} R = e^{-\lambda} \left(\frac{1}{r^2} - \frac{\lambda'}{r} \right) - \frac{1}{r^2} \tag{3.3.155}$$

$$G_r^r = R_r^r - \frac{1}{2} R \delta_r^r = R_r^r - \frac{1}{2} R = e^{-\lambda} \left(\frac{1}{r^2} + \frac{\nu'}{r} \right) - \frac{1}{r^2} \tag{3.3.156}$$

$$G_\theta^\theta = R_\theta^\theta - \frac{1}{2} R \delta_\theta^\theta = R_\theta^\theta - \frac{1}{2} R = e^{-\lambda} \left(\frac{\nu''}{2} - \frac{\nu' \lambda'}{4} + \frac{\nu'^2}{4} + \frac{\nu' - \lambda'}{2r} \right) \tag{3.3.157}$$

Now, if we consider the Einstein field equation in mixed mode:

$$E_{\mu}^{\nu} = \chi T_{\mu}^{\nu} \tag{3.3.158}$$

We can express its components within the same mathematical context:

$$\begin{aligned} e^{-\lambda} \left(\frac{1}{r^2} - \frac{\lambda'}{r} \right) - \frac{1}{r^2} &= \chi T_t^t \\ e^{-\lambda} \left(\frac{1}{r^2} + \frac{\nu'}{r} \right) - \frac{1}{r^2} &= \chi T_r^r \\ e^{-\lambda} \left(\frac{\nu''}{2} - \frac{\nu' \lambda'}{4} + \frac{\nu'^2}{4} + \frac{\nu' - \lambda'}{2r} \right) &= \chi T_\theta^\theta \end{aligned} \tag{3.3.159}$$

Then:

$$\chi T_t^t - \chi T_r^r = -\left(\nu' + \lambda' \right) \frac{e^{-\lambda}}{r} \tag{3.3.160}$$

Let us examine the classical construction of the interior metric starting from the expression of the energy-momentum tensor $T_{\mu}^{\nu(g,g)}$ from the first field equation 3.3.98 in its classical mixed-mode form[34]:

$$T_{\mu}^{\nu(g,g)} = \begin{pmatrix} \rho & 0 & 0 & 0 \\ 0 & -\frac{p}{c^2} & 0 & 0 \\ 0 & 0 & -\frac{p}{c^2} & 0 \\ 0 & 0 & 0 & -\frac{p}{c^2} \end{pmatrix} \tag{3.3.161}$$

[34] (13.1) page 425 de [1]

The equations 3.3.159 and 3.3.160 are then expressed as follows:

$$e^{-\lambda}\left(\frac{1}{r^2}-\frac{\lambda'}{r}\right)-\frac{1}{r^2}=\chi\rho \tag{3.3.162}$$

$$e^{-\lambda}\left(\frac{1}{r^2}+\frac{\nu'}{r}\right)-\frac{1}{r^2}=-\chi\frac{p}{c^2} \tag{3.3.163}$$

$$e^{-\lambda}\left(\frac{\nu''}{2}-\frac{\nu'\lambda'}{4}+\frac{\nu'^2}{4}+\frac{\nu'-\lambda'}{2r}\right)=-\chi\frac{p}{c^2} \tag{3.3.164}$$

$$-\frac{\nu'+\lambda'}{r}e^{-\lambda}=\chi\left(\rho+\frac{p}{c^2}\right) \tag{3.3.165}$$

From which we can deduce:

$$e^{-\lambda}\left(\frac{1}{r^2}-\frac{\lambda'}{r}\right)-\frac{1}{r^2}=e^{-\lambda}\left[\frac{\nu''}{2}-\frac{\nu'\lambda'}{4}+\frac{\nu'^2}{4}+\frac{\nu'-\lambda'}{2r}\right] \tag{3.3.166}$$

$$e^{\lambda}\frac{1}{r^2}=\frac{1}{r^2}-\frac{\nu'^2}{4}+\frac{\nu'\lambda'}{4}+\frac{\nu'+\lambda'}{2r}-\frac{\nu''}{2} \tag{3.3.167}$$

To solve these differential equations, we can proceed in a manner similar to expression (14.15) from reference [1] in chapter 14 by setting:

$$e^{-\lambda}=1-\frac{2m(r)}{r}\implies 2m(r)=r\left(1-e^{-\lambda}\right) \tag{3.3.168}$$

With :

$$m=\frac{GM}{c^2} \tag{3.3.169}$$

Considering 3.3.162, if we derive this expression, we obtain[35]:

$$2m'=\left(1-e^{-\lambda}\right)+r\lambda'e^{-\lambda} \tag{3.3.170}$$

$$-\frac{2m'}{r^2}=\frac{-1+e^{-\lambda}-r\lambda'e^{-\lambda}}{r^2}=-\frac{1}{r^2}+e^{-\lambda}\left(\frac{1}{r^2}-\frac{\lambda'}{r}\right) \tag{3.3.171}$$

$$m'=-\frac{r^2\chi\rho}{2}=\frac{4\pi r^2G}{c^2}\rho \tag{3.3.172}$$

Similarly to equation (14.18) from [1], we can deduce:

$$m(r)=\frac{G\rho}{c^2}\int_0^r 4\pi r^2\mathrm{d}r=\frac{4}{3}\pi r^3\rho\frac{G}{c^2} \tag{3.3.173}$$

Thus, expression 3.3.163 coupled with expression 3.3.168 allows us to obtain:

$$\nu'=\frac{r}{r(r-2m)}\left(-\chi\frac{pr^2}{c^2}+1\right)-\frac{(r-2m)}{r(r-2m)} \tag{3.3.174}$$

[35]By convention, we adopt the value of Einstein's gravitational constant $\chi=-\frac{8\pi G}{c^2}$ according to (10.98) in [1].

Then :

$$\nu' = 2\frac{m + \frac{4\pi G p r^3}{c^4}}{r(r-2m)} \tag{3.3.175}$$

However, by deriving expression 3.3.163, we obtain:

$$-\chi\frac{p'}{c^2} = \frac{2}{r^3} - \lambda' e^{-\lambda}\left(\frac{1}{r^2} + \frac{\nu'}{r}\right) + e^{-\lambda}\left(\frac{-2}{r^3} + \frac{\nu''}{r} - \frac{\nu'}{r^2}\right) \tag{3.3.176}$$

From which by simplification:

$$-\chi\frac{p'}{c^2} = \frac{2}{r^3} - e^{-\lambda}\left(\frac{\lambda'}{r^2} + \frac{\lambda'\nu'}{r} + \frac{2}{r^3} - \frac{\nu''}{r} + \frac{\nu'}{r^2}\right) \tag{3.3.177}$$

$$-\chi\frac{p'}{c^2} = \frac{2}{r^3} - 2\frac{e^{-\lambda}}{r}\left(\frac{\lambda'}{2r} + \frac{\lambda'\nu'}{2} + \frac{1}{r^2} - \frac{\nu''}{2} + \frac{\nu'}{2r}\right) \tag{3.3.178}$$

$$-\chi\frac{p'}{c^2} = \frac{2}{r^3} - 2\frac{e^{-\lambda}}{r}\left(\frac{1}{r^2} - \frac{\nu'^2}{4} + \frac{\lambda'\nu'}{4} + \frac{\lambda' + \nu'}{2r} - \frac{\nu''}{2} + \frac{\nu'^2}{4} + \frac{\lambda'\nu'}{4}\right) \tag{3.3.179}$$

By combining this result with expression 3.3.167, we can deduce:

$$-\chi\frac{p'}{c^2} = -e^{-\lambda}\frac{\nu'}{2r}(\nu' + \lambda') \tag{3.3.180}$$

Hence, the following expression by coupling with relation 3.3.165:

$$-\chi\frac{p'}{c^2} = -\frac{e^{-\lambda}}{r}(\nu' + \lambda')\frac{\nu'}{2} = \chi\left(\rho + \frac{p}{c^2}\right)\frac{\nu'}{2} \implies \frac{p'}{c^2} = -\frac{\nu'}{2}\left(\rho + \frac{p}{c^2}\right) \tag{3.3.181}$$

Considering expression 3.3.175, we then arrive at the classical Tolman–Oppenheimer–Volkoff (TOV) equation ([49], (14.25c) from [1]):

$$\frac{p'}{c^2} = -\frac{m + \frac{4\pi G p r^3}{c^4}}{r(r-2m)}\left(\rho + \frac{p}{c^2}\right) \tag{3.3.182}$$

We can conclude this calculation by obtaining the explicit form of the interior metric, still within this quasi-Newtonian framework.

Indeed, taking into account relation (14.28) from [1][36] for $r \leq R_s$, and the obtained mass 3.3.173, we can already establish one of the terms of the metric from 3.3.168:

$$e^{-\lambda} = 1 - \frac{2m(r)}{r} = 1 - \frac{8}{3}\pi r^2 \rho\frac{G}{c^2} \implies e^{-\lambda} = 1 - \frac{r^2}{\hat{r}^2} \tag{3.3.183}$$

The interior metric 3.3.115 can then be written as follows:

$$\mathrm{d}s^2 = e^{\nu(r)}\mathrm{d}x^{0\,2} - \frac{\mathrm{d}r^2}{1 - \frac{r^2}{\hat{r}^2}} - r^2\mathrm{d}\phi^2 - r^2\sin^2\theta\mathrm{d}\phi^2 \tag{3.3.184}$$

[36] corresponding to 6.1.2 which will be studied in section 8

Let us now determine the function $\nu(r)$ knowing that the density of the star is assumed to be constant. We then obtain from 3.3.181:

$$\nu' = -\frac{2p'}{\rho c^2 + p} \quad \Rightarrow \quad \nu' = -\frac{2(\rho c^2 + p)'}{\rho c^2 + p} = -2\ln(\rho c^2 + p)' \tag{3.3.185}$$

Then :

$$-\frac{\nu}{2} = \ln(\rho c^2 + p) + C_1 \quad \Longrightarrow \quad {}^{37} \quad De^{-\frac{\nu}{2}} = \frac{8\pi G}{c^2}\left(\rho + \frac{p}{c^2}\right) = -\chi\left(\rho + \frac{p}{c^2}\right) \tag{3.3.186}$$

Considering 3.3.165, we can solve this equation as follows:

$$-\frac{\nu' + \lambda'}{r}e^{-\lambda} = \chi\left(\rho + \frac{p}{c^2}\right) = -De^{-\frac{\nu}{2}} \quad \Longrightarrow \quad rDe^{-\frac{\nu}{2}} = \nu' e^{-\lambda} + \lambda' e^{-\lambda} = \nu' e^{-\lambda} - \frac{\mathrm{d}}{\mathrm{d}r}(e^{-\lambda}) \tag{3.3.187}$$

Thus, from 3.3.183, we obtain:

$$rDe^{-\frac{\nu}{2}} = \nu'\left(1 - \frac{r^2}{\hat{r}^2}\right) - \frac{\mathrm{d}}{\mathrm{d}r}\left(1 - \frac{r^2}{\hat{r}^2}\right) = \nu'\left(1 - \frac{r^2}{\hat{r}^2}\right) + \frac{2r}{\hat{r}^2} \tag{3.3.188}$$

By setting:

$$e^{\frac{\nu}{2}} = \gamma(r) \quad \Longrightarrow \quad \gamma' = \frac{\nu'}{2}e^{\frac{\nu}{2}} \tag{3.3.189}$$

Hence, 3.3.188 allows us to obtain:

$$rD = \nu' e^{\frac{\nu}{2}}\left(1 - \frac{r^2}{\hat{r}^2}\right) + \frac{2r}{\hat{r}^2}e^{\frac{\nu}{2}} = 2\gamma'\left(1 - \frac{r^2}{\hat{r}^2}\right) + \frac{2r}{\hat{r}^2}\gamma \tag{3.3.190}$$

The resolution of first-order linear differential equations relies on the superposition of solutions. The general solution is the sum of a particular solution to the nonhomogeneous equation and the general solution of the homogeneous equation. This method exploits the linearity of differential operators to construct a comprehensive solution that encompasses all possible behaviors of the equation[38].

Thus, a particular solution to this equation is $\gamma_p = \frac{\hat{r}^2 D}{2}$.[39]

[37] By applying the exponential to each side of the equation, we introduce a new integration constant $D = e^{C_1}$ that must be consistent with the structure of Einstein's field equations for a perfect fluid. In these equations, the energy-momentum tensor $T_{\mu\nu}$ is proportional to the Einstein tensor $G_{\mu\nu}$ via Einstein's gravitational constant $\frac{8\pi G}{c^4}$, linking spacetime curvature to matter distribution. Thus, the equation $De^{-\frac{\nu}{2}} = \rho c^2 + p$ can be rewritten as follows: $De^{-\frac{\nu}{2}} = \frac{8\pi G}{c^2}\left(\rho + \frac{p}{c^2}\right)$, where D is determined by the specific boundary conditions for a constant matter density ρ.

[38] The resolution of first-order linear differential equations often involves using the superposition of solutions. This method is based on the fact that differential operators are linear, meaning if two functions f_1 and f_2 are solutions to a linear differential equation, then any linear combination of these functions $af_1 + bf_2$ is also a solution.

[39] Indeed, this solution applied to the right-hand side of equation 3.3.190 yields the left-hand side.

And the general solution of the homogeneous equation is given by[40]:

$$u'\left(1-\frac{r^2}{\hat{r}^2}\right)+\frac{r}{\hat{r}^2}u=0 \quad \Rightarrow \quad u=-B\left(1-\frac{r^2}{\hat{r}^2}\right)^{1/2} \tag{3.3.191}$$

Proof. Let's integrate both sides of the equation.

The integration of the left-hand side involves u and its derivative u', while the integration of the right-hand side is with respect to r.

$$\int \frac{u'}{u}\,\mathrm{d}u=-\int \frac{r}{\hat{r}^2-r^2}\,\mathrm{d}r \tag{3.3.192}$$

This yields:

$$\ln u=\frac{1}{2}\ln(\hat{r}^2-r^2)+C \tag{3.3.193}$$

From which we get:

$$u=-B\left(1-\frac{r^2}{\hat{r}^2}\right)^{1/2} \quad {}^{41} \tag{3.3.194}$$

□

Hence, the general solution is given by:

$$\gamma=e^{\frac{\nu}{2}}=\frac{\hat{r}^2D}{2}-B\left(1-\frac{r^2}{\hat{r}^2}\right)^{\frac{1}{2}} \tag{3.3.195}$$

This allows us to obtain the temporal component of the metric tensor:

$$g_{00}=e^{\nu}=\left[A-B\left(1-\frac{r^2}{\hat{r}^2}\right)^{\frac{1}{2}}\right]^2 \tag{3.3.196}$$

By identification and considering 6.1.2, we obtain:

$$\frac{\hat{r}^2D}{2}=A\Rightarrow D=2\frac{A}{\hat{r}^2}=\frac{2\rho}{3}\frac{8\pi G}{c^2}A=-\chi\frac{2\rho}{3}A \tag{3.3.197}$$

Thus, by coupling 3.3.187 and 3.3.195, we obtain:

$$De^{-\frac{\nu}{2}}=-\chi\left(\rho+\frac{p}{c^2}\right)=-\chi\frac{2\rho}{3}A\left[\frac{\hat{r}^2D}{2}-B\left(1-\frac{r^2}{\hat{r}^2}\right)^{1/2}\right]^{-1} \tag{3.3.198}$$

[40] By setting $u=2\gamma$

[41] B is an integration constant determined in such a way that the solution applied to the left-hand side of the differential equation 3.3.191 cancels it out.

Which enables us to deduce:

$$\rho + \frac{p}{c^2} = \frac{2\rho}{3} \frac{A}{\left[A - B\left(1 - \frac{r^2}{\hat{r}^2}\right)^{1/2}\right]} \tag{3.3.199}$$

However, if we consider that the pressure vanishes at the surface of the sphere at $r = r_n$[42], we can deduce the following relation:

$$A = 3B\left(1 - \frac{{r_n}^2}{\hat{r}^2}\right)^{1/2} \tag{3.3.200}$$

To determine B, we must match the interior and exterior metrics at the sphere's surface[43], which can be expressed as follows by considering 3.3.196:

$$g_{00}^{int}(r_n) = e^{\nu(r_n)} = \left[A - B\left(1 - \frac{{r_n}^2}{\hat{r}^2}\right)^{1/2}\right]^2 = g_{00}^{ext}(r_n) = \left(1 - \frac{2GM}{r_n c^2}\right) \tag{3.3.201}$$

Thus, considering 3.3.200, we can deduce[44]:

$$B^2\left[3\left(1 - \frac{{r_n}^2}{\hat{r}^2}\right)^{1/2} - \left(1 - \frac{{r_n}^2}{\hat{r}^2}\right)^{1/2}\right]^2 = \left(1 - \frac{{r_n}^2}{\hat{r}^2}\right) \implies B = \frac{1}{2} \tag{3.3.202}$$

From which we can obtain:

$$A = \frac{3}{2}\left(1 - \frac{{r_n}^2}{\hat{r}^2}\right)^{1/2} \tag{3.3.203}$$

Then:

$$g_{00}^{int}(r) = \left[\frac{3}{2}\left(1 - \frac{{r_n}^2}{\hat{r}^2}\right)^{1/2} - \frac{1}{2}\left(1 - \frac{r^2}{\hat{r}^2}\right)^{1/2}\right]^2 \tag{3.3.204}$$

Hence, the Schwarzschild interior metric:

$$\mathrm{d}s^2 = \left[\frac{3}{2}\sqrt{\left(1 - \frac{{r_n}^2}{\hat{r}^2}\right)} - \frac{1}{2}\sqrt{\left(1 - \frac{r^2}{\hat{r}^2}\right)}\right]^2 \mathrm{d}{x^0}^2 - \frac{\mathrm{d}r^2}{1 - \frac{r^2}{\hat{r}^2}} - r^2\left(\mathrm{d}\theta^2 + \sin^2\theta \mathrm{d}\phi^2\right) \tag{3.3.205}$$

This metric connects with the Schwarzschild exterior metric :

$$\mathrm{d}s^2 = \left(1 - \frac{2GM}{c^2 r}\right) c^2 \mathrm{d}{x^0}^2 - \frac{\mathrm{d}r^2}{1 - \frac{2GM}{c^2 r}} - r^2\left(\mathrm{d}\theta^2 + \sin^2\theta \mathrm{d}\phi^2\right) \tag{3.3.206}$$

We can thus deduce, according to the classical theory of General Relativity, that a particle of ordinary matter will undergo an attractive gravitational field due to the effect of a distribution of positive masses.

[42] As we will see later 8.2.9

[43] For $r = r_n$, as seen in section 2.3.8

[44] Considering 3.3.173, 3.3.169 et 6.1.2.

Solution to the Second Field Equation 3.3.99

Let's consider the impact of the presence of positive masses on the spacetime geometry structured by $h_{\mu\nu}$ from the second field equation 3.3.99 associated with the population of negative masses. It is worth mentioning that we are entirely free to choose the interaction tensor $T_{\mu}^{\nu(g,h)}$, as this choice can stem from a Lagrangian derivation.

Thus, we have chosen the expression 3.3.108, which we can classically define as follows:

$$T_{\mu}^{\nu(g,h)} = \begin{pmatrix} \rho & 0 & 0 & 0 \\ 0 & \frac{p}{c^2} & 0 & 0 \\ 0 & 0 & \frac{p}{c^2} & 0 \\ 0 & 0 & 0 & \frac{p}{c^2} \end{pmatrix} \tag{3.3.207}$$

We can construct the left-hand side from the metric 3.3.116, which are the same as for the previous case of positive masses[45]. On the right-hand side of the second field equation 3.3.99, the ratio of determinants will be considered almost unity insofar as we perform this calculation within the Newtonian approximation.

Thus, we obtain:

$$\sqrt{\frac{|g|}{|h|}} = \sqrt{\frac{e^{\nu}e^{\lambda}r^4\sin^2\theta}{e^{\bar{\nu}}e^{\bar{\lambda}}r^4\sin^2\theta}} \approx 1 \tag{3.3.208}$$

Then:

$$e^{-\bar{\lambda}}\left(\frac{1}{r^2} - \frac{\bar{\lambda}'}{r}\right) - \frac{1}{r^2} = -\chi\rho \tag{3.3.209}$$

$$e^{-\bar{\lambda}}\left(\frac{1}{r^2} + \frac{\bar{\nu}'}{r}\right) - \frac{1}{r^2} = -\chi\frac{p}{c^2} \tag{3.3.210}$$

$$e^{-\bar{\lambda}}\left(\frac{\bar{\nu}''}{2} - \frac{\bar{\nu}'\bar{\lambda}'}{4} + \frac{\bar{\nu}'^2}{4} + \frac{\bar{\nu}' - \bar{\lambda}'}{2r}\right) = -\chi\frac{p}{c^2} \tag{3.3.211}$$

$$-\frac{\bar{\nu}' + \bar{\lambda}'}{r}e^{-\bar{\lambda}} = -\chi\left(\rho - \frac{p}{c^2}\right) \tag{3.3.212}$$

Hence:

$$e^{\bar{\lambda}}\frac{1}{r^2} = \frac{1}{r^2} - \frac{\bar{\nu}'^2}{4} + \frac{\bar{\nu}'\bar{\lambda}'}{4} + \frac{\bar{\nu}' + \bar{\lambda}'}{2r} - \frac{\bar{\nu}''}{2} \tag{3.3.213}$$

[45] To simplify the notation, the superscripts (g) and (h) will not be taken into account throughout the demonstration. Given that the source of the gravitational field in the second field equation 3.3.99 is created by a positive mass, we will retain the classical form of the variables ρ, c, and p on the right-hand side. However, the left-hand side of this equation describes the geometry induced by this source on the geodesics traveled by negative masses. Therefore, we will use the notations $\bar{\lambda}$, $\bar{\nu}$ on the left-hand side to represent this physical phenomenon.

To solve these differential equations, we can proceed in a manner similar to the previous case by setting:

$$e^{-\bar{\lambda}} = 1 - \frac{2\bar{m}(r)}{r} \implies 2\bar{m}(r) = r\left(1 - e^{-\bar{\lambda}}\right) \tag{3.3.214}$$

From which:

$$-\frac{2\bar{m}'}{r^2} = -\frac{1}{r^2} + e^{-\bar{\lambda}}\left(\frac{1}{r^2} - \frac{\bar{\lambda}'}{r}\right) \tag{3.3.215}$$

$$\tag{3.3.216}$$

However, in a manner similar to equation (14.18) of [1], we can write:

$$\bar{m}' = -\frac{4\pi r^2 G}{c^2}\rho \implies \bar{m}(r) = -\frac{G\rho}{c^2}\int_0^r 4\pi r^2 \mathrm{d}r = -\frac{4}{3}\pi r^3 \rho \frac{G}{c^2} = -m(r) \tag{3.3.217}$$

The expression 3.3.210 thus allows us to obtain:

$$\bar{\nu}' = 2\frac{-m + \frac{4\pi G p r^3}{c^4}}{r(r+2m)} \tag{3.3.218}$$

By deriving expression 3.3.210, we obtain:

$$-\chi\frac{p'}{c^2} = \frac{2}{r^3} - \bar{\lambda}' e^{-\bar{\lambda}}\left(\frac{1}{r^2} + \frac{\bar{\nu}'}{r}\right) + e^{-\bar{\lambda}}\left(\frac{-2}{r^3} + \frac{\bar{\nu}''}{r} - \frac{\bar{\nu}'}{r^2}\right) \tag{3.3.219}$$

From which by simplification:

$$-\chi\frac{p'}{c^2} = \frac{2}{r^3} - e^{-\bar{\lambda}}\left(\frac{\bar{\lambda}'}{r^2} + \frac{\bar{\lambda}'\bar{\nu}'}{r} + \frac{2}{r^3} - \frac{\bar{\nu}''}{r} + \frac{\bar{\nu}'}{r^2}\right) \tag{3.3.220}$$

$$-\chi\frac{p'}{c^2} = \frac{2}{r^3} - 2\frac{e^{-\bar{\lambda}}}{r}\left(\frac{\bar{\lambda}'}{2r} + \frac{\bar{\lambda}'\bar{\nu}'}{2} + \frac{1}{r^2} - \frac{\bar{\nu}''}{2} + \frac{\bar{\nu}'}{2r}\right) \tag{3.3.221}$$

$$-\chi\frac{p'}{c^2} = \frac{2}{r^3} - 2\frac{e^{-\bar{\lambda}}}{r}\left(\frac{1}{r^2} - \frac{\bar{\nu}'^2}{4} + \frac{\bar{\lambda}'\bar{\nu}'}{4} + \frac{\bar{\lambda}' + \bar{\nu}'}{2r} - \frac{\bar{\nu}''}{2} + \frac{\bar{\nu}'^2}{4} + \frac{\bar{\lambda}'\bar{\nu}'}{4}\right) \tag{3.3.222}$$

By combining this result with expression 3.3.213, we can deduce:

$$-\chi\frac{p'}{c^2} = -e^{-\bar{\lambda}}\frac{\bar{\nu}'}{2r}(\bar{\nu}' + \bar{\lambda}') \tag{3.3.223}$$

Hence, the following expression by coupling with relation 3.3.212:

$$-\chi\frac{p'}{c^2} = -\frac{e^{-\bar{\lambda}}}{r}(\bar{\nu}' + \bar{\lambda}')\frac{\bar{\nu}'}{2} = -\chi\left(\rho - \frac{p}{c^2}\right)\frac{\bar{\nu}'}{2} \implies \frac{p'}{c^2} = \frac{\bar{\nu}'}{2}\left(\rho - \frac{p}{c^2}\right) \tag{3.3.224}$$

Considering expression 3.3.218, we then arrive at the Tolman–Oppenheimer–Volkoff (TOV) solution for the population of negative masses:

$$\frac{p'}{c^2} = -\frac{m - \frac{4\pi G p r^3}{c^4}}{r(r+2m)}\left(\rho - \frac{p}{c^2}\right) \tag{3.3.225}$$

The two solutions 3.3.182 and 3.3.225 tend towards the Euler equation in the Newtonian approximation. This also corresponds to the asymptotic satisfaction of the Bianchi identities in the same context[46].

We will now establish the Schwarzschild interior metric associated with the population of negative masses by applying the same calculation scheme as for the population of positive masses, thus constituting the solution to the second field equation 3.3.99.

Indeed, taking into account relation (14.28) from [1] for $r \leq R_s$ and 3.3.214, we can establish the following relation:

$$e^{-\bar{\lambda}} = 1 - \frac{2\bar{m}(r)}{r} \implies e^{-\lambda} = 1 + \frac{r^2}{\hat{r}^2} \tag{3.3.226}$$

The interior metric 3.3.116 can then be written as follows:

$$\bar{\mathrm{d}s}^2 = e^{\bar{\nu}(r)}\mathrm{d}x^{0\,2} - \frac{\mathrm{d}r^2}{1+\frac{r^2}{\hat{r}^2}} - r^2\mathrm{d}\phi^2 - r^2\sin^2\theta\mathrm{d}\phi^2 \tag{3.3.227}$$

Let us now determine the function $\bar{\nu}(r)$ knowing that the density of the star is assumed to be constant. We then obtain from 3.3.224:

$$\bar{\nu}' = -\frac{2p'}{-\rho c^2 + p} \quad \Rightarrow \quad \bar{\nu}' = -\frac{2(\rho c^2 - p)'}{\rho c^2 - p} = -2\ln(\rho c^2 - p)' \tag{3.3.228}$$

Then:

$$-\frac{\bar{\nu}}{2} = \ln(\rho c^2 - p) + C_2 \quad \Longrightarrow \quad \bar{D}e^{-\frac{\bar{\nu}}{2}} = -\chi\left(\rho - \frac{p}{c^2}\right) \tag{3.3.229}$$

Considering 3.3.212, we can solve this equation as follows:

$$-\frac{\bar{\nu}' + \bar{\lambda}'}{r}e^{-\bar{\lambda}} = -\chi\left(\rho - \frac{p}{c^2}\right) = \bar{D}e^{-\frac{\bar{\nu}}{2}} \quad \Longrightarrow \quad -r\bar{D}e^{-\frac{\bar{\nu}}{2}} = \bar{\nu}'e^{-\bar{\lambda}} - \frac{\mathrm{d}}{\mathrm{d}r}(e^{-\bar{\lambda}}) \tag{3.3.230}$$

Thus, from 3.3.226, we obtain:

$$-r\bar{D}e^{-\frac{\bar{\nu}}{2}} = \bar{\nu}'\left(1+\frac{r^2}{\hat{r}^2}\right) - \frac{\mathrm{d}}{\mathrm{d}r}\left(1+\frac{r^2}{\hat{r}^2}\right) = \bar{\nu}'\left(1+\frac{r^2}{\hat{r}^2}\right) - \frac{2r}{\hat{r}^2} \tag{3.3.231}$$

[46] The inequality $r \gg 2m$ (where m is often replaced by $\frac{GM}{c^2}$ to obtain a dimension of length, M being the mass of the object and G the gravitational constant) indicates that we are sufficiently far from the gravitational source for the effects of general relativity to be negligible. Indeed, at great distances, the length $\frac{2GM}{c^2}$ is completely negligible.

By setting:

$$e^{\frac{\bar{\nu}}{2}} = \bar{\gamma}(r) \quad \Longrightarrow \quad \bar{\gamma}' = \frac{\bar{\nu}'}{2} e^{\frac{\bar{\nu}}{2}} \tag{3.3.232}$$

Hence, 3.3.231 allows us to obtain:

$$-r\bar{D} = \nu' e^{\frac{\bar{\nu}}{2}} \left(1 + \frac{r^2}{\hat{r}^2}\right) - \frac{2r}{\hat{r}^2} e^{\frac{\bar{\nu}}{2}} = 2\bar{\gamma}' \left(1 + \frac{r^2}{\hat{r}^2}\right) - \frac{2r}{\hat{r}^2}\bar{\gamma} \tag{3.3.233}$$

A particular solution of this equation is $\bar{\gamma}_p = \frac{\hat{r}^2 \bar{D}}{2}$.

And the general solution of the homogeneous equation is given by[47]:

$$u' \left(1 + \frac{r^2}{\hat{r}^2}\right) - \frac{r}{\hat{r}^2} u = 0 \quad \Rightarrow \quad u = \bar{B} \left(1 + \frac{r^2}{\hat{r}^2}\right)^{1/2} \tag{3.3.234}$$

Hence, the general solution:

$$\bar{\gamma} = e^{\frac{\bar{\nu}}{2}} = \frac{\hat{r}^2 \bar{D}}{2} + \bar{B} \left(1 + \frac{r^2}{\hat{r}^2}\right)^{\frac{1}{2}} \tag{3.3.235}$$

This allows us to obtain the temporal component of the metric tensor:

$$\bar{g}_{00} = e^{\bar{\nu}} = \left[\bar{A} + \bar{B} \left(1 + \frac{r^2}{\hat{r}^2}\right)^{\frac{1}{2}}\right]^2 \tag{3.3.236}$$

By identification and considering 6.1.2, we obtain:

$$\frac{\hat{r}^2 \bar{D}}{2} = \bar{A} \Rightarrow \bar{D} = 2\frac{\bar{A}}{\hat{r}^2} = \frac{2\rho}{3} \frac{8\pi G}{c^2} \bar{A} = -\chi \frac{2\rho}{3} \bar{A} \tag{3.3.237}$$

Thus, by coupling 3.3.230 and 3.3.235, we obtain:

$$\bar{D} e^{-\frac{\nu}{2}} = -\chi \left(\rho - \frac{p}{c^2}\right) = -\chi \frac{2\rho}{3} \bar{A} \left[\frac{\hat{r}^2 \bar{D}}{2} + \bar{B} \left(1 + \frac{r^2}{\hat{r}^2}\right)^{1/2}\right]^{-1} \tag{3.3.238}$$

This enables us to deduce:

$$\rho - \frac{p}{c^2} = \frac{2\rho}{3} \frac{\bar{A}}{\left[\bar{A} + \bar{B} \left(1 + \frac{r^2}{\hat{r}^2}\right)^{1/2}\right]} \tag{3.3.239}$$

However, if we consider that the pressure vanishes at the surface of the sphere at $r = r_n$, we can deduce the following relation:

$$\bar{A} = -3\bar{B} \left(1 + \frac{{r_n}^2}{\hat{r}^2}\right)^{1/2} \tag{3.3.240}$$

[47] By setting $u = 2\bar{\gamma}$

To determine $\bar{B}$, a matching of the interior and exterior metrics at the sphere's surface is required, which can be expressed as follows by considering 3.3.236:

$$\bar{g}_{00}^{int}(r_n) = e^{\bar{\nu}(r_n)} = \left[\bar{A} + \bar{B}\left(1 + \frac{{r_n}^2}{\hat{r}^2}\right)^{1/2}\right]^2 = \bar{g}_{00}^{ext}(r_n) = \left(1 + \frac{2GM}{r_n c^2}\right) \tag{3.3.241}$$

Thus, taking into account expression 3.3.240, we can deduce:

$$\left[-3\bar{B}\left(1 + \frac{{r_n}^2}{\hat{r}^2}\right)^{1/2} + \bar{B}\left(1 + \frac{{r_n}^2}{\hat{r}^2}\right)^{1/2}\right]^2 = \left(1 + \frac{{r_n}^2}{\hat{r}^2}\right) \implies B = \frac{1}{2} \tag{3.3.242}$$

From which we can obtain:

$$\bar{A} = -\frac{3}{2}\left(1 + \frac{{r_n}^2}{\hat{r}^2}\right)^{1/2} \tag{3.3.243}$$

Then:

$$\bar{g}_{00}^{int}(r) = \left[-\frac{3}{2}\left(1 + \frac{{r_n}^2}{\hat{r}^2}\right)^{1/2} + \frac{1}{2}\left(1 + \frac{r^2}{\hat{r}^2}\right)^{1/2}\right]^2 \tag{3.3.244}$$

Hence, the Schwarzschild interior metric:

$$\bar{\mathrm{d}s}^2 = \left[\frac{3}{2}\sqrt{\left(1 + \frac{{r_n}^2}{\hat{r}^2}\right)} - \frac{1}{2}\sqrt{\left(1 + \frac{r^2}{\hat{r}^2}\right)}\right]^2 \mathrm{d}{x^0}^2 - \frac{\mathrm{d}r^2}{1 + \frac{r^2}{\hat{r}^2}} - r^2\left(\mathrm{d}\theta^2 + \sin^2\theta \mathrm{d}\phi^2\right) \tag{3.3.245}$$

This metric must join the Schwarzschild exterior metric:

$$\bar{\mathrm{d}s}^2 = \left(1 + \frac{2GM}{c^2 r}\right) c^2 \mathrm{d}{x^0}^2 - \frac{\mathrm{d}r^2}{1 + \frac{2GM}{c^2 r}} - r^2\left(\mathrm{d}\theta^2 + \sin^2\theta \mathrm{d}\phi^2\right) \tag{3.3.246}$$

We can deduce that a particle with negative mass will undergo a repulsive gravitational field due to the effect of a distribution of positive masses.

Thus, the general form is given by:

$$\mathrm{d}s^{(f)2} = \left[\frac{3}{2}\sqrt{\left(1 - \varepsilon\frac{{r_n}^2}{\hat{r}^2}\right)} - \frac{1}{2}\sqrt{\left(1 - \varepsilon\frac{r^2}{\hat{r}^2}\right)}\right]^2 \mathrm{d}{x^0}^2 - \frac{\mathrm{d}r^2}{1 - \varepsilon\frac{r^2}{\hat{r}^2}} - r^2\left(\mathrm{d}\theta^2 + \sin^2\theta \mathrm{d}\phi^2\right) \tag{3.3.247}$$

With $\varepsilon = 1$ to represent masses of the same sign that attract each other, and $\varepsilon = -1$ for masses of opposite signs that repel each other.

The paradigm of General Relativity (GR) can be summarized as follows:

> *The universe is a manifold M_4, equipped with a metric, solution to Einstein's field equation 2.3.1.*

The Janus model is an extension of GR:

> *The universe is a manifold M_4, equipped with two metrics, solutions of the coupled field equations system 3.3.54 and 3.3.55.*

Under these conditions, GR represents an approximation of this model, in regions where negative mass can be neglected, for example in the vicinity of the Sun. This is obviously an extremely ambitious proposition, which requires observational confirmations to be credible.

3.3.8 Compatibility of Field Equations Near the Dipole Repeller

Consider now the regions where negative masses dominate, for example, near the Dipole Repeller. We can determine the solution for each of the field equations 3.3.102 and 3.3.103.

Solution to the First Field Equation 3.3.102

Let's consider the impact of the presence of negative masses on the geometry of space-time structured by $g_{\mu\nu}$ from the first field equation 3.3.102 associated with the population of positive masses. As we have already mentioned, we can choose the interaction tensor $T_{\mu}^{\nu(h,g)}$ as follows, insofar as this choice can stem from a Lagrangian derivation[48]:

$$T_{\mu}^{\nu(h,g)} = \begin{pmatrix} \bar{\rho} & 0 & 0 & 0 \\ 0 & -\frac{\bar{p}}{\bar{c}^2} & 0 & 0 \\ 0 & 0 & -\frac{\bar{p}}{\bar{c}^2} & 0 \\ 0 & 0 & 0 & -\frac{\bar{p}}{\bar{c}^2} \end{pmatrix} \tag{3.3.248}$$

We can construct the left-hand sides from the metric 3.3.115, which are the same as for the previous cases. On the right-hand side of the first field equation 3.3.102, the ratio of the determinants will be considered nearly unitary.

Thus, we obtain:

$$\sqrt{\frac{|h|}{|g|}} = \sqrt{\frac{e^{\bar{\nu}} e^{\bar{\lambda}} r^4 \sin^2\theta}{e^{\nu} e^{\lambda} r^4 \sin^2\theta}} \approx 1 \tag{3.3.249}$$

$$e^{-\lambda}\left(\frac{1}{r^2} - \frac{\lambda'}{r}\right) - \frac{1}{r^2} = -\chi\bar{\rho} \tag{3.3.250}$$

$$e^{-\lambda}\left(\frac{1}{r^2} + \frac{\nu'}{r}\right) - \frac{1}{r^2} = -\chi\frac{\bar{p}}{\bar{c}^2} \tag{3.3.251}$$

$$e^{-\lambda}\left(\frac{\nu''}{2} - \frac{\nu'\lambda'}{4} + \frac{\nu'^2}{4} + \frac{\nu' - \lambda'}{2r}\right) = -\chi\frac{\bar{p}}{\bar{c}^2} \tag{3.3.252}$$

$$-\frac{\nu' + \lambda'}{r} e^{-\lambda} = -\chi\left(\bar{\rho} - \frac{\bar{p}}{\bar{c}^2}\right) \tag{3.3.253}$$

[48] To simplify the notation, the superscripts (g) and (h) will not be taken into account throughout the demonstration. Given that the source of the gravitational field from the first field equation 3.3.102 is created by a negative mass, we will use the notations $\bar{\rho}$, $\bar{c}$, and $\bar{p}$ on the right-hand side to represent this physical phenomenon. However, the left-hand side of this equation describes the geometry induced by this source on the geodesics traveled by positive masses. Therefore, we will retain the classical form of the variables λ and ν on the left-hand side.

Hence:

$$e^{\lambda}\frac{1}{r^2} = \frac{1}{r^2} - \frac{\nu'^2}{4} + \frac{\nu'\lambda'}{4} + \frac{\nu'+\lambda'}{2r} - \frac{\nu''}{2} \tag{3.3.254}$$

To solve these differential equations, we can proceed in a manner similar to the previous study:

$$e^{-\lambda} = 1 - \frac{2m(r)}{r} \implies 2m(r) = r\left(1 - e^{-\lambda}\right) \quad \text{with} \quad m = \frac{GM}{c^2} \tag{3.3.255}$$

Hence:

$$-\frac{2m'}{r^2} = -\frac{1}{r^2} + e^{-\lambda}\left(\frac{1}{r^2} - \frac{\lambda'}{r}\right) \tag{3.3.256}$$

$$\tag{3.3.257}$$

However, in a manner similar to equation (14.18) of [1], we can write:

$$m' = \frac{4\pi r^2 G}{c^2}\rho \implies m(r) = \frac{G\rho}{c^2}\int_0^r 4\pi r^2 \mathrm{d}r = \frac{4}{3}\pi r^3 \rho \frac{G}{c^2} \tag{3.3.258}$$

The expression 3.3.251 coupled with the expression 3.3.255 thus allows us to obtain:

$$\nu' = 2\frac{-m + \frac{4\pi G\bar{p}r^3}{\bar{c}^4}}{r(r+2m)} \tag{3.3.259}$$

However, by proceeding with the derivation of the expression 3.3.251, we obtain:

$$-\chi\frac{\bar{p}'}{\bar{c}^2} = \frac{2}{r^3} - \lambda' e^{-\lambda}\left(\frac{1}{r^2} + \frac{\nu'}{r}\right) + e^{-\lambda}\left(\frac{-2}{r^3} + \frac{\nu''}{r} - \frac{\nu'}{r^2}\right) \tag{3.3.260}$$

Therefore, by simplification:

$$-\chi\frac{\bar{p}'}{\bar{c}^2} = \frac{2}{r^3} - e^{-\lambda}\left(\frac{\lambda'}{r^2} + \frac{\lambda'\nu'}{r} + \frac{2}{r^3} - \frac{\nu''}{r} + \frac{\nu'}{r^2}\right) \tag{3.3.261}$$

$$-\chi\frac{\bar{p}'}{\bar{c}^2} = \frac{2}{r^3} - 2\frac{e^{-\lambda}}{r}\left(\frac{\lambda'}{2r} + \frac{\lambda'\nu'}{2} + \frac{1}{r^2} - \frac{\nu''}{2} + \frac{\nu'}{2r}\right) \tag{3.3.262}$$

$$-\chi\frac{\bar{p}'}{\bar{c}^2} = \frac{2}{r^3} - 2\frac{e^{-\lambda}}{r}\left(\frac{1}{r^2} - \frac{\nu'^2}{4} + \frac{\lambda'\nu'}{4} + \frac{\lambda'+\nu'}{2r} - \frac{\nu''}{2} + \frac{\nu'^2}{4} + \frac{\lambda'\nu'}{4}\right) \tag{3.3.263}$$

By combining this result with the expression 3.3.254, we can deduce:

$$-\chi\frac{\bar{p}'}{\bar{c}^2} = -e^{-\lambda}\frac{\nu'}{2r}(\nu'+\lambda') \tag{3.3.264}$$

Hence, the following expression by coupling with the relation 3.3.253:

$$-\chi\frac{\bar{p}'}{\bar{c}^2} = -\frac{e^{-\lambda}}{r}(\nu'+\lambda')\frac{\nu'}{2} = -\chi\left(\bar{\rho} - \frac{\bar{p}}{\bar{c}^2}\right)\frac{\nu'}{2} \implies \frac{\bar{p}'}{\bar{c}^2} = \frac{\nu'}{2}\left(\bar{\rho} - \frac{\bar{p}}{\bar{c}^2}\right) \tag{3.3.265}$$

Considering the expression 3.3.259, we then arrive at the Tolman–Oppenheimer–Volkoff (TOV) solution for the population of positive masses[49]:

$$\frac{\bar{p}'}{\bar{c}^2} = -\frac{m - \frac{4\pi G\bar{p}r^3}{\bar{c}^4}}{r(r+2m)}\left(\bar{\rho} - \frac{\bar{p}}{\bar{c}^2}\right) \tag{3.3.266}$$

We will now establish the Schwarzschild interior metric solution of the first field equation 3.3.102.

Indeed, taking into account relation (14.28) from [1] for $r \leq R_s$ and 3.3.255, we can establish the following relation:

$$e^{-\lambda} = 1 - \frac{2m(r)}{r} \implies e^{-\lambda} = 1 + \frac{r^2}{\hat{r}^2} \tag{3.3.267}$$

The interior metric 3.3.115 can then be written as follows:

$$\mathrm{d}s^2 = e^{\nu(r)}\mathrm{d}x^{0^2} - \frac{\mathrm{d}r^2}{1 + \frac{r^2}{\hat{r}^2}} - r^2\mathrm{d}\phi^2 - r^2\sin^2\theta\mathrm{d}\phi^2 \tag{3.3.268}$$

Let's now determine the function $\nu(r)$, knowing that the density of the sphere is constant by assumption. We then obtain from 3.3.224:

$$\nu' = -\frac{2\bar{p}'}{-\bar{\rho}\bar{c}^2 + \bar{p}} \quad \Rightarrow \quad \nu' = -\frac{2(\bar{\rho}\bar{c}^2 - \bar{p})'}{\bar{\rho}\bar{c}^2 - \bar{p}} = -2\ln(\bar{\rho}\bar{c}^2 - \bar{p})' \tag{3.3.269}$$

Then:

$$-\frac{\nu}{2} = \ln(\bar{\rho}\bar{c}^2 - \bar{p}) + C_2 \quad \Longrightarrow \quad De^{-\frac{\nu}{2}} = -\chi\left(\bar{\rho} - \frac{\bar{p}}{\bar{c}^2}\right) \tag{3.3.270}$$

Considering 3.3.253, we can solve this equation as follows:

$$-\frac{\nu' + \lambda'}{r}e^{-\lambda} = -\chi\left(\bar{\rho} - \frac{\bar{p}}{\bar{c}^2}\right) = De^{-\frac{\nu}{2}} \quad \Longrightarrow \quad -rDe^{-\frac{\nu}{2}} = \nu' e^{-\lambda} - \frac{\mathrm{d}}{\mathrm{d}r}(e^{-\lambda}) \tag{3.3.271}$$

Thus, from 3.3.267, we obtain:

$$-rDe^{-\frac{\nu}{2}} = \nu'\left(1 + \frac{r^2}{\hat{r}^2}\right) - \frac{\mathrm{d}}{\mathrm{d}r}\left(1 + \frac{r^2}{\hat{r}^2}\right) = \nu'\left(1 + \frac{r^2}{\hat{r}^2}\right) - \frac{2r}{\hat{r}^2} \tag{3.3.272}$$

However, by setting:

$$e^{\frac{\nu}{2}} = \gamma(r) \quad \Longrightarrow \quad \gamma' = \frac{\nu'}{2}e^{\frac{\nu}{2}} \tag{3.3.273}$$

Hence, 3.3.272 allows us to obtain:

$$-rD = \nu' e^{\frac{\nu}{2}}\left(1 + \frac{r^2}{\hat{r}^2}\right) - \frac{2r}{\hat{r}^2}e^{\frac{\nu}{2}} = 2\gamma'\left(1 + \frac{r^2}{\hat{r}^2}\right) - \frac{2r}{\hat{r}^2}\gamma \tag{3.3.274}$$

[49]The impact of the pressure gradient of negative masses on the geodesics traveled by ordinary matter and photons of positive energy

A particular solution of this equation is $\gamma_p = \frac{\hat{r}^2 D}{2}$.

And the general solution of the homogeneous equation is given by[50]:

$$u'\left(1+\frac{r^2}{\hat{r}^2}\right) - \frac{r}{\hat{r}^2}u = 0 \quad \Rightarrow \quad u = B\left(1+\frac{r^2}{\hat{r}^2}\right)^{1/2} \tag{3.3.275}$$

Hence, the general solution:

$$\gamma = e^{\frac{\nu}{2}} = \frac{\hat{r}^2 D}{2} + B\left(1+\frac{r^2}{\hat{r}^2}\right)^{\frac{1}{2}} \tag{3.3.276}$$

Thus, we obtain the temporal component of the metric tensor:

$$g_{00} = e^{\nu} = \left[A + B\left(1+\frac{r^2}{\hat{r}^2}\right)^{\frac{1}{2}}\right]^2 \tag{3.3.277}$$

By identification and considering 6.1.2, we obtain:

$$\frac{\hat{r}^2 D}{2} = A \Rightarrow D = 2\frac{A}{\hat{r}^2} = \frac{2\bar{\rho}}{3}\frac{8\pi G}{\bar{c}^2}A = -\chi\frac{2\bar{\rho}}{3}A \tag{3.3.278}$$

Thus, by coupling 3.3.271 and 3.3.276, we obtain:

$$De^{-\frac{\nu}{2}} = -\chi\left(\bar{\rho} - \frac{\bar{p}}{\bar{c}^2}\right) = -\chi\frac{2\bar{\rho}}{3}A\left[\frac{\hat{r}^2 D}{2} + B\left(1+\frac{r^2}{\hat{r}^2}\right)^{1/2}\right]^{-1} \tag{3.3.279}$$

Which allows us to deduce:

$$\bar{\rho} - \frac{\bar{p}}{\bar{c}^2} = \frac{2\bar{\rho}}{3}\frac{A}{\left[A + B\left(1+\frac{r^2}{\hat{r}^2}\right)^{1/2}\right]} \tag{3.3.280}$$

However, if we consider that the pressure vanishes at the surface of the sphere at $r = r_n$, we can deduce the following relation:

$$A = -3B\left(1+\frac{{r_n}^2}{\hat{r}^2}\right)^{1/2} \tag{3.3.281}$$

To determine B, it is necessary to match the interior and exterior metrics at the surface of the sphere, which can be translated as follows, considering 3.3.277:

$$g_{00}^{int}(r_n) = e^{\nu(r_n)} = \left[A + B\left(1+\frac{{r_n}^2}{\hat{r}^2}\right)^{1/2}\right]^2 = g_{00}^{ext}(r_n) = \left(1+\frac{2GM}{r_n c^2}\right) \tag{3.3.282}$$

[50]By setting $u = 2\gamma$

Thus, taking into account the expression 3.3.281, we can deduce:

$$\left[-3B\left(1+\frac{{r_n}^2}{\hat{r}^2}\right)^{1/2}+B\left(1+\frac{{r_n}^2}{\hat{r}^2}\right)^{1/2}\right]^2=\left(1+\frac{{r_n}^2}{\hat{r}^2}\right)\implies B=\frac{1}{2} \tag{3.3.283}$$

From which we can obtain:

$$A=-\frac{3}{2}\left(1+\frac{{r_n}^2}{\hat{r}^2}\right)^{1/2} \tag{3.3.284}$$

Then:

$$g_{00}^{int}(r)=\left[-\frac{3}{2}\left(1+\frac{{r_n}^2}{\hat{r}^2}\right)^{1/2}+\frac{1}{2}\left(1+\frac{r^2}{\hat{r}^2}\right)^{1/2}\right]^2 \tag{3.3.285}$$

Hence, the Schwarzschild interior metric solution:

$$\mathrm{d}s^2=\left[\frac{3}{2}\sqrt{\left(1+\frac{{r_n}^2}{\hat{r}^2}\right)}-\frac{1}{2}\sqrt{\left(1+\frac{r^2}{\hat{r}^2}\right)}\right]^2\mathrm{d}x^{0^2}-\frac{\mathrm{d}r^2}{1+\frac{r^2}{\hat{r}^2}}-r^2\left(\mathrm{d}\theta^2+\sin^2\theta\mathrm{d}\phi^2\right) \tag{3.3.286}$$

This metric matches the Schwarzschild exterior metric:

$$\mathrm{d}s^2=\left(1+\frac{2GM}{c^2r}\right)c^2\mathrm{d}x^{0^2}-\frac{\mathrm{d}r^2}{1+\frac{2GM}{c^2r}}-r^2\left(\mathrm{d}\theta^2+\sin^2\theta\mathrm{d}\phi^2\right) \tag{3.3.287}$$

We can deduce that a particle of ordinary matter will undergo a repulsive gravitational field due to the effect of a distribution of negative masses.

Solution of the Second Field Equation 3.3.103

Here, the source of the gravitational field of the second field equation 3.3.103 is created by a negative mass. Therefore, we will adopt the same form of the variables $\bar{\rho}$, $\bar{c}$, and $\bar{p}$ on the right-hand side. The left-hand side of this equation, describing the geometry induced by this source on the geodesics traveled by negative masses, we will also use the notations $\bar{\lambda}$, $\bar{\nu}$ on the left-hand side to represent this physical phenomenon.

Let's examine the classic construction of the interior metric starting from the expression of the energy-momentum tensor $T_{\mu}^{\nu(h,h)}$ of the second field equation 3.3.103 associated with the population of negative masses that we are perfectly free to define in the following way:

$$T_{\mu}^{\nu(h,h)}=\begin{pmatrix}\bar{\rho} & 0 & 0 & 0\\ 0 & \frac{\bar{p}}{\bar{c}^2} & 0 & 0\\ 0 & 0 & \frac{\bar{p}}{\bar{c}^2} & 0\\ 0 & 0 & 0 & \frac{\bar{p}}{\bar{c}^2}\end{pmatrix} \tag{3.3.288}$$

Thus, we can set the following differential equations:

$$e^{-\bar{\lambda}}\left(\frac{1}{r^2}-\frac{\bar{\lambda}'}{r}\right)-\frac{1}{r^2}=\chi\bar{\rho} \tag{3.3.289}$$

$$e^{-\bar{\lambda}}\left(\frac{1}{r^2}+\frac{\bar{\nu}'}{r}\right)-\frac{1}{r^2}=-\chi\frac{\bar{p}}{\bar{c}^2} \tag{3.3.290}$$

$$e^{-\bar{\lambda}}\left(\frac{\bar{\nu}''}{2}-\frac{\bar{\nu}'\bar{\lambda}'}{4}+\frac{\bar{\nu}'^2}{4}+\frac{\bar{\nu}'-\bar{\lambda}'}{2r}\right)=-\chi\frac{\bar{p}}{\bar{c}^2} \tag{3.3.291}$$

$$-\frac{\bar{\nu}'+\bar{\lambda}'}{r}e^{-\bar{\lambda}}=\chi\left(\bar{\rho}+\frac{\bar{p}}{\bar{c}^2}\right) \tag{3.3.292}$$

Hence:

$$e^{-\bar{\lambda}}\left(\frac{1}{r^2}-\frac{\bar{\lambda}'}{r}\right)-\frac{1}{r^2}=e^{-\bar{\lambda}}\left[\frac{\bar{\nu}''}{2}-\frac{\bar{\nu}'\bar{\lambda}'}{4}+\frac{\bar{\nu}'^2}{4}+\frac{\bar{\nu}'-\bar{\lambda}'}{2r}\right] \tag{3.3.293}$$

$$e^{\bar{\lambda}}\frac{1}{r^2}=\frac{1}{r^2}-\frac{\bar{\nu}'^2}{4}+\frac{\bar{\nu}'\bar{\lambda}'}{4}+\frac{\bar{\nu}'+\bar{\lambda}'}{2r}-\frac{\bar{\nu}''}{2} \tag{3.3.294}$$

To solve these differential equations, we can proceed in a manner similar to expression (14.15) from reference [1] in chapter 14 by setting:

$$e^{-\bar{\lambda}}=1-\frac{2\bar{m}(r)}{r}\implies 2\bar{m}(r)=r\left(1-e^{-\bar{\lambda}}\right) \tag{3.3.295}$$

Considering 3.3.289, if we derive this expression, we obtain:

$$2\bar{m}'=\left(1-e^{-\bar{\lambda}}\right)+r\bar{\lambda}'e^{-\bar{\lambda}} \tag{3.3.296}$$

$$-\frac{2\bar{m}'}{r^2}=\frac{-1+e^{-\bar{\lambda}}-r\bar{\lambda}'e^{-\bar{\lambda}}}{r^2}=-\frac{1}{r^2}+e^{-\bar{\lambda}}\left(\frac{1}{r^2}-\frac{\bar{\lambda}'}{r}\right) \tag{3.3.297}$$

$$\bar{m}'=-\frac{r^2\chi\bar{\rho}}{2}=\frac{4\pi r^2G}{\bar{c}^2}\bar{\rho} \tag{3.3.298}$$

In a manner similar to equation (14.18) from [1], we can deduce:

$$\bar{m}(r)=\frac{G\bar{\rho}}{\bar{c}^2}\int_0^r 4\pi r^2\mathrm{d}r=\frac{4}{3}\pi r^3\bar{\rho}\frac{G}{\bar{c}^2} \tag{3.3.299}$$

The expression 3.3.290 coupled with the expression 3.3.295 allows us to obtain:

$$\bar{\nu}'=\frac{r}{r(r-2\bar{m})}\left(-\chi\frac{\bar{p}r^2}{\bar{c}^2}+1\right)-\frac{(r-2\bar{m})}{r(r-2\bar{m})} \tag{3.3.300}$$

Hence:

$$\bar{\nu}'=2\frac{\bar{m}+\frac{4\pi G\bar{p}r^3}{\bar{c}^4}}{r(r-2\bar{m})} \tag{3.3.301}$$

However, by deriving the expression 3.3.290, we obtain:

$$-\chi\frac{\bar{p}'}{\bar{c}^2} = \frac{2}{r^3} - \bar{\lambda}' e^{-\bar{\lambda}}\left(\frac{1}{r^2} + \frac{\bar{\nu}'}{r}\right) + e^{-\bar{\lambda}}\left(\frac{-2}{r^3} + \frac{\bar{\nu}''}{r} - \frac{\bar{\nu}'}{r^2}\right) \tag{3.3.302}$$

Therefore, by simplification:

$$-\chi\frac{\bar{p}'}{\bar{c}^2} = \frac{2}{r^3} - e^{-\bar{\lambda}}\left(\frac{\bar{\lambda}'}{r^2} + \frac{\bar{\lambda}'\bar{\nu}'}{r} + \frac{2}{r^3} - \frac{\bar{\nu}''}{r} + \frac{\bar{\nu}'}{r^2}\right) \tag{3.3.303}$$

$$-\chi\frac{\bar{p}'}{\bar{c}^2} = \frac{2}{r^3} - 2\frac{e^{-\bar{\lambda}}}{r}\left(\frac{\bar{\lambda}'}{2r} + \frac{\bar{\lambda}'\bar{\nu}'}{2} + \frac{1}{r^2} - \frac{\bar{\nu}''}{2} + \frac{\bar{\nu}'}{2r}\right) \tag{3.3.304}$$

$$-\chi\frac{\bar{p}'}{\bar{c}^2} = \frac{2}{r^3} - 2\frac{e^{-\bar{\lambda}}}{r}\left(\frac{1}{r^2} - \frac{\bar{\nu}'^2}{4} + \frac{\bar{\lambda}'\bar{\nu}'}{4} + \frac{\bar{\lambda}' + \bar{\nu}'}{2r} - \frac{\bar{\nu}''}{2} + \frac{\bar{\nu}'^2}{4} + \frac{\bar{\lambda}'\bar{\nu}'}{4}\right) \tag{3.3.305}$$

By combining this result with expression 3.3.294, we can deduce:

$$-\chi\frac{\bar{p}'}{\bar{c}^2} = -e^{-\bar{\lambda}}\frac{\bar{\nu}'}{2r}(\bar{\nu}' + \bar{\lambda}') \tag{3.3.306}$$

Hence, the following expression by coupling with relation 3.3.292:

$$-\chi\frac{\bar{p}'}{\bar{c}^2} = -\frac{e^{-\bar{\lambda}}}{r}(\bar{\nu}' + \bar{\lambda}')\frac{\bar{\nu}'}{2} = \chi\left(\bar{\rho} + \frac{\bar{p}}{\bar{c}^2}\right)\frac{\bar{\nu}'}{2} \implies \frac{\bar{p}'}{\bar{c}^2} = -\frac{\bar{\nu}'}{2}\left(\bar{\rho} + \frac{\bar{p}}{\bar{c}^2}\right) \tag{3.3.307}$$

Considering expression 3.3.301, we can deduce the classical Tolman–Oppenheimer–Volkoff (TOV) equation:

$$\frac{\bar{p}'}{\bar{c}^2} = -\frac{\bar{m} + \frac{4\pi G\bar{p}r^3}{\bar{c}^4}}{r(r - 2\bar{m})}\left(\bar{\rho} + \frac{\bar{p}}{\bar{c}^2}\right) \tag{3.3.308}$$

The two solutions 3.3.266 and 3.3.308 tend towards the Euler equation in the Newtonian approximation. The compatibility of the two field equations is ensured asymptotically.

The form of the interaction tensor 3.3.248 and the energy-momentum tensor 3.3.288 satisfies the Bianchi conditions. This would obviously not be the case if the negative mass were to fall outside of this framework. For that, there would need to exist neutron stars of negative mass. However, the characteristic time of evolution of conglomerates of negative mass, their "cooling time", exceeds the age of the universe. These spheroidal conglomerates cannot evolve, so the content of this negative spacetime will be limited to a mixture of negative mass anti-hydrogen and anti-helium. Since nucleosynthesis cannot occur, there can be no anti-galaxies or anti-stars, regardless of their mass. Consequently, there cannot exist anti-neutron stars.

Moreover, in the case where this negative spacetime would generate hyperdense stars through an as yet unknown mechanism, it would then be necessary to reconsider the

form of these tensors. However, the current configuration satisfies all currently available and potentially available observational data.

Photons of positive energy emitted by sources located behind the Dipole Repulsor will experience a significant decrease in their magnitude due to the negative gravitational lensing effect. These photons then freely traverse this vast void. The effect will be maximal when the photons brush past this spheroidal conglomerate, where the entirety of the mass must be taken into account. However, it will be negligible when these photons pass through the central neighborhood (Figure 3.16).

Thus, we predict that when a map is established by the JWST telescope, the invisible mass will manifest its presence by a brightness attenuation, not over the entire disk, but in a ring.

Let's now determine the explicit form of the interior metric.

Taking into account relation (14.28) from [1] for $r \leq R_s$, we can establish one of the terms of the metric from 3.3.295:

$$e^{-\bar{\lambda}} = 1 - \frac{2\bar{m}(r)}{r} = 1 - \frac{8}{3}\pi r^2 \bar{\rho}\frac{G}{\bar{c}^2} \implies e^{-\bar{\lambda}} = 1 - \frac{r^2}{\hat{r}^2} \tag{3.3.309}$$

The interior metric 3.3.116 can then be written as follows:

$$\bar{\mathrm{d}s}^2 = e^{\bar{\nu}(r)}\mathrm{d}x^{0^2} - \frac{\mathrm{d}r^2}{1-\frac{r^2}{\hat{r}^2}} - r^2\mathrm{d}\phi^2 - r^2\sin^2\theta\mathrm{d}\phi^2 \tag{3.3.310}$$

Let's now determine the function $\bar{\nu}(r)$ knowing that the density of the sphere is constant by assumption. Then, according to 3.3.307, we obtain:

$$\bar{\nu'} = -\frac{2\bar{p}'}{\bar{\rho}\bar{c}^2 + \bar{p}} \quad \Rightarrow \quad \bar{\nu'} = -\frac{2(\bar{\rho}\bar{c}^2 + \bar{p})'}{\bar{\rho}\bar{c}^2 + \bar{p}} = -2\ln(\bar{\rho}\bar{c}^2 + \bar{p})' \tag{3.3.311}$$

Then:

$$-\frac{\bar{\nu}}{2} = \ln(\bar{\rho}\bar{c}^2 + \bar{p}) + C_1 \quad \Longrightarrow \quad \bar{D}e^{-\frac{\bar{\nu}}{2}} = \frac{8\pi G}{\bar{c}^2}\left(\bar{\rho} + \frac{\bar{p}}{\bar{c}^2}\right) = -\chi\left(\bar{\rho} + \frac{\bar{p}}{\bar{c}^2}\right) \tag{3.3.312}$$

Considering 3.3.292, we can solve this equation as follows:

$$-\frac{\bar{\nu'} + \bar{\lambda}'}{r}e^{-\bar{\lambda}} = \chi\left(\bar{\rho} + \frac{\bar{p}}{\bar{c}^2}\right) = -\bar{D}e^{-\frac{\bar{\nu}}{2}} \quad \Longrightarrow \quad r\bar{D}e^{-\frac{\bar{\nu}}{2}} = \bar{\nu'}e^{-\bar{\lambda}} + \bar{\lambda}'e^{-\bar{\lambda}} = \bar{\nu'}e^{-\bar{\lambda}} - \frac{\mathrm{d}}{\mathrm{d}r}(e^{-\bar{\lambda}}) \tag{3.3.313}$$

Thus, according to 3.3.309, we obtain:

$$r\bar{D}e^{-\frac{\bar{\nu}}{2}} = \bar{\nu'}\left(1 - \frac{r^2}{\hat{r}^2}\right) - \frac{\mathrm{d}}{\mathrm{d}r}\left(1 - \frac{r^2}{\hat{r}^2}\right) = \bar{\nu'}\left(1 - \frac{r^2}{\hat{r}^2}\right) + \frac{2r}{\hat{r}^2} \tag{3.3.314}$$

Now, by setting:

$$e^{\frac{\bar{\nu}}{2}} = \bar{\gamma}(r) \quad \Longrightarrow \quad \bar{\gamma}' = \frac{\bar{\nu}'}{2} e^{\frac{\bar{\nu}}{2}} \tag{3.3.315}$$

Hence, 3.3.314 allows us to obtain:

$$r\bar{D} = \bar{\nu}' e^{\frac{\bar{\nu}}{2}} \left(1 - \frac{r^2}{\hat{r}^2}\right) + \frac{2r}{\hat{r}^2} e^{\frac{\bar{\nu}}{2}} = 2\bar{\gamma}' \left(1 - \frac{r^2}{\hat{r}^2}\right) + \frac{2r}{\hat{r}^2}\bar{\gamma} \tag{3.3.316}$$

A particular solution of this equation is $\bar{\gamma}_p = \frac{\hat{r}^2 \bar{D}}{2}$. [51]

And the general solution of the homogeneous equation is given by [52]:

$$\bar{u}' \left(1 - \frac{r^2}{\hat{r}^2}\right) + \frac{r}{\hat{r}^2}\bar{u} = 0 \quad \Rightarrow \quad \bar{u} = -\bar{B} \left(1 - \frac{r^2}{\hat{r}^2}\right)^{1/2} \tag{3.3.317}$$

The general solution is therefore given by:

$$\bar{\gamma} = e^{\frac{\bar{\nu}}{2}} = \frac{\hat{r}^2 \bar{D}}{2} - \bar{B} \left(1 - \frac{r^2}{\hat{r}^2}\right)^{\frac{1}{2}} \tag{3.3.318}$$

Thus, we obtain the temporal component of the metric tensor:

$$\bar{g}_{00} = e^{\bar{\nu}} = \left[\bar{A} - \bar{B} \left(1 - \frac{r^2}{\hat{r}^2}\right)^{\frac{1}{2}}\right]^2 \tag{3.3.319}$$

By identification and considering 6.1.2, we obtain:

$$\frac{\hat{r}^2 \bar{D}}{2} = \bar{A} \Rightarrow \bar{D} = 2\frac{\bar{A}}{\hat{r}^2} = \frac{2\bar{\rho}}{3} \frac{8\pi G}{\bar{c}^2} \bar{A} = -\chi \frac{2\bar{\rho}}{3} \bar{A} \tag{3.3.320}$$

Thus, by coupling 3.3.313 and 3.3.318, we obtain:

$$\bar{D} e^{-\frac{\bar{\nu}}{2}} = -\chi \left(\bar{\rho} + \frac{\bar{p}}{\bar{c}^2}\right) = -\chi \frac{2\bar{\rho}}{3} \bar{A} \left[\frac{\hat{r}^2 \bar{D}}{2} - \bar{B} \left(1 - \frac{r^2}{\hat{r}^2}\right)^{1/2}\right]^{-1} \tag{3.3.321}$$

Which allows us to deduce:

$$\bar{\rho} + \frac{\bar{p}}{\bar{c}^2} = \frac{2\bar{\rho}}{3} \frac{\bar{A}}{\left[\bar{A} - \bar{B}\left(1 - \frac{r^2}{\hat{r}^2}\right)^{1/2}\right]} \tag{3.3.322}$$

Now, if we consider that the pressure vanishes at the surface of the sphere at $r = \bar{r_n}$, we can deduce the following relation:

$$\bar{A} = 3\bar{B} \left(1 - \frac{\bar{r_n}^2}{\hat{r}^2}\right)^{1/2} \tag{3.3.323}$$

[51] Indeed, this solution applied to the right-hand side of equation 3.3.316 yields the left-hand side.
[52] By setting $\bar{u} = 2\bar{\gamma}$

To determine B, we need to match the interior and exterior metrics at the surface of the sphere, which can be translated as follows, considering 3.3.319:

$$\bar{g}_{00}^{int}(\bar{r_n}) = e^{\bar{\nu}(\bar{r_n})} = \left[\bar{A} - \bar{B}\left(1 - \frac{\bar{r_n}^2}{\hat{r}^2}\right)^{1/2}\right]^2 = \bar{g}_{00}^{ext}(\bar{r_n}) = \left(1 - \frac{2G\bar{M}}{\bar{r_n}\bar{c}^2}\right) \tag{3.3.324}$$

Thus, considering 3.3.323, we can deduce:

$$\bar{B}^2\left[3\left(1 - \frac{\bar{r_n}^2}{\hat{r}^2}\right)^{1/2} - \left(1 - \frac{\bar{r_n}^2}{\hat{r}^2}\right)^{1/2}\right]^2 = \left(1 - \frac{\bar{r_n}^2}{\hat{r}^2}\right) \implies \bar{B} = \frac{1}{2} \tag{3.3.325}$$

From which we can obtain:

$$\bar{A} = \frac{3}{2}\left(1 - \frac{\bar{r_n}^2}{\hat{r}^2}\right)^{1/2} \tag{3.3.326}$$

Then:

$$\bar{g}_{00}^{int}(r) = \left[\frac{3}{2}\left(1 - \frac{\bar{r_n}^2}{\hat{r}^2}\right)^{1/2} - \frac{1}{2}\left(1 - \frac{r^2}{\hat{r}^2}\right)^{1/2}\right]^2 \tag{3.3.327}$$

Hence, the interior Schwarzschild metric:

$$\bar{\mathrm{d}s}^2 = \left[\frac{3}{2}\sqrt{\left(1 - \frac{\bar{r_n}^2}{\hat{r}^2}\right)} - \frac{1}{2}\sqrt{\left(1 - \frac{r^2}{\hat{r}^2}\right)}\right]^2 \mathrm{d}x^{0^2} - \frac{\mathrm{d}r^2}{1 - \frac{r^2}{\hat{r}^2}} - r^2\left(\mathrm{d}\theta^2 + \sin^2\theta\mathrm{d}\phi^2\right) \tag{3.3.328}$$

This metric matches the exterior Schwarzschild metric:

$$\bar{\mathrm{d}s}^2 = \left(1 - \frac{2G\bar{M}}{\bar{c}^2 r}\right)\bar{c}^2\mathrm{d}x^{0^2} - \frac{\mathrm{d}r^2}{1 - \frac{2G\bar{M}}{\bar{c}^2 r}} - r^2\left(\mathrm{d}\theta^2 + \sin^2\theta\mathrm{d}\phi^2\right) \tag{3.3.329}$$

We can deduce that a particle of negative mass will undergo an attractive gravitational field due to the effect of a distribution of negative masses.

Chapter 4

Modeling Galactic Dynamics

It has been possible to construct a model of a galaxy with spherical symmetry surrounded by a halo of negative masses. This has a confining effect that explains a number of phenomena generally attributed to dark matter in the context of the Standard Model, notably its deceleration resulting from its interaction through *dynamic friction* with its negative mass environment, as well as its spiral structure. This model also explains why stars in the outer regions of galaxies move at higher speeds than those predicted by the gravity of visible matter alone. Without negative masses, the laws of Newtonian gravity would suggest that these stars should move more slowly, being further from the galaxy's massive center. However, observations show that these stars have relatively high speeds, suggesting the additional anti-gravitational influence of an invisible mass, namely negative mass matter.

Elliptical galaxies constitute a significant proportion of the mass of the visible Universe. They are primarily composed of old stars, characterized by a high velocity dispersion and distributed in the disk[1] as well as in the galactic halo, and contain very little gas[2]. In contrast, spiral galaxies contain about 10% of their mass in the form of interstellar gas. This gas is primarily concentrated around the diametral plane, forming a very flattened disk. Its distribution is not uniform, but shows condensations, the most significant of which contribute to the galaxy's spiral structure. In these galaxies, young stars, with low velocity dispersion and concentrated near the plane of symmetry, are primarily found in the spiral arms.

Globular clusters, on the other hand, are systems with spherical symmetry, virtually devoid of gas.

[1] The disk refers to a flat and extended structure, distinct from the denser central regions of galaxies, called bulges, and from the external galactic halos, which contain older stars and less gas.

[2] Elliptical galaxies are distinguished by their spheroidal or elliptical shape without distinct spiral arms. They generally have a homogeneous distribution of old stars and little ongoing star formation, due to the scarcity of gas necessary for the birth of new stars. These galaxies are often found in densely populated environments like the centers of galaxy clusters.

Therefore, to study the dynamics of stellar systems, such as galaxies or globular clusters, it is reasonable as a first approximation to neglect the presence of gas and focus solely on the population of old stars, with high velocity dispersion. It is noteworthy that on the scale of a galactic rotation, these systems are virtually collisionless and can be described by *the Vlasov equation*.

4.1 The Vlasov Equation and Its Components

Self-gravitating stellar systems had already been modeled in 1942 by S. Chandrasekhar [14] using a Maxwell-Boltzmann type solution of *the Vlasov equation*, coupled with *the Poisson equation*. The stars in galaxies form non-collisional ensembles[3].

Indeed, *the Vlasov equation* is a fundamental equation in plasma physics and stellar dynamics that describes the temporal evolution of the *distribution function* $f(\vec{r}, \vec{v}, t)$ in *phase space* for a system of particles under the influence of a conservative force field. This equation helps scientists understand how groups of particles, like stars in a galaxy or particles in a plasma, move and behave over time.

The *distribution function* mentioned in this equation represents the distribution of particles in a space that accounts for both their position and velocity. This *phase space* is a conceptual tool that allows for visualizing and calculating the behavior of a large number of particles simultaneously.

The Vlasov equation is given by:

$$\frac{\partial f}{\partial t} + \vec{v} \cdot \nabla_{\vec{r}} f - \nabla_{\vec{r}} \Psi \cdot \nabla_{\vec{v}} f = 0 \tag{4.1.1}$$

where:

- $f(\vec{r}, \vec{v}, t)$ is the distribution function representing the number density of particles in phase space at a position $\vec{r}$, with a velocity $\vec{v}$, at time t.

- $\frac{\partial f}{\partial t}$ is the partial derivative of the distribution function with respect to time, representing the change in the distribution function over time.

[3]When the distribution function evolves *collisionlessly* according to *the Vlasov equation*, it means that it describes the motion of particles considering that they do not directly collide with each other. This is a useful approximation for studying systems like galaxies, where stars are so far apart from one another that they interact primarily through gravity and not through direct collisions.

- $\vec{v}\cdot\nabla_{\vec{r}}f$ represents the convective derivative[4] in position space, which describes how the distribution function changes due to the motion of particles through space at velocity $\vec{v}$.

- $\Psi(\vec{r},t)$ is the scalar potential field, which depends on position and time, and its negative gradient $-\nabla_{\vec{r}}\Psi$ gives the force per unit mass acting on the particles.

- $-\nabla_{\vec{r}}\Psi\cdot\nabla_{\vec{v}}f$ is the force term, representing how the distribution function changes due to forces acting on the particles, altering their velocities.

The equation asserts that the distribution function is constant along the particle trajectories in the absence of collisions, which is known as *Liouville's theorem*. This property is crucial for the conservation of phase space density and underlies the collisionless dynamics described by the Vlasov equation.

NB:

- In a physical context, the term $-\nabla_{\vec{r}}\Psi$ represents the force acting on a particle. For a scalar potential $\Psi(\vec{r},t)$, the negative gradient with respect to position, written as $-\nabla_{\vec{r}}\Psi$, gives us the force vector $\vec{F}$. This relationship is a cornerstone of classical mechanics and is described by the equation:

$$\vec{F} = -\nabla_{\vec{r}}\Psi \tag{4.1.2}$$

  where:

  - $\vec{F}$ is the force vector experienced by a particle,

  - $\nabla_{\vec{r}}$ denotes the gradient with respect to position,

  - $\Psi(\vec{r},t)$ is the scalar potential field that depends on the position $\vec{r}$ and time t.

  The negative sign indicates that the force acts in the direction of decreasing potential energy, aligning with the physical principle that particles tend to move from regions of high potential energy to regions of low potential energy.

[4]The convective derivative describes how a quantity (like density, velocity, temperature, etc.) changes following the general movement of a fluid system. It takes into account both the variation of the quantity over time and the variation due to the movement of the fluid.

- **The Maxwell-Boltzmann Distribution**, named after James Clerk Maxwell and Ludwig Boltzmann, is a fundamental statistical law in physics that plays a crucial role in describing the distribution of particle velocities in a gas at a specific temperature. When a gas is heated, energy is imparted to its particles, causing them to move at different velocities. This distribution mathematically characterizes how these velocities are distributed among the particles in an equilibrium gas, meaning that the overall velocity distribution remains constant over time, even though individual particles may exchange energy during collisions.

  To illustrate this concept, imagine a room filled with bouncing balls, each representing a particle in the gas. These balls collide with each other, sometimes changing speeds. Some may slow down, while others speed up. Over time, you would observe that some balls move slowly, most at moderate speeds, and a few move very quickly. The Maxwell velocity distribution is a mathematical model that predicts the proportion of particles moving at each speed in the gas.

  The distribution is expressed by the probability density function $f(v)$, where v is the velocity of a particle, m is the mass of a particle, k is the Boltzmann constant, T is the temperature of the gas, and e is the base of the natural logarithm. The formula for $f(v)$ is given by:

$$f(v) = \left(\frac{m}{2\pi kT}\right)^{\frac{3}{2}} 4\pi v^2 e^{-\frac{mv^2}{2kT}} \tag{4.1.3}$$

  Understanding the Maxwell-Boltzmann distribution is essential not only for grasping the behavior of gases but also forms the basis of the kinetic theory of gases, which helps scientists predict the properties of gases such as diffusion, viscosity, and thermal conductivity.

4.2 The Vlasov-Poisson System

The Vlasov-Poisson system describes the evolution of a self-gravitating system in the absence of collisions. As we have mentioned, the Vlasov equation governs the evolution of the distribution function $f(\vec{r}, \vec{v}, t)$ in phase space, and the Poisson equation relates the gravitational potential Ψ to the mass density ρ:

$$\Delta\Psi = 4\pi G\rho \tag{4.2.1}$$

where ρ is related to the distribution function by $\rho(\vec{r}, t) = \int f(\vec{r}, \vec{v}, t)\, \mathrm{d}^3\vec{v}$, which is the mass density obtained by integrating the distribution function over all velocities. This system of equations is fundamental in the study of the dynamics of stellar systems

and galaxies.

NB: The connection between the Poisson equation and the Vlasov equation is made through the gravitational potential Ψ. In a system composed of many particles, such as stars in a galaxy or molecules in a gas, the Vlasov equation governs the evolution of the particle distribution function in phase space, and the Poisson equation relates the collective effect of these particles' mass distribution to the potential field in which they move. When the Vlasov equation is used to describe a self-gravitating system of particles, like the stars in a galaxy, it is often coupled with the Poisson equation. The gravitational potential that appears in the Vlasov equation is the same potential that satisfies the Poisson equation. In this coupled system, the Poisson equation provides the field equation that determines the gravitational potential Ψ resulting from the mass distribution ρ, and the Vlasov equation uses this potential to determine how the distribution function evolves over time.

In the context of astrophysics, when describing the motion of particles in a system, it is common to distinguish between the average velocity of the particles and their individual or residual velocities. The average velocity, denoted $\mathbf{c}_o = \langle \mathbf{c} \rangle$, is the mean velocity of all the particles in the system. The residual velocity $\mathbf{C}$, also known as peculiar velocity (relative or proper velocity) of a particle, is then defined as its individual velocity (or absolute velocity) $\mathbf{c}$ minus this average velocity[5]:

$$\mathbf{C} = \mathbf{c} - \mathbf{c}_o \tag{4.2.2}$$

This residual velocity represents the deviation of a particle's velocity from the average flow and can be associated with the concept of thermal velocity in fluid mechanics, which is the random motion of particles in a fluid. Indeed, in a system like a galaxy or a fluid, the particles (such as stars or molecules) move around. The average velocity is the mean velocity of all these particles. However, each particle has its own velocity, which might be different from this average. The residual velocity of a particle is the difference between its individual velocity and the average velocity of the system. It's like measuring how much faster or slower a particle's motion is compared to the average movement in the system.

Furthermore, an operator D is defined that combines the time derivative with convection by the mean flow (Page 48 - Section 3.12 of [16]) :

$$\frac{D}{Dt} = \frac{\partial}{\partial t} + \mathbf{c}_o \cdot \nabla_{\mathbf{r}} \tag{4.2.3}$$

where $\frac{\partial}{\partial t}$ is the temporal partial derivative, and $\mathbf{c}_o \cdot \nabla_{\mathbf{r}}$ denotes the advection operator acting on a scalar or vector field with respect to the mean velocity (Page 9 - Section

[5] We will now use a bold letter to define a vector and a regular letter to denote a scalar. Additionally, we will use c instead of v to define the velocity according to [16]

1.33 of [16]).

This operator D is used to describe the change of a quantity both in terms of time and as it is transported by the mean flow. Indeed, this operator is a way of accounting for two things at once: how particles change over time (that's the $\frac{\partial}{\partial t}$ part) and how they move with the flow or the average movement of the system (that's the $\mathbf{c}_o \cdot \nabla_\mathbf{r}$ part). $\mathbf{c}_o$ is the average velocity, and $\nabla_\mathbf{r}$ is a mathematical operator that measures how particles change from one place to another. By combining these two, the operator D helps us understand how a quantity (like density or pressure) changes not only over time but also as it moves with the general flow of the system.

It is particularly useful in the study of fluid dynamics and plasma physics, where it can simplify the equations governing the system's behavior by focusing on fluctuations rather than the overall movement.

We can then consider two Vlasov equations, written in terms of residual velocities, coupled by the Poisson equation. These equations are written:

$$\frac{Df}{Dt} + \mathbf{C} \cdot \nabla_\mathbf{r} f - \left(\nabla_\mathbf{r} \Psi + \frac{D\mathbf{c}_o}{Dt} \right) \cdot \nabla_\mathbf{C} f - \nabla_\mathbf{C} f \cdot \mathbf{C} : \nabla_\mathbf{r} \mathbf{c}_o = 0 \tag{4.2.4}$$

$$\frac{\underline{D}\underline{f}}{\underline{D}\underline{t}} + \underline{\mathbf{C}} \cdot \nabla_\mathbf{r} \underline{f} - \left(\nabla_\mathbf{r} \Psi + \frac{\underline{D}\underline{\mathbf{c}}_o}{\underline{D}\underline{t}} \right) \cdot \nabla_{\underline{\mathbf{C}}} \underline{f} - \nabla_{\underline{\mathbf{C}}} f \cdot \underline{\mathbf{C}} : \nabla_\mathbf{r} \underline{\mathbf{c}}_o = 0 \tag{4.2.5}$$

where, I remind you, D is the convective derivative with respect to the mean flow, $\mathbf{c}_o$ is the average velocity, $\mathbf{C}$ is the residual velocity or the proper thermal agitation velocity of a particle, f is the distribution function, and Ψ is the gravitational potential.

The terms $\nabla_\mathbf{C} f \cdot \mathbf{C}$ and $\nabla_\mathbf{r} \mathbf{c}_o$ are called dyadic products[6], which are tensor operations resulting in matrices (in this context, called dyadic matrices according to [16] and [79]). The term $\nabla_\mathbf{C} f \cdot \mathbf{C} : \nabla_\mathbf{r} \mathbf{c}_o$ represents the scalar product of two dyads defined ([16] page 16 eq. 1.31.4 and [79] section 3.3) by the notation $A : B = A_i^j B_i^j$.

NB: $A : B$ represents the scalar (dot) product of two matrices or dyads, where each element of the first matrix A is multiplied by the corresponding element of the second matrix B, and the products are summed:

$$A : B = \sum_{i=1}^{3} \sum_{j=1}^{3} A_{ij} B_{ij} \tag{4.2.6}$$

[6]These are complex mathematical operations that transform velocities and other quantities into matrices (a type of mathematical table). These matrices are used to describe the relationships between different velocities and to understand how they change together.

Now, we know from 4.2.3 that:

$$\frac{Df}{Dt} = \frac{\partial f}{\partial t} + \mathbf{c}_o \frac{\partial f}{\partial \mathbf{r}} = \nabla_t f + \mathbf{c}_o \cdot \nabla_{\mathbf{r}} f \tag{4.2.7}$$

Then,

$$\frac{D\ln(f)}{Dt} = \frac{1}{f}\frac{Df}{Dt} = \frac{\partial \ln(f)}{\partial t} + \mathbf{c}_o \frac{\partial \ln(f)}{\partial \mathbf{r}} = \nabla_t \ln(f) + \mathbf{c}_o \cdot \nabla_{\mathbf{r}} \ln(f) \tag{4.2.8}$$

Thus, the equations 4.2.4 and 4.2.5 become:

$$\nabla_t \ln(f) + \mathbf{c}_o \cdot \nabla_{\mathbf{r}} \ln(f) + \mathbf{C} \cdot \nabla_{\mathbf{r}} \ln(f) - \left(\nabla_{\mathbf{r}} \Psi + \frac{D\mathbf{c}_o}{Dt} \right) \cdot \nabla_{\mathbf{C}} \ln(f) - \nabla_{\mathbf{C}} \ln(f) \cdot \mathbf{C} : \nabla_{\mathbf{r}} \mathbf{c}_o = 0 \tag{4.2.9}$$

$$\nabla_{\underline{t}} \underline{\ln(f)} + \underline{\mathbf{c}}_o \cdot \nabla_{\mathbf{r}} \underline{\ln(f)} + \underline{\mathbf{C}} \cdot \nabla_{\mathbf{r}} \underline{\ln(f)} - \left(\nabla_{\mathbf{r}} \Psi + \frac{D\mathbf{c}_o}{\underline{Dt}} \right) \cdot \nabla_{\underline{\mathbf{C}}} \underline{\ln(f)} - \nabla_{\underline{\mathbf{C}}} \underline{\ln(f)} \cdot \underline{\mathbf{C}} : \nabla_{\mathbf{r}} \underline{\mathbf{c}}_o = 0 \tag{4.2.10}$$

To search for solutions to these equations, the principle is as follows:

1. We start by taking a distribution f as a function of velocities and time.
2. Then, we substitute it into the Vlasov equation.
3. We group the terms according to the monomials of velocity components, which generates as many individual equations.

4.3 Modeling a Galaxy with an Ellipsoidal Velocity Distribution

The velocity distribution in a stellar system can often be described by a Maxwell-Boltzmann distribution function. The natural logarithm of this distribution function f is expressed in terms of the residual velocity components C_x, C_y, C_z, which in the case of the Maxwell-Boltzmann distribution leads to a spherical polynomial.

If the distribution is not isotropic[7], which is often the case, for example, in the solar system around the Sun, the velocity distribution can take an ellipsoidal shape, as shown in Figure 4.1. Indeed, the velocity ellipsoid represents a velocity space where the distribution is more ellipsoidal than spherical, indicating an anisotropic distribution[8].

[7] The term *isotropic* refers to a property being identical in all directions. An isotropic velocity distribution would mean that the velocities of objects in space are evenly distributed in all directions.

[8] The velocities of stars or particles within a galaxy are not distributed uniformly in all directions (isotropic), but rather anisotropically, with direction preferences that can be described by an ellipsoid

The distribution of stellar residual velocities around the Sun is not isotropic but corresponds to a velocity ellipsoid where one of the axes is roughly double the other two. Figure 4.1 represents the velocity ellipsoid of a galaxy rotating around the axis $\overrightarrow{OZ}$[9]. A model of a galaxy (or globular cluster) has been constructed corresponding to this figure.

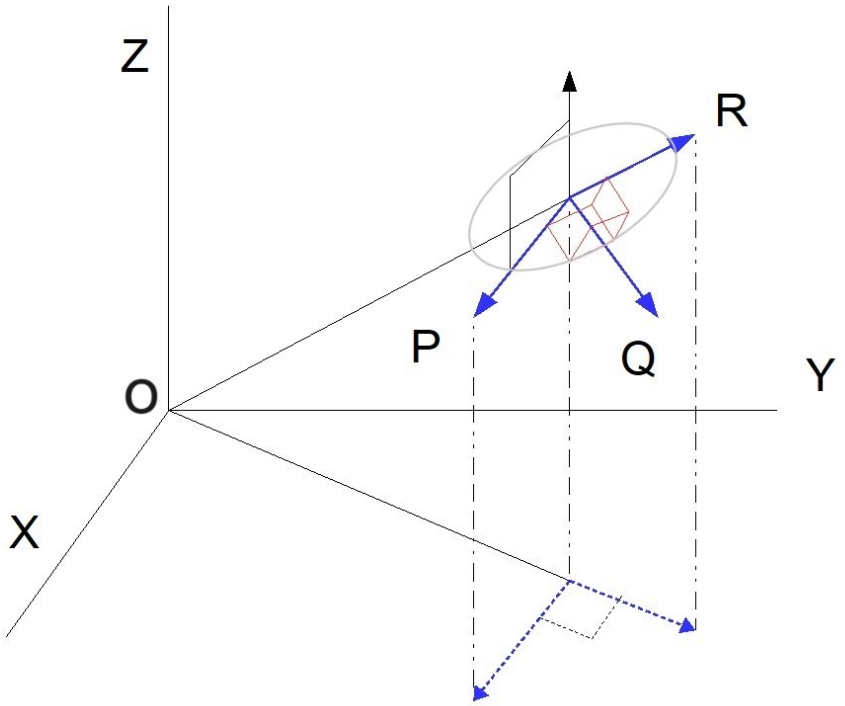

Figure 4.1: Velocity ellipsoid with cylindrical symmetry.

An ellipsoidal distribution is chosen where the velocities form an ellipsoid defined by a logarithmic function of the quadratic velocity distribution:

$$\ln(f) = \ln(B) + a_r \mathbf{C}_r^2 + a_p \mathbf{C}_p^2 + a_q \mathbf{C}_q^2 \tag{4.3.1}$$

These velocity terms are quadratic because they are proportional to the square of the velocity components in each respective direction:

[9]In a spherical galaxy, the distribution of positions exhibits spherical symmetry. However, if the galaxy rotates around the axis $\overrightarrow{OZ}$, like a spiral galaxy, then the velocity distribution can no longer be spherically symmetrical. In reality, the average agitation speed of the matter composing the galaxy becomes perpendicular to the rotation axis. A cylindrical symmetry distribution is then more appropriate to represent this scenario. We seek a velocity distribution where the average speed is primarily tangential to the galaxy's plane of rotation (with a possible radial component). To achieve this, we decompose the agitation speed by introducing radial and tangential components, with three unknowns (H, a, and α) that we aim to determine using the Vlasov equation.

- $\mathbf{C}_r$ is the unit vector in the direction of $\mathbf{r}$, and a_r is the velocity component $\mathbf{C}$ along this axis.
- $\mathbf{C}_p$ is the unit vector in the direction perpendicular to both $\mathbf{r}$ and Z, and a_p is the velocity component $\mathbf{C}$ along this axis.
- $\mathbf{C}_q$ is the unit vector in the direction perpendicular to the two previous directions, thus forming a trihedron. a_q is the velocity component $\mathbf{C}$ along this axis.

Within the framework of an ellipsoidal velocity distribution, 4.3.1 can also be written in the following form:

$$\ln(f) = \ln(B) - \frac{m}{2kH}\mathbf{C}^2 + a(\mathbf{C}\cdot\mathbf{r})^2 + \alpha[\mathbf{C}\cdot(\mathbf{k}\times\mathbf{r})]^2 \tag{4.3.2}$$

where :

- $\mathbf{k}$ is the unit vector along $\overrightarrow{OZ}$ around which the galaxy rotates[10]
- $\mathbf{R}$ is the unit vector along the radial axis collinear to $\mathbf{r}$ given by the following relation: $\mathbf{R} = \frac{\mathbf{r}}{\|\mathbf{r}\|}$
- $\mathbf{P}$ is the unit vector in the direction perpendicular to $\mathbf{r}$ and Z given by the following relation: $\mathbf{P} = \frac{\mathbf{k}\times\mathbf{R}}{\|\mathbf{k}\times\mathbf{R}\|}$[11]
- $\mathbf{Q}$ is the unit vector perpendicular to the two previous vectors given by the following relation: $\mathbf{Q} = \frac{\mathbf{P}\times\mathbf{R}}{\|\mathbf{P}\times\mathbf{R}\|}$
- B, H, a, and α depend a priori on time and space.

However, we can make the following assumptions:

1. We will consider a steady-state regime, which means there is no implicit dependence on time.
2. We will consider a solution exhibiting symmetry around the axis $\overrightarrow{OZ}$, characterized by rotation around this axis with an average tangential speed.

[10] Unit vector $\mathbf{k} = \begin{bmatrix}0\\0\\1\end{bmatrix}$ along the Z axis in the frame (X, Y, Z).

[11] The cross product generates a vector orthogonal to two given vectors. Then, the normalization of this resultant vector is performed by dividing it by its own norm.

This translates into the following simplifications:

$$\frac{\partial \ln(f)}{\partial t} = 0 \tag{4.3.3}$$

$$\frac{D\mathbf{c}_o}{Dt} = \frac{\partial \mathbf{c}_o}{\partial t} + \mathbf{c}_o \cdot \frac{\partial \mathbf{c}_o}{\partial \mathbf{r}} = \mathbf{c}_o \cdot \frac{\partial \mathbf{c}_o}{\partial \mathbf{r}} \tag{4.3.4}$$

$$\mathbf{c}_o \cdot \frac{\partial \ln(f)}{\partial \mathbf{r}} = 0 \tag{4.3.5}$$

The Vlasov equations 4.2.9 and 4.2.10 then reduce to the following expressions:

$$\mathbf{C} \cdot \nabla_{\mathbf{r}} \ln(f) - \left(\nabla_{\mathbf{r}} \Psi + \mathbf{c}_o \cdot \frac{\partial \mathbf{c}_o}{\partial \mathbf{r}} \right) \cdot \nabla_{\mathbf{C}} \ln(f) - \nabla_{\mathbf{C}} \ln(f) \cdot \mathbf{C} : \nabla_{\mathbf{r}} \mathbf{c}_o = 0 \tag{4.3.6}$$

$$\underline{\mathbf{C}} \cdot \nabla_{\mathbf{r}} \underline{\ln(f)} - \left(\nabla_{\mathbf{r}} \Psi + \underline{\mathbf{c}_o} \cdot \frac{\partial \underline{\mathbf{c}_o}}{\partial \mathbf{r}} \right) \cdot \nabla_{\underline{\mathbf{C}}} \underline{\ln(f)} - \nabla_{\underline{\mathbf{C}}} \underline{\ln(f)} \cdot \underline{\mathbf{C}} : \nabla_{\mathbf{r}} \underline{\mathbf{c}_o} = 0 \tag{4.3.7}$$

4.3.1 Attempts to Develop Solutions for the First Vlasov Equation

Let's try to establish a solution to the Vlasov equation 4.3.6. Indeed, this expression contains three terms. The first given by $\mathbf{C} \cdot \nabla_{\mathbf{r}} \ln(f)$ will yield solutions of velocity of order three and one. The second $\left(\nabla_{\mathbf{r}}\Psi + \mathbf{c}_o \cdot \frac{\partial \mathbf{c}_o}{\partial \mathbf{r}}\right) \cdot \nabla_{\mathbf{C}} \ln(f)$ will allow us to obtain solutions of velocity of order one and the last $\nabla_{\mathbf{C}} \ln(f) \cdot \mathbf{C} : \nabla_{\mathbf{r}} \mathbf{c}_o$ of order two.

Third-Order Solution Solution for the Elliptical Velocity Distribution Function

The first term of the Vlasov equation 4.3.6 must satisfy the following relation:

$$\mathbf{C} \cdot \nabla_{\mathbf{r}} \ln(f) = 0 \tag{4.3.8}$$

However, to further simplify the calculations, we can set:

$$\mathbf{c}_o = \omega(\mathbf{k} \times \mathbf{r}) = \omega \begin{pmatrix} -y \\ x \\ 0 \end{pmatrix} \tag{4.3.9}$$

$$\implies \frac{\partial \mathbf{c}_0}{\partial \mathbf{r}} = \omega \frac{\partial(\mathbf{k} \times \mathbf{r})}{\partial \mathbf{r}} \tag{4.3.10}$$

Then :

$$\mathbf{C} \cdot (\mathbf{k} \times \mathbf{r}) = -yC_x + xC_y \tag{4.3.11}$$

$$[\mathbf{C} \cdot (\mathbf{k} \times \mathbf{r})](\mathbf{k} \times \mathbf{r}) = \begin{pmatrix} y^2 C_x - xyC_y \\ -xyC_x + x^2 C_y \\ 0 \end{pmatrix} \tag{4.3.12}$$

Thus, introducing equation 4.3.2 into 4.3.8 allows us to obtain the following relation, retaining only the terms of order three:

$$-\frac{m}{2k}\mathbf{C}^2\mathbf{C} \cdot \frac{\partial}{\partial \mathbf{r}}\left(\frac{1}{H}\right) + 2a(\mathbf{C} \cdot \mathbf{r}) \cdot \mathbf{C} \cdot \mathbf{C} + \mathbf{C} \cdot \frac{\partial a}{\partial \mathbf{r}}(\mathbf{C} \cdot \mathbf{r})^2 + \mathbf{C} \cdot \frac{\partial \alpha}{\partial \mathbf{r}}[\mathbf{C} \cdot (\mathbf{k} \times \mathbf{r})]^2 = 0 \tag{4.3.13}$$

We can express it in terms of the components C_x, C_y, C_z of the residual velocity, collinear to the trihedron formed by the axes $(\mathbf{X}, \mathbf{Y}, \mathbf{Z})$, in order to take advantage of the symmetry around the axis $\overrightarrow{OZ}$ and then group the monomials:

$$\begin{aligned}
&-\frac{m}{2k}\left(C_x^2 + C_y^2 + C_z^2\right)\left(C_x \frac{\partial}{\partial x}\left(\frac{1}{H}\right) + C_y \frac{\partial}{\partial y}\left(\frac{1}{H}\right) + C_z \frac{\partial}{\partial z}\left(\frac{1}{H}\right)\right) \\
&+ 2a\left(C_x^2 + C_y^2 + C_z^2\right)(xC_x + yC_y + zC_z) \\
&+ \left(C_x \frac{\partial a}{\partial x} + C_y \frac{\partial a}{\partial y} + C_z \frac{\partial a}{\partial z}\right)(xC_x + yC_y + zC_z)^2 \\
&+ \left(C_x \frac{\partial \alpha}{\partial x} + C_y \frac{\partial \alpha}{\partial y} + C_z \frac{\partial \alpha}{\partial z}\right)(-yC_x + xC_y)^2 = 0
\end{aligned} \tag{4.3.14}$$

Thus, we obtain 45 terms which, when grouped by monomials, allow us to deduce the following ten partial differential equations:

$$C_x^3 : -\frac{m}{2k}\frac{\partial}{\partial x}\left(\frac{1}{H}\right) + 2ax + x^2\frac{\partial a}{\partial x} + y^2\frac{\partial \alpha}{\partial x} = 0 \tag{4.3.15}$$

$$C_y^3 : -\frac{m}{2k}\frac{\partial}{\partial y}\left(\frac{1}{H}\right) + 2ay + y^2\frac{\partial a}{\partial y} + x^2\frac{\partial \alpha}{\partial y} = 0 \tag{4.3.16}$$

$$C_z^3 : -\frac{m}{2k}\frac{\partial}{\partial z}\left(\frac{1}{H}\right) + 2az + z^2\frac{\partial a}{\partial z} = 0 \tag{4.3.17}$$

$$C_x^2 C_y : -\frac{m}{2k}\frac{\partial}{\partial y}\left(\frac{1}{H}\right) + 2ay + x^2\frac{\partial a}{\partial y} + 2xy\frac{\partial a}{\partial x} + y^2\frac{\partial \alpha}{\partial y} - 2xy\frac{\partial \alpha}{\partial x} = 0 \tag{4.3.18}$$

$$C_y^2 C_x : -\frac{m}{2k}\frac{\partial}{\partial x}\left(\frac{1}{H}\right) + 2ax + y^2\frac{\partial a}{\partial x} + 2xy\frac{\partial a}{\partial y} + x^2\frac{\partial \alpha}{\partial x} - 2xy\frac{\partial \alpha}{\partial y} = 0 \tag{4.3.19}$$

$$C_x^2 C_z : -\frac{m}{2k}\frac{\partial}{\partial z}\left(\frac{1}{H}\right) + 2az + x^2\frac{\partial a}{\partial z} + 2xz\frac{\partial a}{\partial x} + y^2\frac{\partial \alpha}{\partial z} = 0 \tag{4.3.20}$$

$$C_y^2 C_z : -\frac{m}{2k}\frac{\partial}{\partial z}\left(\frac{1}{H}\right) + 2az + y^2\frac{\partial a}{\partial z} + 2yz\frac{\partial a}{\partial y} + x^2\frac{\partial \alpha}{\partial z} = 0 \tag{4.3.21}$$

$$C_z^2 C_x : -\frac{m}{2k}\frac{\partial}{\partial x}\left(\frac{1}{H}\right) + 2ax + z^2\frac{\partial a}{\partial x} + 2xz\frac{\partial a}{\partial z} = 0 \tag{4.3.22}$$

$$C_z^2 C_y : -\frac{m}{2k}\frac{\partial}{\partial y}\left(\frac{1}{H}\right) + 2ay + z^2\frac{\partial a}{\partial y} + 2yz\frac{\partial a}{\partial z} = 0 \tag{4.3.23}$$

$$C_x C_y C_z : 2yz\frac{\partial a}{\partial x} + 2xz\frac{\partial a}{\partial y} + 2xy\frac{\partial a}{\partial z} - 2xy\frac{\partial \alpha}{\partial z} = 0 \tag{4.3.24}$$

Assuming that a and α do not depend on r, we obtain:

$$C_x^3 \equiv C_z^2 C_x \equiv C_y^2 C_x : -\frac{m}{2k}\frac{\partial}{\partial x}\left(\frac{1}{H}\right) + 2ax = 0 \tag{4.3.25}$$

$$C_y^3 \equiv C_x^2 C_y \equiv C_z^2 C_y : -\frac{m}{2k}\frac{\partial}{\partial y}\left(\frac{1}{H}\right) + 2ay = 0 \tag{4.3.26}$$

$$C_z^3 \equiv C_x^2 C_z \equiv C_y^2 C_z : -\frac{m}{2k}\frac{\partial}{\partial z}\left(\frac{1}{H}\right) + 2az = 0 \tag{4.3.27}$$

However, we know that the radius of the ellipsoid on its plane of rotation defined according to the frame $(\mathbf{X}, \mathbf{Y})$ around the axis $\mathbf{Z}$ is given by[12]:

$$\rho^2 = x^2 + y^2 \implies \begin{cases} \dfrac{\partial \rho^2}{\partial x} = 2x \\ \dfrac{\partial \rho^2}{\partial y} = 2y \end{cases} \tag{4.3.28}$$

[12]Knowing that $r^2 = \rho^2 + z^2$ where $\rho^2 = x^2 + y^2$

We then obtain in terms of ρ:

$$\frac{\partial}{\partial \rho^2}\left(\frac{1}{H}\right) = \frac{2k}{m}a \Rightarrow \frac{1}{H} = \frac{2k}{m}a\rho^2 + f_1(z^2) \tag{4.3.29}$$

$$\frac{\partial}{\partial z^2}\left(\frac{1}{H}\right) = \frac{2k}{m}a \Rightarrow \frac{1}{H} = \frac{2k}{m}az^2 + f_2(\rho^2) \tag{4.3.30}$$

The function f_1 depends only on z^2, therefore, if we differentiate (4.3.29) with respect to z^2, we obtain 4.3.30, which is:

$$\frac{\partial}{\partial z^2}\left(\frac{2k}{m}a\rho^2 + f_1(z^2)\right) = \frac{\partial}{\partial z^2}f_1(z^2) = \frac{\partial}{\partial z^2}\left(\frac{1}{H}\right) = \frac{2k}{m}a \tag{4.3.31}$$

Then:

$$f_1(z^2) = \frac{2k}{m}az^2 + k_z \tag{4.3.32}$$

Consequently:

$$\frac{1}{H} = \frac{2k}{m}a\rho^2 + \frac{2k}{m}az^2 + k_z \tag{4.3.33}$$

However, by setting $r = 0$ ($\rho^2 = 0$ and $z^2 = 0$), we have $\frac{1}{H} = k_z$ which we decide to associate with $\frac{1}{T_0}$[13].

Thus, the coherent solution that satisfies these equations is written in the following form:

$$\frac{1}{H} = \frac{1}{T_0}\left(1 + \frac{2kaT_0}{m}r^2\right) \tag{4.3.34}$$

Let us set:

$$r_0^2 = \frac{m}{2akT_0} \implies H = \frac{T_0}{1 + \frac{r^2}{r_0^2}} \tag{4.3.35}$$

However, we know that the component of any vector $\mathbf{C}$ along one of the axes of the frame is the orthogonal projection, which is obtained by performing the dot product of the vector $\mathbf{C}$ with the unit vector of the respective axis. Thus, we can express the components of 4.3.1 in the following way:

$$\mathbf{C}_r = \mathbf{C} \cdot \mathbf{R} = \mathbf{C} \cdot \frac{\mathbf{r}}{\|\mathbf{r}\|} = \frac{\mathbf{C} \cdot \mathbf{r}}{\|\mathbf{r}\|} \tag{4.3.36}$$

$$\mathbf{C}_p = \mathbf{C} \cdot \mathbf{P} = \mathbf{C} \cdot \frac{\mathbf{k} \times \mathbf{r}}{\|\mathbf{k} \times \mathbf{r}\|} = \frac{\mathbf{C} \cdot (\mathbf{k} \times \mathbf{r})}{\|\mathbf{k} \times \mathbf{r}\|} \tag{4.3.37}$$

$$\mathbf{C}_q = \mathbf{C} - \mathbf{C}_r - \mathbf{C}_p \tag{4.3.38}$$

[13] T_0 being a function of time

And taking into account the fact that[14]:

$$\|\mathbf{k}\times\mathbf{r}\|^2 = (\mathbf{k}\times\mathbf{r})\cdot(\mathbf{k}\times\mathbf{r}) = (\mathbf{k}\cdot\mathbf{k})(\mathbf{r}\cdot\mathbf{r}) - (\mathbf{k}\cdot\mathbf{r})(\mathbf{k}\cdot\mathbf{r}) = r^2 - z^2 = \rho^2 \tag{4.3.39}$$

After introduction into 4.3.1 and grouping the terms, we obtain:

$$\ln(f) = \ln(B) + \frac{(a_r - a_q)}{r^2}(\mathbf{C}\cdot\mathbf{r})^2 + \frac{(a_p - a_q)}{\rho^2}[\mathbf{C}\cdot(\mathbf{k}\times\mathbf{r})]^2 + a_q\mathbf{C}^2 \tag{4.3.40}$$

Thus, by identification with 4.3.2, we can deduce that:

$$a_q = -\frac{m}{2kH} \tag{4.3.41}$$

$$a = \frac{(a_r - a_q)}{r^2} \Rightarrow a_r = -\frac{m}{2kH} + ar^2 \tag{4.3.42}$$

$$\alpha = \frac{(a_p - a_q)}{\rho^2} \Rightarrow a_p = -\frac{m}{2kH} + a\rho^2 \tag{4.3.43}$$

If we also set:

$$\rho_0^2 = \frac{m}{2\alpha k T_0} \tag{4.3.44}$$

Then, we obtain:

$$a_r = -\frac{m}{2kT_0} \tag{4.3.45}$$

$$a_p = -\frac{m}{2kT_0}\left(1 + \frac{r^2}{r_0^2} - \frac{\rho^2}{\rho_0^2}\right) \tag{4.3.46}$$

$$a_q = -\frac{m}{2kT_0} + \left(1 + \frac{r^2}{r_0^2}\right) \tag{4.3.47}$$

We can deduce the logarithmic function of the quadratic velocity distribution:

$$f = f_0 e^{\left(-\frac{m}{2kT_0}\left[\mathbf{C}_r^2 + \mathbf{C}_p^2\left(1+\frac{r^2}{r_0^2}-\frac{\rho^2}{\rho_0^2}\right) + \mathbf{C}_q^2\left(1+\frac{r^2}{r_0^2}\right)\right]\right)} \tag{4.3.48}$$

with:

$$f_0 = n\left(\frac{m}{2\pi k T_0}\right)^{\frac{3}{2}}\left(1 + \frac{r^2}{r_0^2}\right)^{\frac{1}{2}}\left(1 + \frac{r^2}{r_0^2} - \frac{\rho^2}{\rho_0^2}\right)^{\frac{1}{2}} \tag{4.3.49}$$

[14] Lagrange's identity is a well-known relation in mathematics that states:

$$\|\mathbf{a}\times\mathbf{b}\|^2 = \|\mathbf{a}\|^2\|\mathbf{b}\|^2 - (\mathbf{a}\cdot\mathbf{b})^2$$

where $\mathbf{a}$ and $\mathbf{b}$ are vectors.

Second-Order Solution for Determining Angular and Circular Velocities

The last term of the Vlasov equation 4.3.6 corresponding to $\nabla_{\mathbf{C}} \ln(f) \cdot \mathbf{C} : \nabla_{\mathbf{r}} \mathbf{c}_o$ involves the double product of

$$\nabla_{\mathbf{C}} \ln(f) \cdot \mathbf{C} : \nabla_{\mathbf{r}} \mathbf{c}_o = \mathrm{Tr}(\mathbf{AB}) = 0 \tag{4.3.50}$$

with:

$$\begin{cases} \mathbf{A} = \nabla_{\mathbf{C}} \ln(f) \cdot \mathbf{C} \\ \mathbf{B} = \nabla_{\mathbf{r}} \mathbf{c}_o \end{cases}$$

Calculating $\mathbf{B}$:

Based on 4.3.9, we can deduce:

$$\mathbf{B} = \frac{\partial \mathbf{c}_0}{\partial \mathbf{r}} = \begin{pmatrix} \frac{\partial \mathbf{c}_{0x}}{\partial x} & \frac{\partial \mathbf{c}_{0y}}{\partial x} & 0 \\ \frac{\partial \mathbf{c}_{0x}}{\partial y} & \frac{\partial \mathbf{c}_{0y}}{\partial y} & 0 \\ \frac{\partial \mathbf{c}_{0x}}{\partial z} & \frac{\partial \mathbf{c}_{0y}}{\partial z} & 0 \end{pmatrix} = \begin{pmatrix} -y\frac{\partial \omega}{\partial x} & x\frac{\partial \omega}{\partial x} + \omega & 0 \\ -y\frac{\partial \omega}{\partial y} - \omega & x\frac{\partial \omega}{\partial y} & 0 \\ -y\frac{\partial \omega}{\partial z} & x\frac{\partial \omega}{\partial z} & 0 \end{pmatrix} \tag{4.3.51}$$

Calculating $\mathbf{A}$:

$$\mathbf{A} = \nabla_{\mathbf{C}} \ln(f) \cdot \mathbf{C} \tag{4.3.52}$$

Based on 4.3.2, we can deduce:

$$\mathbf{A} = -\frac{m}{kH} \mathbf{C} \cdot \mathbf{C} + 2a(\mathbf{C} \cdot \mathbf{r}) \cdot \mathbf{r} \cdot \mathbf{C} + 2\alpha[\mathbf{C} \cdot (\mathbf{k} \times \mathbf{r})] \cdot (\mathbf{k} \times \mathbf{r}) \cdot \mathbf{C} \tag{4.3.53}$$

$$= \mathbf{A_1} + \mathbf{A_2} + \mathbf{A_3} \tag{4.3.54}$$

Let's calculate each term:

$$\mathbf{A_1} = -\frac{m}{kH} \begin{pmatrix} C_x^2 & C_x C_y & C_x C_z \\ C_y C_x & C_y^2 & C_y C_z \\ C_z C_x & C_z C_y & C_z^2 \end{pmatrix}, \tag{4.3.55}$$

$$\mathbf{A_2} = 2a(xC_x + yC_y + zC_z) \begin{pmatrix} xC_x & xC_y & xC_z \\ yC_x & yC_y & yC_z \\ zC_x & zC_y & zC_z \end{pmatrix}, \tag{4.3.56}$$

$$\mathbf{A_3} = 2\alpha \begin{pmatrix} y^2 C_x - xyC_y \\ -xyC_x + x^2 C_y \\ 0 \end{pmatrix} \begin{pmatrix} C_x & C_y & C_z \end{pmatrix} \tag{4.3.57}$$

$$= 2\alpha \begin{pmatrix} y^2 C_x C_x - xyC_y C_x & y^2 C_x C_y - xyC_y C_y & y^2 C_x C_z - xyC_y C_z \\ -xyC_x C_x + x^2 C_y C_x & -xyC_x C_y + x^2 C_y C_y & -xyC_x C_z + x^2 C_y C_z \\ 0 & 0 & 0 \end{pmatrix}. \tag{4.3.58}$$

Let's consider the following two matrices $\mathbf{A}$ and $\mathbf{B}$:

$$\mathbf{A} = \begin{pmatrix} A_{xx} & A_{xy} & A_{xz} \\ A_{yx} & A_{yy} & A_{yz} \\ A_{zx} & A_{zy} & A_{zz} \end{pmatrix} \quad \text{and} \quad \mathbf{B} = \begin{pmatrix} B_{xx} & B_{xy} & B_{xz} \\ B_{yx} & B_{yy} & B_{yz} \\ B_{zx} & B_{zy} & B_{zz} \end{pmatrix} \tag{4.3.59}$$

The trace of their matrix product is given by:

$$\mathrm{Tr}(\mathbf{AB}) = A_{xx}B_{xx} + A_{xy}B_{yx} + A_{xz}B_{zx} + A_{yx}B_{xy} + A_{yy}B_{yy} + A_{yz}B_{zy} + 0 \tag{4.3.60}$$

Let's calculate each term of this trace:

$$A_{xx} = -\frac{m}{kH}C_x^2 + 2a(x^2C_x^2 + yxC_xC_y + zxC_xC_z) + 2\alpha(y^2C_x^2 - xyC_yC_x) \tag{4.3.61}$$

$$= C_x^2\left(-\frac{m}{kH} + 2ax^2 + 2\alpha y^2\right) + C_xC_y2(a-\alpha)xy + C_xC_z2axz \tag{4.3.62}$$

$$A_{yy} = -\frac{m}{kH}C_y^2 + 2a(xC_xyC_y + yC_yyC_y + zC_zyC_y) + 2\alpha(-xyC_xC_y + x^2C_yC_y) \tag{4.3.63}$$

$$= C_y^2\left(-\frac{m}{kH} + 2ay^2 + 2\alpha x^2\right) + C_xC_y2(a-\alpha)xy + C_yC_z2ayz \tag{4.3.64}$$

$$A_{xy} = -\frac{m}{kH}C_xC_y + 2a(xC_xxC_y + yC_yxC_y + zC_zxC_y) + 2\alpha(y^2C_xC_y - xyC_yC_y) \tag{4.3.65}$$

$$= C_xC_y\left(-\frac{m}{kH} + 2\alpha x^2 + 2\alpha y^2\right) + C_y^2 2(a-\alpha)xy + C_yC_z2axz \tag{4.3.66}$$

$$A_{yx} = -\frac{m}{kH}C_yC_x + 2a(xC_xyC_x + yC_yyC_x + zC_zyC_x) + 2\alpha(-xyC_xC_x + x^2C_yC_x) \tag{4.3.67}$$

$$= C_x^2 2(a-\alpha)xy + C_xC_y\left(-\frac{m}{kH} + 2ay^2 + 2\alpha x^2\right) + C_xC_z2ayz \tag{4.3.68}$$

$$A_{xz} = -\frac{m}{kH}C_xC_z + 2a(xC_xxC_z + yC_yxC_z + zC_zxC_z) + 2\alpha(y^2C_xC_z - xyC_yC_z) \tag{4.3.69}$$

$$= C_z^2 2axz + C_xC_z\left(-\frac{m}{kH} + 2ax^2 + 2\alpha y^2\right) + C_yC_z2(a-\alpha)xy \tag{4.3.70}$$

$$A_{yz} = -\frac{m}{kH}C_yC_z + 2a(xC_xyC_z + yC_yyC_z + zC_zyC_z) + 2\alpha(-xyC_xC_z + x^2C_yC_z) \tag{4.3.71}$$

$$= C_z^2 2ayz + C_xC_z2(a-\alpha)xy + C_yC_z\left(-\frac{m}{kH} + 2ay^2 + 2\alpha x^2\right) \tag{4.3.72}$$

$$\tag{4.3.73}$$

The terms in C_x^2 come from $A_{xx}\ B_{xx}$ and $A_{yx}\ B_{xy}$:

$$\left(-\frac{m}{kH} + 2ax^2 + 2\alpha y^2\right)\left(-y\frac{\partial\omega}{\partial x}\right) + 2(a-\alpha)xy\left(x\frac{\partial\omega}{\partial x} + \omega\right) = 0 \tag{4.3.74}$$

The terms in C_y^2 come from $A_{xy}\ B_{yx}$ and $A_{yy}\ B_{yy}$:

$$\left(-\frac{m}{kH}+2ay^2+2\alpha x^2\right)\left(x\frac{\partial\omega}{\partial y}\right)+2(a-\alpha)xy\left(-y\frac{\partial\omega}{\partial y}-\omega\right)=0 \tag{4.3.75}$$

The terms in C_z^2 come from $A_{xz}\ B_{zx}$ and $A_{yz}\ B_{zy}$:

$$2axz\left(-y\frac{\partial\omega}{\partial z}\right)+2ayz\left(x\frac{\partial\omega}{\partial z}\right)=0 \tag{4.3.76}$$

The terms in C_xC_y come from $A_{xy}\ B_{yx}$, $A_{xx}\ B_{xx}$, $A_{yx}\ B_{xy}$, and $A_{yy}\ B_{yy}$:

$$\left(-\frac{m}{kH}+2ax^2+2\alpha y^2\right)\left(-y\frac{\partial\omega}{\partial y}-\omega\right)+2(a-\alpha)xy\left(-y\frac{\partial\omega}{\partial x}\right) \tag{4.3.77}$$

$$+\left(-\frac{m}{kH}+2ay^2+2\alpha x^2\right)\left(x\frac{\partial\omega}{\partial x}+\omega\right)+2(a-\alpha)xy\left(x\frac{\partial\omega}{\partial y}\right)=0 \tag{4.3.78}$$

The terms in C_xC_z come from $A_{xz}\ B_{zx}$, $A_{xx}\ B_{xx}$, $A_{yx}\ B_{xy}$, and $A_{yz}\ B_{zy}$:

$$(2axz)\left(-y\frac{\partial\omega}{\partial x}\right)+\left(-\frac{m}{kH}+2ax^2+2\alpha y^2\right)\left(-y\frac{\partial\omega}{\partial z}\right) \tag{4.3.79}$$

$$+(2axy)\left(x\frac{\partial\omega}{\partial x}+\omega\right)+2(a-\alpha)xy\left(x\frac{\partial\omega}{\partial z}\right)=0 \tag{4.3.80}$$

The terms in C_yC_z come from $A_{xy}\ B_{yx}$, $A_{xz}\ B_{zx}$, $A_{yy}\ B_{yy}$, and $A_{yz}\ B_{zy}$:

$$(2axz)\left(-y\frac{\partial\omega}{\partial y}-\omega\right)+2(a-\alpha)xy\left(-y\frac{\partial\omega}{\partial z}\right) \tag{4.3.81}$$

$$+(2ayz)\left(x\frac{\partial\omega}{\partial y}\right)+\left(-\frac{m}{kH}+2ay^2+2\alpha x^2\right)\left(x\frac{\partial\omega}{\partial z}\right)=0 \tag{4.3.82}$$

Let's now exploit the fact that ω depends only on ρ^2 and z^2 to simplify the expressions. Thus, according to 4.3.28, we obtain:

$$\frac{\partial\omega}{\partial x}=\frac{\partial\omega}{\partial\rho^2}\frac{\partial\rho^2}{\partial x}=2x\frac{\partial\omega}{\partial\rho^2} \tag{4.3.83}$$

$$\frac{\partial\omega}{\partial y}=\frac{\partial\omega}{\partial\rho^2}\frac{\partial\rho^2}{\partial y}=2y\frac{\partial\omega}{\partial\rho^2} \tag{4.3.84}$$

$$\frac{\partial\omega}{\partial z}=\frac{\partial\omega}{\partial z^2}\frac{\partial z^2}{\partial z}=2z\frac{\partial\omega}{\partial z^2} \tag{4.3.85}$$

The equation for C_x^2 becomes:

$$\frac{\partial\ln\omega}{\partial\rho^2}=-\frac{(a-\alpha)}{\left(\frac{m}{kH}-2\alpha\rho^2\right)} \tag{4.3.86}$$

In the particular context where a and α are constants in space (independent of r), starting from 4.3.34, we can deduce the following relation:

$$\frac{\partial \ln \omega}{\partial \rho^2} = -\frac{1}{2}\frac{2(a-\alpha)}{\left(\frac{m}{kT_0} + 2(a-\alpha)\rho^2 + 2az^2\right)} \tag{4.3.87}$$

$$= -\frac{1}{2}\frac{\partial}{\partial \rho^2}\left[\ln\left(\frac{m}{kT_0} + 2(a-\alpha)\rho^2 + 2az^2\right)\right] \tag{4.3.88}$$

Thus, the obtained solution is given by:

$$\omega = \frac{\omega_{\rho_0}(z^2)}{\sqrt{\frac{m}{kT_0} + 2(a-\alpha)\rho^2 + 2az^2}} \tag{4.3.89}$$

The solutions of the other equations are compatible[15].

In the same way as before, the equation for C_xC_z gives us:

$$\frac{\partial \ln \omega}{\partial z^2} = -\frac{a}{\left(\frac{m}{kH} - 2\alpha\rho^2\right)} \tag{4.3.90}$$

In the same particular context where a and α are independent of r, we can deduce the angular velocity of the galaxy:

$$\omega = \frac{\omega_{z_0}(\rho^2)}{\sqrt{\frac{m}{kT_0} + 2(a-\alpha)\rho^2 + 2az^2}} \tag{4.3.91}$$

This solution being compatible with the last term in C_yC_z[16].

In the context of galaxy dynamics, if ω represents the angular velocity of the galaxy[17], then the circular velocity v at a radius ρ is given by:

$$v = \rho \cdot \omega = \rho \cdot \frac{\omega_0}{\sqrt{\frac{m}{kT_0} + 2(a-\alpha)\rho^2 + 2az^2}} \tag{4.3.92}$$

Thus, we can establish a relationship between the gravitational force exerted by the galaxy and the centrifugal force experienced by an object in circular orbit as follows:

$$-\frac{\partial \Psi}{\partial \rho} = \rho\omega^2 = \frac{\rho\omega_0^2}{\frac{m}{kT_0} + 2a\rho^2 + 2(a-\alpha)z^2} \tag{4.3.93}$$

[15] For the terms in C_y^2, $C_z^2 = 0$ and C_xC_y.

[16] $\left(\frac{m}{kH} - 2\alpha\rho^2\right)\left(\frac{\partial \omega}{\partial z^2}\right) = -a\omega$

[17] This is because the circular velocity is the speed at which a star (or any other object) must move along a circular path to maintain a stable orbit around the center of the galaxy, due to the centripetal force provided by the gravitational attraction of the galaxy.

The partial derivative of the gravitational potential Ψ with respect to the radial coordinate ρ, denoted $-\frac{\partial \Psi}{\partial \rho}$, represents the gravitational acceleration. For an object to maintain a circular orbit, this acceleration must be equal to the centrifugal force, which is given by $\rho\omega^2$[18].

[18]The constraint on the gravitational potential indicates that for a star in a stable orbit, the gravitational force must exactly counterbalance the centrifugal force at each radius ρ. This condition is fundamental for determining the mass distribution in galaxies using observed rotation curves.

First-Order Solution

The terms contributing to the solution of the Vlasov equation are $\mathbf{C} \cdot \nabla_{\mathbf{r}} \ln(f)$ and $\left(\nabla_{\mathbf{r}} \Psi + \mathbf{c}_o \cdot \frac{\partial \mathbf{c}_o}{\partial \mathbf{r}}\right) \cdot \nabla_{\mathbf{C}} \ln(f)$, and must satisfy the relation:

$$\mathbf{C} \cdot \nabla_{\mathbf{r}} \ln(f) + \left(\nabla_{\mathbf{r}} \Psi + \mathbf{c}_o \cdot \frac{\partial \mathbf{c}_o}{\partial \mathbf{r}}\right) \cdot \nabla_{\mathbf{C}} \ln(f) = 0 \tag{4.3.94}$$

We need to express $\mathbf{C} \cdot \nabla_{\mathbf{r}} \ln(f)$ while retaining only the first-order terms, namely:

$$\mathbf{C} \frac{\partial \ln B}{\partial \mathbf{r}} = C_x \frac{\partial \ln B}{\partial x} + C_y \frac{\partial \ln B}{\partial y} + C_z \frac{\partial \ln B}{\partial z} \tag{4.3.95}$$

Regarding $\left(\nabla_{\mathbf{r}} \Psi + \mathbf{c}_o \cdot \frac{\partial \mathbf{c}_o}{\partial \mathbf{r}}\right) \cdot \nabla_{\mathbf{C}} \ln(f)$, we know that the angular velocity of a galaxy ω depends only on ρ^2 and z^2. Thus, equations 4.3.83, 4.3.84, and 4.3.85 allow us to transform relation 4.3.51 as follows:

$$\frac{\partial \mathbf{c}_0}{\partial \mathbf{r}} = \begin{pmatrix} -2xy \frac{\partial \omega}{\partial r^2} & 2x^2 \frac{\partial \omega}{\partial r^2} + \omega & 0 \\ -2y^2 \frac{\partial \omega}{\partial r^2} - \omega & 2xy \frac{\partial \omega}{\partial r^2} & 0 \\ -2yz \frac{\partial \omega}{\partial z^2} & 2xz \frac{\partial \omega}{\partial z^2} & 0 \end{pmatrix} \tag{4.3.96}$$

Thus, its dot product with 4.3.9 allows us to deduce that:

$$\mathbf{c}_0 \frac{\partial \mathbf{c}_0}{\partial \mathbf{r}} = -\omega_{c_0}^2 (x, y, 0) \tag{4.3.97}$$

Then :

$$\left(\nabla_{\mathbf{r}} \Psi + \mathbf{c}_o \cdot \frac{\partial \mathbf{c}_o}{\partial \mathbf{r}}\right) = -\left(\tfrac{\partial \Psi}{\partial x}, \tfrac{\partial \Psi}{\partial y}, \tfrac{\partial \Psi}{\partial z}\right) + \omega_{c_0}^2 \left(x, y, 0\right) \tag{4.3.98}$$

Now we know that[19] :

$$\omega_{c_0}^2 (x, y, 0) = -\left(\frac{\partial \Psi_0}{\partial \mathbf{r}}\right) = -\left(\frac{\partial \Psi_0}{\partial x}, \frac{\partial \Psi_0}{\partial y}, \frac{\partial \Psi_0}{\partial z}\right) \quad \text{with} \quad \Psi_0 = -\frac{1}{2} \omega_{c_0}^2 \rho^2 \tag{4.3.99}$$

Consequently:

$$\left(\nabla_{\mathbf{r}} \Psi + \mathbf{c}_o \cdot \frac{\partial \mathbf{c}_o}{\partial \mathbf{r}}\right) = -\frac{\partial (\Psi + \Psi_0)}{\partial \mathbf{r}} \tag{4.3.100}$$

Thus, according to 4.3.9, 4.3.12, and 4.3.53, we can deduce:

$$\nabla_{\mathbf{C}} \ln(f) = -\frac{m}{kH} \begin{pmatrix} C_x \\ C_y \\ C_z \end{pmatrix} + 2a \begin{pmatrix} xxC_x + xyC_y + xzC_z \\ xyC_x + yyC_y + yzC_z \\ xzC_x + yzC_y + zzC_z \end{pmatrix} + 2\alpha \begin{pmatrix} y^2 C_x - xyC_y \\ -xyC_x + x^2 C_y \\ 0 \end{pmatrix} \tag{4.3.101}$$

[19] Considering 4.3.28, we can deduce that $\frac{\partial \Psi_0}{\partial \rho} = -\frac{1}{2} \omega_{c_0}^2 \frac{\partial \rho^2}{\partial \rho} = -\omega_{c_0}^2 (x, y, 0)$

This yields:

$$\nabla_{\mathbf{C}} \ln(f) = \begin{pmatrix} C_x\left(-\frac{m}{kH} + 2ax^2 + 2\alpha y^2\right) + C_y 2xy(a-\alpha) + C_z 2axz \\ C_x 2xy(a-\alpha) + C_y\left(-\frac{m}{kH} + 2ay^2 + 2\alpha x^2\right) + C_z 2ayz \\ C_x 2axz + C_y 2ayz + C_z\left(-\frac{m}{kH} + 2az^2\right) \end{pmatrix} \tag{4.3.102}$$

We thus obtain:

$$\left(\nabla_{\mathbf{r}}\Psi + \mathbf{c}_o \cdot \frac{\partial \mathbf{c}_o}{\partial \mathbf{r}}\right)\cdot\nabla_{\mathbf{C}} \ln(f) = -\frac{\partial(\Psi+\Psi_0)}{\partial \mathbf{r}} \begin{pmatrix} C_x\left(-\frac{m}{kH} + 2ax^2 + 2\alpha y^2\right) + C_y 2xy(a-\alpha) + C_z 2axz \\ C_x 2xy(a-\alpha) + C_y\left(-\frac{m}{kH} + 2ay^2 + 2\alpha x^2\right) + C_z 2ayz \\ C_x 2axz + C_y 2ayz + C_z\left(-\frac{m}{kH} + 2az^2\right) \end{pmatrix} \tag{4.3.103}$$

Thus, the three partial differential equations that satisfy the first-order terms of the Vlasov equation 4.3.94 are as follows[20] :

$$\frac{\partial \ln B}{\partial x} + \frac{\partial(\Psi+\Psi_0)}{\partial x}\left(\frac{m}{kT_0} + 2(a-\alpha)y^2 + 2az^2\right) - 2\frac{\partial(\Psi+\Psi_0)}{\partial y}xy(a-\alpha) - 2\frac{\partial(\Psi+\Psi_0)}{\partial z}axz = 0 \tag{4.3.104}$$

$$\frac{\partial \ln B}{\partial y} - 2\frac{\partial(\Psi+\Psi_0)}{\partial x}xy(a-\alpha) + \frac{\partial(\Psi+\Psi_0)}{\partial y}\left(\frac{m}{kT_0} + 2(a-\alpha)x^2 + 2az^2\right) - 2\frac{\partial(\Psi+\Psi_0)}{\partial z}ayz = 0 \tag{4.3.105}$$

$$\frac{\partial \ln B}{\partial z} + 2\frac{\partial(\Psi+\Psi_0)}{\partial x}axz + 2\frac{\partial(\Psi+\Psi_0)}{\partial y}ayz - \frac{\partial(\Psi+\Psi_0)}{\partial z}\left(\frac{m}{kT_0} + 2az^2\right) = 0 \tag{4.3.106}$$

4.3.2 Modeling the Effects of Negative Mass Environment on Velocity Distribution

In spherical symmetry, the two transverse axes of the velocity ellipsoid, which are equal, differ from the axis pointing towards the center of the galaxy. For an axisymmetric system, the two transverse axes differ, which was developed in reference [65]. In the configuration of figure 4.2, the form of the velocity distribution function corresponds to a particular spherically symmetric configuration:

$$\ln(f) = \ln B(r) - \frac{\mathbf{C}^2}{\langle c^2\rangle} + a(r)(\mathbf{C}\cdot\mathbf{r})^2 \tag{4.3.107}$$

The equation takes into account the mean square velocity of particles, denoted $\langle c^2\rangle$, and a potential function $B(r)$, as well as a function $a(r)$ that adjusts the distribution based on the radial distance r. The term $\mathbf{C}$ represents the residual thermal agitation velocity, and $\mathbf{C}\cdot\mathbf{r}$ represents the dot product of the residual velocity with the position

[20] Still in the specific context where a and α are constants in space and knowing that according to 4.3.34, we obtain $\frac{m}{kH} = \frac{m}{kT_0} + 2ar^2 = \frac{m}{kT_0} + 2ax^2 + 2ay^2 + 2az^2$

vector, which would have significance in the context of a velocity distribution in a galaxy or a similar system.

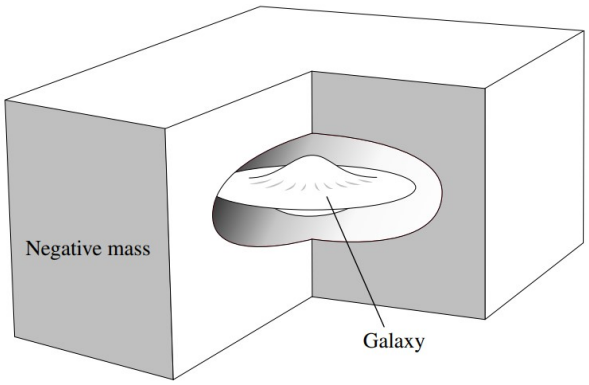

Figure 4.2: Galaxy surrounded by a confining negative mass.

For the negative mass environment, a Maxwellian velocity distribution is used:

$$\ln(f) = \ln B(r) - \frac{\mathbf{C}^2}{\langle c^2 \rangle} \tag{4.3.108}$$

By introducing these functions into the two Vlasov equations 4.3.6 and 4.3.7 and using dyadic algebra ([16] [79]), we obtain exact solutions that model the confinement of this spheroidal galaxy corresponding to Figure 4.3.

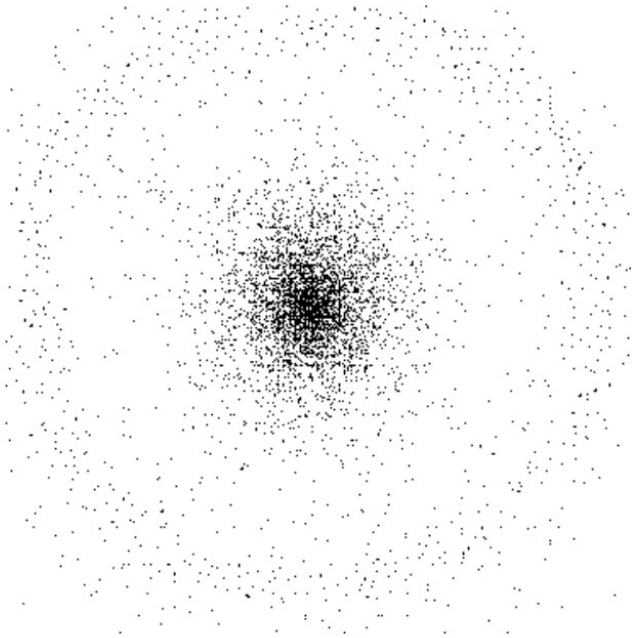

Figure 4.3: Spheroidal galaxy, globular cluster, or galaxy cluster.

This model highlights the role of the negative mass environment in confining spheroidal galaxies, galaxy clusters, and, in the case of galaxies, gives the possibility to reconstruct their flat rotation curves. The positive mass objects are located in voids of the negative mass distribution. These voids, equivalent to a positive mass, are primarily responsible for the observed gravitational lensing effects. Thus, the model accounts for this set of observations.

From this perspective, it offers an alternative to the dark matter model. In this context, a solid body rotation[21] is introduced.

The image in figure 3.7 comes from numerical simulations conducted at the Deutsches Elektronen-Synchrotron (DESY) laboratory in Hamburg in 1992 by student Frédéric Descamp, who used the pseudonym F. Landsheat in his publications. Within just a few cycles, after a transient phase, a barred spiral galaxy forms, which persists for about thirty cycles [64].

The evolution of the galaxy's angular momentum, as well as the establishment of its rotation curve differing from the initial solid body rotation, are illustrated in figure 3.8.

The phenomenon of deceleration serves as an illustration in systems where collisions are minimal and transport phenomena such as heat and angular momentum are negligible. In the context of spiral galaxies, these interactions are orchestrated by density waves, which become evident in the distribution of positive masses and their counterparts in the realm of negative masses, as demonstrated by numerical simulations.

For three decades, astrophysicists have linked the observed spiral structures in galaxies to a phenomenon of deceleration. A recent research paper [18] presents observational evidence for this phenomenon, known as *dynamical friction*. The authors conclude that this supports the hypothesis of the existence of a dark matter halo, which, in their view, explains this deceleration. Nevertheless, an alternative interpretation remains plausible. This study can be seen as providing an argument in favor of the idea that deceleration results from the interaction between the mass of the galaxy and its negative mass environment.

NB:

- *Angular momentum* is a physical property that describes the rotation of an object. For a galaxy, this means how it spins in space. The *evolution of angular momentum* indicates that over time, the way the galaxy rotates changes. This can

[21] This means that all parts of the object rotate at the same speed, like a spinning top. However, the actual rotation curve of the galaxy differs from this simple solid-body model. In other words, the galaxy's rotational speed varies at different distances from the center, which is typical for real galaxies.

be due to several factors, such as gravitational interactions with other galaxies or its negative mass environment, internal movements of stars, or even the formation of new structures within the galaxy.

- The *rotation curve* of a galaxy shows how the rotation speed varies at different distances from its center. Typically, one would expect the far parts of the galaxy to rotate more slowly than the parts closer to the center, much like the planets in our solar system - the farther they are from the sun, the slower their orbital speed.

- A phenomenon of *dynamical friction* exists within the galaxy. It is a process that occurs when a massive object, like a star or a group of stars, moves through a dense field of matter made up of gas and stars in a galaxy. As it moves, this massive object attracts the surrounding matter due to gravity. This matter in return pulls on the object, gradually slowing it down. Imagine running through a crowd. Even if people do not stop you directly, their presence slows your movement. This is a simple analogy for dynamical friction. When many objects in a galaxy undergo dynamical friction, it can slow down the overall rotation of the galaxy. This slowing is usually not uniform; it can affect different parts of the galaxy differently, depending on the distribution of matter and the movements of stars and other objects.

Chapter 5

Contribution to Cosmology & Particle Physics

5.1 Introduction to Dynamic Groups

Dynamical Systems Theory is a mathematical discipline focused on the analysis of the evolution over time of various systems, taking into account initial conditions and external influences. *Symplectic Geometry*, which merges aspects of dynamical systems theory with those of differential geometry, examines the properties and deformations of curved spaces under the action of external forces. This field, based on the principles of Hamiltonian mechanics, explores structures named *"symplectic varieties"*, endowed with a unique configuration useful for measuring volumes. Unlike Riemannian geometry, which uses a metric tensor to measure lengths and angles, symplectic geometry employs a mathematical form, the *"symplectic form"*, for the calculation of areas.

Jean-Marc Souriau was a leading pioneer in symplectic topological geometry. He developed the concept of geometric quantization, transforming fundamental physical quantities like energy and momentum into purely geometric objects. Souriau's work gave physical meaning to the reversal of time's arrow in our cosmological model ([9], [38]).

What is a group?

In mathematical terms, it refers to certain matrices acting upon other matrices. But physically, what does this represent?

According to J-M Souriau, a group is created for transportation, and the method of transport is more significant than the transported entity: *"Tell me how you move, and I will tell you who you are."*

Our focus is primarily on Lie groups(see [11]), which are both groups and differential manifolds (locally projected *"curved spaces"* onto an n-dimensional Euclidean space). They are instrumental in describing movements and transformations in space. Two key

groups are the orthogonal group O(3) and the Euclidean group E(3):

- **The orthogonal group O(3)** is used to describe rotations and symmetries in three dimensions, preserving distances in space. It includes a crucial subgroup called SO(3), the rotation group, which manages rotations around an axis.
- **The Euclidean group E(3)** describes three-dimensional movements like rotations, symmetries, and translations. Built upon the orthogonal group O(3), it can be broken down into a force and a couple applied to an object in solid mechanics. It's a group within which the Pythagorean theorem can be used to calculate the length between two points. This group transforms a point with coordinates x, y, z to a new point with coordinates x', y', z'. The unique feature of this dynamic group is its ability to generate a family of geometric objects invariant within the group. For example, a line subjected to translation remains a line, making it a one-dimensional invariant geometric object. A sphere is a perfect example of a three-dimensional symmetric object. Its unique property is that it remains unchanged under rotations around its center, showcasing rotational symmetry. In geometric terms, this implies that when a sphere undergoes a rotational movement, it maintains its geometric properties uniformly at every point. In the field of physics, particularly in the study of space-time in general relativity, Schwarzschild's solution is an important concept. It describes the gravitational field outside a non-rotating, spherically symmetric mass such as a star. The Schwarzschild metric, a solution to Einstein's field equations, is invariant under rotations and translations in time and space, resembling the invariance observed in Euclidean geometry but applied to the curved space-time of general relativity. In Schwarzschild space-time, geodesics are determined by the curvature of space-time, which is described by the Schwarzschild metric. For an object moving along a geodesic, certain quantities such as its angular momentum and energy relative to the mass causing the curvature of space-time are conserved. This conservation is the result of the symmetries of space-time, analogous to the laws of conservation in classical mechanics.

Lie groups thus describe movements in space while preserving distances and lengths. They are groups of isometry when the geometric properties of moving objects remain unchanged (distances and angles) in space during a transformation. Rotations are examples of three-dimensional space symmetries, as they do not alter the geometric properties of the space. For instance, rotating a cube does not change the distances between its vertices. In other words, the geometric properties of the object remain unchanged, even though its position has been modified.

According to the theory of special relativity, instead of living in a three-dimensional Euclidean space $[x, y, z]$ with a signature $(+++)$ where time is a distinct entity, we actually exist in a four-dimensional spacetime where the three spatial dimensions are perpendicular to one temporal dimension $[t, x, y, z]$ called Minkowski spacetime, with a

signature of $(-+++)$.

The Poincaré group, associated with this space, plays a crucial role in describing motion in the spacetime of special relativity. This group allows for modeling specific behaviors, especially those of massless particles like photons, which move invariably at the speed of light. While their speed remains constant, gravity affects their energy, leading to phenomena such as gravitational redshift. Furthermore, the Poincaré group also applies to particles with nonzero mass, each following its own dynamics dictated by the principles of relativity. This dynamic group applied to special relativity, includes the motion of masses or photons with a possible reversal of the time arrow[1] and can be represented in matrix form as follows :

$$\begin{pmatrix} L & C \\ 0 & 1 \end{pmatrix} \tag{5.1.1}$$

where L represents the matrix of the Lorentz group ($\mathcal{L}or$) which describes how space-time coordinates change between different inertial frames. These transformations include rotations in space as well as Lorentz transformations (boosts), which are changes of reference frames moving at a constant speed relative to each other. And C is the vector corresponding to spatio-temporal translations in $\mathbb{R}^{1,3}$.

Indeed, half of the elements of the dynamic group reverse time, implying that if we consider a space-time element like a mass or a photon and apply a temporal motion from past to future, we can achieve the same motion in the reverse direction using the Poincaré group. Consequently, according to Souriau's theory from his work *"Structure of Dynamic Systems"* ([38]), if the dynamic group can circulate photons or masses with a time arrow in opposition, then their energy, and thus their mass, can also be reversed.

N.B.: The restricted Poincaré group exclusively handles *"orthochronous"* relativistic movements in four-dimensional Minkowski space, transitioning from past to future. Its matrix form includes the matrix L_o of the *"orthochronous"* Lorentz group $\mathcal{L}or_o$ as follows:

$$\begin{pmatrix} L_o & C \\ 0 & 1 \end{pmatrix} \tag{5.1.2}$$

Can we now consider these movements with negative energy and mass and an opposing time arrow as part of Physics? Can they be measured or observed?

Particles with negative energy emit photons of negative energy, so they cannot be observed or measured optically. However, it has been observed and measured that the expansion of the universe is accelerating due to negative pressure linked to dark energy ([52]). Indeed, pressure is an energy density per unit volume.

[1] From past to future and vice versa.

Thus, the expansion of the universe is directly linked to negative energy. This suggests that a substantial part of the universe, currently defined as dark energy, affects this expansion through gravitational effect. This dynamic group and geometric approach, therefore, provide an answer to its origin and nature. It could be content with masses or photons charged with negative energy.

5.2 Various Symmetries Associated with Each Inversion Operator

The restricted Poincaré group handles relativistic movements in four-dimensional Minkowski space. The Poincaré group is the group according to the following matrix :

$$\begin{pmatrix} L & C \\ 0 & 1 \end{pmatrix} \tag{5.2.1}$$

where C is the vector corresponding to spatio-temporal translations in $\mathbb{R}^{1,3}$:

$$C = \begin{pmatrix} \Delta t \\ \Delta x \\ \Delta y \\ \Delta z \end{pmatrix} \tag{5.2.2}$$

It acts on points in Minkowski space:

$$\xi = \begin{pmatrix} t \\ x \\ y \\ z \end{pmatrix} \tag{5.2.3}$$

This Lie group with 10 independent parameters[2] is the isometry group of this space, defined by its metric:

$$\mathrm{d}s^2 = \mathrm{d}t^2 - \mathrm{d}x^2 - \mathrm{d}y^2 - \mathrm{d}z^2 \tag{5.2.4}$$

The *Lorentz group* $\mathcal{L}or$ has four connected components:

- $\mathcal{L}or_n$ is the neutral component (its *restricted subgroup*), does not invert either space or time and is defined by:

$$\mathcal{L}or_n = \{L \in \mathcal{L}or,\ \det(L) = 1\ \wedge\ [L]_{00} \geq 1\}$$

- $\mathcal{L}or_s$ inverts space and is defined by:

$$\mathcal{L}or_s = \{L \in \mathcal{L}or,\ \det(L) = -1\ \wedge\ [L]_{00} \geq 1\}$$

[2]Including the 6 independent parameters of the Lorentz group (3 rotations and 3 boosts) and 4 independent transformations, which are translations in the 4 directions of Minkowski space.

- $\mathcal{L}or_t$ inverts time but not space and is defined by:

$$\mathcal{L}or_t = \{L \in \mathcal{L}or,\ \det(L) = 1\ \wedge\ [L]_{00} \leq -1\}$$

- $\mathcal{L}or_{st}$ inverts both space and time and is defined by:

$$\mathcal{L}or_{st} = \{L \in \mathcal{L}or,\ \det(L) = -1\ \wedge\ [L]_{00} \leq -1\}$$

And we have:

$$\mathcal{L}or = \mathcal{L}or_n \sqcup\ \mathcal{L}or_s \sqcup\ \mathcal{L}or_t \sqcup\ \mathcal{L}or_{st} \tag{5.2.5}$$

The first two components are grouped to form the so-called *"orthochronous"* subgroup:

$$\mathcal{L}or_o = \mathcal{L}or_n \sqcup\ \mathcal{L}or_s \tag{5.2.6}$$

It includes *P-symmetry*, which poses no problem for physicists who know that there are photons of *"right"* and *"left"* helicity whose motions are derived from this symmetry. This corresponds to the phenomenon of the polarization of light.

The last two components form the subset *"retrochronous"* or *"antichronous"*, whose components invert time:

$$\mathcal{L}or_a = \mathcal{L}or_t \sqcup\ \mathcal{L}or_{st} \tag{5.2.7}$$

Thus, we have:

$$\mathcal{L}or = \mathcal{L}or_o \sqcup\ \mathcal{L}or_a \tag{5.2.8}$$

Noting that:

$$\mathcal{L}or_t = -\mathcal{L}or_s \quad \mathcal{L}or_{st} = -\mathcal{L}or_n \tag{5.2.9}$$

The *Poincaré group* inherits the properties of the Lorentz group and thus has four connected components, it's defined by:

$$\mathcal{P}oin := \left\{ \begin{pmatrix} L & C \\ 0 & 1 \end{pmatrix},\quad L \in \mathcal{L}or \wedge C \in \mathbb{R}^{1,3} \right\} \tag{5.2.10}$$

5.3 Lorentz Dynamic Group

The application of the coadjoint action of a dynamic group on the dual of its Lie algebra, initiated by mathematician Jean-Marie Souriau, has shed light on specific aspects of the approach followed in physics. The restricted dynamic Lorentz group, limited to its two orthochronous components, translates, through its resulting invariance properties, aspects of special relativity. In 1970, J-M Souriau established that the analysis of the components of its moment highlights the geometric nature of a (non-quantified) spin ([76] [78]). The Lorentz group has two connected orthochronous components, namely its first neutral component, containing the neutral element of the group, and its second enantiomorphic component, inverting space synonymous with *P-Symmetry*.

In dynamic group theory, a classification in terms of movements is made apparent. At this stage, the action of these space-inverting elements is illustrated in the phenomenon of light polarization, where any *"right"* photon can be converted into a *"left"* photon. This group can be represented by a family of 4×4 matrices L, axiomatically defined by $L^T G L = G$, where L^T is the transpose of the Lorentz matrix L, and G is the Minkowski metric matrix, often referred to as the Gram matrix in this context. In special relativity, it is generally represented by a diagonal matrix with elements $\text{diag}(1, -1, -1, -1)$. This equation signifies that the Lorentz transformation preserves the Minkowski inner product, a crucial condition for the coherence of the theory of special relativity.

5.4 Restricted Poincaré Dynamic Group

The product of the Lorentz group with the spatiotemporal translation group allows us to construct the restricted Poincaré dynamic group, still limited to its two orthochronous components. In its moment, we first find the energy related to the subgroup of temporal translations. Then the momentum, related to spatial translations, both being linked by the invariance of the modulus of the energy-momentum four-vector under the action of the Lorentz group. The matrix associated with this group must include the *"orthochronous"* Lorentz matrix L_o of dimension 3×3, as well as the translation vector C and additional components to complete its structure(See 5.1.2).

5.5 Restricted Kaluza & Janus Dynamic Groups

By adding a translation along a fifth dimension to the restricted Poincaré group, we form a Lie group to which we will give the name *Restricted Kaluza Group* ([6], [8], [9], [38], [40]). This group is not the 15-parameter Kaluza group associated with a 5-dimensional Lorentzian manifold, but a new group with 11 independent parameters, including a translation parameter in addition to the 10 parameters of the Poincaré group. This new dimension endows the momentum with an additional scalar that can be identified with the electric charge q, which may be positive, negative, or zero, and is still not quantized. We then bring out the geometric translation according to a scalar ϕ due to endowing the masses with an invariant electric charge. Then, by bringing in a new symmetry reflecting the inversion of the fifth dimension, synonymous with an inversion of the scalar from q to $-q$, we double the number of its connected components from 2 to 4. The action on the moment then links this new symmetry to the inversion of the electric charge q. We thus deduce the geometric modeling of charge conjugation or *C-Symmetry*, which translates the matter-antimatter symmetry introduced by Dirac. It's then logical to name this new extension, the *Restricted Janus Group*.

5.6 Janus Dynamic Group

By introducing a new symmetry to the previous group, which we describe as *T-Symmetry* and which converts matter into antimatter with negative mass – a concept we could name *antimatter in the Feynman sense* – we build the *Janus Dynamic Group*. Thus, we double the number of connected components from four to eight, grouped into two subsets: *"Orthochronous"*, conserving time and energy properties, and *"Antichronous"*, reversing time and energy. Therefore, we bring forth the geometric translation of endowing masses with an invariant electric charge. As the Jean-Marie Souriau demonstrated as early as 1970, a pioneer in the theory of dynamic groups ([76], [78]), this approach has allowed key elements, which have marked the progress of relativistic physics, to be given a purely geometric nature.

Here is the matrix associated with the Janus Dynamic Group from which it is possible to reconstruct all the symmetry groups:

$$\mathcal{J}an = \left\{ \begin{pmatrix} (-1)^{\mu} & 0 & \phi \\ 0 & T^{\lambda}S^{\nu}L_n & C \\ 0 & 0 & 1 \end{pmatrix},\ \lambda,\mu \in \{0,1\} \wedge\ \phi \in \mathbb{R} \wedge\ L \in \mathcal{L}or \wedge\ C \in \mathbb{R}^{1,3} \right\} \tag{5.6.1}$$

- ***P-Symmetry*** :
  By setting $\mu = 0$, $\lambda = 0$, and $\nu = 1$, we obtain:

$$\mathcal{J}an = \left\{ \begin{pmatrix} 1 & 0 & \phi \\ 0 & L_s & C \\ 0 & 0 & 1 \end{pmatrix},\ \phi \in \mathbb{R} \wedge\ L_s = SL_n \in \mathcal{L}or \wedge\ C \in \mathbb{R}^{1,3} \right\} \tag{5.6.2}$$

  This symmetry operator corresponds to the inversion of space where an element of the second connected component of the orthochronous group is considered. It is this symmetry that inverts the helicity of a photon, transforming a *"right-handed photon"* into a *"left-handed photon"* which corresponds to the phenomenon of light polarization.

- ***C-Symmetry*** :
  We must apply $\mu = 1$, $\lambda = 0$ and $\nu = 0$.
  Starting from the Ln element of the restricted Lorentz orthochronous group, by inverting the fifth dimension carrying the electric charge q, we obtain the *"C-symmetry"* operator or *"charge conjugation"* (quantum) such that:

$$\mathcal{J}an = \left\{ \begin{pmatrix} -1 & 0 & \phi \\ 0 & L_n & C \\ 0 & 0 & 1 \end{pmatrix},\ \phi \in \mathbb{R} \wedge\ L_n \in \mathcal{L}or \wedge\ C \in \mathbb{R}^{1,3} \right\} \tag{5.6.3}$$

It is this symmetry that represents the *"Matter-Antimatter"* transformation.

- ***T-Symmetry*** :
  By setting $\mu = 0$, $\lambda = 1$, and $\nu = 0$, we remove the *symmetry C* ($\mathcal{J}an_{11} = 1$) and the *symmetry P* ($\mathcal{J}an_{22} = -L_s$). We obtain:

$$\mathcal{J}an = \left\{ \begin{pmatrix} 1 & 0 & \phi \\ 0 & -L_s & C \\ 0 & 0 & 1 \end{pmatrix}, \ \phi \in \mathbb{R} \wedge \ L_s = -L_t = -TL_n \in \mathcal{L}or \wedge \ C \in \mathbb{R}^{1,3} \right\} \tag{5.6.4}$$

- ***CP-Symmetry*** :
  By setting $\mu = 1$, $\lambda = 0$, and $\nu = 1$, we add the *symmetry C* ($\mathcal{J}an_{11} = -1$) and the *symmetry P* ($\mathcal{J}an_{22} = L_s$) to obtain:

$$\mathcal{J}an = \left\{ \begin{pmatrix} -1 & 0 & \phi \\ 0 & L_s & C \\ 0 & 0 & 1 \end{pmatrix}, \ \phi \in \mathbb{R} \wedge \ L_s = SL_n \in \mathcal{L}or \wedge \ C \in \mathbb{R}^{1,3} \right\} \tag{5.6.5}$$

  NB : We can deduce it also by removing the *T-symmetry* ($\mathcal{J}an_{22} = L_s$) from the *CPT-symmetry* following this operation : $\mathbf{CP} = \mathbf{T} \cdot \mathbf{CPT}$

- ***CPT-Symmetry*** :
  We must apply $\mu = 1$, $\lambda = 1$ and $\nu = 1$.
  We know that the element L_n of the Neutral group does not reverse either time or space, so the element $\mathcal{J}an_{22} = -L_n$ reverses both space and time to form the *PT-symmetry* operator. However, if we add the *C-symmetry* ($\mathcal{J}an_{11} = -1$), we form the CPT Janus group with charge symmetry such as:

$$\mathcal{J}an = \left\{ \begin{pmatrix} -1 & 0 & \phi \\ 0 & -L_n & C \\ 0 & 0 & 1 \end{pmatrix}, \ \phi \in \mathbb{R} \wedge \ L_n = -TSL_n \in \mathcal{L}or \wedge \ C \in \mathbb{R}^{1,3} \right\} \tag{5.6.6}$$

- ***PT-Symmetry*** :
  We must apply $\mu = 0$, $\lambda = 1$ and $\nu = 1$.
  By removing the *C-symmetry* ($\mathcal{J}an_{11} = 1$) from the *CPT-symmetry* following

this operation : $\mathbf{PT} = \mathbf{C} \cdot \mathbf{CPT}$ we obtain :

$$\mathcal{J}an = \left\{ \begin{pmatrix} 1 & 0 & \phi \\ 0 & -L_n & C \\ 0 & 0 & 1 \end{pmatrix}, \ \phi \in \mathbb{R} \wedge \ L_n = -TSL_n \in \mathcal{L}or \wedge \ C \in \mathbb{R}^{1,3} \right\} \tag{5.6.7}$$

- ***CT-Symmetry*** :
  We must apply $\mu = 1$, $\lambda = 1$ and $\nu = 0$.
  Then, by removing the *P-symmetry* ($\mathcal{J}an_{22} = -L_s$) from the *CPT-symmetry* following this operation : $\mathbf{CT} = \mathbf{P} \cdot \mathbf{CPT}$ we obtain :

$$\mathcal{J}an = \left\{ \begin{pmatrix} -1 & 0 & \phi \\ 0 & -L_s & C \\ 0 & 0 & 1 \end{pmatrix}, \ \phi \in \mathbb{R} \wedge \ L_s = -TL_n \in \mathcal{L}or \wedge \ C \in \mathbb{R}^{1,3} \right\} \tag{5.6.8}$$

- ***Neutral Operator*** :
  By setting $\mu = 0$, $\lambda = 0$, and $\nu = 0$, the object moves through the five dimensions without changing its nature. Only the neutral element of the *"orthochronous"* subgroup is considered ($\mathcal{J}an_{22} = L_n$). We obtain:

$$\mathcal{J}an = \left\{ \begin{pmatrix} 1 & 0 & \phi \\ 0 & L_n & C \\ 0 & 0 & 1 \end{pmatrix}, \ \phi \in \mathbb{R} \wedge \ L_n \in \mathcal{L}or \wedge \ C \in \mathbb{R}^{1,3} \right\} \tag{5.6.9}$$

It should be noted that Feynman considers that applying *PT-symmetry* to the motions of particles leads to the creation of antimatter through the application of *C-symmetry*. Therefore, *PT-symmetry* is equivalent to *C-symmetry*, i.e. a particle of matter *"seen in a mirror"* and moving backward in time is antimatter.

This perspective is derived from Weinberg's work, *"The Quantum Theory of Fields"* in Section 2.6, titled *"Space Inversion and Time-Reversal"* ([85]). Indeed, an arbitrary choice is applied for the inversion operator T, resulting in the fact that the *CPT* operator becomes the identity.

Thus, given that $\mathbf{CPT} = \mathbf{I}$, it follows that $\mathbf{PT} = \mathbf{PT} \cdot \mathbf{I} = \mathbf{PT} \cdot \mathbf{CPT} = \mathbf{C}$. Consequently, Feynman's viewpoint relies primarily on Quantum Mechanics, where quantum theorists make a priori, entirely arbitrary choices regarding the P and T operators,

constrained by the *"need to avoid the emergence of negative energy states (considered non-physical)"*. Therefore, the P operator must be linear and unitary, and the T operator antilinear and antiunitary. And to conclude by adding on page 104 that: *"No examples are known of particles that furnish unconventional representations of inversions, so these possibilities will not be pursued further here. From now on, the inversions will be assumed to have the conventional action assumed in Section 2.6"*.

Negative energy states (associated with negative pressure) exist because they're responsible for the acceleration of cosmic expansion, as evidenced by Perlmutter's Nobel Prize-winning work in 2011 ([52]). However, at the time when Quantum Field Theory emerged, this phenomenon was not yet known.

Therefore, for Feynman, the presence of the time inversion operator T in its global *PT-symmetry* does not lead to mass inversion but transforms matter into positive-mass antimatter by charge inversion through the *C-symmetry*.

In the view of the Janus group, starting from the motion of a particle with positive mass in 5D space, *C-symmetry* (carried by the inversion of the fifth dimension) transforms this particle (this motion) into a positive-mass antiparticle that can be called a *"Dirac-like antiparticle"*, which is the kind produced in laboratories and has recently been demonstrated to behave in the same way as ordinary matter under the influence of gravity ([5]).

On the other hand, the PT-symmetric transformation applied to a particle produces an antiparticle with negative energy and mass, due to *T-symmetry*, which can be called a *"Feynman-like antiparticle"* which corresponds to primordial antimatter located between galaxies and is notably found as conglomerates in the *Great Repeller* ([36]). The equivalence $PT = C$, according to Feynman, is then no longer applicable.

5.7 Implications

This study's significant contributions primarily affect the fields of Quantum Mechanics and Cosmology:

- **In Quantum Mechanics**, a notable aspect is the reversal of energy of certain objects. An intriguing question arises regarding the feasibility of objects with negative energy states in Quantum Mechanics. In addressing *T-Symmetry*, quantum physicists traditionally adopt an anti-linear and anti-unitary perspective for the T-operator, aiming to exclude negative energy states, which are generally not considered intrinsic to physics. Similarly, a P-operator is chosen to be unitary and linear for analogous reasons (see [85]). These selections underpin the CPT-theorem, reinforcing the notion that *PT-Symmetry* aligns with *C-Symmetry*. Contrarily, adopting a linear and unitary T-operator reveals that negative energy states are a

natural outcome in the Schrödinger and Dirac equations(see [23]), paving the way for novel research avenues. Moreover, cosmological observations have confirmed that the universe's expansion is accelerating, attributed to a negative pressure associated with dark energy, as demonstrated by the Nobel Prize-winning work of Perlmutter in 2011. Since pressure represents energy density per volume, this phenomenon directly correlates with negative energy influencing the universe's expansion.

- **In the realm of Cosmology**, general relativity firmly dismisses the concept of negative masses, citing the emergence of the Runaway phenomenon and conflicts with the principles of action-reaction and equivalence (see [10]). Therefore, any new model proposing the integration of negative energy and mass states would necessitate an expansion of the foundational geometric framework of relativity. The dynamic group theory, revolving around various groups such as Lorentz, Poincaré, or Kaluza, provides a framework for depicting a universe devoid of forces, characterized by a flat, uncurved structure. In such a universe, particles trace the geodesics of Minkowski space within a Lorentzian metric or navigate a fibered space influenced by a fifth dimension, be it open or closed. This theoretical approach intimates the coexistence of two distinct types of matter, existing in isolation without mutual interaction. Thus, particles within these spaces do not interact with each other. This innovative perspective opens new pathways in understanding particle-space-time interactions.

5.8 Appendix

In the theory of dynamic groups developed by J.M. Souriau in 1970, the connection between the geometric structure and the physical content of a system is explored using specific dynamic groups ([76],[78]). These dynamic groups describe the symmetries and transformations that preserve the geometric properties of the system. By studying the nature of the dynamic group associated with a given physical system, we can determine the relationships between geometry and the associated physical quantities.

Every movement of an object in space-time has its moment. However, this is not synonymous with an *instant* or the physical concepts of linear or angular momentum. The term *moment* in group theory refers to movement, that is, a physical displacement between points in space.

To determine this moment, it is necessary to first define what a group action is. This refers to the way in which a group of matrices can act by multiplication on another group of matrices in order to manage, for example in the Euclidean group, rotations, symmetries, and translations in a single operation.

But J.M. Souriau discovered that a group can also act on moments, in turn generating a new geometric space. Thus, there may be another action of the group on another space. In fact, there is a space where movements are inscribed: space-time. In the four-dimensional Minkowski space-time, a group acts on a point t_1, x_1, y_1, z_1 to give another point t_2, x_2, y_2, z_2. However, what is inscribed in space-time is only the trajectory. Yet, the movement acts in two spaces, the second being the space of movement parameters, which Souriau calls the space of moments[3].

The Coadjoint Action of the Poincaré Group on its Space of Moments

Consider the movement of an object in space. Such movement is also defined by its moment μ. The physicist can then apply an element g, for example from the Galilean group, to this moment μ. This produces a new moment μ'. This action can be written

[3]Souriau's approach, thanks to the Poincaré group which is the isometry group of Minkowski space encompassing the Lorentz group (with its four connected components), allows the parameters associated with each of these movements, whose representative points belong to a vector space, *the space of moments*, to emerge. The dimension of this space is equal to that of the group: ten. Indeed, the Lorentz group is made up of transformations that preserve the quadratic form of space-time. It consists of the orthochronous Lorentz transformations and the translation group. The transformations of the orthochronous Lorentz group have 6 degrees of freedom, while the translation group has 4 degrees of freedom. This structure leads to 10 independent parameters of the Poincaré group. By combining them into an antisymmetrical matrix called a *torseur*, the parameters of the space of movements can thus be defined.

as follows:

$$\mu' = g \times \mu \times g^T \tag{5.8.1}$$

g^T represents the transpose of this matrix, and μ is the matrix of moments. It is an antisymmetric matrix of size 5×5, meaning that symmetric elements with respect to the main diagonal have opposite signs. The elements of the main diagonal are equal to zero (which is its own opposite). We can define this matrix as follows:

$$\mu = \begin{pmatrix} 0 & -l_z & l_y & f_x & -p_x \\ l_z & 0 & -l_x & f_y & -p_y \\ -l_y & l_x & 0 & f_z & -p_z \\ -f_x & -f_y & -f_z & 0 & -E \\ p_x & p_y & p_z & E & 0 \end{pmatrix} \tag{5.8.2}$$

For example, to better understand what μ represents, this 5×5 matrix can be broken down as follows:

- A matrix M of dimension 4×4 given by:

$$M = \begin{pmatrix} 0 & -l_z & l_y & f_x \\ l_z & 0 & -l_x & f_y \\ -l_y & l_x & 0 & f_z \\ -f_x & -f_y & -f_z & 0 \end{pmatrix} \tag{5.8.3}$$

- An energy-momentum vector P of dimension 4×1 given by[4]:

$$P = \begin{pmatrix} p_x \\ p_y \\ p_z \\ E \end{pmatrix} \tag{5.8.4}$$

- Its transpose, the row vector P^T of dimension 1×4 given by:

$$P^T = \begin{pmatrix} p_x & p_y & p_z & E \end{pmatrix} \tag{5.8.5}$$

We can deduce the more compact form of μ as follows:

$$\mu = \begin{pmatrix} M & -P \\ P^T & 0 \end{pmatrix} \tag{5.8.6}$$

The coadjoint action is the action of a group on its space of moments. More specifically, it is the action of a Lie group on the dual vector space of its Lie algebra[5]

[4]We specify the word *vector* to indicate the nature of the variable used, in order not to overload the expressions.

[5]The dual of a Lie algebra, in the context of physics, is a mathematical space composed of covectors.

Poincaré Group

In General Relativity, the Poincaré group governs the motion of relativistic material particles (5.2.10) and can be defined by the matrix group[6]:

$$g := \left\{ \begin{pmatrix} L & C \\ 0 & 1 \end{pmatrix}, L = \lambda L_o \in \mathcal{L}or \wedge \lambda = \pm 1 \wedge C \in \mathbb{R}^{1,3} \right\} \tag{5.8.7}$$

acting on Minkowski space as follows:

$$g(X) = L.X + C \tag{5.8.8}$$

The action of the group on its space of moments is the action on the dual of the Lie algebra of the group. The element of the Lie algebra is obtained by differentiating the ten components of the group. Souriau designates by the Greek letter Λ the differential of the square matrix Z representing the element of the Poincaré group, and by the Greek letter Γ the element of the subgroup of spatio-temporal translations[7]:

$$Z := \left\{ \begin{pmatrix} \Lambda & \Gamma \\ 0 & 0 \end{pmatrix}, \bar{\Lambda} = -\Lambda \wedge \Gamma \in \mathbb{R}^{1,3} \right\} \tag{5.8.9}$$

We have shown that the moment matrix μ includes elements with a physical interpretation, such as the four-vector P, where E represents the energy and $p = \{p_x, p_y, p_z\}$ the linear momentum.

However, what is the essence and physical significance of this antisymmetric matrix M ?

These covectors are mathematical entities that assign scalar values to vectors in the Lie algebra, representing physical quantities that do not have a specific direction, such as energy or temperature. Moments, in this context, are measures that describe how the transformations associated with a Lie group modify the Lie algebra itself. The coadjoint representation is a method by which a group acts on the dual of its Lie algebra. This action allows for the examination of the transformation of covectors, like moments, under the influence of the group. The interest of this approach lies in its ability to reveal information about the geometric and physical characteristics of systems studied, by analyzing how these systems evolve or remain invariant under the transformations of the group.

[6] (13.51) and (13.52) of [78]

[7] (13.54) of [78]. He then writes μ, an element of the space of movements, in the form (13.57) and expresses the invariance in the form of the constancy of the scalar (13.58), where M is an antisymmetric matrix.

Let's proceed to decompose it to find out:

$$
\begin{aligned}
M &= \begin{pmatrix} 0 & -l_z & l_y & f_x \\ l_z & 0 & -l_x & f_y \\ -l_y & l_x & 0 & f_z \\ -f_x & -f_y & -f_z & 0 \end{pmatrix} \\
S &= \begin{pmatrix} 0 & -l_z & l_y \\ l_z & 0 & -l_x \\ -l_y & l_x & 0 \end{pmatrix} \\
f &= \begin{pmatrix} f_x \\ f_y \\ f_z \\ 0 \end{pmatrix}
\end{aligned}
\tag{5.8.10}
$$

In its compact form:

$$
M = \begin{pmatrix} S & f \\ -f^T & 0 \end{pmatrix} \tag{5.8.11}
$$

The velocity V is implicitly integrated into the L matrix of the Lorentz group. When examining a motion occurring in a specific direction, for example along an axis, with a velocity V and a translation $\Delta z = c$, and $c = V\Delta t$, we then place ourselves in a coordinate system that follows the motion of the particle along this translation in space-time. In this context, the vector f turns out to be null.

The matrix S can then be expressed as follows:

$$
S = \begin{pmatrix} 0 & -s & 0 \\ s & 0 & 0 \\ 0 & 0 & 0 \end{pmatrix} \tag{5.8.12}
$$

The term refers to the *spin* of a particle. As Souriau demonstrated in 1970, it has a purely geometric nature: it is represented by an antisymmetric matrix of size 3×3. The method of geometric quantization he developed reveals that spin can only be an integer multiple of $\hbar$ (the reduced Planck constant). Souriau also explored, in [78], how the existence of an electric charge in a particle suggests its movement in a spacetime endowed with a fifth dimension of extremely small size[8], similar to the Kaluza dimension, which is looped onto itself like a bundle of fibers. This fifth dimension, being looped onto itself, could lead to the geometric quantization of electric charge, thanks to a *"closure form"* in spacetime, allowing an object to become identical to itself after a 360° rotation. This characteristic is fundamental for understanding the quantification of spin.

[8]The Planck length

The quantity $f = [f_x, f_y, f_z]$, designated by Souriau as the *"passage"*, cancels out in the frame of the moving particle and is only perceptible from another frame, illustrating an effect of motion[9].

The relationship $C_m = f + pt$ establishes a link between the passage f and the position of the center of mass C_m at time $t = 0$.

The complete Galilean moment consists of the following elements:

$$\mu = \{\text{energy, mass, momentum, passage, spin}\}$$

Every movement of an object is characterized by its own moment, which can only be partially transferred from one object to another, without the possibility of creation or disappearance. This allows the moment to be measured by transferring a part of the object's moment to the measuring instrument.

It is important to note that rest mass is considered a parameter of the moment. Unlike classical mass, which was treated as an arbitrary additive constant in the Galilean group, mass in the Poincaré group is defined as relativistic mass $m = \frac{E}{c^2}$, and thus varies with velocity. This treatment also differs from the non-relativistic dynamic group by the absence of barycentric decomposition[10], a feature of the Galilean group resulting from the existence of a privileged subgroup absent in the Poincaré group[11]. Any virtual movement can be interpreted as a real movement by changing the frame of reference[12]. The Poincaré group thus describes the properties of elementary particles using only two physically interpretable parameters: rest mass and spin[13].

For massless particles such as the photons, helicity, in addition to polarization (linear or elliptical), is also crucial. The helicity of the photon, which can take the values ± 1, corresponds respectively to left circular polarization (LCP) and right circular polarization (RCP). The helicity of a particle is determined by the orientation of its spin

[9]For example, you are sitting in a flying plane at the back of the cabin, and you are asked to move forward. You can only pass if you *"borrow some passage"* from the plane. This will cause it to deviate slightly from its initial flight plan. It is the conservation of passage that establishes the following rule: If an object is in free space, its center of mass moves in a straight line, at a constant speed, in the direction of the momentum unless disturbed by external forces such as gravity. If the momentum is zero, the center of mass is stationary.

[10]The concept of barycentric decomposition refers to the ability to separate the motion of a system into a motion of the center of mass and relative motions of the particles around this center.

[11]As we have already studied, the Galilean group governs the transformations between inertial frames. An important feature of the Galilean group is the ability to identify a center of mass (or barycenter) for a system of particles, which behaves simply under these transformations. In special relativity, the concept of the center of mass is not as simple or universal as in classical mechanics, because the definition of the center of mass depends on the frame of reference.

[12]In special relativity, what may appear as purely hypothetical movement in one frame can be observed as a concrete physical movement in another.

[13]or intrinsic angular momentum

relative to its motion vector.

Now that we have introduced the main tools, we can show the coadjoint action of the Poincaré group on its space of moments.

We know that the coadjoint action is the action of a Lie group on the dual vector space of its Lie algebra.

Thus, by applying the action of the Poincaré group on the dual of its Lie algebra, i.e., on its space of moments, we obtain the following action from 5.8.1 :

$$\mu' = \begin{pmatrix} L & C \\ 0 & 1 \end{pmatrix} \times \begin{pmatrix} M & -P \\ P^T & 0 \end{pmatrix} \times \begin{pmatrix} L^T & 0 \\ C^T & 1 \end{pmatrix} \tag{5.8.13}$$

$$\mu' = \begin{pmatrix} LML^T - LPC^T + CP^TL^T & -LP \\ P^TL^T & 0 \end{pmatrix} \tag{5.8.14}$$

By identification with 5.8.6, we can deduce that[14]:

$$M' = LML^T - LPC^T + CP^TL^T \quad \text{and} \quad P' = LP \tag{5.8.15}$$

What then is the meaning of the different components of the space of moments[15]?

$$\mu = \{M, P\} = \{l, g, p, E\} \tag{5.8.16}$$

M is the moment matrix associated with μ and P is the energy-momentum vector. l is the angular momentum of M, g is the relativistic barycenter of M, p is the linear momentum of P and E is the energy of P.

In Chapter 5 of [78], J.M. Souriau develops a method of geometric quantization that leads to the quantization of spin, considered as a geometric attribute[16].

$$s = n\frac{\hbar}{2} \tag{5.8.17}$$

Thus, we obtain a description of particles in their space of moment, with different spin values.

The mass is defined on page 188[17] as follows:

$$m = \sqrt{P^T \cdot P}\,\mathrm{sgn}(E) \tag{5.8.18}$$

[14] (13.107) of [78]
[15] (13.57) of [78]
[16] (18.82) of [78]
[17] (14.57) of [78]

Time and Energy Inversion

The elements of the Lorentz group act on points in spacetime that constitute a movement. By acting an element L of the Lorentz group on a given movement, we obtain another movement.

As mentioned through expression 5.2.5, the Lorentz group has four connected components.

The neutral component $\mathcal{L}or_n$ is a subgroup containing the identity matrix that inverts neither space nor time.

Consider the 4-component matrix ω made up of two parameters λ_1 and λ_2:

$$\omega_{(\lambda_1,\lambda_2)} = \begin{pmatrix} \lambda_1 & 0 & 0 & 0 \\ 0 & \lambda_2 & 0 & 0 \\ 0 & 0 & \lambda_2 & 0 \\ 0 & 0 & 0 & \lambda_2 \end{pmatrix} \quad \text{with} \quad \begin{cases} \lambda_1 = \pm 1 \\ \lambda_2 = \pm 1 \end{cases} \tag{5.8.19}$$

Thus, the four components of the Lorentz group can be easily expressed using the four possible combinations of these two parameters applied to its neutral component, of which an element $L_n \in \mathcal{L}or_n$ is expressed according to the expression $L = \omega L_n$:

$$\omega_{(1,1)} \times L_n = \begin{pmatrix} 1 & 0 & 0 & 0 \\ 0 & 1 & 0 & 0 \\ 0 & 0 & 1 & 0 \\ 0 & 0 & 0 & 1 \end{pmatrix} \in \mathcal{L}or_n \qquad \omega_{(1,-1)} \times L_n = \begin{pmatrix} 1 & 0 & 0 & 0 \\ 0 & -1 & 0 & 0 \\ 0 & 0 & -1 & 0 \\ 0 & 0 & 0 & -1 \end{pmatrix} \in \mathcal{L}or_s$$

$$\omega_{(-1,1)} \times L_n = \begin{pmatrix} -1 & 0 & 0 & 0 \\ 0 & 1 & 0 & 0 \\ 0 & 0 & 1 & 0 \\ 0 & 0 & 0 & 1 \end{pmatrix} \in \mathcal{L}or_t \quad \omega_{(-1,-1)} \times L_n = \begin{pmatrix} -1 & 0 & 0 & 0 \\ 0 & -1 & 0 & 0 \\ 0 & 0 & -1 & 0 \\ 0 & 0 & 0 & -1 \end{pmatrix} \in \mathcal{L}or_{st} \tag{5.8.20}$$

We note that $\lambda_1 = -1$ inverts time while $\lambda_2 = -1$ inverts space. The four components are grouped into two subsets *"orthochronous"* and *"retrochronous"* according to the respective expressions 5.2.6 and 5.2.7.

The Poincaré group can then be written according to these four connected components as follows:

$$g := \left\{ \begin{pmatrix} \omega L_n & C \\ 0 & 1 \end{pmatrix}, \omega L_n \in \mathcal{L}or \wedge C \in \mathbb{R}^{1,3} \right\} \tag{5.8.21}$$

Thus, the action of this Poincaré group on the spacetime coordinates yields the

following space of movements:

$$\begin{bmatrix} \omega L_n & C \\ 0 & 1 \end{bmatrix} \times \begin{bmatrix} \xi \\ 1 \end{bmatrix} = \begin{bmatrix} \omega L_n \xi + C \\ 1 \end{bmatrix}. \tag{5.8.22}$$

In fact, this is the action of the Poincaré group on its space of moments μ having ten independent scalars:

- The energy E
- The momentum $p = \{p_x, p_y, p_z\}$
- The passage $f = \{f_x, f_y, f_z\}$
- The spin $s = \{l_x, l_y, l_z\}$

The action of the Poincaré group on the dual of its Lie algebra is the coadjoint action on its space of moments M (passage f and spin s) and the energy-momentum vector P (energy E and momentum p), which yields:

$$M' = (\omega L_n) M (\omega L_n)^T - (\omega L_n) P C^T + C P^T (\omega L_n)^T \quad \text{et} \quad P' = (\omega L_n) P \tag{5.8.23}$$

To highlight the effects of the symmetries P, T, and PT on $\{E, p, f, s\}$, we will choose the simplest possible action, where there is no translation in spacetime, so that the vector $\mathbf{C}$ cancels out and $L_n = 1$[18]:

$$M' = [\omega_{(\lambda_2,\lambda_1)}] M [\omega_{(\lambda_2,\lambda_1)}]^T \quad \text{et} \quad P' = [\omega_{(\lambda_2,\lambda_1)}] P \tag{5.8.24}$$

Now, consider for example the symmetry T, where there is only a time inversion ($\lambda_1 = -1$), without space inversion ($\lambda_2 = 1$), in a case where there is also no translation in spacetime ($C = 0$). We thus have:

$$\omega_{(1,-1)} \times L_n = L_t \tag{5.8.25}$$

Hence:

$$L_t \times \xi = \begin{pmatrix} 1 & 0 & 0 & 0 \\ 0 & 1 & 0 & 0 \\ 0 & 0 & 1 & 0 \\ 0 & 0 & 0 & -1 \end{pmatrix} \times \begin{pmatrix} x \\ y \\ z \\ t \end{pmatrix} = \begin{pmatrix} x \\ y \\ z \\ -t \end{pmatrix}. \tag{5.8.26}$$

Thus, we obtain the action of time inversion in the space of trajectories or in spacetime.

[18] The matrix $\omega_{(\lambda_2,\lambda_1)}$ is here expressed according to a 4D spacetime convention noted {x, y, z, t} instead of the usual relativity convention {t, x, y, z} that we use elsewhere, in order to align with the graphical and matrix representations of M and P shown previously.

Let's determine the coadjoint action, that is, the action of the group on its space of moments according to 5.8.10:

$$M' = L_t M L_t^T = \begin{pmatrix} 1 & 0 & 0 & 0 \\ 0 & 1 & 0 & 0 \\ 0 & 0 & 1 & 0 \\ 0 & 0 & 0 & -1 \end{pmatrix} \begin{pmatrix} 0 & -l_z & l_y & f_x \\ l_z & 0 & -l_x & f_y \\ -l_y & l_x & 0 & f_z \\ -f_x & -f_y & -f_z & 0 \end{pmatrix} \begin{pmatrix} 1 & 0 & 0 & 0 \\ 0 & 1 & 0 & 0 \\ 0 & 0 & 1 & 0 \\ 0 & 0 & 0 & -1 \end{pmatrix} \tag{5.8.27}$$

Hence :

$$M' = \begin{pmatrix} 0 & -l_z & l_y & -f_x \\ l_z & 0 & -l_x & -f_y \\ -l_y & l_x & 0 & -f_z \\ f_x & f_y & f_z & 0 \end{pmatrix} \tag{5.8.28}$$

On the other hand, we have:

$$P' = L_t P = \begin{pmatrix} 1 & 0 & 0 & 0 \\ 0 & 1 & 0 & 0 \\ 0 & 0 & 1 & 0 \\ 0 & 0 & 0 & -1 \end{pmatrix} \begin{pmatrix} p_x \\ p_y \\ p_z \\ E \end{pmatrix} = \begin{pmatrix} p_x \\ p_y \\ p_z \\ -E \end{pmatrix} \tag{5.8.29}$$

Thus, we can deduce that the application of the L_t component of the Lorentz group to the movement of a particle induces an inversion of its energy from E to $-E$ and its passage from f to $-f$.

The T symmetry applied to the movement of a particle thus inverts its energy (page 189–193 of [78]).

The same process can be applied to the 4 connected components of the Lorentz group and we will discover that:

- Symmetry P: the momentum and passage are inverted. The energy and spin remain unchanged.
- Symmetry T: the energy and passage are inverted. The momentum and spin remain unchanged.
- Symmetry PT: the momentum and energy are inverted. The passage and spin remain unchanged.

No transformation changes the spin.

Restricted Kaluza Group

Let's apply an extension of the Poincaré group to form the following dynamic group:

$$g := \left\{ \begin{pmatrix} 1 & 0 & \phi \\ 0 & L & C \\ 0 & 0 & 1 \end{pmatrix}, \phi \in \mathbb{R} \wedge L = \lambda L_o \in \mathcal{L}or \wedge \lambda = \pm 1 \wedge C \in \mathbb{R}^{1,3} \right\} \tag{5.8.30}$$

Starting from Minkowski space:

$$\xi = \begin{pmatrix} t \\ x \\ y \\ z \end{pmatrix} = \begin{pmatrix} t \\ r \end{pmatrix} \tag{5.8.31}$$

Let's introduce Kaluza space[19] that incorporates a 5×5 Gram matrix:

$$\Gamma = \begin{pmatrix} 1 & 0 & 0 & 0 & 0 \\ 0 & -1 & 0 & 0 & 0 \\ 0 & 0 & -1 & 0 & 0 \\ 0 & 0 & 0 & -1 & 0 \\ 0 & 0 & 0 & 0 & -1 \end{pmatrix} = \begin{pmatrix} G & 0 \\ 0 & -1 \end{pmatrix} \quad \text{where} \quad G = \begin{pmatrix} 1 & 0 & 0 & 0 \\ 0 & -1 & 0 & 0 \\ 0 & 0 & -1 & 0 \\ 0 & 0 & 0 & -1 \end{pmatrix} \tag{5.8.32}$$

In the considered group, we just add a translation ϕ to the fifth dimension ζ. Thus, the dimension of the group becomes 11 (section 5.5). It is the isometry group of Kaluza space, defined by its metric:

$$\mathrm{d}s^2 = \mathrm{d}X^T \Gamma \mathrm{d}X = \mathrm{d}t^2 - \mathrm{d}x^2 - \mathrm{d}y^2 - \mathrm{d}z^2 - \mathrm{d}\zeta^2 \tag{5.8.33}$$

With :

$$X = \begin{pmatrix} \xi \\ \zeta \end{pmatrix} = \begin{pmatrix} t \\ x \\ y \\ z \\ \zeta \end{pmatrix} \tag{5.8.34}$$

According to Noether's theorem[20], this new symmetry is accompanied by the invariance of a scalar that we will call q. The torsor of this Kaluza group then incorporates an additional parameter:

$$\mu = \{M, P, q\} = \{l, g, p, E, q\} \tag{5.8.35}$$

[19] Kaluza space is a hyperbolic Riemannian manifold with signature $(+----)$

[20] Noether's theorem states that for every continuous symmetry of a physical action, there exists a conserved quantity. In our context, if a new symmetry ensures the invariance of a scalar q, this scalar is the conserved quantity. This means that q remains constant when the symmetry is applied to the system's action.

Let's introduce the action of the group on its Lie algebra:

$$Z' = g^{-1} Z g \tag{5.8.36}$$

However, if we consider an element of the Lie algebra of this group:

$$Z = \begin{pmatrix} 0 & 0 & \delta\phi \\ 0 & G\omega & \gamma \\ 0 & 0 & 0 \end{pmatrix} \quad Z' = \begin{pmatrix} 0 & 0 & \delta\phi' \\ 0 & G\omega' & \gamma' \\ 0 & 0 & 0 \end{pmatrix} \tag{5.8.37}$$

The inverse matrix of g [21] gives :

$$\begin{pmatrix} 1 & 0 & \phi \\ 0 & L & C \\ 0 & 0 & 1 \end{pmatrix}^{-1} = \begin{pmatrix} 1 & 0 & -\phi \\ 0 & L^{-1} & -L^{-1}C \\ 0 & 0 & 1 \end{pmatrix} \tag{5.8.38}$$

And :

$$\begin{pmatrix} 0 & 0 & \delta\phi \\ 0 & G\omega & \gamma \\ 0 & 0 & 0 \end{pmatrix} \begin{pmatrix} 1 & 0 & \phi \\ 0 & L & C \\ 0 & 0 & 1 \end{pmatrix} = \begin{pmatrix} 0 & 0 & \delta\phi \\ 0 & G\omega L & G\omega C + \gamma \\ 0 & 0 & 0 \end{pmatrix} \tag{5.8.39}$$

We can then calculate 5.8.36 as follows:

$$Z' = \begin{pmatrix} 1 & 0 & -\phi \\ 0 & L^{-1} & -L^{-1}C \\ 0 & 0 & 1 \end{pmatrix} \begin{pmatrix} 0 & 0 & \delta\phi \\ 0 & G\omega & \gamma \\ 0 & 0 & 0 \end{pmatrix} \begin{pmatrix} 1 & 0 & \phi \\ 0 & L & C \\ 0 & 0 & 1 \end{pmatrix} \tag{5.8.40}$$

Hence :

$$Z' = \begin{pmatrix} 1 & 0 & -\phi \\ 0 & L^{-1} & -L^{-1}C \\ 0 & 0 & 1 \end{pmatrix} \begin{pmatrix} 0 & 0 & \delta\phi \\ 0 & G\omega L & G\omega C + \gamma \\ 0 & 0 & 0 \end{pmatrix} = \begin{pmatrix} 0 & 0 & \delta\phi \\ 0 & L^{-1}G\omega L & L^{-1}G\omega C + L^{-1}\gamma \\ 0 & 0 & 0 \end{pmatrix} \tag{5.8.41}$$

Then :

$$Z' = \begin{pmatrix} 0 & 0 & \delta\phi' \\ 0 & G\omega' & \gamma' \\ 0 & 0 & 0 \end{pmatrix} = \begin{pmatrix} 0 & 0 & \delta\phi \\ 0 & L^{-1}G\omega L & L^{-1}G\omega C + L^{-1}\gamma \\ 0 & 0 & 0 \end{pmatrix} \tag{5.8.42}$$

[21] For example, to find the inverse of a 2×2 matrix, we use the following formula when the matrix is of the form:

$$\begin{pmatrix} a & b \\ c & d \end{pmatrix}$$

The inverse is :

$$\frac{1}{ad - bc} \begin{pmatrix} d & -b \\ -c & a \end{pmatrix}$$

Thus, by identification, we can deduce :

$$\frac{1}{2}T_r(M\cdot\omega)+P^T\cdot G\gamma+q\delta\phi=\frac{1}{2}T_r(M'\cdot\omega')+P'^T\cdot G\gamma'+q'\delta\phi' \tag{5.8.43}$$

This allows us to deduce the action of the following group:

$$q'=q \tag{5.8.44}$$
$$M'=LML^T-LPC^T+CP^TL^T \tag{5.8.45}$$
$$P'=LP \tag{5.8.46}$$

If we identify q as the electric charge, this would show that the motion of a massive particle in a five-dimensional space would transform it into an electrically charged particle.

Restricted Janus Group

Consider the following dynamic group:

$$g:=\left\{\begin{pmatrix}\mu&0&\phi\\0&L&C\\0&0&1\end{pmatrix},\mu=\pm1\wedge\phi\in\mathbb{R}\wedge L=\lambda L_o\in\mathcal{L}or\wedge\lambda=\pm1\wedge C\in\mathbb{R}^{1,3}\right\} \tag{5.8.47}$$

The action of the group on the coordinates of the 5-dimensional spacetime defined by 5.8.34 yields the space of the following motions:

$$\begin{pmatrix}\mu&0&\phi\\0&L&C\\0&0&1\end{pmatrix}\begin{pmatrix}\zeta\\\xi\\1\end{pmatrix}=\begin{pmatrix}\mu\zeta+\phi\\L\xi+C\\1\end{pmatrix} \tag{5.8.48}$$

A similar calculation to the previous one yields the action of the group:

$$q'=\mu q \tag{5.8.49}$$
$$M'=LML^T-LPC^T+CP^TL^T \tag{5.8.50}$$
$$P'=LP \tag{5.8.51}$$

This group acts on the five-dimensional Kaluza space. We observe that $\mu=-1$ reverses the fifth dimension ζ and the scalar q.

Through a dynamic interpretation of the group, we find the idea suggested by J.M. Souriau [78]: the inversion of the fifth dimension is associated with the inversion of electric charge. However, this is only one of the quantum charges.

Indeed, the *C-Symmetry* translating the *"Matter-Antimatter"* symmetry introduced by Dirac, reverses all quantum charges. This inversion operation is only obtained by

adding as many compactified dimensions as there are quantum charges. The action of the group on the coordinates of n-dimensional spacetime yields the space of the following motions:

$$\begin{pmatrix} \mu & 0 & 0 & \cdots & 0 & \phi^1 \\ 0 & \mu & 0 & \cdots & 0 & \phi^2 \\ 0 & 0 & \ddots & \cdots & 0 & \vdots \\ \vdots & \vdots & \cdots & \mu & 0 & \phi^p \\ 0 & 0 & \cdots & 0 & L & C \\ 0 & 0 & \cdots & 0 & 0 & 1 \end{pmatrix} \begin{pmatrix} \zeta^1 \\ \zeta^2 \\ \vdots \\ \zeta^p \\ \xi \\ 1 \end{pmatrix} = \begin{pmatrix} \mu\zeta^1 + \phi^1 \\ \mu\zeta^2 + \phi^2 \\ \vdots \\ \mu\zeta^p + \phi^p \\ L\xi + C \\ 1 \end{pmatrix} \tag{5.8.52}$$

The torsor of this group incorporates several additional scalars q^p:

$$\mu = \{M, P, \sum_1^p q^i\} = \{l, g, p, E, q^1, q^2, \ldots, q^p\} \tag{5.8.53}$$

This allows us to obtain the action of the group on its momentum space:

$$q'^1 = \mu q^1 \tag{5.8.54}$$
$$q'^1 = \mu q^1 \tag{5.8.55}$$
$$\ldots \tag{5.8.56}$$
$$q'^p = \mu q^p \tag{5.8.57}$$
$$M' = LML^T - LPC^T + CP^TL^T \tag{5.8.58}$$
$$P' = LP \tag{5.8.59}$$

Moreover, Souriau considers that electric charge can be geometrically quantized into discrete values $(+e, 0, -e)$ when the associated fifth dimension is closed.

Imagine representing motion in Minkowski space along a simple straight line oriented in time. At each point, we add a closed dimension, which extends Minkowski space into a bundle. In the didactic figure 5.1, it is represented as a cylinder.

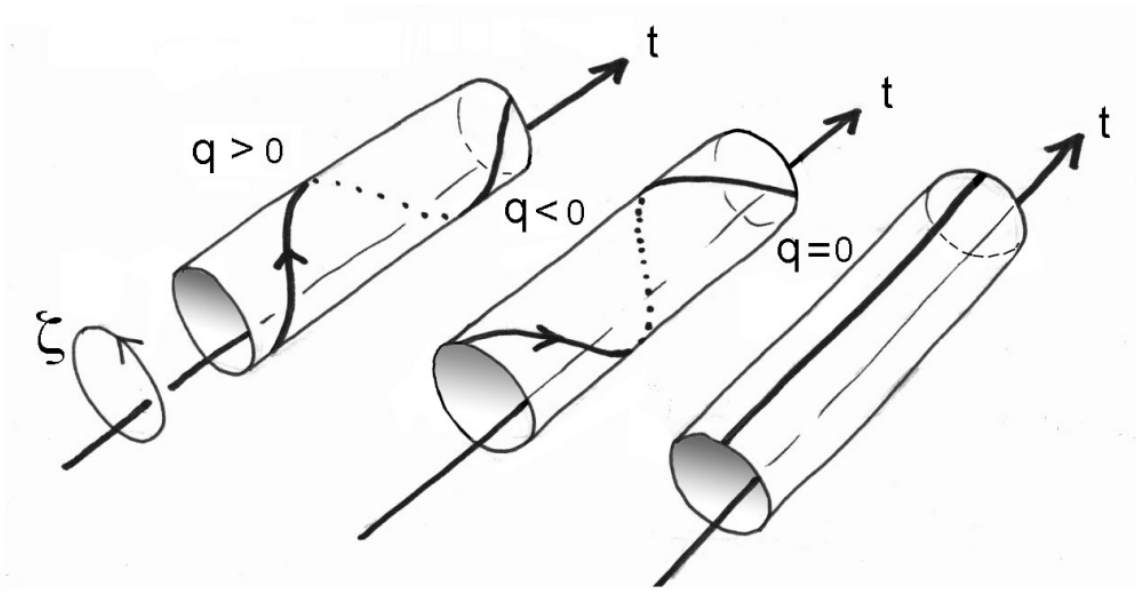

Figure 5.1: Inversion of the winding direction of a particle's motion reflecting the symmetry C

Janus Dynamic Group

As studied in section 5.6, if we introduce a new symmetry to the previous group, which we can call *PT Symmetry* allowing the conversion of matter into antimatter with negative mass[22], we thus combine *C Symmetry* and PT to form the *Janus Dynamic Group*[23] as follows:

$$g := \left\{ \begin{pmatrix} \lambda\mu & 0 & \phi \\ 0 & \lambda L_o & C \\ 0 & 0 & 1 \end{pmatrix}, \lambda, \mu \in \{-1, 1\} \wedge \phi \in \mathbb{R} \wedge L_o \in \mathcal{L}or_o \wedge C \in \mathbb{R}^{1,3} \right\} \quad (5.8.60)$$

We can consider that particles of matter and antimatter can coexist in the same space sheet. However, no coexistence is possible for the motion of particles deduced by T-symmetry (or PT-symmetry).

This space is of dimension $4 + p$ (for p quantum charges).

We will therefore consider the two-sheet covering of this manifold M_{n+p}.

[22] A concept we could call *antimatter in the sense of Feynman*

[23] Whose general form is given by 5.6.1

In each of these two sheets, there remains a possibility to perform the symmetry corresponding to $\mu = -1$, that is, the inversion of all quantum charges.

In other words, the *"Matter-Antimatter"* duality exists in both sheets.

To understand the nature of the different components of these sheets, we will consider the motion of a particle of matter with energy and mass:

- By acting on this motion with elements of the group corresponding to $(\lambda = 1; \mu = 1)$, we will obtain other motions of particles of matter with positive mass and energy.

- By acting on this motion with elements of the group corresponding to $(\lambda = 1; \mu = -1)$, we will obtain other motions of antimatter particles with positive mass and energy[24].

- By acting on this motion with elements of the group corresponding to $(\lambda = -1; \mu = 1)$, we will obtain other motions of particles of matter with negative mass and energy.

- By acting on this motion with elements of the group corresponding to $(\lambda = -1; \mu = -1)$, we will obtain other motions of antimatter particles with negative mass and energy[25].

Its isometry group is that of Janus space, defined by the same metric as structuring Kaluza space 5.8.33, and its dimension is 11[26]. The torsor of the group is also the same as 5.8.35.

However, if we consider an element of the Lie algebra of this group:

$$Z = \begin{pmatrix} 0 & 0 & \delta\phi \\ 0 & \lambda G\omega & \gamma \\ 0 & 0 & 1 \end{pmatrix} \tag{5.8.61}$$

[24] These are *"antimatter in the sense of Dirac"* (C-symmetry).
[25] These are *"antimatter in the sense of Feynman"* (PT-symmetry).
[26] $10 + 1$ dimension associated with the fifth space dimension ζ that J.M. Souriau identifies with the electric charge q.

The inverse matrix of g (5.8.60) yields:

$$\begin{pmatrix} \lambda\mu & 0 & \phi \\ 0 & \lambda L_o & C \\ 0 & 0 & 1 \end{pmatrix}^{-1} = \begin{pmatrix} \lambda\mu & 0 & -\lambda\mu\phi \\ 0 & \lambda L_o^{-1} & -\lambda L_o^{-1}C \\ 0 & 0 & 1 \end{pmatrix} \tag{5.8.62}$$

And :

$$\begin{pmatrix} 0 & 0 & \delta\phi \\ 0 & \lambda G\omega & \gamma \\ 0 & 0 & 0 \end{pmatrix} \begin{pmatrix} \lambda\mu & 0 & \phi \\ 0 & \lambda L_o & C \\ 0 & 0 & 1 \end{pmatrix} = \begin{pmatrix} 0 & 0 & \delta\phi \\ 0 & \lambda^2 G\omega L_o & \lambda G\omega C + \gamma \\ 0 & 0 & 0 \end{pmatrix} \tag{5.8.63}$$

We can then calculate 5.8.36 as follows:

$$Z' = \begin{pmatrix} \lambda\mu & 0 & -\lambda\mu\phi \\ 0 & \lambda L_o^{-1} & -\lambda L_o^{-1}C \\ 0 & 0 & 1 \end{pmatrix} \begin{pmatrix} 0 & 0 & \delta\phi \\ 0 & \lambda^2 G\omega L_o & \lambda G\omega C + \gamma \\ 0 & 0 & 0 \end{pmatrix} \tag{5.8.64}$$

Hence :

$$Z' = \begin{pmatrix} 0 & 0 & \delta\phi' \\ 0 & \lambda G\omega' & \gamma' \\ 0 & 0 & 1 \end{pmatrix} = \begin{pmatrix} 0 & 0 & (\lambda\mu)\delta\phi \\ 0 & \lambda^3 L_o^{-1} G\omega L_o & \lambda^2 L_o^{-1} G\omega C + \lambda L_o^{-1}\gamma \\ 0 & 0 & 0 \end{pmatrix} \tag{5.8.65}$$

Thus, by identification, we can deduce:

$$\delta\phi' = \lambda\mu\delta\phi \tag{5.8.66}$$
$$\omega' = \lambda^2 G L_o^{-1} G\omega L_o \tag{5.8.67}$$
$$\gamma' = \lambda^2 L_o^{-1} G\omega C + \lambda L_o^{-1}\gamma \tag{5.8.68}$$
$$\tag{5.8.69}$$

However :

$$L_o^{-1} = G L_o^T G \tag{5.8.70}$$

Then[27] :

$$\begin{aligned} \delta\phi' &= \lambda\mu\delta\phi \\ \omega' &= \lambda^2 L_o^T \omega L_o \\ \gamma' &= \lambda^2 G L_o^T \omega C + \lambda G L_o^T G\gamma \end{aligned} \tag{5.8.71}$$

However, inspired by J.M. Souriau, we could add as many additional closed dimensions as quantum charges and write the dynamic group as follows:

$$\begin{pmatrix} \lambda\mu & 0 & 0 & \cdots & 0 & \phi^1 \\ 0 & \lambda\mu & 0 & \cdots & 0 & \phi^2 \\ 0 & 0 & \ddots & \cdots & 0 & \vdots \\ \vdots & \vdots & \cdots & \lambda\mu & 0 & \phi^p \\ 0 & 0 & \cdots & 0 & \lambda L_o & C \\ 0 & 0 & \cdots & 0 & 0 & 1 \end{pmatrix} \tag{5.8.72}$$

[27] GG=I (Identity matrix)

The isometry group of this space can be defined by the following metric:

$$\mathrm{d}s^2 = (\mathrm{d}t)^2 - (\mathrm{d}x)^2 - (\mathrm{d}y)^2 - (\mathrm{d}z)^2 - (\mathrm{d}\zeta^1)^2 - (\mathrm{d}\zeta^2)^2 - \ldots - (\mathrm{d}\zeta^p)^2 \tag{5.8.73}$$

With :

$$X = \begin{pmatrix} \xi \\ \zeta \end{pmatrix} = \begin{pmatrix} t \\ x \\ y \\ z \\ \zeta^1 \\ \zeta^2 \\ \vdots \\ \zeta^p \end{pmatrix} \tag{5.8.74}$$

The action of this Janus group on the coordinates of $10+p$ independant parameters then yields the space of the following motions:

$$\begin{pmatrix} \lambda\mu & 0 & 0 & \cdots & 0 & \phi^1 \\ 0 & \lambda\mu & 0 & \cdots & 0 & \phi^2 \\ 0 & 0 & \ddots & \cdots & 0 & \vdots \\ \vdots & \vdots & \cdots & \lambda\mu & 0 & \phi^p \\ 0 & 0 & \cdots & 0 & \lambda L_o & C \\ 0 & 0 & \cdots & 0 & 0 & 1 \end{pmatrix} \begin{pmatrix} \zeta^1 \\ \zeta^2 \\ \vdots \\ \zeta^p \\ \xi \\ 1 \end{pmatrix} = \begin{pmatrix} \lambda\mu\zeta^1 + \phi^1 \\ \lambda\mu\zeta^2 + \phi^2 \\ \vdots \\ \lambda\mu\zeta^p + \phi^p \\ \lambda L_o\xi + C \\ 1 \end{pmatrix} \tag{5.8.75}$$

According to Noether's theorem, this new symmetry is accompanied by the invariance of additional scalars q^p. Therefore, the torsor of the group integrates them according to this relation:

$$\mu = \{M, P, \sum_1^p q^i\} = \{l, g, p, E, q^1, q^2, \ldots, q^p\} \tag{5.8.76}$$

Thus, the duality relation[28] gives us:

$$\frac{1}{2}T_r(M \cdot \omega) + P^T \cdot G\gamma + \delta\phi \sum_1^p q^i = \frac{1}{2}T_r(M' \cdot \omega') + P'^T \cdot G\gamma' + \delta\phi \sum_1^p q'^i \tag{5.8.77}$$

This allows us to deduce the action of the group by identification with 5.8.71:

$$\sum_1^p q'^i = \lambda\mu \sum_1^p q^i \tag{5.8.78}$$

$$M' = LML^T - LPC^T + CP^TL^T \tag{5.8.79}$$

$$P' = LP \tag{5.8.80}$$

[28] (13.58) from [78]

Chapter 6

Alternative Interpretation of the Wormhole Model Coupled with a White Fountain as a *One-Way Membrane*

The exterior metric developed by K. Schwarzschild in 1916, as a solution to Einstein's equation in vacuum, is invariant by the time symmetry $t \mapsto -t$. This property, commonly called "*staticity*", precludes the presence of a cross term drdt in the metric. This cross-term was later reintroduced through a change of variables by Arthur Eddington to show that the singularity at the horizon is due to a bad choice of coordinates ([25]). In a recent paper [41] by Pascal Koiran, it was demonstrated that in Eddington coordinates, the infall time to the horizon occurs in finite time *from the point of view of a distant observer*. This new study aims to build on this result as well as the study [26] by Einstein and Rosen to construct a model of a *wormhole* coupled with a *white fountain* as a *one-way membrane*, connecting two semi-Riemannian *PT-symmetric* spaces through a *bridge* that can only be crossed in one direction.

6.1 Solutions of Einstein's Equation Reflecting Different Topologies

We begin this chapter by a review of some the work stemming from the discovery by Schwarzschild of an exact solution to the Einstein field equations in vacuum. The work of Einstein and Rosen [26] is of particular importance for this study since we will be interested in the fate of a particle crossing an Einstein-Rosen bridge. At first sight this line of inquiry may look like a dead end to some readers. Indeed, the Einstein-Rosen bridge has often been presented as non-traversable in the literature. In Section 6.2, we point out that this conclusion is in fact based on an analysis of the Kruskal-Szekeres extension, which as a geometric object is very different from an Einstein-Rosen bridge.

The main developments of this chapter take place in Sections 6.3 and 6.4. We show that a particle crossing the bridge undergoes a *PT-symmetry*, and we discuss its physical significance.

In 1916, Karl Schwarzschild successively published two papers ([75],[74]). The first one presented the construction of the solution to Einstein's equation in vacuum, based on the following assumptions:

- *Stationarity*: Independence of the metric terms with respect to the time coordinate[1].
- *Isotropy* and spherical symmetry[2].
- Absence of the drdt cross term.
- Lorentzian at infinity.

He rapidly completed this solution, called the exterior Schwarzschild metric, with an interior metric [74] describing the geometry inside a sphere filled with a fluid of constant density ρ_o and solution to Einstein's equation with a second member. The conditions for connecting the two metrics (Continuity of geodesics) were ensured. The phenomena of the advance of Mercury's perihelion and gravitational lensing confirm this solution (Figure 3.3). K. Schwarzschild worked to ensure that the conditions governing these two metrics were in accordance with physical reality.

As an example, in the present day, neutron stars, owing to their staggering density and formidable mass, stand as natural cosmic laboratories, probing realms of density and gravity unreachable within terrestrial laboratories. Let us consider two distinct ways through which a neutron star might reach a state of physical criticality.

In a scenario where the star's density, ρ_o, remains constant, a characteristic radius $\hat{r}$ can be defined. Then, a physical criticality is reached when the star's radius is :

$$R_{\mathrm{cr}_\phi} = \sqrt{\frac{8}{9}}\hat{r} = \sqrt{\frac{c^2}{3\pi G\rho_o}} \tag{6.1.1}$$

with

$$\hat{r} = \sqrt{\frac{3c^2}{8\pi G\rho_o}} \tag{6.1.2}$$

Thus,

- For the exterior metric, it was necessary that the radius of the star be less than $\hat{r}$.

[1]Invariance by time translation.
[2]Invariance by *SO(3)*.

- As for the interior metric, the radius of the star had to be less than R_{cr_ϕ} because a larger radius leads the pressure to rise to infinity at the center of the star.

Next, for massive stars, an imploding iron sphere can present a complex scenario. Assuming the sphere's mass M is conserved during implosion, we must consider two important critical radius :

- In the core part, the geometric criticality radius is given by the *Schwarzschild Radius* which is:
$$R_{\mathrm{cr}_\gamma} = R_s = 2\frac{GM}{c^2} \tag{6.1.3}$$
- Outside of this mass, the physical critical radius is given by 6.1.1

With mass conservation expressed as $M = \frac{4}{3}\pi R^3 \rho_o$, we can explore how the variable density ρ_o during implosion impacts these critical radius.

Indeed, if physical criticality is reached during implosion, we have $R = R_{\mathrm{cr}_\phi}$.
Then, substituting the mass conservation equation into 6.1.1, we get :

$$R = R_{\mathrm{cr}_\phi} = 2.25\frac{GM}{c^2} > R_{\mathrm{cr}_\gamma} \tag{6.1.4}$$

We can deduce that if the physical criticality is reached for a mass M, then it occurs before geometric criticality appears.

K. Schwarzschild also emphasized that the measurements pertained to conditions far exceeding what was understood within the framework of the astrophysical reality of his time.

It is also important to note that the topology of this geometric solution is built by connecting two bounded manifolds along their common boundary, a sphere S^2 with an area of $4\pi R_o^2$ (R_o is the *radius of the star*).

In 1916, Ludwig Flamm considered the external solution as describing potentially a geometric object. The concern was then an attempt to describe masses as a non-contractible region of space ([29]).

In 1934, Richard Tolman was the first to consider a possible handling of the most general metric solution introducing a cross term $\mathrm{d}r\mathrm{d}t$. However, for the sake of simplification, he immediately eliminated it using a simple change of variable ([82]).

In 1935, Einstein and Rosen proposed, within the framework of a geometric modeling of particles, a non-contractible geometric structure, through the following coordinate change ([26]):

$$u^2 = r - 2m \tag{6.1.5}$$

The metric solution then becomes:

$$\mathrm{d}s^2 = \frac{u^2}{u^2+2m}\mathrm{d}t^2 - 4u^2(u^2+2m)\mathrm{d}u^2 - (u^2+2m)^2(\mathrm{d}\theta^2 + \sin^2\theta\mathrm{d}\phi^2) \tag{6.1.6}$$

The authors thus obtain a non-contractible geometric structure, termed a *"space bridge"*, where a closed surface of area $4\pi\alpha^2$, corresponding to the value $u = 0$, connects two *"sheets"*: one corresponding to the values of u from 0 to $+\infty$ and the other from $-\infty$ to 0. It is noteworthy that this metric is not Lorentzian at infinity[3]. Although this metric, expressed in this new coordinate system, is regular, the authors point out that at the throat surface, its determinant becomes zero. In this geometric structure, two bounded semi-Riemannian sheets are distinguished, the first corresponding to $u > 0$ and the second to $u < 0$. It corresponds to their joining along their common boundary. The overall spacetime does not fit within the standard framework of semi-Riemannian geometry since it does not fulfill the requirement $\det(g_{\mu\nu}) \neq 0$ at the throat. As pointed out in [80], it does fit within the more general framework of singular semi-Riemannian geometry, which allows for degenerate metric tensors.

In 1939, Oppenheimer and Snyder, capitalizing on the complete decoupling between proper time and the time experienced by a distant observer, in the absence of a cross term in $\mathrm{d}r\mathrm{d}t$, suggested using the external metric solution to describe the *"freeze frame"* of the implosion of a massive star at the end of its life. By considering that the variable t is identified with the proper time of a distant observer, it creates this *"freeze frame"* pattern such as a collapse phenomenon whose duration, in proper time, measured in days, seems for a distant observer to unfold in infinite time ([49]). This paper was considered as the foundation of the black hole model.

In 1960, Kruskal extended the geometric solution to encompass a contractible spacetime, organized around a central singularity corresponding to $r = 0$. The geodesics are extended for $r < \alpha$. The black hole model (with spherical symmetry[4]) then takes its definitive form as the implosion of a mass, in a brief moment, perceived as a *"freeze-frame"* by a distant observer ([42]). The Schwarzschild sphere is then termed the *"event horizon"*.

In 1988, M. Morris and K. S. Thorne revisited this geometric interpretation by abandoning contractibility, not to attempt to obtain a geometric modeling of the solution, but to study the possibility of interstellar travel, through *"wormholes"*, using the following metric ([46]):

$$\mathrm{d}s^2 = -c^2\mathrm{d}t^2 + \mathrm{d}l^2 + (b_o^2 + l^2)(\mathrm{d}\theta^2 + \sin^2\theta\mathrm{d}\phi^2) \tag{6.1.7}$$

[3] For this reason, the change of variables $r^2 = \rho^2 + 4m^2$ was proposed by Chruściel ([19], page 77) as an alternative to (6.1.5). See also Section 6.4 of the present study, where we propose an alternative to the change of variables from [19].

[4] In 1963, Roy Kerr constructed the stationary axisymmetric solution to Einstein's equation in vacuum. However, in this study, we limit ourselves to the interpretations of the stationary solution with spherical symmetry (2.3.10).

By focusing their study on the feasibility of interstellar travel, the authors highlight the enormous constraints associated with such geometry as well as its unstable and transient nature.

6.2 Distinction between the Kruskal-Szekeres Extension and the Einstein-Rosen Bridge

The Kruskal-Szekeres extension and the Einstein-Rosen bridge are two major constructions in the study of spacetime geometry around a wormhole. However, their geometric natures differ significantly.

The Kruskal-Szekeres spacetime is defined by a traditional *semi-Riemannian manifold*, characterized by a non-degenerate metric at every point. This makes it consistent with the general framework of general relativity, where the metric's signature is homogeneous and does not vary.

In contrast, the Einstein-Rosen spacetime has a degenerate metric at certain points, namely, at the bridge's throat. This characteristic places it in the class of *singular semi-Riemannian manifolds* as defined by Ovidiu Stoica [80]. This fundamental distinction shows that the Kruskal-Szekeres spacetime is not simply an extension of Einstein-Rosen but a fundamentally different construction.

Thus, these two spacetimes cannot be considered versions of each other but rather two distinct interpretations of the geometry around a wormhole. This was already pointed out in several papers by Guendelman et al. Consider in particular [33], where they write:

> [29] The nomenclature of "Einstein-Rosen bridge" in several standard textbooks (e.g. [15]) uses the Kruskal-Szekeres manifold. The latter notion of "Einstein-Rosen bridge" is not equivalent to the original construction in [14]. Namely, the two regions in Kruskal-Szekeres space-time corresponding to the outer Schwarzschild space-time region (r $>$ 2m) and labeled (I) and (III) in [15] are generally *disconnected* and share only a two-sphere (the angular part) as a common border (U $=$ 0, V $=$ 0 in Kruskal-Szekeres coordinates), whereas in the original Einstein-Rosen "bridge" construction the boundary between the two identical copies of the outer Schwarzschild space-time region (r $>$ 2m) is a three-dimensional hypersurface (r $=$ 2m).

We can also cite two other papers whose authors make the same observation regarding the Kruskal-Szekeres extension's inadequacy in properly analyzing the Einstein-Rosen bridges: that of Guendelman et al. [32] and that of Poplawski [67]. Indeed, to distinguish these spacetimes, Poplawski uses the terms *"Schwarzschild bridge"* and

"Einstein-Rosen bridge".

For all these reasons, we will *not* work with the Kruskal-Szekeres extension in this study. We note in particular that the common claim [31, 81] that the Einstein-Rosen bridge is not traversable is actually based on an analysis of the Kruskal-Szekeres extension; but, as pointed out in [33, 41], the original Einstein-Rosen bridge [26] is in fact traversable.

6.3 Construction of a Lorentzian Geometric Solution at Infinity with Two Sheets

Let us consider the exterior Schwarzschild metric in its classical form under the signature $(+---)$:

$$\mathrm{d}s^2 = \left(1-\frac{\alpha}{r}\right)c^2\mathrm{d}t^2 - \left(1-\frac{\alpha}{r}\right)^{-1}\mathrm{d}r^2 - r^2(\mathrm{d}\theta^2+\sin^2\theta\mathrm{d}\varphi^2) \tag{6.3.1}$$

6.3.1 T-Symmetry

This metric built in 1916 ([75]), as a solution to Einstein's equation in vacuum, was endowed with an additional hypothesis, which its author did not mention, that of invariance by time symmetry. It is important to note that this hypothesis has no physical basis and results in the elimination of a cross term $\mathrm{d}r\mathrm{d}t$ in the metric, as Tolman had envisaged as early as 1934 (Page 239 of [82]).

Conversely, A. Eddington introduced it with the aim of eliminating the coordinate singularity at the Schwarzschild surface in $r=\alpha$, using the variable change ([25],[41]):

$$t_E^+ = t + \frac{\alpha}{c}\ln\left|\frac{r}{\alpha}-1\right| \tag{6.3.2}$$

The metric becomes:

$$\mathrm{d}s^2 = \left(1-\frac{\alpha}{r}\right)c^2\mathrm{d}t_E^{+2} - \left(1+\frac{\alpha}{r}\right)\mathrm{d}r^2 - \frac{2\alpha c}{r}\mathrm{d}r\mathrm{d}t_E^+ - r^2\left(\mathrm{d}\theta^2+\sin^2\theta\mathrm{d}\varphi^2\right) \tag{6.3.3}$$

We know that under these conditions, from the point of view of a distant observer, the free fall time is finite, i.e., a massive infalling particle will reach the surface $r=\alpha$ for a finite value of t_E^+ [41]. By contrast, escape time remains infinite. The metric for which the escape time is finite will be obtained by performing this change of variable:

$$t_E^- = -t - \frac{\alpha}{c}\ln\left|\frac{r}{\alpha}-1\right| \tag{6.3.4}$$

Thus, the metric becomes:

$$\mathrm{d}s^2 = \left(1-\frac{\alpha}{r}\right)c^2\mathrm{d}t_E^{-2} - \left(1+\frac{\alpha}{r}\right)\mathrm{d}r^2 + \frac{2\alpha c}{r}\mathrm{d}r\mathrm{d}t_E^- - r^2\left(\mathrm{d}\theta^2+\sin^2\theta\mathrm{d}\varphi^2\right) \tag{6.3.5}$$

This is equivalent to inverting the time coordinate in 6.3.3. Thus, this choice of associating two metrics describing two semi-Riemannian spaces leads us to consider a global geometric solution of two *T-symmetric* sheets connected by a *"bridge"* in this particular coordinate system as well as in the coordinate system of Einstein and Rosen ([26]).

Now, let us demonstrate that these transformations are also accompanied by a *P-symmetry*.

6.3.2 P-Symmetry

In this representation, the radial geodesics of the first sheet are orthogonal to the tangent plane at the *"space bridge"* when they reach it. These same geodesics, emerging in the second sheet, are also orthogonal to this same tangent plane. Let's now consider four points forming a tetrahedron, which converge towards the *"space bridge"* along radial trajectories. We can set a 3D orientation by defining a direction of traversal of the points on each of the equilateral triangles forming the tetrahedron. With respect to the coordinate r, it seems as if these points bounce off a rigid surface, leading to an inversion of the orientation of the tetrahedron. The upstream and downstream tetrahedra then become *enantiomorphic* (Figure 6.1).

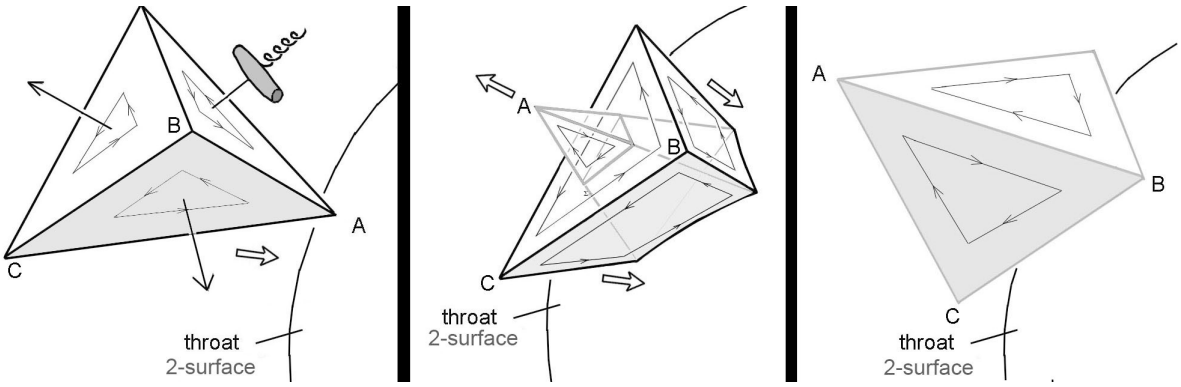

Figure 6.1: Inversion of space when crossing the *"space bridge"*

The change of orientation is already visible in the simplified 2-dimensional representation of a wormhole in Figure 6.2. Let us look at this figure from above, and imagine a triangle gliding on the surface of the top sheet toward the throat. After crossing the throat, the triangle starts gliding on the bottom sheet and we now see it upside now from our position above the top sheet. From our point of view, its orientation has therefore changed. The physical meaning of this change of orientation will be discussed in Section 6.3.3.

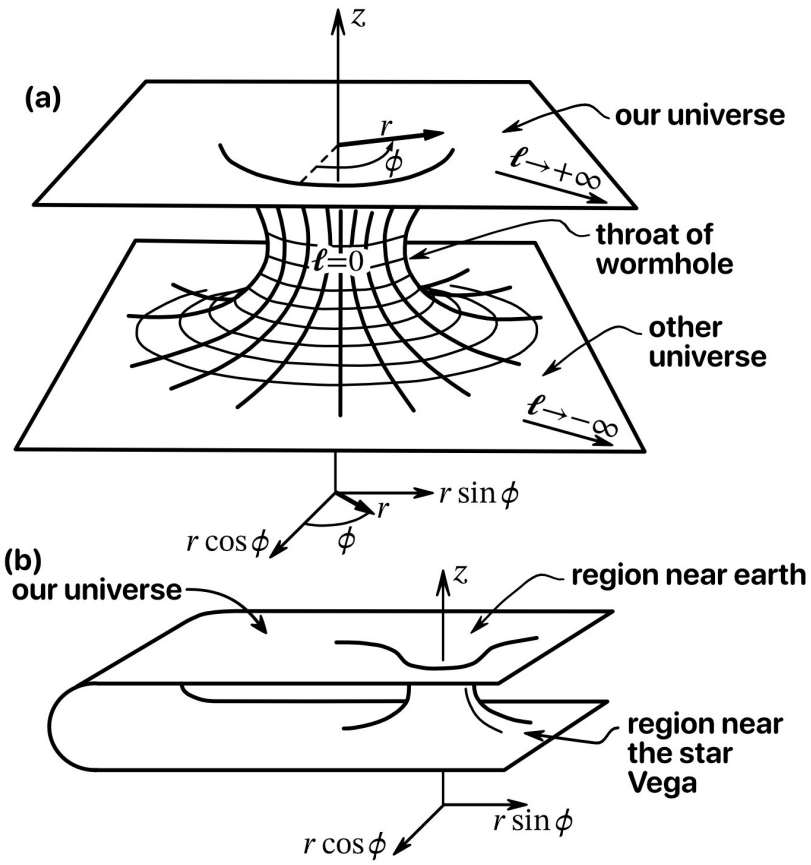

Figure 6.2: Page 396 of the article by M. Morris and K.S. Thorne (1988)

The geometric structure of the pair of metrics 6.1.6 and 6.3.1 thus represents a *"bridge"* connecting two *PT-symmetric* semi-Riemannian spaces.

The element of this 2D-surface is then given by:

$$\sqrt{|\det(g_{\mu\nu})|} = \sqrt{|g_{\theta\theta}g_{\phi\phi}|} = \alpha^2 \sin(\theta) \tag{6.3.6}$$

As this metric describes a 2D-surface sphere (like a sphere of constant radius in a 4D spacetime), then the differential area element is given by :

$$\mathrm{d}A = \sqrt{|\det(g_{\mu\nu})|}\mathrm{d}\theta\mathrm{d}\phi = \alpha^2 \sin(\theta)\mathrm{d}\theta\mathrm{d}\phi \tag{6.3.7}$$

To find the minimal area of this *"space bridge"*, we must integrate this area element over all possible angles :

$$A = \int_0^{2\pi}\int_0^{\pi} \alpha^2 \sin(\theta)\mathrm{d}\theta\mathrm{d}\phi = 4\pi\alpha^2 \tag{6.3.8}$$

It's therefore non-contractible with a minimal area of $4\pi\alpha^2$.

6.3.3 Identification of the Two Sheets

In Section 6.3.2 we have described the change of orientation of a tetrahedron crossing the wormhole throat in Figure 6.1, and of a triangle crossing the throat in Figure 6.2. The change of orientation of the triangle is only visible for a person looking at Figure 6.2 in its entirety. Therefore, it does not correspond to any physically observable phenomenon since any physical observer must be located on one of the two sheets and cannot see directly the other sheet. The situation is the same in Figure 6.1 : The middle picture represents the situation from a point of view where we could look simultaneously at the two sides of the wormhole (B and C have not reached the throat yet, while A has already crossed it and emerges on the other side). This is again impossible for a physical observer: it seems that the *P-symmetry* as described so far does not correspond to any physically observable phenomenon. We can however give it a real physical meaning with an additional ingredient introduced by Einstein and Rosen [26].

Recall that their motivation was not to investigate interstellar travel as in Figure 6.2, but to describe elementary particles by solutions to the equations of general relativity. Quoting from the abstract of their paper: *"These solutions involve the mathematical representation of physical space by a space of two identical sheets, a particle being represented by a "bridge" connecting these sheets."* Einstein and Rosen also suggest that the multi-particle problem might be studied by similar methods, but this work is not carried out in their paper.

Quoting again from [26] : *"If several particles are present, this case corresponds to finding a solution without singularities of the modified Eqs. (3a), the solution representing a space with two congruent sheets connected by several discrete "bridges.""* From their point of view, two points in the mathematical representation 6.1.6 with identical values of θ, ϕ but opposite values of u therefore correspond to two points in physical space with the same value of r ($r = u^2 + m$). If we make the same identification of points with opposite values of u, the situation represented in the middle picture of Figure 6.1 can be seen by a physical observer. The *P-symmetry* described in Section 6.3.2 now has a real physical meaning. We will elaborate on the interpretation of the combined *PT-symmetry* in the next section.

6.4 Another Representation of this Geometry

By performing the following change of variable to 6.3.3 and 6.3.5 :

$$r = \alpha\,(1 + \log\,\mathrm{ch}(\rho)) \tag{6.4.1}$$

We obtain the following two metrics:

$$\begin{aligned} \mathrm{d}s^2 = &\left(\frac{\log\cosh(\rho)}{1+\log\cosh(\rho)}\right) c^2 \mathrm{d}t_E^{+2} - \left(\frac{2+\log\cosh(\rho)}{1+\log\cosh(\rho)}\right) \alpha^2 \tanh^2(\rho)\mathrm{d}\rho^2 \\ &- 2c\alpha\left(\frac{\tanh(\rho)}{1+\log\cosh(\rho)}\right)\mathrm{d}\rho\mathrm{d}t_E^{+} - \alpha^2(1+\log\cosh(\rho))^2(\mathrm{d}\theta^2 + \sin^2\theta\mathrm{d}\varphi^2) \end{aligned} \tag{6.4.2}$$

$$\begin{aligned} \mathrm{d}s^2 = &\left(\frac{\log\cosh(\rho)}{1+\log\cosh(\rho)}\right) c^2 \mathrm{d}t_E^{-2} - \left(\frac{2+\log\cosh(\rho)}{1+\log\cosh(\rho)}\right) \alpha^2 \tanh^2(\rho)\mathrm{d}\rho^2 \\ &+ 2c\alpha\left(\frac{\tanh(\rho)}{1+\log\cosh(\rho)}\right)\mathrm{d}\rho\mathrm{d}t_E^{-} - \alpha^2(1+\log\cosh(\rho))^2(\mathrm{d}\theta^2 + \sin^2\theta\mathrm{d}\varphi^2) \end{aligned} \tag{6.4.3}$$

Therefore, to obtain the metric that structures the second sheet for $\rho < 0$ in order to ensure the continuity of the geodesics translating the transit of matter through the *"bridge"* with a finite escape time on this sheet, we must apply the *T-symmetry* where the time coordinate is reversed upon crossing[5].

Those metrics, which are Lorentzian at infinity, structures two sheets corresponding to ρ varying respectively from 0 to $+\infty$ and $-\infty$ to 0. On the *"space bridge"* for $\rho = 0$, the components g_{tt} and $g_{\rho\rho}$ of the metric tensor disappear, leaving only the last two spatial components $g_{\theta\theta}$ and $g_{\phi\phi}$, which are:

$$g_{\mu\nu} = \begin{pmatrix} 0 & 0 & 0 & 0 \\ 0 & 0 & 0 & 0 \\ 0 & 0 & -\alpha^2 & 0 \\ 0 & 0 & 0 & -\alpha^2\sin^2\theta \end{pmatrix} \tag{6.4.4}$$

On this particular coordinate system, we can infer that its determinant is zero. The *P-symmetry* arises from the fact that adjacent points, this time explicitly differentiated, are inferred by $\rho \to -\rho$. This transformation plays the same role as $u \to -u$ in 6.1.6.

By associating these metric solutions under these two conditions, we would obtain a *Wormhole* and a *White Fountain* as a *One-Way Membrane*, connecting two semi-Riemannian spaces through a *"bridge"* that can be crossed only in one direction. Let us assume further that the wormhole does not lead to another universe as in Figure 6.2.a, or to a distant point in the same universe as in Figure 6.2.b; but that the two congruent sheets correspond to the same points in the physical universe through

[5] $t_E^{+} = -t_E^{-}$

the transformation $u \to -u$ (or $\rho \to -\rho$), as suggested in [26] and in Section 6.3.3. We can then conclude that the two sheets are *PT-symmetric*.

In the literature, the inversion of the time coordinate has been analyzed in various ways. In particular:

(i) According to the theory of dynamic groups by J-M Souriau ([76], [78]), where it has been demonstrated to induce an energy inversion. Consequently, time reversal transforms every motion of a particle of mass m into a motion of a particle of mass $-m$ ([48], page 191). On page 192 of the same book, the author offers an alternative analysis which avoids negative masses. Souriau points out that these alternatives should be judged according to their ability to explain experiments.

(ii) Feynman has offered an interpretation of antimatter as ordinary matter traveling backward in time.

(iii) It is known from theoretical analysis (the *CPT* theorem) and from experiments that elementary particles obey physical laws that are invariant under *CPT-symmetry*.

The *PT-symmetry* uncovered in Section 6.3 can be viewed as a *CPT-symmetry* followed by a *C-symmetry* (inversion of electric charge). We would therefore obtain antimatter on the second sheet. If the second sheet already contains ordinary matter, it could interact with the antimatter coming from the first sheet and this would constitute a source of energy, whose applications can be multiple, both ecologically, through the recycling of radioactive waste for example, and in the energy or military sectors by producing energy by converting 100% of the mass of interacting particles and antiparticles[6].

6.5 Conclusion

We introduce a new geometric construction based on the stationary solution with spherical symmetry of Einstein's equation in vacuum, by limiting ourselves to the two only hypotheses, inspired by physics : *isotropy* (invariance by $SO(3)$) and *stationarity* (invariance by time translation). In doing so, we do not add, as has been done previously without any real physical justification, the invariance by *"time reflection"* symmetry from $t \to -t$ ("*static*" solution). This new set of less restrictive assumptions introduces

[6]For instance, in the military sector, to quantify the difference between conventional nuclear weapons and *"antimatter weapons,"* consider that in nuclear weapons, only a small fraction of the mass is converted into energy. For example, in the bomb dropped on Hiroshima, less than one gram of matter was actually converted into energy to produce the explosion. In contrast, in a matter-antimatter reaction, if 1 gram of matter meets 1 gram of antimatter, the entirety of this mass (i.e., 2 grams) is converted into energy, following the relation 2.2.5, thus releasing a considerably larger amount of energy. To put this into perspective, 1 gram of matter in contact with 1 gram of antimatter would release about 1.8×10^{14} joules of energy, which is comparable to the energy released by about 43 kilotons of TNT. For comparison, the atomic bomb dropped on Hiroshima had a yield of about 15 kilotons of TNT.

the presence of a cross term drdt, which the *staticity* assumption had previously prohibited. This new geometric object behaves as a *"One-Way Membrane"*, an union of a wormhole and a white fountain through a *"bridge"*. With a Lorentzian metric at infinity, this structure connects two *PT-symmetric* enantiomorphic semi-Riemannian spaces with opposing time arrows. Therefore, this object corresponds to the two-sheets covering of a four-dimensional spacetime, presenting themselves as *PT-symmetric*, connected along a *"bridge"*. Taking our inspiration from Einstein and Rosen, we have suggested to represent a point in physical space by a pair of congruent points, one on each of the two sheets. We have shown that this identification of congruent points should lead to observable physical effects when an object crosses the space bridge between the two sheets.

6.6 Application Domains

Civil Application

The application of matter-to-antimatter conversion in the field of ecology would offer an innovative solution for the recycling of radioactive waste. It would be conceivable to reverse the mass of radioactive matter particles with positive mass into antiparticles with negative mass through the application of *PT symmetry*. This revolutionary approach would allow the transformation of radioactive waste into a clean[7] and abundant source of energy, thus proposing a doubly beneficial solution: reducing radioactive pollution and producing sustainable energy.

Nathalie Debergh has opened this field of research in relativistic quantum mechanics, notably through the publication [23], which explores the emergence of negative energy states by showing that anti-fermions[8] with positive energy and mass can be transformed into anti-fermions with negative energy and mass by the linear and unitary application of the two inversion operators T and P to the Dirac equation. She was able to demonstrate that this application preserves the norm of the quantum state, which is an essential property for physical transformations. This unitary approach has

[7] Without neutron emission.

[8] Fermions are subatomic particles, meaning they are fundamental constituents of matter, smaller than atoms. They follow a unique principle known as the Pauli Exclusion Principle, which states that two fermions cannot occupy the same quantum state simultaneously. In other words, each fermion in a system must be unique in terms of its quantum properties, such as its position, momentum, and spin orientation. This rule is what allows atoms to form and structure themselves in complex ways, leading to the vast diversity of matter in the universe. Fermions are also described by a statistical rule known as Fermi-Dirac statistics, which predicts how they behave in groups at different temperatures. This statistic helps to understand why matter behaves differently at the quantum scale compared to our macroscopic daily experience. Among the fermions, we find quarks and leptons. Quarks combine to form protons and neutrons, which make up the nuclei of atoms. Leptons include electrons, which orbit around the atomic nucleus, as well as neutrinos, very light and weakly interacting elementary particles. Together, quarks and leptons form ordinary matter.

thus allowed for the exploration of solutions to the Dirac equation that include negative energies and masses in a manner consistent with the fundamental principles of quantum field theory.

Military Application

The manipulation of matter antiparticles with positive mass in interaction with matter particles of the same mass type through the application of *C symmetry* could present significant military interest. The energy released by matter-antimatter annihilation is described by Einstein's equation 2.2.5, illustrating the conversion of mass m into energy E. This principle reveals that a small amount of matter can transform into a huge amount of energy. During annihilation, the entire mass of the particles and antiparticles converts into energy, primarily in the form of gamma radiation. Consequently, the military application of this technology paves the way for the development of antimatter weapons of unmatched power, far surpassing the destructive capabilities of conventional nuclear weapons, while raising significant ethical and security questions.

Ethical and Security Considerations

The safe manipulation and storage of antimatter pose major challenges for its use in both civilian and military contexts. The risks of accidents and the moral implications of exploiting this technology, especially in a military context, would require the establishment of strict safety protocols and thorough reflection on the implications for international law and disarmament agreements.

6.7 Appendix

Now, let us consider the case of matter transfer to a second layer of the universe, wherein we are free to define the outgoing metric of the second sheet. By applying the new variable change 6.7.1 to the Schwarzschild metric 6.3.1, struck with the sign change of the integration constant $\alpha \to -\alpha$, we can thus build a *"repulsive"* metric on the second sheet:

$$t_E^+ = t + \frac{\alpha}{c} \ln \left| \frac{r}{\alpha} + 1 \right| \tag{6.7.1}$$

It ensures the continuity of the geodesics from the first sheet to the second with a finite free-fall time on the first and a finite escape time on the second.

The incoming metric structuring the first sheet becomes:

$$\mathrm{d}s^2 = \left(1 + \frac{\alpha}{r}\right) c^2 \mathrm{d}t_E^{+2} - \left(1 - \frac{\alpha}{r}\right) \mathrm{d}r^2 - \frac{2\alpha c}{r} \mathrm{d}r\mathrm{d}t_E^+ - r^2(\mathrm{d}\theta^2 + \sin^2\theta \mathrm{d}\varphi^2) \tag{6.7.2}$$

And the outgoing metric structuring the second sheet becomes:

$$\mathrm{d}s^2 = \left(1 + \frac{\alpha}{r}\right) c^2 \mathrm{d}t_E^{-2} - \left(1 - \frac{\alpha}{r}\right) \mathrm{d}r^2 + \frac{2\alpha c}{r} \mathrm{d}r\mathrm{d}t_E^- - r^2(\mathrm{d}\theta^2 + \sin^2\theta \mathrm{d}\varphi^2) \tag{6.7.3}$$

Taking the general form:

$$\mathrm{d}s^2 = \left(1 + \frac{\alpha}{r}\right) c^2 \mathrm{d}t_E^2 - \left(1 - \frac{\alpha}{r}\right) \mathrm{d}r^2 + \delta \frac{2\alpha c}{r} \mathrm{d}r\mathrm{d}t_E - r^2(\mathrm{d}\theta^2 + \sin^2\theta \mathrm{d}\phi^2) \qquad (6.7.4)$$

where $\delta = -1$ for the metric structuring the first sheet and $\delta = +1$ for the outgoing metric structuring the second sheet. Thus, as the two metrics are symmetric by time inversion $t \to -t$, the continuity of the geodesics is assured from one sheet to the other with a finite free-fall time on the first and a finite escape time on the second.

This implies that regular matter could potentially be converted into antimatter with negative mass, which would then be transferred to a separate layer of the universe. This process essentially involves the transformation of matter into antimatter with negative mass. By combining this geometric solution with the previously developed solution in Section 6.3, we can explore the feasibility of interstellar travel by exploiting the metric properties of this second layer.

Chapter 7

Topological Nature of the Model

7.1 Definition

Topology in cosmology refers to the study of the fundamental spatial properties of the universe that remain invariant under continuous transformations. Unlike geometry, which focuses on precise distances and angles, topology is more concerned with how space is connected and structured on a large scale. It examines aspects such as connectivity, continuity, and the boundaries of cosmic space, irrespective of its exact shape and size.

In a cosmological context, topology helps to understand the overall structure of the universe, including questions such as whether the universe is finite or infinite, whether it has *"edges"* or is limitless, and whether it could be connected in non-trivial ways (as in multi-connected universe models). This includes examining the large-scale shape and structure of the universe, as determined by the distribution of galaxies, cosmic background radiations, and other astrophysical observations.

Topology is particularly relevant for advanced cosmological models, like the Janus Cosmological Model, as it provides a framework to explore concepts such as the multi-layered universe, connectivity between different regions of space-time, and other non-intuitive properties that may arise from advanced theoretical physics.

In summary, topology in cosmology is a powerful tool for exploring and understanding the fundamental structure and nature of our universe, beyond the constraints of classical geometry.

Before proceeding with this chapter, it is crucial to read and fully grasp the comic book *Topologicon* [53], written by Dr. Jean-Pierre Petit, which is freely accessible through this website `http://www.savoir-sans-frontieres.com/`. This work popularizes concepts of topology in connection with cosmology and general relativity. Indeed, this chapter primarily deals with conceptual tools that are quite counterintuitive. Therefore, a prior reading of this comic book is highly recommended for better understanding.

7.2 Model of the Wormhole

Extending the new interpretation of the wormhole model discussed in the previous chapter 6, we propose a deeper topological perspective in relation with general relativity. For example, let's consider the throat sphere S^2 that connects two layers of spacetime through *PT-symmetry*. Could this configuration be analogous to a projective plane? In topology, a projective plane is a non-orientable surface with unique properties, such as lines that diverge at one point but rejoin on the opposite side. This suggests that the connection between spacetime layers through the wormhole's throat might defy the traditional orientation of space, thus evoking the projective plane.

Our conjecture is based on the observation that the nullity of the metric determinant on this surface would indicate a non-orientable nature in 2D. If this throat sphere is closed and has a limited surface area, it could be identified with a projective plane P^2. Although this idea may seem counterintuitive, it arises directly from the topology of the object as described by Schwarzschild exterior solution 2.3.119.

In the context of general relativity, the concept of elementary volume in curved spacetime is crucial. The elementary volume in n dimensions, defined by a Riemannian metric, is given by $\mathrm{d}V = \sqrt{|\det(g)|}\,\mathrm{d}^n x$, where g is the metric tensor and $\det(g)$ its determinant. This elementary volume is not simply the product of coordinate differentials, as in Euclidean space, but is instead modified by the curved structure of spacetime. The factor $\sqrt{|\det(g)|}$ reflects how spacetime is deformed by the presence of mass and energy, according to Einstein's equations. Thus, in regions of strong curvature, this elementary volume can behave in non-intuitive ways, revealing fascinating and sometimes surprising topological characteristics of spacetime.

Let's revisit the sphere S^2, whose metric is defined by the expression:

$$\mathrm{d}s^2 = \alpha^2(\mathrm{d}\theta^2 + \sin^2\theta \mathrm{d}\varphi^2) \tag{7.2.1}$$

The metric of a sphere is a mathematical function that describes the distances between points on the sphere's surface. As this metric describes a 2D-surface sphere (like a sphere of constant radius in a 4D spacetime), then the differential area element is given by:

$$\mathrm{d}A = \sqrt{|\det(g_{\mu\nu})|}\mathrm{d}\theta\mathrm{d}\phi = \alpha^2 \sin(\theta)\mathrm{d}\theta\mathrm{d}\phi \tag{7.2.2}$$

And it's actually a surface element because a sphere is a two-dimensional surface in three-dimensional space. When we integrate this surface element, we obtain the area described by the expression:

$$A = \int_0^{2\pi}\int_0^{\pi} \alpha^2 \sin(\theta)\mathrm{d}\theta\mathrm{d}\phi = 4\pi\alpha^2 \tag{7.2.3}$$

Which is the area of a sphere with radius α. We can also observe that this surface is analogous to that of a projective plane P^2, a concept rarely addressed in standard geometry.

7.3 Model of the Universe

In geometry, a sphere S^2 can be easily visualized because we can embed it in our familiar three-dimensional space $\mathbb{R}^3$. However, a projective plane, such as P^2, cannot be embedded in the same way. The projective plane is a type of non-orientable surface, which means it cannot be flattened out in three-dimensional space without self-intersection. To visualize a projective plane, we need to use *"immersion"*, a method where the surface *self-intersects* along a set of *self-intersections*. This concept challenges our traditional understanding of shapes and spaces.

Understanding higher-dimensional projective planes, like P^3 or P^n, requires us to abandon visual representations and embrace abstract thinking. This mental shift is necessary to explore complex topological structures that extend beyond our dimensions.

For example, turning a sphere inside out is conceivable if we consider each strip forming the meridians that cover it as being able to intersect through *"immersion"* to form a two-sheeted covering of a Möbius strip with three half-twists ([45]). This *"self-intersection"* effect is only linked to the immersion of this covering in our three-dimensional representation space $\mathbb{R}^3$. We can then make the pole M of one sheet of this sphere S^2 coincide with the opposite pole M' of the other sheet of the same covering. This is referred to as the *"conjunction of antipodal points"*. This transformation allows the arrows of time, carried by the meridians of this sphere, to meet but in opposition on each sheet of the same covering as on the next Figure 7.1.

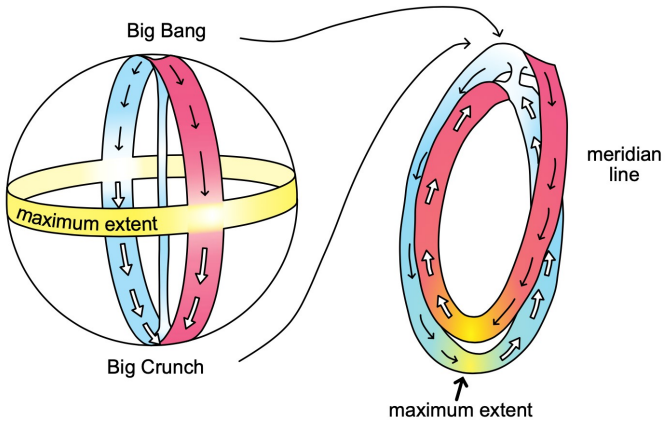

Figure 7.1: Turning a Sphere Inside Out by Conjoining Antipodal Points

NB : The Möbius strip, or Möbius band, is a surface with only one side and one edge. It is a classic mathematical object in topology, a branch of mathematics that studies properties of spaces that remain invariant under continuous transformations. The Möbius strip can be created by taking a strip of paper, giving it a half-twist, and then joining the two ends of the strip together. This configuration results in a surface that, if you start drawing a line along it, will return to its starting point after having traversed both *"sides"* of the strip without ever lifting your pen. What makes the Möbius strip fascinating is its non-orientable nature. In a normal space, like a sheet of paper, there is a clear distinction between *"top"* and *"bottom"*. However, on a Möbius strip, this distinction doesn't exist: as you traverse the surface, you seamlessly transition from top to bottom and back again. The Möbius strip is often used to illustrate important concepts in topology and geometry, such as the idea of a one-sided surface and the limits of our spatial intuition. In theoretical physics and cosmology, the Möbius strip can also serve as a model to explore complex spatial structures and phenomena such as the twisting of space-time or the connection between different dimensions.

Thus, PT-symmetry can be interpreted as the traversal of a projective plane from one sheet of the covering to the other (Figure 7.2).

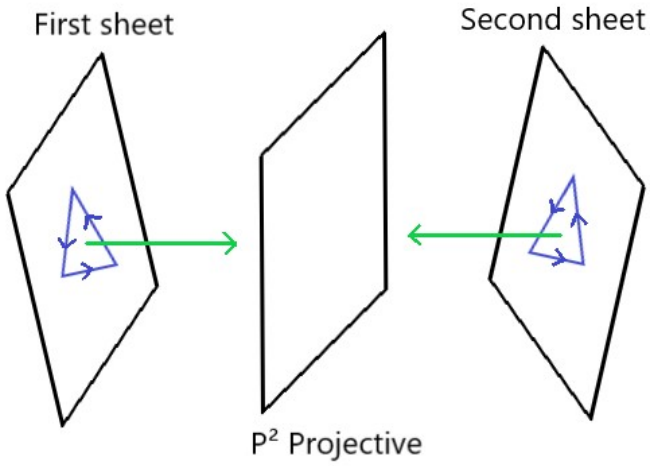

Figure 7.2: P^2 Projective

For a geometric object to be equipped with a functional coordinate system, the non-nullity of the determinant of its metric is then essential. Particularly, in the context of *"Gaussian coordinates"*, this principle is crucial. In a four-dimensional space, this requirement enables the foliation of space by a set of three-dimensional hypersurfaces. These hypersurfaces are *"orthogonal"* to the geodesics, meaning perpendicular to the paths a freely moving object would follow, and are characterized solely by the time coordinate. The distinction between the *"arrow of time"* and *"proper time"* is important

here: the arrow of time refers to a unidirectional temporal dimension, while proper time is a measure of time specific to the observer.

In the context of the two-dimensional spacetime we are examining, the foliation is performed using a series of circles. Each point on these circles can be associated with a *"time vector"*, which is orthogonal to the circles. Orthogonality in this case means that the time vector is positioned to be perpendicular to the surface of each circle, thus forming a distinct temporal component of spacetime (7.3).

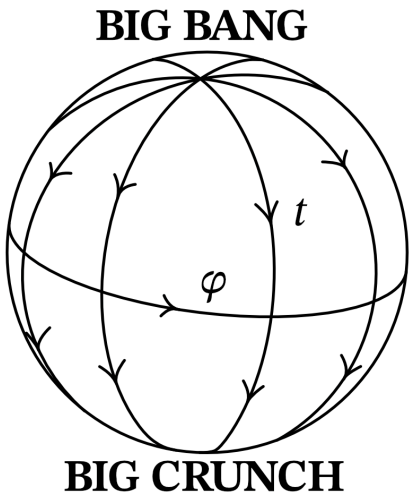

Figure 7.3: Illustration of the *"Time Vector"* Orthogonal to a Circle in a Family of Circles Foliating a Sphere S^2

Even in this case, this *"object"* has two singular points: its poles, where the azimuth is undefined. These poles represent unavoidable *"mesh singularities"*. There are two of them because the Euler-Poincaré characteristic of this object equals 2. For instance, if we consider a simple polyhedron like a tetrahedron to represent an approximation of the sphere, which is a pyramid with a triangular base, its Euler-Poincaré characteristic is 4 (vertices) - 6 (edges) + 4 (faces) = 2. The Euler-Poincaré characteristic of a sphere S^n equals 2 if n is even and zero if n is odd (6.3.3).

From our viewpoint, the universe would be an S^4 sphere with two singularities, the Big Bang and the Big Crunch. A four-dimensional sphere S^4 is an analog of a regular sphere, extending the concept into higher dimensions. Considering this sphere with its two poles, the Big Bang and the Big Crunch, it can be foliated by *"parallels"* (similar to parallel circles on a 2D surface S^2). This foliation process involves creating layers, or *"slices"*, through the sphere, which are analogous to the lines of latitude on Earth. The past-future orientation then becomes uniform everywhere. In this context, the past-future orientation refers to the direction of time from the Big Bang to the Big Crunch,

which becomes consistent throughout this foliated structure. Relative to this normal to the parallel surfaces, spacetime is orientable, meaning that there is a well-defined notion of *"up"* and *"down"* in the spacetime structure.

However, by *"folding"* this surface (whether S^2 or S^4), we create a situation where two parallels overlap. Folding in this sense means manipulating the structure of the sphere in such a way that different parts of the surface come into contact. Their time vectors then become antiparallel or opposed, as mentioned earlier. The time vector is a way of representing the direction of time at each point in spacetime. When these vectors become antiparallel, it signifies that the direction of time is reversed at the points of contact. This leads to what we might call an *"induced orientation"*. Induced orientation here refers to the new orientation of time vectors that results from the folding process. At every point in this spacetime, structured as a two-sheeted covering of a Möbius strip with three half-twists (*two-folds cover*), the *"antipodal matter"* (both spatial and temporal) appears *"retrochronal"*. A Möbius strip with three half-twists is a one-sided surface that can be visualized by twisting a strip of paper three times before joining the ends.

In Jean-Pierre Petit's article [55], he considers the interaction of the universe with the gravitational field created by its antipode, assuming that the laws of interaction are:

1. Ordinary masses attract each other according to Newton.

2. *"Antipodal"* masses attract each other according to Newton.

3. Ordinary masses and *"antipodal"* masses repel each other according to an *"anti-Newton"* law.

This hypothesis led him to *"fold"* the universe by giving it the topology of a *"two-sheeted covering"* of a 2D surface.

Thus *"folded"*, the S^2 sphere (closed surface) becomes the covering of another closed surface, the Boy's surface, which has a single pole and whose Euler-Poincaré characteristic equals 1 as on Figure 7.4. The Boy's surface[1] is an unique 3D non-orientable surface with only one face and one edge, featuring a singular point where all antipodal points converge.

[1]The Boy's surface is an example of a non-orientable 3D surface with only one face and one edge. It is intriguing because, unlike the classical sphere, it has a singular point where all antipodal points converge. This means that if you start drawing a line on the Boy's surface, you will eventually return to your starting point without ever having crossed an edge or used the other side, as there isn't one.

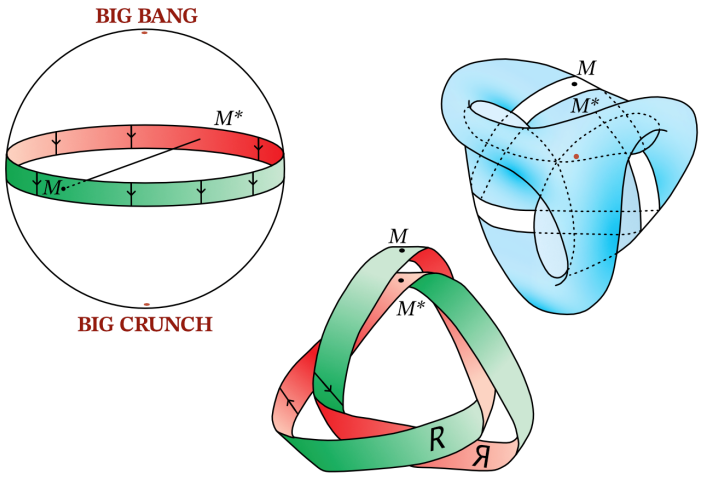

Figure 7.4: The vicinity of the equator of a 2-Sphere and its location on a Boy's surface

At this point, the Big Bang and the Big Crunch *"coincide"*.

A *"tube"* could then be envisioned in place of this polar singularity to connect these two mesh singularities:

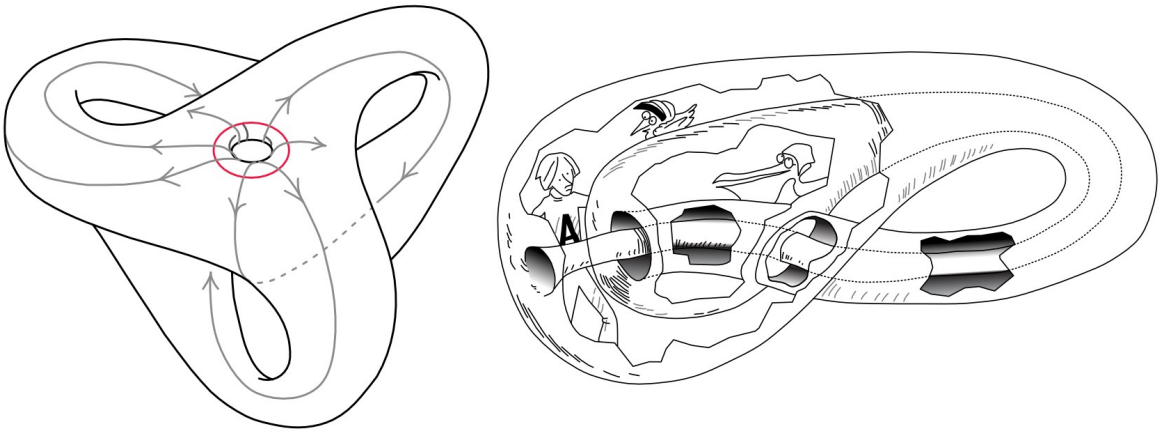

Figure 7.5: Boy's surface after Sphere S^2 foliation and the K^2 Klein bottle at the right

The singular nature disappears, and the object then becomes the covering of a K^2 Klein bottle, a non-orientable surface without distinct boundaries or interior, whose Euler-Poincaré characteristic is zero, as illustrated in the Figure 7.5. The Klein bottle is another non-orientable surface that neither has a distinct boundary nor an interior. Imagine a Möbius strip whose edges are also joined together. Unlike the Boy's surface, the Klein bottle cannot be realized in our three-dimensional space without

self-intersection. Its interest lies in its topological behavior, where *"inside"* and *"outside"* are not separate concepts, thus offering a useful representation for certain ideas in topology and theoretical cosmology.

I believe the limitations in theoretical physics and cosmology during the 1950s can be attributed to the field's delay in embracing topology. Topology, the study of properties preserved through continuous deformations, could have provided new ways to understand the fabric of the universe and its complex structures.

Chapter 8

Alternative Interpretation of the Supermassive Subcritical Objects M87* and Sagittarius A*

The first images of supermassive objects located at the centers of galaxies, published in the *Astrophysical Journal*, have been predominantly interpreted as representations of giant black holes. This interpretation is grounded in the lack of widely accepted alternative explanations. This study reexamines these images, particularly those of objects at the center of the M87 galaxy and the Milky Way. It highlights the possibility of subcritical supermassive entities, with radius only 5.72% shorter than the Schwarzschild radius calculated from their masses. We will also see that the central parts of these entities are darkened due to the gravitational redshift effect, represented by $z+1$. This redshift is calculated as the ratio of the wavelength of light received by a distant observer to that emitted from the surface, corresponding to the ratio of the maximum to minimum observed temperatures from the center to the edge of these objects, a value remarkably close to 3. We'll explore the notion that their stability might result from a balance between gravitational collapse, due to a physical criticality occurring long before geometric criticality, and an extremely high radiative pressure at constant density emanating from their centers, proportional to the square of the speed of light - a phenomenon initially considered by Karl Schwarzschild in his second paper published in February 1916. Our analysis aims to enrich the understanding of supermassive objects in galactic centers by proposing an alternative interpretation.

8.1 Introduction

The images of the two supermassive objects located at the center of the galaxies M87 and the Milky Way have sparked great media interest, being immediately dubbed "*the first images of giant black holes*". These images were published in the prestigious *Astrophysical Journal* (M87* [2] and Sagittarius A* at the center of the Milky Way

[3]). Below, a bar connects the color shade to what is referred to as the "*brightness temperature*":

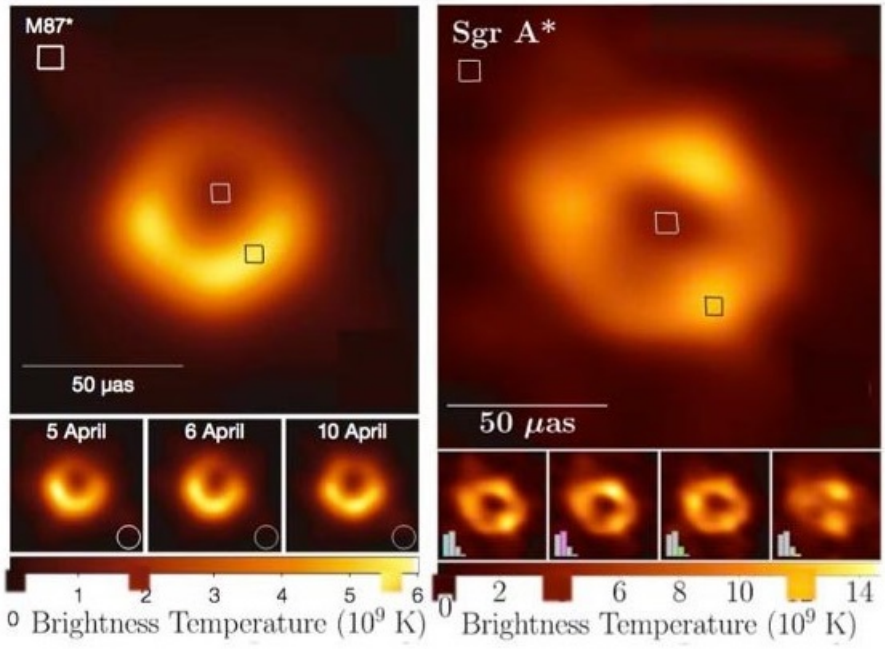

Figure 8.1: Images of M87* and Sagittarius A* objects

On this Figure 8.1, at the left, the first image of the object at the center of the M87 galaxy was published in 2019, showing minimal brightness temperatures of 1.8 billion degrees and maximum temperatures of 5.7 billion degrees, with a ratio close to 3. Three years later, in 2022, a second image at the right was published, showing minimal temperatures of 4 billion degrees and maximum temperatures of 12 billion degrees, with a ratio also close to 3. These two objects have vastly different masses, with the first being 1625 times more massive than the second. It seems peculiar that, under these circumstances, for both objects, a hot gas cloud in the foreground exhibits characteristics such that the ratio of maximum to minimum temperatures is so close to 3 in both cases.

Two new images of the object at the center of galaxy M87 were published in the journal *Astronomy & Astrophysics* on January 18, 2024 ([4]), and we can observe in Figure 8.2 a difference in the ratio of maximum to minimum brightness temperatures. On the new image from April 11, 2017, the ratio between the maximum and minimum brightness temperatures gives an approximate value of 3.4 (5.8×10^9 K divided by 1.7×10^9 K). Conversely, the image on the right, taken almost a year later, shows an approximate temperature ratio of 4.8 (8×10^9 K divided by 1.7×10^9 K).

Despite the fact that the most recent observation of M87* shows a temperature ratio very different from that calculated for the same object observed a year earlier,

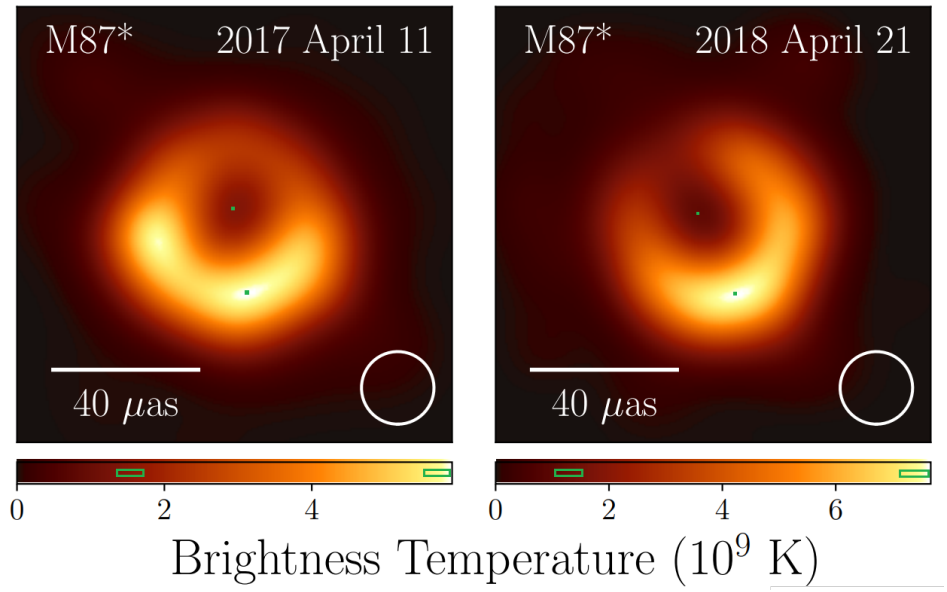

Figure 8.2: New images of object M87* published on January 18, 2024.

determining which of the two observations is more reliable requires thorough analysis. This discrepancy can be attributed to several factors, ranging from the collection of interferometric data to their subsequent processing. Indeed, these measurements depend on the combination of signals from several radio telescopes spread over large distances. Measurement errors, atmospheric variations, differences in instrument calibration, and image reconstruction techniques can all contribute to the observed differences. Nonetheless, the common point among all these observations is that the central part of this celestial object always exhibits a temperature exceeding 1 billion degrees Kelvin.

If the image of a third object at the center of a new galaxy led to a temperature ratio close to 3, it would be prudent to question the true nature of these objects.

The first images of supermassive objects located at the center of galaxies were associated with giant black holes, and the non-perfectly black central part seems to be due to the light emanating from a disk of hot gas orbiting around the black hole. However, as we will see later in this study, a neutron star can reach criticality in two scenarios:

- Abruptly, involving the sudden collapse of a supermassive star onto its iron core before transforming into a supernova.

- More gradually, in binary systems, a subcritical neutron star slowly accumulates mass by absorbing gas emitted by a companion star through a "*stellar wind*". The critical mass at which it could potentially undergo further transformation depends on the equation of state of the matter inside the neutron star and can

vary. Typically, current models estimate that the critical mass required for further transformation is approximately within the range of 2 to 3 times the solar mass, near the Tolman-Oppenheimer-Volkoff limit.

The peculiarity of such a model is that the massive object must exhibit a brightness temperature ratio of 3 between its corona and its center (maximum and minimum temperatures). As we will demonstrate later, a more consistent alternative interpretation would be to attribute the darkening of the central part of these objects to a gravitational redshift effect, which slows down time near their horizon.

Indeed, a massive object curves the space-time around it, affecting the trajectory of not only massive objects but also light. When a photon passes near such an object, its path is bent due to this curvature of space-time, a phenomenon known as gravitational lensing (See the figure 3.3). However, it's not just the path of the photon that changes: as it moves away from the massive object, the photon loses energy to escape the strong gravitational field. This loss of energy results in a decrease in its frequency, which extends its wavelength towards the red end of the light spectrum, a phenomenon known as redshift.

To calculate the energy lost by a photon due to gravitational redshift, it is essential to understand that a photon's energy is directly related to its frequency f through the equation $E = hf$, where h is the Planck constant.

If we consider a photon emitted with a frequency f_e and observed with a reduced frequency f_r due to gravitational redshift, the energy lost by the photon can be expressed as the difference between the initial and final energies:

$$\Delta E = h(f_\mathrm{e} - f_\mathrm{r}) \tag{8.1.1}$$

Using the relationship between frequency and wavelength ($f = \frac{c}{\lambda}$), where c is the speed of light, this equation can be rewritten in terms of wavelengths:

$$\Delta E = hc\left(\frac{1}{\lambda_\mathrm{r}} - \frac{1}{\lambda_\mathrm{e}}\right) \tag{8.1.2}$$

And using the definition of redshift $z = \frac{\lambda_\mathrm{r} - \lambda_\mathrm{e}}{\lambda_\mathrm{e}}$, we can rearrange to obtain an expression in terms of z:

$$\Delta E = hc\left(\frac{1}{\lambda_\mathrm{e}(1+z)} - \frac{1}{\lambda_\mathrm{e}}\right) \tag{8.1.3}$$

$$\Delta E = -\frac{hc}{\lambda_\mathrm{e}}\left(\frac{z}{1+z}\right) \tag{8.1.4}$$

This equation shows that the energy lost by a photon due to gravitational redshift depends on the wavelength at which it was emitted and the value of the redshift z, with the negative sign indicating a loss of energy.

This loss of energy is not merely apparent. For example, the cosmic microwave background is the radiation that has undergone the greatest redshift, with a z factor of

about 1,100, corresponding to a very low temperature and energy of around 3 Kelvin (-270°C), much lower than the original energy (See the figure 3.9).

It is also important to note that the very thin and collimated jets observed in the vicinity of supermassive objects indicate the presence of a strong magnetic field that opposes the collapse of the object by exerting intense magnetic pressure against gravity. These objects, like neutron stars at their maximum mass, are subcritical, resulting in a gravitational redshift effect limited to 3. This suggests that these objects might be subcritical massive objects.

In science, when an observation does not match the theory, the theory is typically questioned. However, in this very recent article published in the *Astrophysical Journal* [43], researchers modified the observations to align them with the black hole model. They generated synthetic images of black holes by manipulating various parameters such as mass, angular momentum, etc., and selecting the one that best matched the observed data using the PRIMO software as on the Figure 8.3:

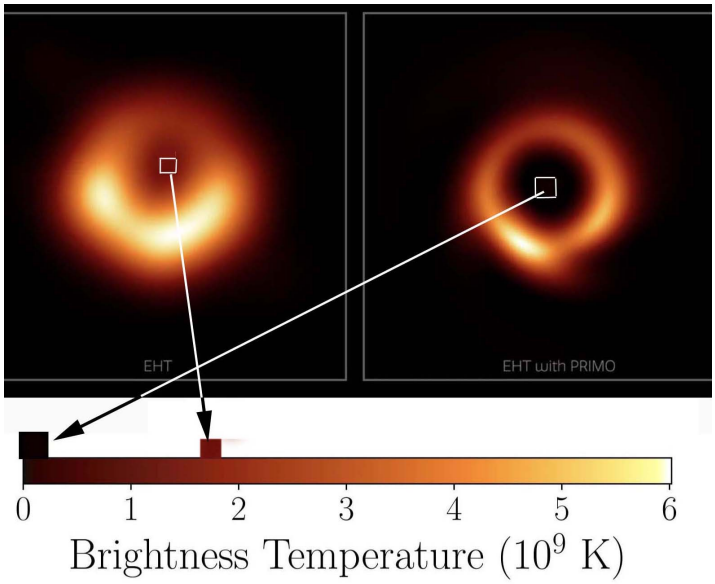

Figure 8.3: Synthetic image of the M87* black hole processed by PRIMO at the right compared the original image at the left

The result was a confirmation of the theory, but it raises questions about scientific rigor and research objectivity.

8.2 Alternative Interpretation of the Phenomenon

There is an alternative interpretation which is to attribute this color variation from the center to the edge to a gravitational redshift, with $z = 2$, leading to a wavelength

elongation by a factor of $1+z=3$. What can we say about such objects?

8.2.1 Comparison of Physical & Geometric Criticalities

In the section 6.1, we examined Schwarzschild's solutions to Einstein's equations, highlighting the Schwarzschild exterior metric and the corresponding interior metric for a fluid of constant density ρ_o. These solutions were confirmed by phenomena such as the advance of Mercury's perihelion and the gravitational lensing phenomenon (Figure 3.3). Karl Schwarzschild worked to ensure that the conditions governing these two metrics were in accordance with physical reality.

In a scenario where the star's density, ρ_o, remains constant, a characteristic radius $\hat{r}$ can be defined. Indeed, if we consider the interior metric published by Schwarzschild in his second article of February 1916 [74]:

$$\mathrm{d}s^2 = \left(\frac{3\cos\chi_a - \cos\chi}{2}\right)\mathrm{d}t^2 - \frac{3}{\kappa\rho_0}\left(\mathrm{d}\chi^2 + \sin^2\chi\mathrm{d}\Theta^2 + \sin^2\chi\sin^2\Theta\mathrm{d}\Phi^2\right) \tag{8.2.1}$$

Schwarzschild considered the speed of light c to be equal to one. Thus, the expression $\frac{3}{\kappa\rho_0}$ should be written as $\frac{3c^2}{\kappa\rho_0}$. Then, K. Schwarzschild defined a constant κ as being equal to $8\pi k^2$ *"where k^2 is Gauss' gravitational constant"*, which then allows him to introduce the characteristic radius $\hat{r}^2$ that equals to $\frac{3}{\kappa\rho_0}$ and, which is also the radius of the circle making up a part of the meridian of Flamm's surface ([49]). Thus, the equation 8.2.1 leads us to:

$$\mathrm{d}s^2 = \left(\frac{3\cos\chi_a - \cos\chi}{2}\right)\mathrm{d}t^2 - \hat{r}^2\left(\mathrm{d}\chi^2 + \sin^2\chi\mathrm{d}\Theta^2 + \sin^2\chi\sin^2\Theta\mathrm{d}\Phi^2\right) \tag{8.2.2}$$

Then, as K. Schwarzschild uses the angle χ to locate points inside the sphere, he switches to the variable r by the application of the variable change $r=\hat{r}\sin\chi$, which allows us to arrive at the modern form of the metric. Tolman provides a precise statement in 1934 by giving the following ([82]):

$$\begin{aligned}\mathrm{d}s^2 = &-\frac{\mathrm{d}r^2}{1-\left(\frac{r^2}{\hat{r}^2}\right)} - r^2\left(\mathrm{d}\theta^2 + \sin^2\theta\mathrm{d}\phi^2\right)\\ &+\left[\frac{3}{2}\sqrt{1-\left(\frac{r_n^2}{\hat{r}^2}\right)} - \frac{1}{2}\sqrt{1-\left(\frac{r^2}{\hat{r}^2}\right)}\right]^2 c^2\mathrm{d}t^2\end{aligned} \tag{8.2.3}$$

Where r_n is the radius of the star and $\hat{r}$ is a stellar constant as a function of its density ρ_o. Note that it formulates the order of the terms, in the metric, according to the signature $(---+)$ but retains the signs of the respective terms.

Let us consider a stationary observer ($\mathrm{d}r = \mathrm{d}\theta = \mathrm{d}\phi = 0$) located inside a star. The metric becomes:

$$\mathrm{d}s = c\mathrm{d}\tau = \left[\frac{3}{2}\sqrt{1-\left(\frac{r_n^2}{\hat{r}^2}\right)} - \frac{1}{2}\sqrt{1-\left(\frac{r^2}{\hat{r}^2}\right)}\right] c\mathrm{d}t = f(r)\mathrm{d}t \tag{8.2.4}$$

where τ is the proper time as seen by the stationary observer inside the star and $f(r)$ is the time factor.

Then, as seen on the section 6.1, when the time factor is null at the center of the star, a physical criticality is reached before geometric criticality appears, when the star's radius is only 5.72% less than the critical radius $\hat{r}$ inferred from its density:

$$r_n = R_{\mathrm{cr}_\phi} = \sqrt{\frac{8}{9}}\hat{r} = \sqrt{\frac{c^2}{3\pi G\rho_0}} \tag{8.2.5}$$

8.2.2 Gravitational Redshift Near Physical Criticality

Next, the Schwarzschild solution was later taken up, in a different form, by Tolman ([82]), Oppenheimer ([49]) and others ([1]), leading to the state equation, known as Tolman–Oppenheimer–Volkoff (TOV) equation, presented in its differential form:

$$\frac{\mathrm{d}p}{\mathrm{d}r} = -\frac{\rho c^2 + p}{r^2}\left(\frac{4\pi G}{c^4}pr^3 + \frac{Gm(r)}{c^2}\right)\left(1 - \frac{2Gm(r)}{c^2 r}\right)^{-1} \tag{8.2.6}$$

Whose integrated value was given by Karl Schwarzschild a century earlier (see the Figure 8.4), where in his second paper [74] published on February 1916, he describes the geometry inside a sphere filled with an incompressible fluid of constant density ρ_0:

$$f_2 = \frac{3}{\varkappa\rho_0}\sin^2\chi, \quad f_4 = \left(\frac{3\cos\chi_a - \cos\chi}{2}\right)^2, \quad f_1 f_2^2 f_4 = 1. \tag{29}$$

$$\rho_0 + p = \rho_0 \frac{2\cos\chi_a}{3\cos\chi_a - \cos\chi} \tag{30}$$

$$3x = r^3 = \left(\frac{\varkappa\rho_0}{3}\right)^{-3/2}\left[\frac{9}{4}\cos\chi_a\left(\chi - \frac{1}{2}\sin 2\chi\right) - \frac{1}{2}\sin^3\chi\right]. \tag{31}$$

Figure 8.4: The pressure law obtained in 1916 by Karl Schwarzschild

In this formula, the speed of light is still adjusted to a unit value. Therefore, this formula is equivalent to:

$$p = \rho_0 c^2 \left(\frac{\cos\chi - \cos\chi_a}{3\cos\chi_a - \cos\chi}\right) \tag{8.2.7}$$

Next, as seen in Section 8.2.1, K. Schwarzschild switched to the variable r by the following simple variable change:

$$r = \widehat{r}\sin\chi \tag{8.2.8}$$

The pressure becomes zero at the star's surface for $\chi = \chi_a$ with a radius given by:

$$r_a = \widehat{r}\sin\chi_a \tag{8.2.9}$$

The center of the star corresponds to $\chi = 0$, so the pressure becomes:

$$p = \rho_0 c^2 \left(\frac{1-\cos\chi_a}{3\cos\chi_a - 1}\right) \tag{8.2.10}$$

This imposes a maximum limit on this radius for $\cos\chi_a = \frac{1}{3}$, meaning:

$$r_a = R_{\mathrm{cr}_\phi} = \widehat{r}\sqrt{\frac{8}{9}} \approx 0,9428\widehat{r} \tag{8.2.11}$$

However, if we consider the mass corresponding to a physical criticality:

$$M_{\mathrm{cr}_\phi} = \frac{4}{3}\pi\hat{r}^3\rho_o \tag{8.2.12}$$

and the one corresponding to a geometric criticality:

$$M_{\mathrm{cr}_\gamma} = \frac{4}{3}\pi r_a^3\rho_o \tag{8.2.13}$$

we obtain the following relation:

$$M_{\mathrm{cr}_\phi} = \left(\frac{8}{9}\right)^{\frac{3}{2}} M_{\mathrm{cr}_\gamma} = 0.838 M_{\mathrm{cr}_\gamma} = 2.5 M_{\mathrm{solar}} \tag{8.2.14}$$

A value compatible with the masses of a few neutron stars that we have been able to deduce directly from available observations and for which, Thorne, Wheeler, and Misner have estimated in their book (page 611 of [81]) as the critical mass beyond which the pressure escalates to infinity as on the Figure 8.5.

Of course, we will never have images of neutron stars comparable to objects located at the center of M87 and the Milky Way. So, let's calculate the gravitational redshift effect $z+1$ corresponding to massive celestial bodies near this physical criticality. This effect impacts the light emitted from their surface in a radial direction toward a distant observer, who will perceive it with an increased wavelength λ_r. It's given by:

$$\frac{\lambda_r}{\lambda_e} = \frac{1}{\sqrt{1-\frac{R_s}{r_a}}} \tag{8.2.15}$$

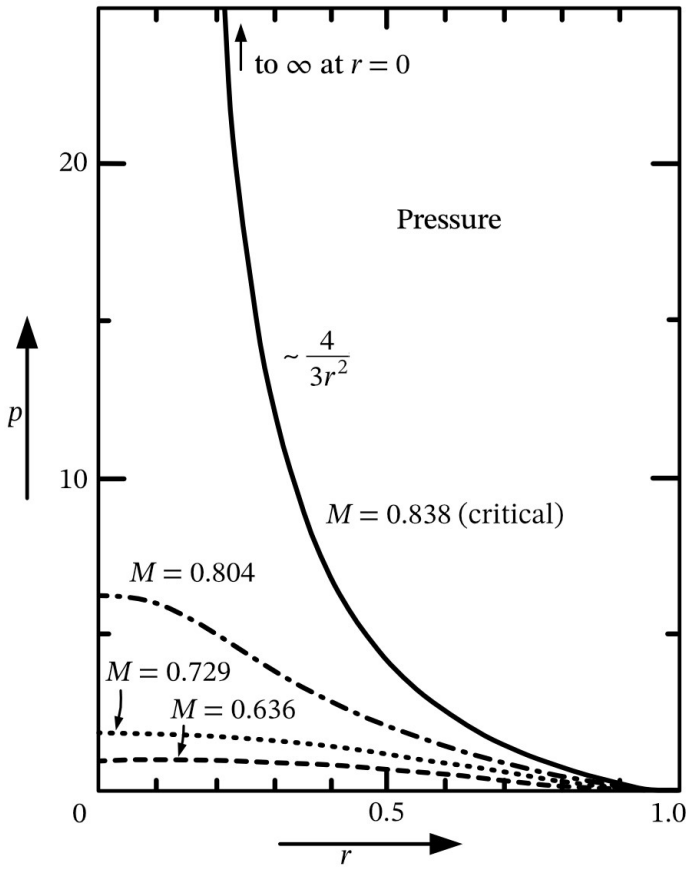

Figure 8.5: Variation of the pressure inside a neutron star of constant density

However, in the core part, the geometric criticality radius is defined by the *Schwarzschild Radius* which is:

$$R_s = \frac{2GM_{\mathrm{cr}_\gamma}}{c^2} = \frac{2G}{c^2}\left(\frac{4}{3}\pi r_a^3 \rho_0\right) = \frac{8\pi G\rho_0}{3c^2} r_a^3 = \frac{r_a^3}{\widehat{r}^2} \tag{8.2.16}$$

Then, the gravitational redshift will give:

$$\frac{\lambda_r}{\lambda_e} = \frac{1}{\sqrt{1-\frac{r_a^2}{\widehat{r}^2}}} = \frac{1}{\sqrt{1-\frac{2GM}{r_a c^2}}} = \frac{1}{\sqrt{1-\frac{8}{9}}} = 3 \tag{8.2.17}$$

This is precisely the value deduced from the ratio of maximum to minimum temperature of the first two images of black holes located at the centers of the M87 galaxy and the Milky Way. Thus, the images of these supermassive objects might also correspond to subcritical entities, where the pressure at their center – defined as a density of energy per unit volume – would be either infinite or at least extremely high.

8.2.3 Variation of Light Speed & Pressure in Constant Density Plasmas

Now, let's consider a fluid (hydrogen plasma) with an assumed constant density. At a temperature below 3000°C, the pressure inside it is given by:

$$p = \frac{\rho_0 v^2}{3} \tag{8.2.18}$$

where v is the average thermal agitation speed of the particles composing the plasma ([16]). Thus, the reasoning that *"if the pressure p tends to infinity, then this velocity should also tend to infinity, which is in contradiction with a central principle of special relativity, the "principle of causality", stating that no physical effect can propagate at a speed $v > c$"* ([81]), would lead to a physical aberration.

Nevertheless, in this region of space-time, the pressure within this plasma becomes radiative:

$$p_r = \frac{\rho_0 c^2}{3} \tag{8.2.19}$$

If we consider increasing this radiative pressure at a constant density, it can only be achieved by considering a variation of the speed of light in the medium, something Karl Schwarzschild was the first to consider [74]:

Die Lichtgeschwindigkeit in unserer Kugel wird:

$$v = \frac{2}{3\cos\chi_a - \cos\chi}, \tag{44}$$

Figure 8.6: Variation of the speed of light in a sphere of constant density

Thus, as he pointed out in his paper, the increase in the speed of light follows the increase in pressure. What happens when this pressure rises, as does the value of the speed of light ? Simple, it's clear according to Karl Schwarzschild (page 433 of [74]) that these two quantities become infinite for $\cos\chi_a = \frac{1}{3}$, which is to be done for $r = R_{\mathrm{cr}_\phi}$ (8.2.11) as seen in Section 8.2.2.

We can deduce, according to Karl Schwarzschild study, that the stability of those supermassive subcritical objects is due to the fact that the gravitational collapse, due to the physical criticality occurring long before the geometric criticality, is compensated by an extremely high radiative pressure at constant density coming from their centers, proportional to the square of the speed of light.

8.3 Conclusion

We have analyzed the images of supermassive objects located at the centers of galaxies, which were initially presented in the *Astrophysical Journal* as the first images of giant black holes. Through our comprehensive study, we propose an alternative interpretation for these objects, which could correspond to supermassive subcritical entities, exhibiting a maximum-to-minimum temperature ratio close to 3. Indeed, their radius are only 5.72% shorter than the Schwarzschild lengths deduced from their masses. This observation aligns well with the gravitational redshift effect, potentially characteristic of neutron stars nearing a physical criticality, as suggested by Schwarzschild's internal geometric solution published in his second paper in February 1916. This solution, largely unrecognized by most post-war cosmologists and not translated into English until 1999, provides a unique lens to view these phenomena. By examining aspects including pressure, the speed of light, and the time factor within these objects, we aim to enrich the existing narrative on the complex astrophysical phenomena at the core of galaxies. This includes an exploration of their stability, which may be maintained by a balance between gravitational collapse, resulting from a physical criticality that occurs long before geometric criticality, and the extremely high radiative pressure at constant density in their centers, proportional to the square of the speed of light. The century-old works of Karl Schwarzschild remind us that there are still mysteries to unravel within well-established theories. The questions we raise, especially regarding the evolution of the time factor and its profound implications for the concept of time itself, are crucial and invite further inquiry. Should future observations confirm our hypotheses, particularly if an image of a third supermassive object is discovered with a similar temperature ratio, it would encourage a reevaluation of some of our current astrophysical models. Ultimately, the universe, in its vastness and complexity, continues to stimulate us in our insatiable quest for knowledge.

Chapter 9

Challenges & Debates

9.1 Challenges Encountered in Communication & Acceptance of the Model

In our journey to disseminate and validate the Janus Cosmological Model (JCM), we encountered formidable challenges, particularly in the domain of scholarly publishing. This section aims to detail these difficulties, shedding light on the inherent complexities and biases present in the international mainstream publishing system.

One of the most significant obstacles we faced was the process of peer review in renowned journals. We found that the system, as it currently stands, is often rigid and impervious to novel ideas, especially those that challenge the established foundations of Physics and Cosmology. Our attempts to publish in prestigious journals such as *Physical Review D*, *Modern Physics Letters A*, *Astrophysical Journal* and *Astrophysics and Space Science*, among others, were met with resistance and skepticism. This resistance seems to stem not from a lack of scientific rigor on our part but from an overarching tendency within the scientific community to maintain the status quo.

In our attempts to publish, we received answers that demonstrate the challenges we faced. For instance, a letter from Dr. Ethan T. Vishniac, Editor-in-Chief of *The Astrophysical Journal*, highlighted the unconventional nature of our work in the context of their publication :

Dear Dr. Zejli,

I am writing to you with regard to your manuscript cited above, which you recently submitted to The Astrophysical Journal.

I have read your manuscript and considered its appropriateness for publication in our journal. Our journal specializes in manuscripts presenting new results on astro-

nomical observations or theory applied directly to astrophysical systems. Unfortunately, the subject matter of your manuscript, which deals with fundamental aspects of bimeric relativity, falls well outside of the subject area of our Journals. Consequently, I regret to inform you that we will be unable to publish your manuscript. Nevertheless, I offer you my best wishes in your future research.

The topic of this paper would be well within the scope of a journal specializing in the phyiscs of gravity. As a general policy, I do not recommend specific journals. I will onlly note that this manuscript is not well organzied as a research paper. The bulk of the paper reviews previous work and the new results and their significance are hard to discern. There is, for example, no mention of either in the abstract.

Regards,
Ethan T. Vishniac
AAS Editor-in-Chief
Johns Hopkins University

Meaning that while our manuscript dealt with fundamental aspects of *"bimeric relativity"* (meaning bimetric), it did not align with the journal's focus on new astronomical results and theories applied to astrophysical systems. This polite and informative answer reflects a general tendency to favor works that fit within the established framework of scientific research.

In contrast, answers from *Physical Review D* were markedly more succinct, often summarized by the phrase *"Non suitable"*. This brief reply underscores the difficulty in gaining acceptance for ideas that significantly deviate from the existing paradigms in theoretical physics and cosmology.

These interactions with leading journals underscore a significant challenge in communicating new scientific theories: the need to align innovative work with the expectations and established standards of scientific journals, while maintaining the integrity and novelty of the research.

Furthermore, recent policy changes at *arXiv*, a prominent preprint repository, have introduced an additional layer of complexity. The new requirement for submissions to be initially published in a major peer-reviewed journal may appear paradoxical and counterintuitive, particularly for pioneering research that might encounter initial resistance in traditional forums. This shift in policy has significantly impeded our capacity to share preliminary findings promptly and engage with the broader scientific community.

Despite these challenges, there have been glimmers of hope and recognition. Two journals, the Russian-based *Gravitation and Cosmology* (Pleiades Publishing) and the

German *Astronomische Nachrichten*, have shown a willingness to seriously consider our work. Their engagement with our research, although not as extensive as we might have hoped, is a positive step towards broader acceptance and understanding of the JCM.

In the following section, we will analyze the answers and reviews from these journals, highlighting both the constructive feedback and the areas where the peer-review process could be improved to accommodate innovative scientific theories.

9.2 Discussion on Criticisms & Provided Responses

During our effort to publish the Janus Cosmological Model, we faced significant challenges, one of which was the prolonged review process by the *Gravitation and Cosmology* journal. After eight months of persistent follow-ups, the journal finally found a referee to review our work. However, the outcome was not as we had hoped. Below is the correspondence that encapsulates the essence of the challenges we faced.

Reply from *Gravitation and Cosmology*

Dear Dr. Zejli,

After numerous attempts, we have received a referee report on your paper GC23-019 'Nature of the Dipole Repeller'. Regretfully, the report contains a number of serious critical remarks. In view of this report, we cannot accept your paper for publication in our journal.

Yours sincerely,
Dr. Sergey V. Bolokhov
Editorial Board of Gravitation and Cosmology

REFEREE REPORT

The authors try to explain the pnenomenon of the so-called Dipole Repeller in the framework of the "Janus cosmological model", which is in fact a kind of a bimetric theory. The model itself contains some entities which are very unlikely to exist in nature, such as particles with negative mass and photons with negative energy. To this end, it is appropriate to recall that recent experiments showed that particles of antimatter are subject of the same forces of gravity as matter particles of the same mass. This makes the authors' assumption of negavite masses still more doubtful. Moreover, it looks strange that the theory in question is invoked to explain just one phenomenon and has no impact on other observed systems. A weak point of the paper is that it contains only qualitative arguments without specific calculations taking into account the observed parameters of the repeller.

Our Answer to the Referee Report

Dear Dr. Sergey V. Bolokhov,

Thank you for forwarding the referee's report on our manuscript, "Nature of the Dipole Repeller." We appreciate the time and effort invested in reviewing our work. However, we believe there may be some misunderstandings regarding the core concepts of our research, which we would like to clarify.

1. On Negative Mass and Antimatter: The referee's concern about negative masses in light of recent experiments with antimatter highlights a fundamental aspect of our model that may have been overlooked. The Janus cosmological model, which forms the basis of our paper, predicts the existence of two distinct types of antimatter. The Type C antimatter, akin to Dirac's antimatter produced in laboratories, responds to gravitational forces similarly to ordinary matter. In contrast, the Type PT antimatter, corresponding to Feynman's concept of negative mass, is proposed to exist at the centers of cosmic voids, such as the Dipole Repeller. This type exerts an antigravitational effect, which is a critical component of our model and is clearly detailed on page 10 of our manuscript.

2. Observational Confirmations and Model Applications: Our model's validity extends beyond explaining the Dipole Repeller. It offers insights into various astronomical phenomena, which the referee might have missed in our paper:

Galaxy Confinement and Stability: Explained by lacunary spaces filled with negative masses.
Gravitational Lensing Effects: The model accounts for gravitational lensing phenomena around galaxies.
Universal Structure: Our theory proposes a lacunar structure of the universe filled with negative mass clusters, resembling interconnected soap bubbles.
Galaxy Rotation Curves and Gravitational Anomalies: We explain the flattening of rotation curves and the unexpected acceleration of stars at galaxy borders.
Early Galaxy Formation: Supported by recent observations from the James Webb Telescope, our model suggests simultaneous formation of galaxies in the universe's first 100 million years.
High-Redshift Galaxies: We address the dimmed luminosity of distant galaxies (redshift > 7) due to the negative gravitational lensing effect of negative mass clusters.
Local Relativistic Verifications: The model aligns with phenomena like Mercury's perihelion precession and light deviation by the Sun.
Supernova Observations: The asymmetry between positive and negative mass populations correlates with observations of Type Ia supernovae.

3. Misinterpretation of the Model's Scope: Finally, the claim that our theory is only invoked to explain a single phenomenon overlooks its broad applicative range. Our model offers explanations for spiral galaxy structures, cosmic antimatter invisibility due to negative energy photons, and the nature of the universe's invisible components, among others.

We believe this additional information and clarification will help address the concerns raised in the referee report. We are prepared to provide further details or revisions if

necessary.

Thank you for considering our response, and we look forward to the opportunity to contribute to the journal.

Yours sincerely

Unfortunately, following our detailed response addressing each of the referee's concerns, we received no further communication. The editor and the referee seemed to have withdrawn from the dialogue, illustrating the challenges and, at times, the seemingly insurmountable barriers faced in pioneering new scientific theories within the established academic publishing framework.

Critical Analysis of Review by *Astronomische Nachrichten*

Our interactions with *Astronomische Nachrichten* also posed challenges but allowed for a deeper exploration of a fundamental issue in the acceptance of new ideas in cosmology. The sole referee, found after a two-month search, initiated a dialogue that shed light on a pervasive problem: the reliance on established hypotheses by renowned physicists, which subsequently shape and solidify the paradigms within which most cosmologists operate.

The objective of our work is to provide an innovative geometric and cosmological interpretation of the Schwarzschild exterior solution, based on two main hypothesis:

- **Isotropy:** Invariance under the action of *SO(3)*[1].
- **Stationarity:** Independence of the metric terms with respect to the time coordinate[2].

The general solution, as originally described by Schwarzschild, is often presented without proper justification. Tolman noted in 1934 ([82]) that the most general form, includes a crossed term in $\mathrm{d}r\mathrm{d}t$. However, this term was later disregarded for convenience. This approach, including Schwarzschild's, has been followed by many researchers, as studied in detail in Chapter 6.

The referee highlighted that the non-existence of such a crossed term stemmed from the assumed symmetry hypotheses. We are accused of neglecting an essential symmetry hypothesis: the solution should be invariant when t is changed to $-t$ (as noted in Wald's book [84], among others). Consequently, a solution with a $\mathrm{d}r\mathrm{d}t$ crossed term would not satisfy this invariance condition, as changing t to $-t$ alters the sign of the crossed term. Yet, what is the physical basis for this symmetry assumption concerning the time variable? None. It was neither mentioned by Schwarzschild nor by many of

[1]The group of 3D rotations and spatial translations.

[2]Invariance by time translation.

his successors.

Indeed, the reasoning (if it can be called that) is based on the *"black hole model"* centered around the *"modern form"*, where the crossed term is absent (6.3.1). This is a purely mathematical hypothesis, meant to align not with tangible observational realities but with the general belief in the existence of black holes. For cosmologists, therefore, this assumption may seem *"natural."*

Our experience with *Astronomische Nachrichten* illustrates how entrenched paradigms can influence the reception of innovative ideas in cosmology, highlighting the need for open-mindedness and reevaluation of fundamental assumptions in the light of new theoretical developments.

9.3 Attempt to Explain the Systematic Rejection of New Ideas

We have recently drafted a detailed article on the symplectic structure of the Janus Cosmological Model, the foundations of which were explained in chapter 5 of this book. This article was then submitted to a renowned journal of mathematical physics. The feedback from the main reviewer was notably positive, describing the content as very innovative and deserving of publication, subject to some adjustments and a thorough clarification of its physical implications.

Taking these recommendations into account, we meticulously revised the article, providing the necessary clarifications, before resubmitting it to the same journal. Although publication is not yet confirmed, the prospects are promising given the initial interest and the detailed and constructive (finally!) analysis of the reviewer.

This experience raises important points about the reception of new ideas in the scientific field. Our article, having benefited from a careful and constructive examination by an expert in the field of mathematical physics, contrasts with the approach of some journals such as *Physical Review D*. These often simply respond with a terse *"non suitable"*, without providing a detailed analysis. An examination of the editorial committees of these journals reveals a predominance of specialists in string theory, but a notable lack of mathematicians-geometers.

This situation illustrates the gap between mathematicians and some theoretical physicists. This divergence recalls the definition given by Souriau of a *"physics without experience and a mathematics without rigor"*. Our experience with the submission of this article highlights the inherent challenges in presenting innovative ideas in the interconnected fields of physics and mathematics, thereby underlining the need for greater openness in academic evaluation.

Chapter 10

Conclusion & Discussions

By considering the principle of Occam's razor, which favors the simplest and most coherent theory with observational data, it is reasonable to argue that the Janus model scores higher than the standard model. The Janus Cosmological Model provides a consistent approach to explaining several astrophysical phenomena while offering a clear interpretation of available observational data. On the other hand, the standard model exhibits inconsistencies with observational data, requiring ad hoc constructions to address these inconsistencies.

Indeed, the Janus model goes beyond just offering alternatives to phenomena usually attributed to dark matter and dark energy, such as the acceleration of cosmic expansion, the confinement of galaxies, pronounced gravitational lensing effects, and the near-homogeneity of the Cosmic Microwave Background (CMB), among others. It provides detailed clarifications on the nature and identity of the universe's invisible components. The model resolves the paradox of the lack of observation of primordial antimatter and offers an explanation for the dipole repeller, considering it as a conglomerate of negative mass. This perspective lends increased credibility to the Janus cosmological model in establishing the large-scale structure of the universe, while explaining the reasons behind the difficulty in detecting negative mass with optical observational instruments. It also accounts for the low magnitude of astronomical objects with a redshift greater than 7 and adheres to the principle of falsifiability by stipulating specific observational tests, such as the presence of negative mass conglomerates, with the dipole repeller as a notable example. Additionally, it proposes an alternative mapping of the universe based on a different interpretation of the weak gravitational lensing effect.

Furthermore, the Janus model finds confirmation in the most recent observational data, particularly those obtained from the James Webb Space Telescope, by predicting the formation of galaxies in their current forms during the first 100 million years of the Universe. Additionally, the structure of its dynamic group confers a *CPT-symmetry* to its geometry for which a specific prediction made in 2017, was confirmed in September 2023. This prediction concerns C-symmetric antimatter (charge symmetry), synthe-

sized in the laboratory and emitting photons of positive energy, which, according to observations, is subject to a downward gravitational attraction, just like ordinary matter.

It also opens up promising avenues of research in quantum mechanics, suggesting that the integration of states of negative energy and mass could be crucial for the quantification of gravitation. The Janus model is in harmony with current observational data, presenting no major contradictions.

Throughout this book, we have delved into the complexities of the model, unraveling its nuances and potential to shed light on the mysteries that have long perplexed cosmologists and physicists.

This journey through the realms of advanced mathematics, theoretical physics, and cosmology demonstrates the model's ability to challenge conventional perspectives and offer alternative explanations to phenomena that current models struggle to fully elucidate. The discussions and analyses presented aim to enrich the reader's understanding and ignite a curiosity to further explore and question the boundaries of our scientific knowledge.

I believe the limitations in theoretical physics and cosmology during the 1950s can be attributed to the field's delay in embracing topology. Topology, the study of properties preserved through continuous deformations, could have provided new ways to understand the fabric of the universe and its complex structures.

In conclusion, I hope that this book will not only serve as a comprehensive guide to the model anchored in a strong theoretical foundation of general relativity, but also inspire and motivate a new generation of thinkers to bravely explore the uncharted territories of cosmology. May it foster a deeper appreciation for the intricate beauty of our universe and the continual quest for understanding that drives us as scientists and as human beings.

This model emerges as an essential and indispensable guiding light in Cosmology, illuminating the path towards uncharted territories and novel prospects. This journey is by no means nearing its conclusion. It continually encourages further research, but above all, the making of new discoveries, which can be summarized by the famous phrase by Pierre Dac ([21]) often attributed to Charles De Gaulle[1]: *"Researchers who search, we find. Researchers who find, we seek."*

[1]Exact quote from Charles De Gaulle pronounced on August 13, 1968: *"Every teacher, every researcher enjoys, after a certain period, the security of a job in the institution where they perform their duties. In other words, they can remain a researcher even if they find nothing, especially from the moment they are no longer of age to find anything."*

Bibliography

[1] R. Adler, M. Bazin, and M. Schiffer. *Introduction to General Relativity*. McGraw-Hill, 1975.

[2] K. Akiyama et al. First M87 Event Horizon Telescope Results. I. The Shadow of the Supermassive Black Hole. *The Astrophysical Journal*, 2019.

[3] K. Akiyama et al. First Sagittarius A* Event Horizon Telescope Results. I. The Shadow of the Supermassive Black Hole in the Center of the Milky Way. *The Astrophysical Journal*, 2022.

[4] K. Akiyama et al. The persistent shadow of the supermassive black hole of M 87. *Astronomy & Astrophysics*, 2024.

[5] E. K. Anderson et al. Observation of the effect of gravity on the motion of antimatter. *Nature*, 2023.

[6] V. Bargmann, P. G. Bergmann, and A. Einstein. On The Five-Dimensional Representation Of Gravitation And Electricity. *Theodore von Karman Anniversary Volume*, page 212, 1941.

[7] A. Benoit-Lévy and G. Chardin. Introducing the Dirac-Milne universe. *Astronomy and Astrophysics*, 537:A78, 2012.

[8] P. Bergmann. *An Introduction To The Theory Of Relativity*. Prentice-Hall, 1942.

[9] P. Bergmann and A. Einstein. On A Generalization Of Kaluza's Theory Of Electricity. *Annals of Mathematics*, 39:683, 1938.

[10] H. Bondi. Negative Mass in General Relativity. *Reviews of Modern Physics*, 29(3), 1957.

[11] N. Bourbaki. *Eléments de mathématique: Groupes et algèbres de Lie*. Springer, 2006.

[12] Michael Boylan-Kolchin. Stress testing ΛCDM with high-redshift galaxy candidates. *Nature Astronomy*, April 2023.

[13] C. E. Brennen. *Cavitation and Bubble Dynamics*. Oxford University Press, 1995.

[14] S. Chandrasekhar. *Principles of Stellar Dynamics*. Dover, 1942.

[15] S. Chandrasekhar. *The Mathematical Theory of Black Holes*. Clarendon Press, 1983.

[16] S. Chapman and T. G. Cowling. *The Mathematical Theory of Non-uniform Gases*. Cambridge University Press, 1970.

[17] Joël Chaskalovic. Gravitation theory for mathematical modelling in geomarketing. *Journal of Interdisciplinary Mathematics*, 12(3):417, 2009.

[18] R. Chiba and R. Schönrich. Tree-ring structure of Galactic bar resonance. *Monthly Notices of the Royal Astronomical Society*, 505:2412, 2021.

[19] P. T. Chruściel. Lectures on Mathematical Relativity. Accessed online at `https://homepage.univie.ac.at/piotr.chrusciel/papers/BeijingAll.pdf`. Lecture notes, revised and extended May 2008 following lectures on black holes in Marrakech, Beijing, July 2006, Mathematical Institute and Hertford College, Oxford, LMPT, Fédération Denis Poisson, Tours.

[20] J. W. Cronin. The Experimental Discovery of CP Violation. *American Physical Society*, 1964.

[21] P. Dac. *Les pensées*. 1972.

[22] T. Damour and Ian I. Kogan. Effective Lagrangians and universality classes of nonlinear bigravity. *Phys. Rev. D*, 2002.

[23] N. Debergh et al. On evidence for negative energies and masses in the Dirac equation through a unitary time-reversal operator. *Journal of Physics Communications*, 2018.

[24] F. W. Dyson, A. S. Eddington, and C. Davidson. A Determination of the Deflection of Light by the Sun's Gravitational Field, from Observations Made at the Total Eclipse of May 29, 1919. *Philosophical Transactions of the Royal Society of London. Series A, Containing Papers of a Mathematical or Physical Character*, pages 291–333, 1920.

[25] A. Eddington. A Comparison with Whitehead's and Einstein's Formulæ. *Nature*, 1924.

[26] A. Einstein and N. Rosen. The Particle Problem in the General Theory of Relativity. *Phys. Rev.*, 48:73, 1935.

[27] H. El-Ad and T. Piran. Voids in the Large-Scale Structure. *The Astrophysical Journal*, 1997.

[28] Leonardo Ferreira et al. Panic! at the Disks: First Rest-frame Optical Observations of Galaxy Structure at z>3 with JWST in the SMACS0723 Field. *The Astrophysical Journal Letters*, 2022.

[29] L. Flamm. Beiträge zur Einsteinschen Gravitationstheorie. *Physikalische Zeitschrift*, 1916.

[30] L. Flamm. Republication of: Contributions to Einstein's theory of gravitation. *General Relativity and Gravitation*, 47(72), 2015.

[31] R. W. Fuller and J. A. Wheeler. Causality and multiply connected space-time. *Physical Review*, 1962.

[32] E. Guendelman, A. Kaganovich, E. Nissimov, and S. Pacheva. Spherically symmetric and rotating wormholes produced by lightlike branes. *International Journal of Modern Physics A*, 25(07):1405–1428, 2010.

[33] E. Guendelman, E. Nissimov, S. Pacheva, and M. Stoilov. Einstein-Rosen "bridge" revisited and lightlike thin-shell wormholes. *Bulgarian Journal of Physics*, 44:84–97, 2017.

[34] G. Heald. The Stronger Case for Gravitational Repulsion between Matter and Antimatter. *Research Gate publication*, (339339776), 2020.

[35] Y. Hoffman et al. The quasi-linear nearby Universe. *Nature Astronomy*, 2018. arXiv:1807.03724.

[36] Y. Hoffman, D. Pomarède, R.B. Tully, and H. Courtois. The dipole repeller. *Nature Astronomy*, 1:0036, 2017.

[37] S. Hossenfelder. Bimetric theory with exchange symmetry. *Phys. Rev. D*, 78:044015, Aug 2008.

[38] T. Kaluza. On the Unification Problem in Physics. *International Journal of Modern Physics D*, 27(14):1870001, 2018.

[39] Roy P. Kerr. Gravitational Field of a Spinning Mass as an Example of Algebraically Special Metrics. *Physical Letters*, 11:237, 1963.

[40] O. Klein. Quantum theory and five-dimensional relativity theory. In *The Oskar Klein Memorial Lectures*, pages 69–82. 2014.

[41] P. Koiran. Infall time in the Eddington–Finkelstein metric, with application to Einstein–Rosen bridges. *Inter. Jr. of Mod. Phys. D*, 15(30), 2021.

[42] M. D. Kruskal. Maximal Extension of Schwarzschild Metric. *Physical Review*, 119(5), 1960.

[43] L. Medeiros et al. Principal-component Interferometric Modeling (PRIMO), an Algorithm for EHT Data. I. Reconstructing Images from Simulated EHT Observations. *The Astrophysical Journal*, 2023.

[44] A. A. Michelson and E. W. Morley. On the Relative Motion of the Earth and the Luminiferous Ether. *American Journal of Science*, 34(203):333–345, 1887.

[45] B. Morin and J.P. Petit. Le Retournement de la Sphère. *Comptes rendus de l'Académie des Sciences Série A*, 287(13):791–794, 1978.

[46] M. Morris and K.S. Thorne. Wormholes in spacetime and their use for interstellar travel: A tool for teaching general relativity. *Am. J. Phys.*, 56:395, 1988.

[47] T.F. Neiser. Fermi Degenerate Antineutrino Star Model of Dark Energy. *Advances in Astronomy*, 2020:Article ID 8654307, 2020.

[48] J. R. Oppenheimer and G. M. Volkoff. On Massive Neutron Cores. *Physical Review*, 55(4):374–381, 1939.

[49] J.R. Oppenheimer and H. Snyder. On Continued Gravitational Contraction. *Phys. Rev.*, 56(5):455–459, 1939.

[50] A. Palatini. Deduzione invariantiva delle equazioni gravitazionali dal principio di Hamilton. *Rend. Circ. Matem. Palermo*, 43:203–212, 1919.

[51] A. I. Pavlovskii. Magnetic Cumulation - A Memoir for Andrei Sakharov. In M. Cowan and R. B. Spielman, editors, *Megagauss Magnetic Field Generation and Pulsed Power Applications*, volume I, pages 9–22. Nova Science Publishers, New York, 1994.

[52] S. Perlmutter et al. Measurements of Ω and Λ from 42 High-Redshift Supernovae. *Astrophysical Journal*, 517(2):565–586, 1999.

[53] J.P. Petit. *Le topologicon*. Edition Belin, 1985.

[54] J.P. Petit. An interpretation of cosmological model with variable light velocity. *Modern Physics Letters A*, 1988.

[55] J.P. Petit. The Missing-Mass Problem. *Il Nuovo Cimento*, 1994.

[56] J.P. Petit. Twin Universe Cosmology. *Astrophysics and Space Science*, 226:273–307, 1995.

[57] J.P. Petit. The Janus Cosmological Model and the fluctuations of the CMB. *Progress in Physics*, 2018.

[58] J.P. Petit and G. D'Agostini. Cosmological Bimetric model with interacting positive and negative masses and two different speeds of light, in agreement with the observed acceleration of the Universe. *Modern Physics Letters A*, 29(34), 2014a.

[59] J.P. Petit and G. D'Agostini. Negative Mass hypothesis in cosmology and the nature of dark energy. *Astrophysics And Space Science*, 354:611–615, 2014b.

[60] J.P. Petit and G. D'Agostini. Bimetric models. When negative mass replaces both dark matter and dark energy. Excellent agreement with observational data. Solving the problem of the primeval antimatter. *Database of the French National Center*, 2021a.

[61] J.P. Petit and G. D'Agostini. Constraints on Janus Cosmological model from recent observations of supernovae type Ia. *Astrophysics and Space Science*, 2021b. hal-03426721f.

[62] J.P. Petit, G. D'Agostini, and N. Debergh. Evidence of negative energies and masses in the Dirac equation through a unitary time-reversal operator. *J. Phys. Comm.*, 2(115012), 2018.

[63] J.P. Petit, G. D'Agostini, and N. Debergh. Physical and mathematical consistency of the Janus Cosmological Model (JCM). *Progress in Physics*, 15, 2019.

[64] J.P. Petit, P. Midy, and F. Landsheat. Twin matter against dark matter. In *Where is the matter? (International Conference on Astrophysics and Cosmology)*, 2001.

[65] J.P. Petit and G. Monnet. Axisymmetrical elliptical exact solution of the couple Vlasov plus Poisson. In L. Weliachew, editor, *La dynamique des galaxies spirales*, page 391. Centre National de la Recherche Scientifique, 1974.

[66] Tsvi Piran. On Gravitational Repulsion. *arXiv*, 2018.

[67] N. Popławski. Radial motion into an Einstein–Rosen bridge. *Physics Letters B*, 687:110–113, 2010.

[68] A. Riess et al. Type Ia Supernova Discoveries at z $>$ 1 from the Hubble Space Telescope, Evidence for Past Deceleration and Constraints on Dark Energy Evolution. *Astrophysical Journal*, 607(2), 2004.

[69] A. D. Sakharov. Violation of CP Invariance, C Asymmetry, and Baryon Asymmetry of the Universe. *Pi'sma ZhÉTF*, 5(1):32–35, 1967.

[70] A. D. Sakharov. Cosmological Models of the Universe with Reversal of Time's Arrow. *Pi'sma ZhÉTF*, 79(3):689–693, 1980.

[71] A. D. Sakharov. Multisheet Models of the Universe. *Pi'sma ZhÉTF*, 82(3):1233–1240, 1982.

[72] A.D. Sakharov. ZhETF Pis'ma. *JETP*, 49:594, 1979. 76 : 1172.

[73] B.P. Schmidt et al. The high-Z supernova search. Measuring cosmic deceleration and global curvature of the universe using type Ia supernovae. *Astrophysical Journal*, 507(1), 1998.

[74] K. Schwarzschild. Über das Gravitationsfeld einer Kugel aus inkompressibler Flüssigkeit nach der Einsteinschen Theorie. *Sitzungsberichte der Königlich Preussischen Akademie der Wissenschaften*, 1916.

[75] K. Schwarzschild. Über das Gravitationsfeld eines Massenpunktes nach der Einsteinschen Theorie. *Sitzungsberichte der Königlich Preussischen Akademie der Wissenschaften*, 1916.

[76] J. M. Souriau. *Géométrie et relativité*. Hermann, 1964.

[77] J. M. Souriau. Prolongements du champ de Schwarzschild. *Bulletin de la Société Mathématique de France*, 93:193–207, 1965.

[78] J. M. Souriau. *Structure of Dynamical Systems, a Symplectic View of Physics*. Birkhäuser Verlag, 1997.

[79] A. J. M. Spencer. *Continuum Mechanics*. Dover Publications, Mineola, 1992.

[80] O. C. Stoica. On singular semi-Riemannian manifolds. *International Journal of Geometric Methods in Modern Physics*, 11, 2014.

[81] K.S. Thorne, J.A. Wheeler, and C.W. Misner. *Gravitation*. 1973.

[82] R. Tolman. *Relativity, Thermodynamics and Cosmology*. Oxford at the Clarendon Press, 1934.

[83] Michael Tsamparlis. On the Palatini method of variation. *Journal of Mathematical Physics*, 19(3):555–557, 1978.

[84] R. Wald. *General relativity*. 1984.

[85] S. Weinberg. *The Quantum Theory of Fields*, volume 1-3. Cambridge University Press, 2000.